2014

A case study of integrated modelling of traffic, vehicular emissions, and air pollutant concentrations for Huron Church Road, Windsor

Hassan Mohseni Nameghi
University of Windsor

A case study of integrated modelling of traffic, vehicular emissions, and air pollutant concentrations for Huron Church Road, Windsor

by

Hassan Mohseni Nameghi

A Dissertation
Submitted to the Faculty of Graduate Studies
through Civil and Environmental Engineering
in Partial Fulfillment of the Requirements for
the Degree of Doctor of Philosophy at the
University of Windsor

Windsor, Ontario, Canada

2013

A case study of integrated modelling of traffic, vehicular emissions, and air pollutant concentrations for Huron Church Road, Windsor

by

Hassan Mohseni Nameghi

APPROVED BY:

_____

Dr. Ashok Kumar, External Examiner
Department of Civil Engineering, The University of Toledo

_____

Dr. Bill Anderson, Outside Reader
Department of Political Science

_____

Dr. Paul Henshaw, Department Reader
Department of Civil and Environmental Engineering

_____

Dr. Rajesh Seth, Department Reader
Department of Civil and Environmental Engineering

_____

Dr. Xiaohong Xu, Advisor
Department of Civil and Environmental Engineering

_____

Dr. Chris Lee, Co-Advisor
Department of Civil and Environmental Engineering

_____

Dr. Stephen Brooks, Chair of Defense
Department of Political Science

02, 05, 2013

DECLARATION OF ORIGINALITY

I hereby certify that I am the sole author of this thesis and that no part of this thesis has been published or submitted for publication.

I certify that, to the best of my knowledge, my thesis does not infringe upon anyone's copyright nor violate any proprietary rights and that any ideas, techniques, quotations, or any other material from the work of other people included in my thesis, published or otherwise, are fully acknowledged in accordance with the standard referencing practices. Furthermore, to the extent that I have included copyrighted material that surpasses the bounds of fair dealing within the meaning of the Canada Copyright Act, I certify that I have obtained a written permission from the copyright owner(s) to include such material(s) in my thesis and have included copies of such copyright clearances to my appendix.

I declare that this is a true copy of my thesis, including any final revisions, as approved by my thesis committee and the Graduate Studies office, and that this thesis has not been submitted for a higher degree to any other University or Institution.

ABSTRACT

The objectives of this research are to examine spatial and temporal variations in traffic-related NO_2 and benzene concentrations and to investigate the sensitivity of estimated vehicular emissions and ambient concentrations on input parameters. The case study was conducted for Huron Church Road (9.5 km) in Windsor, Ontario. Observed vehicle counts and emission factors from Mobile6.2 were used to estimate vehicular emissions. Ambient concentrations were estimated using the AERMOD dispersion model.

Results showed that traffic on Huron Church Road significantly contributes to near-road air quality. The simulated annual mean NO_2 concentration of 2008 was 27 $\mu g/m^3$ at 40 m from the road, which was higher than the background concentration of 21 $\mu g/m^3$. Concentrations sharply decreased with distance from the road. At 600 m from the road, the simulated annual concentration was 9% of the concentrations at a distance of 40 m from the road (=2.4 $\mu g/m^3$, less than background concentration). Similar patterns were observed for benzene.

Ambient concentrations were higher during the nighttime than the daytime due to poor mixing. Traffic counts and wind speed explained 40% of variations in the both observed and simulated NO_2 concentrations. The relationship between the truck/car counts and NO_2/benzene concentration ratios was linear.

The model-measurement comparison showed that Mobile6.2 and AERMOD reasonably reproduced the hour-of-day variations and spatial fall-off pattern of NO_2 concentrations. However, AERMOD underestimated concentrations during the daytime potentially due to over-mixing.

Sensitivity analysis of the Mobile6.2 showed that the emission factors were most

sensitive to the choice of Vehicle Mile Traveled compositions (Ontario versus US), followed by the choice of vehicle age distribution (Ontario versus US), and the average speed of vehicles. In AERMOD simulations, the hour-of-day variation in emission should be considered.

Stop-and-go movements increased the total NOx emission over the 9.5 km road by 24% compared to the case of cruise speed of 50km/h during the morning peak hour. Two correction (multiplication) factors were devised to adjust uniform emissions by Mobile6.2 near signalized intersections: an upstream correction factor of 3.2 to account for idling and acceleration emissions, and a downstream correction factor of 1.6 to account for acceleration emissions.

DEDICATION

This dissertation is dedicated to my wife.

ACKNOWLEDGEMENTS

I would like to sincerely acknowledge all who supported my Ph.D. research at University of Windsor. In particular, my special thanks to my advisors, Dr. Xiaohong Xu and Dr. Chris Lee, for supervision, financial support and giving me the opportunity to learn and to grow, to think critically, to write professionally, and to manage the time wisely. I would like to thank my committee for providing great insights towards my research: Dr. Paul Henshaw, Dr. Bill Anderson, and Dr. Rajesh Seth from University of Windsor and Dr. Ashok Kumar from The University of Toledo. I would like to thank Dr. Amanda Wheeler from Health Canada for providing valuable and insightful suggestions and Mr. John Wolf from City of Windsor for providing Windsor vehicle counts used in this study. I acknowledge Health Canada for providing average NO_2 concentrations at 11 sites near Huron Church Road used for validation of fall-off patterns.

I would like to acknowledge the University of Windsor and the Ontario Ministry of Education for scholarships. Funding for the research contained in this dissertation was provided by Health Canada and the Natural Sciences and Engineering Research Council of Canada (NSERC).

TABLE OF CONTENTS

LIST OF TABLES

LIST OF FIGURES

CHAPTER I

1. INTRODUCTION

1.1 Background

On-road vehicles are the major source of urban air pollution which contribute to poor air quality. On-road vehicles produce large amounts of primary pollutants such as nitrogen oxides (NOx), volatile organic compounds (VOC), carbon monoxide (CO), and particulate matter (PM) and some of them also contribute to production of secondary pollutants such as ozone (O_3) and secondary aerosols (EPA, 2012a). For instance, in Ontario, NOx, VOC, and CO emissions by on-road vehicles accounted for 28%, 14%, and 45% of total anthropogenic emissions, respectively, in 2006 (MOE, 2011). Although strict regulations on vehicular emissions have decreased air pollutant concentrations in North America during recent years, both the number of on-road vehicles and the distance traveled have continuously increased (HEI, 2010).

Windsor, Ontario – located on the Canada-US border across from Detroit, Michigan – "is known to have relatively high levels of air pollution compared to other Canadian cities" (Health Canada, 2010a). Air pollution in Windsor originates from both local and international sources. Local sources include local transportation, manufacturing facilities in Windsor and Detroit, and Windsor-Detroit border crossing traffic. The Ambassador Bridge, one of two Windsor-Detroit entry ports, has the highest number of Canada-US border crossings (Transport Canada, 2010). In the year 2008, 2.9 million heavy duty trucks and 4 million passenger cars crossed the Ambassador Bridge (Transport Canada, 2010). Almost all trucks and the majority of those passenger cars travel along Huron Church Road, an arterial road leading to the Bridge. To mitigate traffic delays at the

border crossing, the Government of Canada plans to build a new Windsor-Detroit Bridge (DRIC, 2008a). Thus, the impact of cross-border traffic on air quality in Windsor is of great interest to the public and researchers.

Ambient air quality in Windsor is also affected by transboundary air pollution from industrialized US states such as Michigan and Ohio. Thus, the Windsor-Detroit area has received lots of attention during recent years. The Border Air Quality Strategy, an agreement between the governments of the US and Canada in 2003, focused on Windsor-Detroit Airshed (Health Canada, 2010b).

Poor air quality can affect respiratory and cardiovascular systems of the human body (Health Canada, 2011). Many epidemiological studies suggest that cardio-respiratory diseases and mortalities are associated with exposures to traffic-related air pollution (Wang, 2008; Gan et al., 2011). As the awareness regarding health effects of vehicular emissions rises, countries implement policies to reduce the human exposure to air pollutants (HEI, 2010). These policies are generally evaluated through the use of simulation tools which estimate traffic counts, vehicular emissions, ambient air concentration of pollutants, and human exposure (Bell et al., 2011). As expected, the accuracy of estimating human exposure largely relies on the accuracy of estimated ambient air concentrations.

Currently, the following three models have commonly been used for estimation of ambient concentrations: 1) geospatial interpolation models using observational data collected at a few government stations, 2) regression models such as Land Use Regression (LUR), which estimates concentrations using observed short term concentrations from a spatial network of monitors and spatially distributed predictors,

e.g. traffic counts within 100m from the receptor, and 3) atmospheric dispersion models such as AERMOD (HEI, 2010). Geospatial interpolation models are limited to the time of observations and do not consider the emission source contribution directly. LUR models consider variables such as traffic counts; however, the actual contribution of traffic to air pollutant concentration "is not known or reported" (HEI, 2010). Therefore, the LUR models may not be suitable for predicting future scenarios caused by changes in emission factors which may occur due to vehicle technology advancement (e.g. cleaner vehicles) or changes in traffic patterns (e.g. reduced congestion). In addition, it is costly to monitor ambient concentrations in a dense network in order to develop regression models.

Dispersion models simulate the air pollutant concentrations by solving mathematical equations. These models require meteorological parameters of the study area, geometric configurations of emission sources and receptors, and the emission rates (EPA, 2012b). To estimate traffic-related concentrations, vehicular emissions are estimated using traffic counts along with emission factors of vehicles, i.e. the amount of emission emitted from each vehicle per distance traveled (mass/vehicle/distance). Emission factors of vehicles are estimated using emission models such as the EPA mobile source emission model Mobile6.2 (EPA, 2003).

There is a growing interest in the use of emission and dispersion models for estimating human exposure to air pollutants. Policy makers rely on these models for evaluating the impacts of emission reduction strategies on human exposure. Thus, it is necessary to validate these models by conducting model-measurement comparisons.

In urban areas, the main source of NO_2 and benzene is on-road vehicles. Wheeler et al. (2008) observed a strong correlation between observed NO_2 and benzene concentrations and suggested that NO_2 could be used as a proxy of benzene for Windsor. Because trucks (diesel vehicles) are high NOx emitters and cars (gasoline vehicles) are high benzene emitters (Transport Canada, 2006), the truck/car and NO_2/benzene ratios are expected to be correlated. As a result, benzene concentrations could be predicted using observed NO_2 concentrations and truck/car count ratios.

Dispersion and emission models require a large amount of inputs including traffic counts, fuel properties, vehicle type and age composition, and meteorological parameters. It is time consuming to process the data for these models. Thus, it is worthwhile to build the simple relationships to predict concentrations using routinely available input data. For this purpose, it is essential to identify major factors explaining large variations in concentrations.

Both the emission and dispersion models are sensitive to some input parameters. The use of more-refined input data over default values of those models is desirable for estimation of emissions and concentrations. However, collecting such data is costly. Thus, it is important to investigate the sensitivity of simulated emissions and concentrations to different levels of detail of input data. EPA (2002a) and Tang et al. (2005) found that Mobile6.2 (EPA, 2003) is sensitive to vehicle age, road type and fuel properties. However, the sensitivity of Mobile6.2 to the use of detailed and local input data over default values was not investigated.

Vehicles produce more emissions when they stop-and-go compared to when they cruise (Ahn and Rakha, 2008), as stop-and-go movement results in induced idling and

acceleration emissions. However, Mobile6.2 does not sufficiently capture the stop-and-go emissions due to the use of an average speed. Thus, it is worthwhile to develop the correction factors using a simple approach to overcome the limitation of this model in estimation of emissions near signalized intersections.

In summary, emissions and dispersion models play an essential role in exposure assessment as well as the evaluation of mitigation strategies and alternative transportation routes. Those models have been extensively validated, and several sensitivity studies have been conducted. However, in order to improve air quality management, there is a need to extend the knowledge and develop new tools by addressing the following research questions:

- To what degree these models can reproduce the observed spatial and temporal distribution of air pollutants?
- If there is a large discrepancy between observed and simulated concentrations, what could be the reason? Is it input parameters or the model performance?
- What are the major factors contributing to the spatial and temporal variations in concentrations?
- Can simplified relationships with fewer input variables be used to predict concentrations instead of the complex dispersion models?
- Can one traffic-related air pollutant be used as a proxy of the other pollutant using the truck/car ratio?
- How are the concentrations estimated by emission and dispersion models sensitive to the more-refined input parameters?

- Can the Mobile6.2 estimated emissions be improved by using a simple approach to taking into account the stop-and-go emissions?

1.2 Objectives

The overall objective of this research is to simulate traffic-related air pollutant concentrations using a multi-model approach and to examine the sensitivity of model results to input parameters. The case study is Huron Church Road in Windsor, Ontario.

The specific objectives are to:

- Estimate the spatial and temporal distributions of vehicle counts, vehicular emissions, and NO_2 and benzene concentrations near Huron Church Road using dispersion modeling.
- Compare observed and estimated concentrations in order to evaluate the performance of the multi-model approach in both spatial and temporal scales.
- Identify major factors contributing to temporal distribution of concentrations using statistical analysis.
- Develop simplified relationships between concentrations and a reduced number of predictor variables
- Find a relationship between NO_2/benzene concentration and truck/car count ratios using regression techniques.
- Investigate the effects of using more detailed input data and considering stop-and-go movement on model estimated vehicular emissions and ambient air concentrations.
- Develop NOx correction factors to adjust Mobile6.2 emissions at signalized

intersections where stop-and-go movement occurs.

1.3 Organization of thesis

The thesis is composed of six chapters including Introduction (Chapter 1), Literature Review (Chapter 2), Methodology (Chapter 3), Results of Part I (Chapter 4), Results of Part II (Chapter 5), and Conclusion (Chapter 6).

Overall, the thesis includes two major parts: 1) Part I: spatial and temporal distributions of vehicle counts, emissions, and concentrations, and 2) Part II: Effects of input data on estimated emissions and concentrations. Methodology for Parts I and II are explained in Sections 3.1 - 3.6 (Chapter 3) and Section 3.7 (Chapter 3), respectively. Results for Parts I and II are explained in Chapter 4 and Chapter 5, respectively.

CHAPTER II

2. REVIEW OF LITERATURE

2.1 Atmospheric dispersion models

Atmospheric dispersion models have been extensively used for estimating spatial and temporal distributions of air pollutant concentrations. They can mimic the dispersion of air pollutants through mathematical simulation. These models predict concentrations of air pollutants downwind of emission sources. They require meteorological parameters of the study area, geometric configurations of emission sources and receptors, and emission rates (EPA, 2012b). The required meteorological parameters are usually wind speed, wind direction, ambient temperature, and stability conditions. As expected, accuracy of estimations by dispersion models depends on input data.

Six well-known atmospheric dispersion models used for estimation of traffic-related air pollutant concentrations were evaluated: AERMOD (EPA, 2004a), CALINE4 (Caltrans, 1998), CAL3QHC (Eckhoff and Braverman, 1995), CALPUFF (Scire et al., 2000a), ADMS-Roads (CERC, 2010) and OSPM (Berkowicz, 2000). Advantages and disadvantages of these methods are compared in Table 2.1. All models are based on steady-state Gaussian plume dispersion except the CALPUFF which is based on non-steady-state Lagrangian equations. Four of these models: AERMOD, CALINE4, CAL3QHC, and CALPUFF, are US EPA recommended regulatory models.

Table 2.1: A comparison of six dispersion models

Dispersion model	Methodology	Advantages	Disadvantages
AERMOD	• Steady-state Gaussian • Boundary layer parameterizations	• Preferred and most advanced model by EPA • Consider the effects of convective mixing.	• Time consuming to setup model and pre-process data
CALINE4	• Steady-state Gaussian • Concept of mixing zone	• Easy to handle • Can model intersections	• Only 20 receptors • Has no meteorological pre-processor
CAL3QHC	• Steady-state Gaussian • Concept of mixing zone • Queuing and hot spot calculations	• Model idling emission near signalized intersections	• Limited number of links (100) and receptors (20)
CALPUFF	• Non-steady-state Lagrangian • Dispersion as a series of continuous puffs	• Consider spatial variability of wind speed and wind direction • Estimate long-range transport of pollutants	• Emissions can not be temporally varied • Not suitable for near-road dispersion
ADAMS-Roads	• Steady-state Gaussian • Boundary layer parameterizations • A Box model for street canyon	• GIS can be linked for visualization and analysis of emission and dispersion • Has been extensively validated for many cases	• No free license is available • Some developed modules, e.g. Emission inventory are for UK, not suitable for other locations
OSPM	• Steady-state Gaussian • Box model for street canyon	• Models recirculation of air pollutant in the street canyon	• No free license is available

The AERMOD is the US EPA preferred dispersion model. In 2010, AERMOD was listed as a recommended regulatory model for PM2.5 and PM10 hot spot analysis (EPA, 2010). AERMOD is a steady-state Gaussian dispersion model which incorporates turbulence effects in "planetary boundary layer" (EPA, 2004a). It is also the

recommended dispersion model for regulatory purposes in Ontario (MOE, 2009b). The major drawback of the AERMOD is the need for extensive input data including surface and upper air meteorological parameters. The AERMOD did not have a line source tool for representing roads until December 2012 (EPA, 2013a). Thus, roads were represented by small volume sources or area sources (EPA, 2004a). This increased the simulation load, and thus the simulation time. In this regard, Wayson (2012) proposed some solutions such as representing road curves with irregularly shaped polygons.

CALINE4 is a line source dispersion model developed by the California Department of Transportation (Caltrans). It can estimate ambient air quality near intersections. The setup and the use of CALINE4 are relatively easy compared to the other dispersion models. However, the number of receptors is limited to 20 in CALINE4. Although CALINE needs hourly mixing heights and atmospheric stability, it has no meteorological pre-processor (Pierce et al., 2008). CALINE4 and Mobile6.2 emission models (EPA, 2003) were used to estimate CO and PM2.5 concentrations near a section of I-75 in Michigan (Zhang and Batterman, 2010). A General Additive Model (GAM) was constructed using measured concentrations, meteorological parameters and traffic counts. By comparing simulation and GAM results, it was concluded that Mobile6.2 tends to underestimate PM2.5 emission factors.

CAL3QHC (CALine3 with Queuing and Hot spot Calculations) is the US EPA preferred dispersion model for identifying air pollution hotspots near signalized intersections. This model is a modified version of the CALINE3 (Benson, 1979) which considers idling emissions in addition to free-flow emissions near signalized intersections. CAL3QHC uses an algorithm to estimate queue length and idling emissions

at signalized intersections. The CAL3QHCR is the revised version of CAL3QHC, and recently the input and output structure of this model was improved (Claggett, 2012).

After release of the new EPA (2009) mobile source emission model, MOVES (MOtor Vehicle Emission Simulator), there has been a growing interest in the use of CALQ3HC. This is because MOVES estimates modal emissions. For instance, Westerlund and Cooper (2012) predicted air toxic concentrations near seven intersections using the CAL3QHC and emission factors from MOVES. The MOVES regulatory manual for hotspot analysis of PM2.5 and PM10 (EPA,2010) recommended a procedure for estimation of idling and free-flow emission factors needed for CAL3QHC simulation.

CALPUFF is a non-steady-state Lagrangian model which assumes that the dispersion of air pollutant takes place as a series of continuous puffs. It considers spatial variability of some meteorological parameters such as wind speed, wind direction, temperature, and heat flux. This is particularly important in a large area where metrological parameters vary considerably over the space. The meteorological pre-processor of CALPUFF called CALMET (Scire et al., 2000b) generates spatial distributions of some meteorological parameters over the space. The CALPUFF can estimate long-range transport of air pollutants. However, it is not suitable for near-road dispersion. CALPUFF and Mobile6.2 were used for estimation of traffic-related NO_2 and NOx concentrations over the Greater Toronto Area (Hatzopoulou et al., 2011).

ADAMS-Roads is the most advanced dispersion model in the UK. It can be linked to GIS for visualization and analysis of emission and dispersion. It has been extensively validated in many studies. The OSPM is a street canyon dispersion model. It considers

recirculation of air pollutant in the street canyon. However, no free license is available for ADAMS-Roads (CERC, 2010) and OSPM (Berkowicz, 2000).

Mohan et al. (2011) compared simulated concentration by AERMOD and ADMS-Urban (an extensive version of ADMS-Roads, which considers emissions from different sources) with observed concentrations. They found that results by both models are comparable. Major differences between results were because of different processing of meteorological parameters.

Dispersion models simulate NOx concentrations using the NOx emissions. However, if NO_2 concentration is desired, there are two methods: 1) use of the chemistry module in dispersion models for transformation of NOx to NO_2, and 2) simulate NOx concentrations with a dispersion model and then use an empirical relationship between NO_2 and NOx from a nearby air quality station.

Generally, the photochemistry of urban smog, the O_3-NOx-VOC chemistry, is composed of two main processes: ozone formation and NOx titration (Sillman, 2003). Ozone formation occurs through the sequence of photochemical reactions; a simplified chain is shown in Reactions 2.1-2.3 (Sillman, 2003). Volatile Organic Compounds (VOCs) convert NO to NO_2, and NO_2 is broken down to radical O and NO in the sunlight. The radical O is combined with O_2 and produces O_3.

$$\text{VOC} + \text{NO} \rightarrow \text{Secondary VOC} + \text{NO}_2 \qquad \text{(Reaction 2.1)}$$

$$\text{NO}_2 + \text{Sunlight} \rightarrow \text{NO} + \text{O} \qquad \text{(Reaction 2.2)}$$

$$\text{O} + \text{O}_2 + \text{M}^* \rightarrow \text{O}_3 + \text{M} \qquad \text{(Reaction 2.3)}$$

where M represents a third body which allows the reaction to occur.

In NOx titration, O_3 is removed by reacting with NO (Reaction 2.4). This process usually occurs during nighttime or in the vicinity of emission sources emitting a large amount of NO (Sillman, 2003).

$NO + O_3 \rightarrow NO_2 + O_2$ (Reaction 2.4)

The chemistry module in dispersion models has been used to simulate NO_2 concentration. The chemistry module in the five above-mentioned dispersion models was compared in Table 2.2.

Table 2.2: A comparison of chemistry modules used in five dispersion models

Dispersion model	Reference	Processes considered for NO_2 chemistry			Requirement for NO_2 simulation	
		NOx titration	O_3 formation	NOx-NO_3-NH_4	emissions	background concentration
AERMOD	EPA (2004a)	√			NOx	O_3
CALINE4	Caltrans (1998)	√			NOx	O_3, NO, and NO_2
CALPUFF	Scire et al. (2000a)	√	√	√	NOx	O_3 and NH_3
ADMS-Roads	CERC (2010)	√	√		NOx and VOC	O_3, NO, and NO_2
OSPM	Berkowicz (2000)	√			NOx	O_3, NO, and NO_2

Because a majority of NO_2 is formed by secondary chemical reactions in the atmosphere, AERMOD, CALINE4 and OPSM only consider the NOx titration process

(Reaction 2.4). However, requirements for NO_2 simulation differ among these three models. The AERMOD only needs the background concentrations of O_3 whereas CALINE4 and OPSM need background concentrations of O_3, NO, and NO_2. This difference in input requirements is due to the assumptions used by each model to represent the NOx titration. The ADMS-Roads considers both NOx titration and O_3 formation processes. It requires both NOx and VOC emissions. The CALPUFF considers the NOx-NO_3-NH_4 process in addition to NOx titration and O_3 formation processes. This is because it is used to estimate long-range transport of pollutants.

2.2 Vehicular emission models

Generally, vehicular emissions are estimated using collected or estimated traffic counts along with emission factors of vehicles: the amount of emission emitted from each vehicle per distance traveled (mass/vehicle/distance). Emission factors of vehicles are determined based on vehicle types (e.g. light-duty, or heavy-duty), fuel types (e.g. gasoline, or diesel), vehicle ages, and vehicle activities (e.g. cold start, or running), traffic conditions (e.g. speed, acceleration, driving cycle), ambient conditions (e.g. temperature and humidity), etc. Based on the above factors, emission factors of vehicles are determined by testing vehicles on the dynamometers under different conditions.

Two types of models have been used for estimating emission factors of vehicles: first, macroscopic models which calculate emission factors of vehicles based on average speed of vehicles using different driving cycles, e.g. Mobile6.2; and second, microscopic emission factor models which calculate emission factors based on instantaneous speed and acceleration of vehicles, e.g. CMEM (University of California, 2003).

For the estimation of emission factors, five models were evaluated: Mobile6.2 (EPA, 2003), Mobile6.2C (Vitale et al., 2004), MOVES (EPA, 2009), CMEM (University of California, 2003) and backward spatial allocation of county-wide emission inventory (Wang et al., 2009). These methods are compared in Table 2.3 with their advantages and disadvantages.

Table 2.3: A comparison of evaluated methods for estimating emission factors

Emission factor model	Advantages	Disadvantages
Mobile6.2	• Incorporate local fuel properties, vehicle registration and ambient temperature • User friendly	• Times consuming for running and creating input/output files
Mobile6.2C	• It is developed for Canada	• No online version was available
MOVES	• Similar to Mobile6.2, incorporate local data • Relational database • Modal emission factors	• Sophisticated as it uses more assumptions
CMEM	• Consider emissions induced by acceleration of vehicles, particularly, heavy-duty trucks	• Trucks emission factors for model year after 2001 is not available • Instantaneous speed and acceleration are not readily available
Spatial allocation of county-wide emission inventory	• High spatial coverage	• Required city-wide vehicle counts • Not suitable for a road

Mobile6.2 released in 2003 is the EPA highway emission estimation model (EPA, 2003). It incorporates local fuel properties, vehicle age distributions, and ambient temperature. Environment Canada developed a Canadian version of Mobile6.2

(Moblie6.2C). Although Mobile6.2C was developed for Canada (Vitale et al., 2004), it might be deemed not suitable for all places in Canada as vehicle age distribution and fuel properties are different by province.

The MOVES is the most recent EPA mobile source emission model. MOVES replaced the Mobile6.2 for regulatory purposes in 2010. In comparison to Mobile6.2, MOVES is more comprehensive as it uses relational database and is able to estimate modal emissions, emissions from alternative fuels and vehicles, GHG emissions, and fuel consumption. In comparison to Moblie6.2, MOVES uses more extensive sets of default input values. This may result in uncertainty in estimation of emissions, where local data are not available or costly to collect.

The Comprehensive Modal Emission Model (CMEM) was developed by the University of California in 2003. The CMEM can simulate instantaneous vehicular emission using instantaneous speed and acceleration of vehicles. The model can estimate emissions induced by acceleration and idling of vehicles. It has been observed that emission rates of vehicles are higher when they accelerate compared to when they cruise (Panis et al., 2006; Chen. et al., 2007). Acceleration and idling of vehicles are more frequent at arterial roads, where vehicles stop and go due to facing signalized intersections. Many studies used traffic simulation and CMEM to estimate vehicular emissions (Kun and Lie, 2007; Boriboonsomsin and Barth, 2008). However, data processing, calibration and validation of traffic simulation models are time consuming and burdensome.

Wang et al. (2009) developed a method to allocate county-wide total mobile source benzene emission (reported as one number), to census tracks (a finer spatial resolution).

This allocation was carried out using some relevant surrogates such as roadway mile traveled. Then, the census track benzene emissions are allocated to roadways using vehicle counts as a surrogate. The backward spatial allocation of county-wide emission inventory requires city-wide vehicle counts for road network which may not be readily available.

An overview of emission and dispersion models used for traffic-related air quality can be found in Fu and Yun (2010). Pierce et al. (2008) also conducted a comprehensive review of these models, and it is suggested for further information.

2.3 Selection of dispersion and emission models

The AERMOD dispersion model was selected. This is because it is the most advanced dispersion model by EPA, and it needs the minimum requirements for NO_2 simulation. It has been used for estimation of NO_2 (Chaix et al., 2006; Lindgren et al., 2009; Lindgren et al., 2010) and benzene (Touma et al., 2007; Cook et al., 2008; Venkatram et al., 2009; Wang et al., 2009) concentrations in several studies. For instance, Touma et al. (2007) modeled benzene concentrations from several sources including roadways. Cook et al. (2008) and Venkatram et al. (2009) estimated the benzene concentrations near roadways. Wang et al. (2009) estimated benzene concentrations in Camden, New Jersey, and then estimated personal exposure to this pollutant.

Among emission models, Mobile6.2 was selected. It has been most widely used for estimating emissions in different studies. For instance, Cook et al. (2008) used Mobil6.2 to generate a look-up table for the calendar year 2002. The table provides emission factor of each vehicle class as a function of temperature and speed. This look-up table was used

for estimation of vehicular emissions and dispersion of air pollutants (Cook et al., 2008; Venkatram et al., 2009).

Mobile6.2 and AERMOD were used in many studies to estimate emissions and concentrations (Sosa et al., 2012; Cook et al., 2008). Sosa et al. (2012) used Mobile6.2 and AERMOD to estimate air pollutant concentrations from border crossing traffic on the Bridge of Americas, a major US-Mexico border. They evaluated effects of different mitigation scenarios, and found that shifting commercial vehicles to other border crossing and replacing them with passenger cars decreased the future level of NOx and PM2.5 concentrations. Hourly vehicle counts were collected for one-week in each of four seasons (spring, summer, fall, and winter), and then hour-of-day emissions by season were estimated. In another study, Cook et al. (2008) used Mobile6.2 and AERMOD to estimate concentrations from traffic on roadways. They also considered emissions from major industrial sources and household activities.

2.4 Relationship between NO_2 and benzene concentrations

NO_2 and benzene are known to be traffic markers in urban air pollution. NO_2 is mainly from diesel vehicles whereas benzene is from gasoline vehicles. NO_2 contributes to formation of photochemical smog and ground-level O_3 through complex chemical and photochemical reactions with NO, O_3, and VOCs. Acute short-term exposure to NO_2 may lead to change in airway responsiveness and lung function (EPA, 2012c). Long-term exposure may lead to chronic bronchitis, and other respiratory infections. Similar to NO_2, the primary source of benzene emission is traffic. Vehicular benzene emissions are from 1) unburned benzene content of fuel, 2) secondary formation through combustion of

some aromatic compounds, and 3) evaporative losses. Short-term exposure to benzene may cause drowsiness and headaches, and long-term exposure may cause cancer (EPA, 2012d).

The major source of NO_2 and benzene in urban areas is traffic. Therefore, it is expected that ambient concentrations of these two pollutants are positively correlated. In this regard, several experimental studies have investigated the correlation between ambient air concentrations of benzene and NO_2 near the roadways (Modig et al., 2004; Schnitzhofer et al., 2008; Beckerman et al., 2008) or in urban areas (Wheeler et al., 2008; Parra et al., 2009). Some of these studies found a significant correlation between ambient air concentrations of NO_2 and benzene. This suggests that NO_2 can be used as an indicator of ambient benzene concentrations (Wheeler et al., 2008; Modig et al., 2004).

Kourtidis et al. (2002) measured ambient air concentration of NO_2, benzene, and some other pollutants in a street canyon. A strong correlation was observed between NO_2 and benzene due to the fact that both were from traffic. Modig et al. (2004) conducted a study to investigate whether "NO_2 could be used to indicate ambient and personal levels of benzene". In this regard, personal levels of NO_2 and benzene were measured for 40 participants for one week. The authors simultaneously collected ambient NO_2 and benzene concentrations at "one urban background station and one street station in the city". Results showed an insignificant correlation between personal levels of NO_2 and benzene ($r=0.1$, $p=0.46$). However, a strong correlation between ambient levels of NO_2 and benzene was observed at both stations ($r=0.7$, $p<0.05$). Beckerman et al. (2008) collected ambient concentrations of NO_2, benzene, and some other air pollutants at two transects perpendicular to a major expressway, Highway 401, in Toronto, Ontario.

Authors found a strong correlation between NO_2 and benzene concentrations at receptors located at one transect, MOE Station, ($r = 0.94$, $p < 0.01$), and no correlation at receptors located at the other transect, the Bayview Station ($r = 0.12$, $p > 0.05$). The correlation was not significant at the Bayview Station because it was located at a hilly area, and there were some emission sources other than the Expressway such as "a major commercial center and busy arterial road". They concluded that "urban landscape, traffic patterns, local topography, atmospheric chemistry and physical processes all appear to influence the correlations between NO_2 and other pollutants" (Beckerman et al., 2008).

Wheeler et al. (2008) collected ambient levels of NO_2, benzene and some other pollutants at 54 locations across Windsor, Ontario over four seasons of the year. They observed significant correlations between NO_2 and benzene concentrations ($r = 0.89$, $p < 0.01$). Parra et al. (2009) measured ambient air concentrations of VOCs and NO_2 at 40 locations of Pamplona in Navarra, Spain. They found a strong correlation between the NO_2 and benzene concentrations ($r = 0.59$, $p < 0.01$), and suggested that NO_2 can be used as an indicator of benzene concentrations.

Schnitzhofer et al. (2008) measured "CO, NO, NO_2, benzene, toluene and PM10 at a motorway location in an Austrian valley" for one year. The authors found strong correlations between heavy-duty vehicle counts and NO_2 concentrations, and between light-duty vehicle counts and CO concentrations. They also observed a strong correlation between CO and benzene. This is because the primary source of these two pollutants is light-duty vehicles. However, the authors did not report the correlation between NO_2 and benzene.

Table 2.4 lists observed ratios of NO_2/benzene concentrations in some of previous studies. Two distinct groups of ratios were 37-39 and 25-26. Because both NO_2 and benzene are mainly from traffic, the ratio of NO_2/benzene concentrations should be similar to the ratio of NOx/benzene emissions. Using default values of Mobile6.2 and the average speed of 60km/h, the NOx/benzene emission ratios were approximately 27 and 700 for passenger cars and heavy duty trucks, respectively. The observed ratio of 25-26 by Modig et al. (2008) and Wheeler et al. (2008) is close to the NOx/benzene emission ratio for passenger cars. This reflects that the major traffic affecting NO_2/benzene concentration ratio was car traffic in these two studies. On the other hand, the observed ratio of 37-39 by Schnitzhofer et al. (2008) and Beckerman et al. (2008) is higher than the NOx/benzene emission ratios of passenger cars.

Table 2.4: Observed NO_2/benzene ratios in previous studies

Study	Source type	Location	NO_2 (ug/m^3)	Benzene (ug/m^3)	NO_2/Benzene
Modig et al. (2004)	Street station	Sweden	53.0	2.1	25.2
	Urban background	Sweden	26.0	1.0	26.0
Schnitzhofer et al., (2008)	Near road	Austria	72.0	1.9*	37.9
Beckerman et al., (2008)	Near expressway	Canada, Toronto	27.4*	0.7	39.2
	Near expressway (Hilly area)	Canada, Toronto	32.9*	0.9	36.6
Wheeler et al., (2008)	Across urban area	Canada, Windsor	23.3*	0.9	25.9

* Converted from ppb to µg/m3, assuming 1 ppb (NO_2)=1.88 µg/m^3(NO_2), 1 ppb (Benzene)=3.19 µg/m^3(Benzene) under standard condition

The cause of the correlation between NO_2 and benzene concentrations in urban areas needs further investigations (Beckerman et al., 2008). The existence of heavy duty trucks

can affect the correlation between NO_2 and benzene concentrations as diesel vehicles are high NOx emitters and gasoline vehicles are high benzene emitters. For example, the NOx emission factor of heavy duty trucks is 16 times that of passenger cars (Transport Canada, 2006). On the other hand, the benzene emission factor of passenger cars is four times that of heavy duty trucks (Claggett & Houk, 2007).

2.5 Limitations in the current literature

2.5.1 Vehicle counts

Accurate estimation of vehicular emission inventory and concentrations relies on accurate estimation of traffic counts. Given that vehicle counts change over time, short-term data collection does not take into account the day-to-day variation in peak-hour volume (Hellinga and Abdy, 2008). To account for the variations in vehicle counts over time, vehicle counts should be collected at various locations for a longer time period. The U.S. Federal Highway Administration (FHWA) (2004) suggested that traffic counts over several days should be adjusted to a typical day using adjustment factors. In this regard, Kim (2003) adjusted vehicle counts collected in different survey times using the annual average daily traffic (AADT) at each intersection.

In particular, the use of short-term data for the estimation of volume and traffic delay may result in a large uncertainty. Some studies addressed this problem by collecting long-term traffic counts. Capparuccini et al. (2008) evaluated the accuracy of design hourly volume (DHV) estimated using short-term traffic counts. They collected hourly traffic counts for a year and found that DHV obtained based on short-term traffic counts was less accurate for roads with higher day-to-day variation in traffic volume. Hellinga and

Abdy (2008) also observed 15-minute traffic counts during the afternoon peak period (3:45-6:30 pm) for the year 2005 and found that average intersection delay estimated using average peak hour volumes underestimated the actual delay by 15%. Furthermore, traffic counts collected at different times at different locations may not be well suited for observing spatial variations of traffic and vehicular emissions. The other limitation of most previous studies is that vehicle counts by vehicle type (e.g. car and truck) were not collected although temporal variations in counts may be different for different vehicle types.

Many studies used annual average daily traffic counts (AADT) to estimate vehicular emissions, and to predict annual mean ambient air concentrations using dispersion models (Carslaw et al., 2002; Pénard-Morand, 2006). Several limitations are associated with the use of AADT for estimation of emissions. First, AADT at each road section are estimated based on short-term counts, and it is hard to justify that short-time counts reflect the actual long-term or annual counts. Second, temporal variations of vehicular emission are not considered when only AADT counts are used.

Wallace and Kanaroglou (2008) considered the hour-of-day variations in traffic counts for the estimation of vehicular emissions and NO_2 concentrations in Hamilton, Ontario. However, the authors observed the hour-of-day pattern of traffic counts from one station and over a short period of time (four weeks), and used it for the city-wide road network. Given that traffic counts change over time and space, short-term data collection on one road section does not take into account the spatial and temporal variation in traffic counts. Thus, to consider temporal variations in traffic, it is suggested that traffic counts are collected at multiple locations over a longer period of time.

2.5.2 Vehicular emissions

Accurate estimate of vehicular emissions are essential for accurate estimation of ambient air concentrations using dispersion models. Generally, total vehicular emissions are estimated using traffic counts along with the emission factor of vehicles. In particular, the emission factor of vehicles by Mobile6.2 can be estimated using either default values of input parameters, which are US nation-wide values, or localized values. Thus, input parameters must be adjusted to reflect local conditions such as composition of vehicle mile traveled, road type, average speed, fuel properties, vehicle age distributions, distribution of vehicle activities (e.g. cold start, or running), ambient conditions (e.g. temperature and humidity), etc. In this regard, several studies investigated the sensitivity of the estimated emission factors by Mobile6.2 to the input parameters.

For instance, Tang et al. (2005) studied the effects of input parameters on estimation of air toxic emission factors by Mobile6.2 and found that not all air toxic emission factors are similarly affected by a change in input parameters. In particular, the benzene emission factor of vehicles is sensitive to the change in fuel properties (RVP, benzene and aromatic contents), road type and average speed, and model year. EPA (2002a) analyzed the sensitivity of CO, HC, and NOx emissions estimated by Mobile6.0 to the input parameters. It was found that change in the following parameters can change emission factors of vehicles by more than 20% compared to the emission factor estimated using default values of the Mobile6.0: vehicle age-distribution, ambient temperature, fuel RVP, and average speed of vehicles. The major limitations with these studies are 1) hypothetical scenarios were used which may not occur in reality, and 2) sensitivity of Mobile6.2 to use of more detailed input data was not investigated.

In calculating the composite emission factor of vehicles, vehicle categories in traffic counts should be mapped to vehicle classes in emission factor models. Traffic counts are usually collected for a few categories of vehicles such as car, truck, bus, etc. However, vehicle classes in emission factor models are more detailed - e.g. 28 classes in Mobile6.2 and 26 classes in CMEM. Some studies used default values of the share of vehicles to obtain composite emission factors of vehicle categories in traffic counts. For instance, Cooper & Arbrandt (2004) used default values from Mobile6.2 for estimation of annual emission inventory in metropolitan Orlando, Florida. However, actual vehicle and fuel compositions in Orlando may be different from those in Mobile6.2. Some others assumed one typical class in emission factor models for each vehicle category in traffic counts. For example, in the estimation of NOx emission, Wallace and Kanaroglou (2008) assumed that all vehicles are classified in the Light Duty Gasoline Vehicle (LDGV) class in Mobile6.2, and ignored all other vehicle classes. Although the number of HDDV is generally small, their contribution to NOx emission is high. This is because the emission factor of HDDV is approximately 16 times that of LDDV (Transport Canada, 2006). According to MOE (2011), NOx emissions of HDDV accounted for 46% of on-road emissions in Ontario in 2009. Therefore, the assumption made by Wallace and Kanaroglou (2008) underestimates NOx concentrations by up to 46%. In another example, Kun and Lie (2007), mapped three vehicle classes in VISSIM, a traffic simulation software, to three typical categories in CMEM. However, it is hard to justify that three out of 26 classes in CMEM can represent the actual vehicle composition in China.

Temporal variations of the emission factor of vehicles were considered in some studies because the emission factor of vehicles varies with ambient conditions. For instance, Cooper & Arbrandt (2004) and Cook et al. (2008) suggested the use of monthly average input into Mobile6.2 instead of the annual input for estimation of the emission inventory.

Effects of stop-and-go traffic movement

Vehicles tend to produce more emissions when they stop and go compared to when they cruise. Thus, driving cycles of vehicles can affect vehicular emissions. Hence, the level of stop-and-go movement is reflected by adjusting the average speed in macro-emission models or considering the instantaneous speed and acceleration in microscopic emission models. In particular, road type and average speed are two parameters used in Mobile6.2 to represent driving cycles. Appropriate choices of these parameters are challenging. This is because the traffic condition along the road varies considerably. In addition, determining the road type in Mobile6.2 based on the observed speed is uncertain.

On arterial roads, stop-and-go traffic movements usually occur near the signalized intersections, and a majority of vehicles cruise on road segments between the intersections. Therefore, it is expected that vehicular emissions and ambient levels of air pollution be higher at areas close to the intersections. As a result, a uniform road type and a single value of average speed for the whole road may not identify the hot spots of air pollution near the signalized intersections. These hotspots are important as higher ambient air concentrations of pollutants have more adverse impacts on health.

Speed profiles during stop-and-go movements are necessary for obtaining spatial variability of emissions at different locations of the road and also for evaluating effects of stop-and-go movement. These profiles are usually collected from a sample of probe vehicles or modeled using microscopic traffic simulation models. For instance, Ahn & Rakha (2008) evaluated the effects of route choice decision on vehicular emissions by collecting instantaneous speed and acceleration of vehicles with GPS equipped vehicles. Alternatively, Panis et al. (2006) estimated instantaneous speed and acceleration of vehicles, and evaluated effects of speed limits on vehicular emissions using a traffic simulation model, DRACULA. Similarly, Kun and Lie (2007) used a traffic simulation model, VISSIM, and a microscopic emission model, CMEM to evaluate effects of "traffic control strategies" on emissions.

Both methods used for obtaining speed profiles, field observation and traffic simulation, have pros and cons. Although the field data are more accurate, they are only collected from a sample of vehicles and for a limited time period. On the other hand, use of traffic simulation provides more detailed results, but simulations require a considerable amount of data for calibration and validation. The other possible method for obtaining stop-and-go speed profiles is the use of an analytical approach for signalized intersections. Analytical approaches are simple, and they require smaller amounts of data than traffic simulation. They are usually used for design and/or phasing of signalized intersections (ITE, 2008).

Use of macroscopic emission models are preferred by researchers due to simplicity of these models and lower data requirements. However, there exist deficiencies of these models in evaluating the effects of stop-and-go on vehicular emissions (Ahn & Rakha,

2008). This is because they cannot capture induced acceleration emissions due to their assumption constant average speed. At the same average speed, emissions of an accelerating vehicle can be much higher compared to a cruising vehicle. For instance, a vehicle with a speed of 40 km/h and an acceleration of 2 m/s^2, emits five times the NOx compared to a cruising vehicle at 40 km/h over the same distance traveled (Panis et al., 2006). Ahn & Rakha (2008) used macroscopic and microscopic emission models to evaluate effects of route choice decisions on vehicular missions and concluded that MOBILE6 is not an appropriate tool "in evaluating the environmental impacts of traffic operational projects".

On the other hand, use of the microscopic emission model is not feasible for estimation of annual mean concentrations, as it requires stop-and-go profiles for finer temporal resolutions, i.e. by day of week, hour of day, and by season. The deficiency of Mobile6.2 in the estimation of emissions near signalized intersections can be overcome by the development of correction factors. This correction factors can be applied to areas near signalized intersections, where vehicles tend to stop and go. This includes the areas behind the stop line of signalized intersections where vehicles decelerate, idle, and accelerate, and the areas after the stop line of signalized intersections where vehicles are likely to accelerate.

2.5.3 Air pollutant concentration

Several studies investigated the sensitivity of AERMOD to input parameters such as meteorological parameters and terrain options (Zou and Zeng., 2010) and site characteristics (Long et al., 2004; Grosch and Lee, 1999). Zou and Zeng (2010) found

that estimated concentrations by AERMOD are insensitive to the choice of urban or rural dispersion coefficients and terrain options. Long et al. (2004) found that among the site characteristics, AERMOD is the most sensitive to surface roughness. Similarly, Grosch and Lee (1999) found that "changes in albedo, Bowen ratio, and surface roughness length can result in changes in design concentrations of factors of 1.5, 2.6, and 160, respectively." A major limitation with the current literature is that no studies investigated the effect of temporal variability of emissions on the estimated concentrations.

Since traffic counts significantly vary by hour of day, day of week, and season, vehicular emissions also vary temporally. In addition, some meteorological parameters such as wind speed, temperature, and atmospheric mixing heights vary temporally. Thus, it is worthwhile to investigate how the estimated concentrations by a dispersion model will be different if a constant emission rate through the year (e.g. use of AADT) is used or the hour-of-day variation in emission is considered.

In order to estimate ambient air concentration of traffic pollutants, usually a series of tools including a vehicle emission factor model and an atmospheric dispersion model are used. In this regard, the US EPA recommended the use of Mobile6.2 and AERMOD for estimation of vehicle emission factor (EPA, 2003) and ambient air concentration of pollutants (EPA, 2004a), respectively. Although many studies estimated effects of input parameters on emissions using Mobile6.2 and on concentrations using AERMOD, few studies considered the combined effects of the two models.

CHAPTER III

3. METHODOLOGY

3.1 Integrated traffic and air quality modeling

Figure 3.1 shows the framework of integrated modeling of traffic, vehicular emissions, and air pollutant concentrations. Air pollutant concentrations were calculated in the following steps. First, vehicle counts at each road section between two successive signalized intersections were estimated for the target year. Second, NOx and benzene emissions for each road section were calculated using emission factors of cars and trucks from Mobile 6.2. Third, air pollutant concentrations in the study area were calculated using the AERMOD dispersion model. Hour of day and falloff patterns of simulated concentrations were compared to observed patterns. The proposed models were applied to the estimation of NO_2 and benzene concentrations on Huron Church Road. The data used for modeling are described in the following sections.

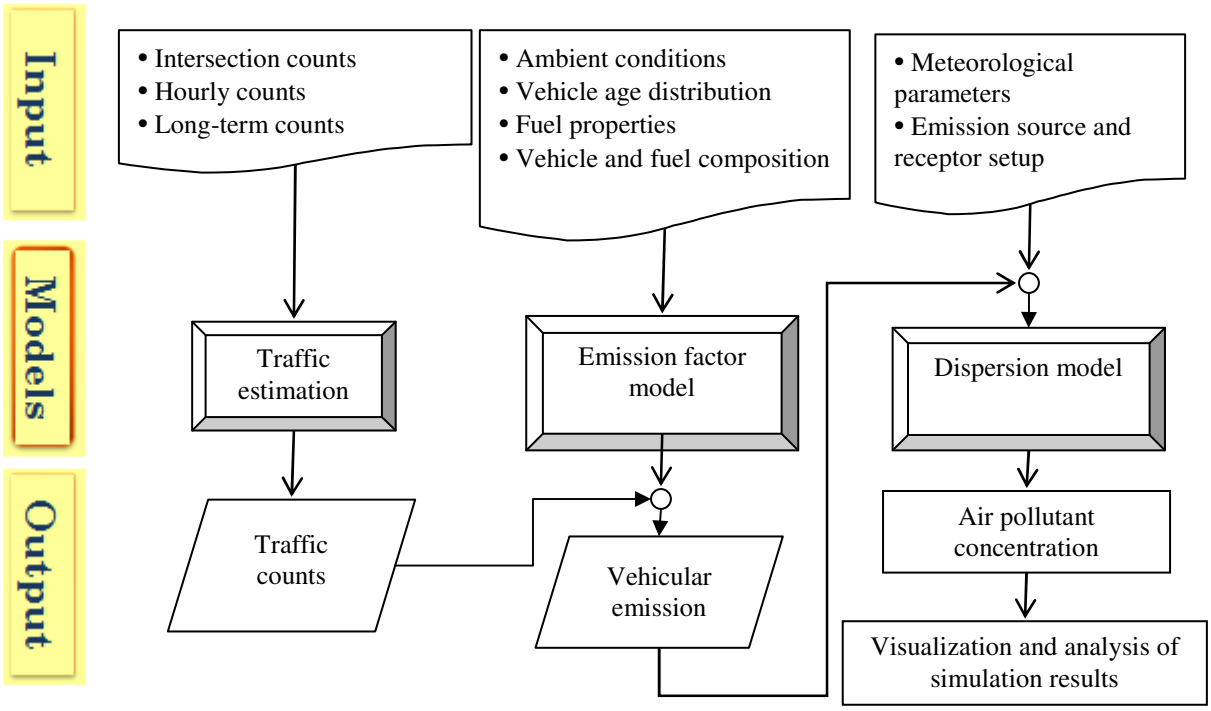

Figure 3.1: Illustration of multi-model approach of traffic, vehicular emissions, and air pollutant concentrations

3.2 Vehicle count data

Border crossing traffic in the City of Windsor contributes to traffic delay and vehicular emissions. Most Canada-to-U.S. heavy duty trucks enter the Ambassador Bridge via Highway 401 then Talbot Road and Huron Church Road as shown in Figure 3.2. Talbot Road is 3.6 km-long with 4-lanes whereas the Huron Church Road is 5.8 km-long with 6-lanes. There are seventeen signalized intersections along the corridor. This 9-km section of road was referred to as Huron Church Road hereafter.

Vehicle counts are needed for estimation of vehicular emissions, and subsequently air pollutant concentrations. However, vehicle counts are sporadically collected in this road. Therefore, it is required to adjust sporadic vehicle counts to a specific period of time

considering their temporal variation. In this study, peak-hour vehicle counts at each road section on Huron Church Road were estimated using sporadically-collected vehicle counts and adjustment factors from long-term traffic data. Then hourly counts at each section were estimated by obtaining temporal profiles of vehicle counts at permanent counts stations.

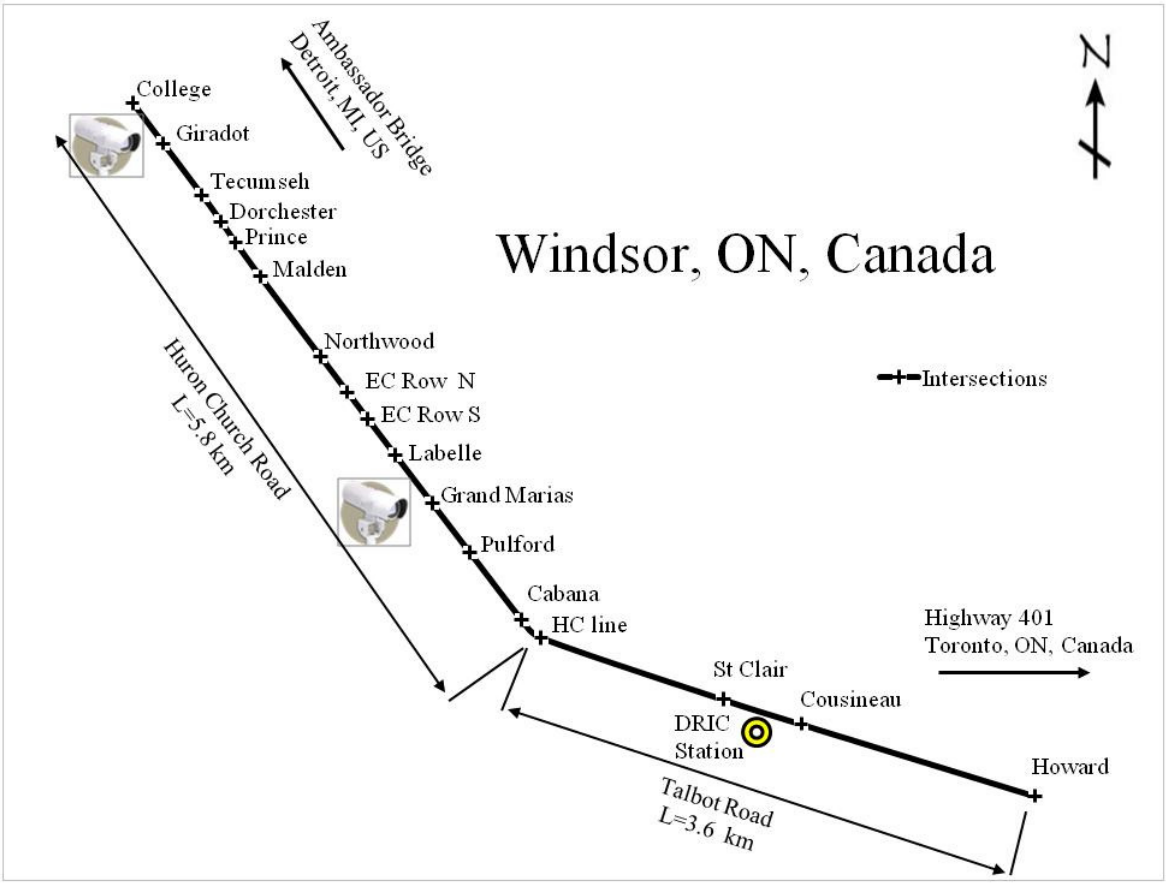

Figure 3.2: A sketch of the Talbot and Huron Church Roads, and the location of traffic count stations

Table 3.1 lists datasets used for estimating vehicle counts on the road. The locations for vehicle count collection are shown in Figure 3.2. Three types of vehicle counts were used in this study. The first type of count was used for estimation of vehicle counts at each

road section, i.e. the City of Windsor intersection counts and DRIC mid-block counts (datasets 1 and 3 in Table 3.1). A road section was designated as the segment between two successive signalized intersections. The second type of count was used for estimating hourly vehicle counts, i.e. the City of Windsor and DRIC hourly counts (datasets 2 and 4 in Table 3.1). The third type of count was used for observing long-term trends in vehicle counts and calculating adjustment factors, i.e. the U.S. entry counts and Bridge counts (datasets 5 and 6 in Table 3.1). Each data set is explained in detail in the following subsections.

Table 3.1: Traffic data used in this study

Dataset	Source	Time	Location (Figure 3.2)	Temporal resolution	Counts
1. City of Windsor intersection counts	City of Windsor	Weekdays in 2004-2008	12 intersections from College to Pulford	AM and PM peak hours	Car and truck counts in each approach
2. City of Windsor hourly counts	City of Windsor	197 days in 2008, 8-28 days in each month	College-Giradot and Labelle-Grand M. road sections	Hourly	Vehicle counts in each lane by vehicle length
3. DRIC mid-block counts	DRIC(2008a)	Feb 2006	16 road sections between College and Howard intersections	AM peak in northbound and PM peak in southbound	Total traffic volume and truck percentage
4. DRIC hourly counts	DRIC(2008b)	Oct 2006-Sep 2007	St. Clair-Cousineau road section	Hourly	Car, short truck, and long truck counts
5. US entry counts	BTS (2009)	2004-2008	Windsor-Detroit port, Canada to US	Monthly and annual	Car and truck counts
6. Bridge counts	Transport Canada (2010)	2008	Ambassador Bridge	Annual	Car and truck counts

3.2.1 City of Windsor intersection counts

The first data set is vehicle counts at the 12 signalized intersections on the road section between College Avenue and Pulford Street as shown in Figure 3.2. These counts were provided by the City of Windsor and hereafter called "City of Windsor intersection counts". These counts were collected on different weekdays in 2004-2008. They include the number of cars and trucks in different approaches (through, left turn and right turn) in both directions (northbound and southbound) at the signalized intersections during morning peak (one busiest hour between 8-10 am) and afternoon peak periods (one busiest hour between 4-6 pm).

3.2.2 City of Windsor hourly counts

The second dataset is bidirectional hourly lane-by-lane vehicle counts in 2008 collected from two traffic count stations at the College-Giradot and Labelle-Grand Marais road sections (Figure 3.2). These counts were provided by the City of Windsor and hereafter called "City of Windsor hourly counts". In these counts, vehicles were classified into three classes according to their length as listed in Table 3.2.

Table 3.2: Vehicle classification by length at two traffic count stations

Class	Length (m)	Hourly average counts (veh/h) [a]	Share of each class from total counts	Vehicle type
A	Less than 7.62	568	77%	Cars
B	Between 7.62 and 10.97	60	8%	Trucks
C and D	Between 10.97 and 48.88	107	15%	
Total	All	735	100%	-

[a] Annual hourly average of two stations and two directions

Since the observed counts in City of Windsor intersections and DRIC mid-blocks were classified by two categories of vehicles - car and truck - the above vehicle classes were categorized into car and truck. Considering average length of cars and trucks, Class A was assumed be cars and Classes B-D were assumed to be trucks.

3.2.3 DRIC mid-block counts

The third data set was total mid-block vehicle counts and the truck percentage in February 2006 for 16 road sections between College and Howard intersections (Figure 3.2). These counts were made during the AM peak hour in the northbound direction and during the PM peak in the southbound direction (DRIC, 2008a). Car and truck counts were calculated using traffic volume and truck percentage at each road section.

3.2.4 DRIC hourly counts

The fourth data set was unidirectional hourly counts of cars, short trucks, and long trucks during October 2006-September 2007. These counts were collected at the St. Clair-Cousineau road section (Figure 3.2) and obtained from a DRIC (2008b) report. For comparing these counts with the City of Windsor hourly counts, short truck and long truck counts were combined into one category, i.e. truck.

3.2.5 Windsor-Detroit US entry counts

The fifth data set was annual and monthly number of cross-border cars and trucks from Canada to the US via Windsor-Detroit port during 2004-2008. These counts were obtained from the US Bureau of Transportation Statistics (BTS, 2009). The Windsor-

Detroit port includes the Ambassador Bridge (Figure 3.2) and the Windsor-Detroit Tunnel.

3.2.6 Ambassador Bridge counts

The sixth dataset was arecord of the annual two-way cross-border counts of cars and trucks at the Ambassador Bridge from Transport Canada (2010).

3.3 Estimation of vehicle counts for spatial variations

Because the vehicle counts at the City of Windsor intersections (dataset 1 in Table 3.1) were obtained at different times, the vehicle counts were adjusted to a specific period of time. Intersection counts were adjusted to the equivalent vehicle counts in 2008. This is because the year 2008 was the most recent year, and City of Windsor hourly counts (data set 2 in Table 3.1) were also collected in 2008.

3.3.1 Adjusting City of Windsor intersection counts

The vehicle counts at each intersection obtained at different times were adjusted to the vehicle counts in a base year on the basis of the observed temporal variations in the long-term data – i.e. the 2004-2008 annual and monthly counts at the Bridge and the 2008 hourly counts at the two traffic count stations. Given that the hourly counts were available in 2008, the year 2008 was selected as the base year.

Adjustment factors for month and year were used to account for monthly and annual variations in car and truck counts. The annual factor (F_{yr}) for each year, applied to all road sections) reflects the difference between counts in a given year, N_{yr}, and the counts in the base year, N_{baseyr}. The monthly factor (F_{mon}) for each month, applied to all road

sections) reflects the difference between the counts in a given month, N_{mon}, and the average monthly counts, N_{avgmon}, as shown in Equations 3.1 and 3.2.

$$F_{mon} = \frac{N_{avgmon}}{N_{mon}} \tag{3.1}$$

$$F_{yr} = \frac{N_{baseyr}}{N_{yr}} \tag{3.2}$$

The adjusted counts at a specific road section in the base year, N_{adj}, were calculated using the observed counts at a specific road section in given month and year, N_{obs}, as in Equations 3.3:

$$N_{adj} = N_{obs} \times F_{mon} \times F_{yr} \tag{3.3}$$

These adjustment factors were estimated for cars and trucks separately.

For truck counts, a majority of trucks travel Huron Church Road to cross the Bridge (northbound) or head to Highway 401 (a major truck route to central and southwestern Ontario) from the Bridge (southbound). Thus, it is expected that temporal variations in truck counts are similar at Huron Church Rd. and the Bridge. Consequently, truck adjustment factors (Equations 3.1 and 3.2) were derived using annual and monthly cross-border truck counts during 2004-2008 reported by the BTS (2009) (data set 5 in Table 3.1).

Unlike trucks, a substantial portion of cars travel Huron Church Road for local trips within the City, rather than crossing the border. Based on 2008 car counts at the Bridge (data set 6 in Table 3.1) and 2008 total car counts at the two traffic count stations (data set 2 in Table 3.1), the proportions of local and cross-border car traffic were estimated to

be 60% and 40%, respectively, in both directions. Considering a difference in temporal variation between local and cross-border car traffic, they were estimated separately.

The annual adjustment factors (Equation 3.2) for local car counts were derived using the populations in the base year and a given year due to unavailability of the long-term local car counts. The annual local car counts are assumed to be proportional to the annual population in the City as the number of travelers generally increases with population. However, the annual adjustment factors were set to one for local car counts, because the population has been almost constant from 2003 to 2007 in the City of Windsor (Artaman, A. Personal communication, 2009). It should be noted that according to the Statistics Canada Census (2012), population of Windsor increased by 3.5% during 2001-2006 and decreased by 2.6 during 2006-2011. For cross-border car counts, the annual adjustment factors (Equation 3.2) were derived using 2004-2008 annual car counts at the Bridge reported by BTS (2009) (data set 5 in Table 3.1). The monthly adjustment factors (Equation 3.1) for both local and cross-border car traffic were calculated using the average of monthly car counts at the two traffic stations (data set 2 in Table 3.1). The adjusted local and cross-border car counts, $N_{adj,localcar}$ and $N_{adj,bordercar}$, were calculated using Equation 3.3 with the observed car counts and local or cross-border adjustment factors. The adjusted total car counts in the base year ($N_{adj,car}$) were calculated using Equation 3.4:

$$N_{adj,car} = p_{local} \times N_{adj,localcar} + (1 - p_{local}) \times N_{adj,bordercar} \quad (3.4)$$

where p_{local} is the fraction of local car traffic.

After car and truck counts at each intersection were adjusted to the equivalent counts in 2008, the counts in each road section were calculated as an average of the arrival counts to the downstream intersection and the departure counts from the upstream intersection of the section.

The adjustment factors were not all close to 1. This indicates that the adjustment of car and truck counts is necessary to account for their annual and monthly variations. The southbound car and truck counts were also estimated using the same adjustment factors as the northbound vehicle counts.

3.3.2. Adjusting DRIC mid-block counts

DRIC mid-block counts were adjusted by month and year from February 2006 to the year 2008 using the same method as the method used for adjusting City of Windsor intersection counts.

3.4 Spatial and temporal distribution of vehicle counts

3.4.1 Spatial distribution

To estimate vehicle counts at each road section on Huron Church Road, both 2008 equivalent City of Windsor and DRIC mid-block counts were used. The strength of City of Windsor mid-block counts compared to DRIC counts was the availability of bidirectional vehicle counts during both AM and PM peak hours. However in comparison with DRIC counts, the City of Windsor counts were not available for five road sections between Pulford and Howard intersections.

For the use in this study, the spatial patterns of adjusted City of Windsor and DRIC mid-block counts are compared in Figure 3.3 and Figure 3.4. Car counts estimated by both data sets have similar patterns (Figure 3.3(a) and Figure 3.4(a)). For instance, in the northbound road during the AM peak hours, cars counts in both data sets decreased towards the Ambassador Bridge north of the EC Row. Truck counts also had similar patterns (Figure 3.3(b) and Figure 3.4(b)). Car counts were consistently lower in City of Windsor than DRIC, but truck counts were opposite. The difference between vehicle counts between the two datasets could be because of difference in collection times. The City of Windsor counts were collected in different weekdays during 2004-2008 whereas the DRIC counts were collected in weekdays of February 2006. The DRIC counts were collected simultaneously, but they were only for one month of a year. On the other hand, the City of Windsor counts were collected during different months of 2004-2006, but they were sparsely collected, i.e. one intersection at a time.

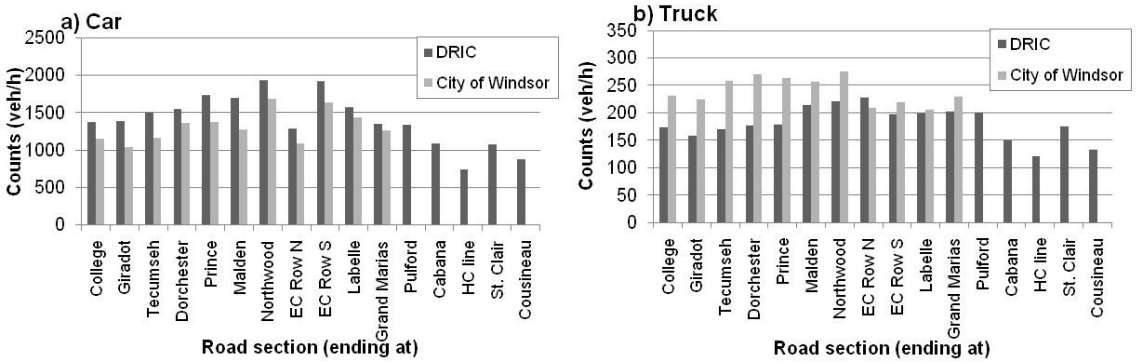

Figure 3.3: Comparisons between DRIC and City of Windsor counts - AM peak in northbound

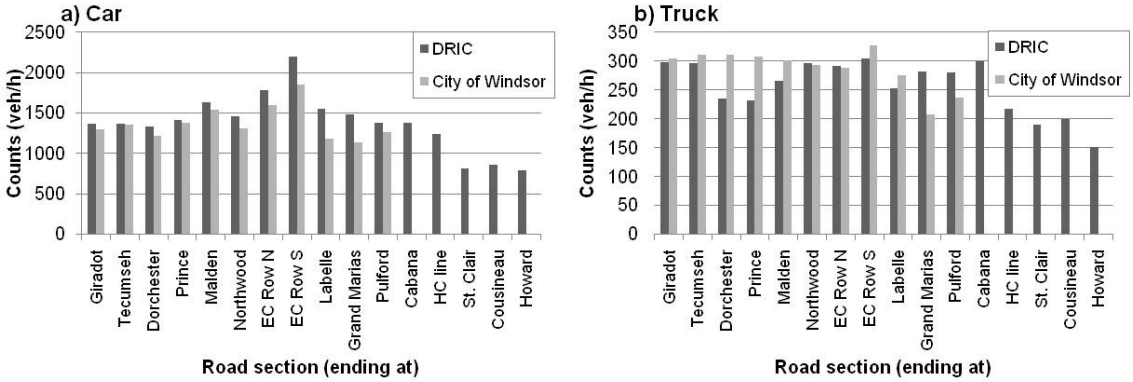

Figure 3.4: Comparisons between DRIC and City of Windsor counts - PM peak in southbound

The City of Windsor mid-block counts during AM and PM peak hours were used for 11 road sections between the College and Pulford intersections. For five remaining road sections – between Howard and Pulford intersections (Figure 3.2) – the DRIC mid block counts were used for estimation of car counts. However, as shown in Figure 3.3(b) and Figure 3.4(b), truck counts in the DRIC mid-block data set over these five road sections change considerably from one road section to the next one. For instance, truck counts in the southbound road during the PM peak (Figure 3.4(b)) decreased from 300veh/h on the Pulford – Cabana section to 215 veh/h on the Cabana - HC Line section. However, the majority of trucks continuously travel along the entire road sections without diverging to the cross streets to cross the border. This is may be the reason that the City of Windsor data were more constant. Therefore, it was assumed that the truck counts on the Howard-Cabana road section are the same as the truck counts on the Pulford-Grand Marais road section.

3.4.2 Temporal distribution

Hourly vehicle counts were collected by the City of Windsor at the College – Giradot and Labelle – Grand Marias road sections, and from DRIC (2008b) at the St. Clair –

Cousineau road section (datasets 2 and 4 in Table 3.1). Hour-of-day patterns of vehicle counts at these three road sections were compared in Figure 3.5. It should be noted that the City of Windsor counts were collected in the year 2008 and DRIC counts in Oct 2006 - Sep 2007. It was observed that hour-of-day car and truck counts at the St. Clair – Cousineau road section were similar to those at the College – Giradot and Labelle – Grand Marias road sections. Lower car counts were observed at the St. Clair – Cousineau road section compared to the other two road sections.

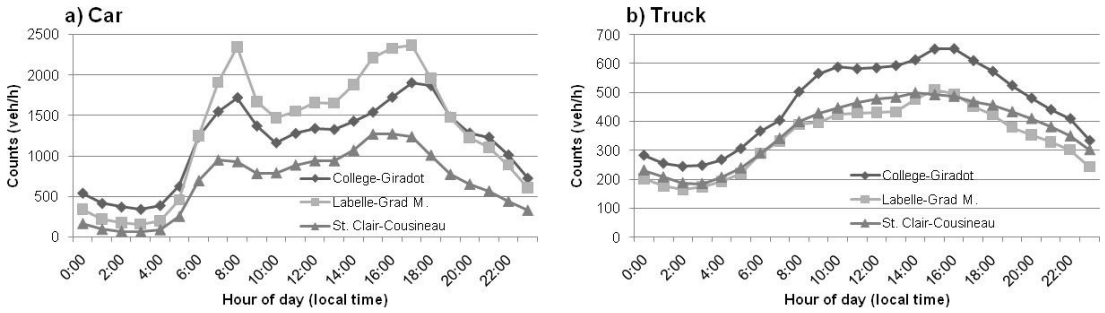

Figure 3.5: Hour of day car and truck counts at three road sections

Since the year 2008 was selected for the estimation of vehicle counts, the City of Windsor hourly counts collected in 2008 were used for observing temporal patterns of vehicle counts. From car and truck counts at the College – Giradot and Labelle – Grand Marias road sections, hour-of-day, day-of-week and seasonal patterns of car and truck counts were observed for each road section and each direction of travel. Each month was classified into four seasons as follows: winter (December, January and February), spring (March – May), summer (June – August) and fall (September – November). An average of the counts at the two road sections was used for estimation of vehicular emissions.

3.5 Estimation of NOx and benzene emission factors

NOx and benzene emission factors (g/veh/km) of car and truck were estimated using Mobile6.2. Traffic emission at each road section is a product of vehicle counts, emission factors of vehicles, and the length of the road.

The observed vehicle counts were available for passenger cars and heavy duty trucks whereas there were 28 classes of vehicles in Mobile6.2. Therefore, car and truck categories in vehicle counts were mapped to vehicle classes in Mobile6.2. However, default vehicle and fuel breakdowns in Mobile6.2 were not specific to the study area and not suitable for calculating composite emission factors of cars and trucks. Thus, local, provincial and national data were utilized to map car and truck categories in vehicle counts into appropriate classes of Mobile6.2. In this regard, emission factors of all classes in Mobile6.2 were estimated first and composite emission factors of cars and trucks were calculated by mapping vehicle classes in Mobile6.2 to car and truck categories.

3.5.1 Mobile6.2 setup parameters

Setup parameters for simulation by Mobile6.2 were determined, and emission factors of all classes in Mobile6.2 were estimated. Table 3.3 lists Mobile6.2 setup parameters. In order to estimate emission factors by hour of day and by season, 96 runs (24 hours × 4 seasons) of Mobile6.2 were executed. Since gasoline vehicles on Huron Church Road used either Michigan or Ontario gasoline, a total of 192 runs (= 96 runs × 2 types of gasoline) were executed.

Table 3.3: Mobile6.2 setup parameters

Parameter	Description
Calendar year	2008
Pollutant	NOx and benzene
Runs	24 hours × 4 seasons × 2 (Michigan and Ontario) = 192 runs
Gasoline Properties	For Michigan and Ontario from DRIC (2008c); refer to Table 3.4
Temperature	Hour of day by season at Windsor Airport (Environment Canada, 2012a); Figure 3.6
Vehicles age distributions	Ontario vehicle registrations in 2008 by year model for three weight classes; obtained from Statistics Canada (2008), refer to Figure 3.7
Average speed and facility type	50 km/h, Arterial road
Emission type	NOx: running and cold-start exhaust emissions Benzene: running and cold-start exhaust emissions, and evaporative running losses
Vehicle activities	Default values of Mobile6.2
Output format	Database format: emission factors of NOx and benzene for all vehicle classes (g/mile)

Input parameters for Mobile6.2 are gasoline properties, ambient temperature, and vehicle age distributions. Ontario and Michigan gasoline properties in the year 2003 were obtained from a DRIC report (2008c) (Table 3.4). Hourly ambient temperatures at the Windsor Airport weather station in 2008 were obtained from Environment Canada (2012a), and then hour-of-day temperature by season was calculated (Figure 3.6).

Table 3.4: Average gasoline properties in Michigan and Ontario, collected in 2003 (DRIC, 2008c)

	Season	RVP [a]	E200 [b]	E300 [c]	Aromatics	Olefins	Benzene	Ethanol	Ethanol Market share
		PSI [d]	vol%	vol%	vol%	vol%	vol%	vol%	%
Michigan	Winter	14.4	53.8	82.7	26.8	6.9	1.7	9.75	25
	Spring	11	47.7	81.2	29.4	8.5	1.6	9.75	25
	Summer	7.6	41.6	79.6	32	10	1.5	9.75	25
	Fall	11	47.7	81.2	29.4	8.5	1.6	9.75	25
Ontario	Winter	14.6	53.9	84.4	25.1	9	0.73	1.92	100
	Spring	12.1	50.9	83.4	26.9	9.3	0.73	1.92	100
	Summer	9.7	47.9	82.4	28.8	9.7	0.73	1.92	100
	Fall	12.1	50.9	83.4	26.9	9.3	0.73	1.92	100

[a] Reid Vapor Pressure

[b] Percentage of gasoline that evaporates at 200 degrees Fahrenheit under 1atm

[c] Percentage of gasoline that evaporates at 300 degrees Fahrenheit under 1atm

[d] Pounds per square inches

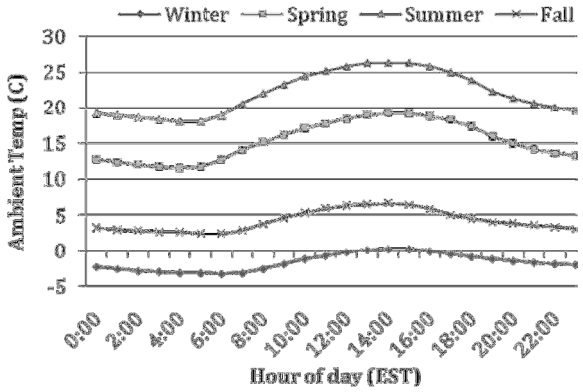

Figure 3.6: Hourly-of-day temperature by season at Windsor Airport in 2008 (Source: Environment Canada, 2012a)

Ontario vehicle registrations in 2008 by model year (1989-2008) for three weight classes were obtained from Statistics Canada (2008). The classes were vehicles up to 4.5 tonnes, trucks 4.5 tonnes to 14.9 tonnes, and trucks 15 tonnes or more. It should be noted

that the number of vehicles with model year earlier than 1989 was included in the number of vehicles with model year 1989. Vehicle registrations by model year were used to calculate vehicle age distributions. In this regard, number of vehicles at each model year was divided by total vehicle registered in 2008. As shown in Figure 3.7, vehicle age distributions were calculated for each of three weight classes. The total number of vehicles registered in Ontario in 2008 was 7,132,435, 101,517, and 115,771 for vehicles up to 4.5 tonnes, trucks 4.5 tonnes to 14.9 tonnes, and trucks 15 tonnes or more, respectively. Since vehicle registration records for Michigan were not available, it was assumed that vehicle models are similar in Ontario and Michigan.

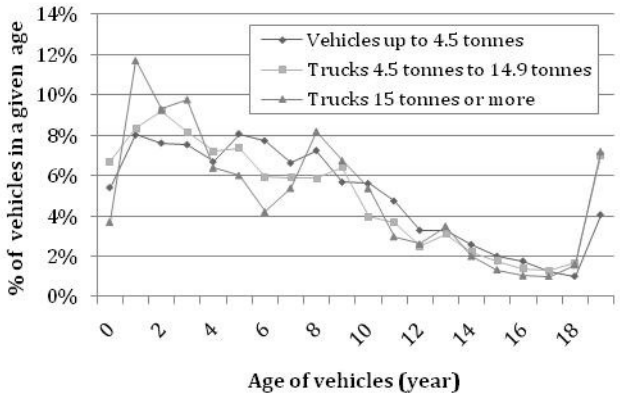

Figure 3.7: Age distribution of Ontario vehicles (Source: Statistics Canada, 2008)

Although the speed limit as posted on the road is 60km/h, it is expected that the average speed is lower than the speed limit due to stop-and-go driving condition. Therefore, average speed and facility type in Mobile6.2 were assumed to be 50km/h and arterial road, respectively.

In the estimation of NOx emission by Mobile6.2, only running and cold-start exhaust emissions were considered. However, in estimation of benzene emissions, evaporative running emissions, those emitted while vehicle is driven along, was considered in addition to exhaust emissions. Default values of Mobile6.2 were used for the distribution of vehicle activities, e.g. hour-of-day distribution of vehicle cold start. Database option was selected for the output format. NOx and benzene emission factors of all 28 vehicle classes in Mobile6.2 were estimated.

3.5.2 Fuel properties

Fuel properties and benzene emission factors

In comparison with NOx emission factors, benzene emission factors are more affected by fuel properties in Mobile6.2 (EPA, 2003). Aromatic and benzene contents of fuel mainly contribute to benzene exhaust emission from vehicles. Part of the benzene content of the fuel, which is not combusted in the engine, is emitted. Combustion of aromatic compounds in an engine may also result in benzene formation (Environment Canada, 2003).

Average volume percentages of aromatic and benzene contents of gasoline in Ontario were 21.5% and 0.7% in 2006, respectively (Environment Canada, 2008). Equation 3.5 shows a typical function used by Mobile6.2 (Cook and Glover, 2002) to calculate the ratio of benzene to Total Organic Gas (TOG) emission for Light Duty Gasoline Vehicle (LDGV) as a function of aromatic and benzene content of fuel.

Benzene/TOG emission = (0.8551* (BNZ) +0.12198 * (ARM) -1.1626)/100 (3.5)

where:

BNZ and ARM = benzene and aromatic contents of gasoline (vol %), respectively.

Equation 3.5 shows that as benzene and aromatic contents of gasoline fuel increase, benzene exhaust emission from LDGV also increases. However, the impact of benzene content is seven times higher than that of aromatic content.

In contrast to gasoline fuel, the benzene content of diesel fuel is negligible. Therefore, benzene emission from diesel vehicles is mainly from aromatic compound combustion. For example, average aromatic content of diesel fuel in Ontario is 30% (Environment Canada, 2003). In particular, average Poly Aromatic Hydrocarbons (PAH) including mono, di, and poly are about 7% of diesel fuel in Ontario (Environment Canada, 2003). Default values of fuel properties in Mobile6.2 were used in the calculation of diesel vehicles emission factor. In conclusion, benzene emission in gasoline vehicles is mainly from the unburned benzene content of gasoline whereas benzene emission in diesel vehicles is mainly formed by secondary chemical reactions of aromatic compounds.

Ontario and Michigan Gasoline properties

In comparison with Michigan gasoline, Ontario gasoline is much cleaner, e.g. benzene content of Ontario gasoline is a half of that of Michigan gasoline (Table 3.4). After endorsement of gasoline regulations in Canada in 1999, the average volume percentage of benzene content of gasoline in Canada decreased significantly from 1.4% in 1998 to 0.8% in 2000 (Environment Canada, 2008). Among two types of gasoline sold in the US,

conventional and Reformulated Gasoline (RFG), only conventional gasoline is sold in Michigan. RFG is a cleaner type of gasoline than conventional gasoline since it has lower average benzene content (0.6%). The average benzene content of conventional gasoline is approximately 1.2%. RFG comprised approximately 25% of the gasoline sold in the U.S. in 2000-2005 (EPA, 2008). It is mainly distributed in major cities such as Los Angeles, New York, Chicago, Washington, and Boston.

Selection of fuel properties

There were two data sets for gasoline properties. The first data set is shown in Table 3.4. The table shows properties of gasoline sold in Michigan and Ontario for four seasons in 2003 (DRIC, 2008c). The second data set is shown in Table 3.5. The table shows projected properties of gasoline sold in Michigan and Ontario in 2007 (EPA, 1999a) and 2006 (Environment Canada, 2008), respectively, for two seasons (summer and winter). The first data set was used since it had gasoline properties for all four seasons.

Table 3.5: Average gasoline properties in Ontario and Michigan.

	Time	RVP	E200	E300	Aromatics	Olefins	Benzene	Ethanol	MTBE [a]
		PSI	Vol%	vol%	Vol%	vol%	vol%	vol%	vol%
Michigan [b]	Summer	8.5	49	80.9	28.4	9.1	1.32	2.9	0.6
	Winter	14	57.6	83.1	25.3	8.4	1.46	2.3	0
Ontario [c]	Year	11.7	51.6	85.1	21.5	6.8	0.7	2.02	0

[a] Methyl Tertiary Butyl Ether

[b] Source: EPA (1999a) ; projected for 2007 from the base year of 1999

[c] Source: Environment Canada (2008); collected in 2006

3.5.3 Vehicle age distribution

Vehicle age distributions in Mobile6.2 were determined using vehicle age distribution of three categories of vehicles in Figure 3.7. Table 3.6 shows vehicle classes in Mobile6.2 classified by vehicle weight and age. The vehicle age distribution in Mobile6.2 can be specified for up to 12 categories. By default, there are five vehicle age distribution categories in Mobile6.2. In this study using the Ontario vehicle registration data from Statistics Canada (2008), three categories of vehicle age distribution were defined (Figure 3.7). These three categories were mapped to 12 registration classes in Mobile6.2 by taking into consideration the weight range in each vehicle class.

Table 3.6: Alignment of vehicle age distribution categories in Mobile6.2 and this study

Vehicle classes in Mobile6.2	Gross Vehicle Weight [a] (lb)	Age distribution categories -Default of Mobile6.2	Age distribution categories (Figure 3.7)
Light duty vehicle	All	1	vehicles up to 4.5 tonnes
Light duty truck 1	up to 6,000 & load≤ 3,750	2	
Light duty truck 2	up to 6,000 & load>3,750		
Light duty truck 3	6,001-8,500 & load≤5,750	3	
Light duty truck 4	6,001-8,500 & load>5,750		
Heavy Duty Vehicle 2B	8,501-10,000	4	trucks 4.5 tonnes to 14.9 tonnes
Heavy Duty Vehicle 3	10,001-14,000		
Heavy Duty Vehicle 4	14,001-16,000	5	
Heavy Duty Vehicle 5	16,001-19,500		
Heavy Duty Vehicle 6	19,501-26,000		
Heavy Duty Vehicle 7	26,001-33,000		
Heavy Duty Vehicle 8A	33,001-60,000		trucks 15 tonnes or more
Heavy Duty Vehicle 8B	>60,000		

3.5.4 Estimation of composite emission factors

Car and truck categories in vehicle counts were mapped to vehicle classes in Mobile6.2 using local, provincial and national data. Table 3.7 lists vehicle classifications in Mobile6.2 manual (Cook and Glover, 2002). In total, there are 28 classes of vehicles classified by vehicle types (e.g. light duty, heavy duty, bus, and motorcycle), fuel type (e.g. gasoline, diesel) and vehicle weight (8,501-10,000 lb).

Table 3.7: Vehicle classification in Mobile6.2 (Cook and Glover, 2002)

Gasoline vehicle categories			Diesel vehicles categories			GVW in lb
Class#	Name	Symbol	Class#	Name	Symbol	
1	Light duty gasoline vehicle	LDGV	14	Light duty diesel vehicle	LDDV	All
2	Light duty gasoline truck 1	LDGT1	15	Light duty diesel truck 1	LDDT1	up to 6,000 & load≤ 3,750
3	Light duty gasoline truck 2	LDGT2		Light duty diesel truck 2	LDDT2	up to 6,000 & load>3,750
4	Light duty gasoline truck 3	LDGT3	28	Light duty diesel truck 3	LDDT3	6,001-8,500 & load≤5,750
5	Light duty gasoline truck 4	LDGT4		Light duty diesel truck 4	LDDT4	6,001-8,500 & load>5,750
6	Heavy duty gasoline vehicle class 2B	HDGV2B	16	Heavy duty diesel vehicle class 2B	HDDV2B	8,501-10,000
7	Heavy duty gasoline vehicle class 3	HDGV3	17	Heavy duty diesel vehicle class 3	HDDV3	10,001-14,000
8	Heavy duty gasoline vehicle class 4	HDGV4	18	Heavy duty diesel vehicle class 4	HDDV4	14,001-16,000
9	Heavy duty gasoline vehicle class 5	HDGV5	19	Heavy duty diesel vehicle class 5	HDDV5	16,001-19,500
10	Heavy duty gasoline vehicle class 6	HDGV6	20	Heavy duty diesel vehicle class 6	HDDV6	19,501-26,000
11	Heavy duty gasoline vehicle class 7	HDGV7	21	Heavy duty diesel vehicle class 7	HDDV7	26,001-33,000
12	Heavy duty gasoline vehicle class 8A	HDGV8A	22	Heavy duty diesel vehicle class 8A	HDDV8A	33,001-60,000
13	Heavy duty gasoline vehicle class 8B	HDGV8B	23	Heavy duty diesel vehicle class 8B	HDDV8B	>60,000
25	Heavy duty gasoline Bus	-	26	Heavy duty diesel Transit Bus	-	All
24	Motorcycle	-	27	Heavy duty diesel School Bus	-	All

Four sets of data were used for mapping car and truck categories with the vehicle classes in Mobile6.2. They are 1) the composition of short and long trucks on the local road in Windsor from DRIC (2008b) counts in 2006-2007; 2) Ontario Light Duty Passenger Vehicles (LDPV) breakdowns in 2006 from Transport Canada (2006); 3) fuel breakdowns of vehicles from Transport Canada (2006) and 4) default values for share of

vehicles in Mobile6.2. These were used for further breakdowns (Table 3.8 and Table 3.9).

Table 3.8 maps the car category in vehicle counts to the vehicle classes in Mobile6.2. It was assumed that the car category was 100% LDPV. The Ontario LDPV breakdown was 70% Light Duty Passenger Cars and 30% Light Duty Passenger Trucks (Transport Canada, 2006). The fuel breakdown for LDPV was 98.5% gasoline and 1.5% diesel in Canada (Transport Canada, 2006).

The default proportions of LDGT1 and LDGT2 in Mobile6.2 were 23% and 77%, respectively. A majority of car categories (92%) were mapped to two classes in Mobile6.2: LDGV (69%) and LDGT2 (23%).

Table 3.8: Mapping car category in vehicle counts with vehicle classes in Mobile6.2

Car breakdown	GVW in lb	Ontario LDPV breakdown [a]	National fuel breakdown [a]	Default breakdown in Mobile6.2 [b]	class # in Mobile6.2 [c]	Final share
LDPV: 100 %	up to 6,000	Light Duty Passenger Car: 70%	Gasoline: 98.5%	LDGV: 100%	1	68.95%
			Diesel: 1.5%	LDDV: 100%	14	1.05%
		Light Duty Passenger Truck: 30%	Gasoline: 98.5%	LDGT1: 23%	2	6.80%
				LDGT2: 77%	3	22.75%
			Diesel: 1.5%	LDDT1&2 100%	15	0.45%

[a] Source: Transport Canada (2006)
[b] Source: EPA (2003) ; refer to Table 3.7 for description of each class
[c] Refer to Table 3.7 for description of each class

Table 3.9 maps truck category in vehicle counts with vehicle classes in Mobile6.2. Using annual hourly average vehicle counts at the St. Clair Station in 2006-2007 by DRIC (2008b), the proportions of short and long trucks in total truck counts were

calculated as 10% and 90%, respectively. Short trucks were assumed to be single trucks or box trucks with gross weight in the range of 8,001 - 33,000 lb (Transport Canada, 2006). Long trucks were assumed to be truck trailer with a gross weight more than 33000 lb (Transport Canada, 2006). Fuel breakdown for short and long trucks in Canada were obtained from Transport Canada (2006). Default values for share of vehicles in Mobile6.2 were used for further breakdowns of trucks as listed in Table 3.9. A majority of trucks (88%) were mapped to two classes in Mobile6.2: HDDV8A (22%) and HDDV8B (78%).

Table 3.9: Mapping truck category in vehicle counts with vehicle classes in Mobile6.2

Truck breakdown on the road [a]	GVW in lb	National fuel breakdown [b]	Default breakdown in Mobile6.2 [c]		Class # in Mobile6.2 [d]	Final share
Short trucks: 10%	8,001-33,000	Gasoline: 34%	HDGV2B: 83%	100%	6	2.82%
			HDGV3: 3%		7	0.10%
			HDGV4: 1%		8	0.03%
			HHGV5: 3%		9	0.10%
			HDGV6: 7%		10	0.24%
			HDGV7: 3%		11	0.10%
		Diesel: 66%	HDDV2B: 27%	100%	16	1.78%
			HDDV3: 8%		17	0.53%
			HDDV4: 9%		18	0.59%
			HHDV5: 4%		19	0.26%
			HDDV6: 21%		20	1.39%
			HDDV7: 31%		21	2.05%
Long trucks: 90%	More than 33,001	Gasoline: 2%	HDGV8A: 100%		12	1.8%
		Diesel: 98%	HDDV8A: 22%	100%	22	19.4%
			HDDV8B: 78%		23	68.8%

[a] Source of raw data: DRIC(2008b)

[b] Source: Transport Canada (2006)

[c] Source: EPA (2003) ; refer to Table 3.7 for description of each class

[d] Refer to Table 3.7 for description of each class

Five classes in Mobile6.2 were mapped to the car category, and 15 classes to the truck category. Thus there are a total of 20 classes. The remaining eight classes, mapped neither to cars nor to trucks, were buses, motorcycles, LDGT3&4, LDDT3&4, and HDGV8B. Buses were counted as HDDVs and motorcycles were not available in vehicle counts. The LDGT3&4 and LDDT3&4 are light duty commercial vehicles which are generally used for local freight movements. Although they could be classified as short trucks, the vehicle counts were not available. It should be noted that Huron Church Road is an international corridor, and most of the trucks on the road are single trucks or truck trailer. Mobil6.2 does not report emission factors for HDGT 8B.

In calculation of composite emission factors for gasoline cars, the shares of Ontario and Michigan gasoline were considered as explained below. The share of cross-border cars on the road was 40%, as estimated in Section 3.3. It was assumed that 60% of fuel was used by cross-border cars in Michigan due to cheaper gasoline price. Thus, 24% (40%×60%) of cars are fueled in Michigan and the other 76% in Ontario. Regarding trucks, 3.4% of total trucks are gasoline, mostly class 16 HDV2B in Mobile6.2 with a gross weight in the range of 8,501 - 10,000 lb (Table 3.2). This means that these gasoline trucks are small and mostly local. Therefore, it was assumed that all gasoline trucks are fueled in Ontario.

3.6 Estimation of NO_2 and benzene concentrations

This section shows how NO_2 and benzene concentrations were estimated from traffic on the Huron Church Road using a dispersion model and analyzing their spatial and

temporal distributions of the output. This section also shows how correlations between NO_2 and benzene concentrations were investigated spatially and temporally.

3.6.1 AERMOD simulation setup

For estimation of NO_2 and benzene concentrations, the AERMOD pollutant dispersion model was used. The model is preferred by the US EPA as it can treat both surface and elevated emission sources in both simple and complex terrain. The AERMOD predicts NOx concentrations using NOx emissions. For estimation of NO_2 concentrations, it has a post-processing tool which estimates NO_2 using NOx modeled and background O_3 concenrtations. The ISC-AERMOD View (Lakes Environmental, 2011) is an interface for AERMOD, and it was used in this study. The AERMOD requires meteorological parameters (e.g. wind speed, wind direction, temperature) of the study area, and geometrical configurations of sources and receptors. In this regard, there are two pre-processors for AERMOD: 1) the AERMET (EPA, 2004b) for pre-processing meteorological parameters, and 2) AERMAP (EPA, 2004c) for pre-processing terrains.

Table 3.10 lists the AERMOD model setup parameters in this study. Windsor terrain is almost flat (elevation = 183-192 m) with a few tall buildings. Therefore, the option for the flat terrain was selected, and AERMAP was not used for pre-processing of the terrain.

Three types of receptors were used as shown in Figure 3.8. The first type of receptorwas placed up to a distance of 1000 m from the road with a spacing of 40 m × 40 m. In total, there were approximately 13 thousand receptors. These receptors were used to estimate annual mean and maximum hourly concentrations. The second type of receptors were the two receptors placed 40 m from the road, one in the east and the other one in the

west. These were used to estimate hourly concentrations and examine temporal variation of concentrations. Finally, one receptor at the Windsor-West air quality station was used to compare observed and simulated hour-of-day variation in concentrations. Simulations were run for benzene and NO_2 separately. In addition, there were two sets of 50 receptors perpendicular to the road and 32 receptors along the road as shown in Figure 3.9; these receptors were used for the sensitivity analysis. The 50 receptors were on a typical traverse for estimation of fall-off pattern of the concentrations.

Table 3.10: Summary of model setup parameters for dispersion calculation in AERMOD

Model Parameters	Settings
Domain	• South-west corner in UTM (zone 17N): 327833 m, 4675873 m • Dimensions: 11 km in north-south direction and 9.4 km in east-west • Flat terrain
Receptors (Figure 3.8)	• Receptors at buffer distance 1000 m from the road with a spacing of 40 m × 40 m, in total 13 thousand • Two receptors for temporal analysis, located 40 m from the road, one to the east and the other to the west • One receptor located at Windsor- West air quality station
Pollutants (One simulation for each)	• Benzene • NO_2
NOx to NO2 conversion	• The PVMRM option: O_3 concentrations from Windsor-West station (MOE, 2009a)
Vehicular emissions	• Vehicle counts at AM and PM peak hours by direction of travel on 16 road sections ; temporal traffic profiles by season/day/hour • NOx and benzene emission factors from Mobile6.2 • Base emissions: peak-hour emissions, AM in northbound and PM in southbound • Variable emission rate: season/day/hour
Emission source parameters (imported volume sources)	• (x, y) center of volume • Emission rate (g/s) • Release height= center of volume=1/2 volume height; volume height=2.5m (Held et al., 2003) • Initial lateral dimension: σy_0= road width/2.15 (EPA, 1995) and initial vertical dimension: σz_0 = volume height/4.3= 0.58 m • # of volume sources: 936 in northbound and 910 in southbound
Meteorological data and pre-processer	• Surface data: Windsor Airport, Station #71538, 42.28 N, 82.96 W, hourly observations in 2008 (Environment Canada, 2012a) • Upper air data: Radiosonde twice daily data at Pontiac, Michigan in 2008. Station: #72632, 42.70 N, 83.47 W (NOAA, 2012) • Period: 1 year (2008) • Pre-processor: AERMET (EPA, 2004b) • Site characteristics (Albedo, Bowen ratio, and surface roughness) for a low-intensity-residential land-use from MOE (2009b)
Outputs	• Annual mean and maximum hourly concentrations for all receptors • Hourly concentrations at three selected receptors
Off	• Dry deposition, wet deposition, plume depletion, and building downwash

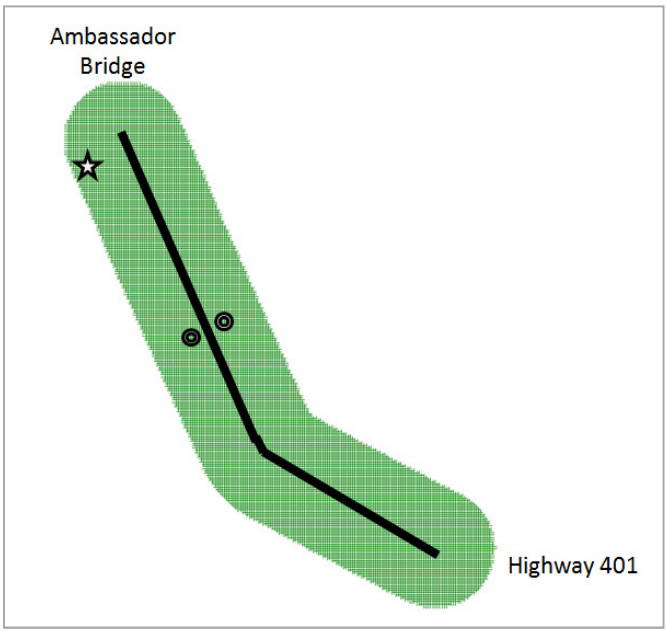

Figure 3.8: Sketch of Huron Church Corridor, receptors in a buffer of 1000 m (13 thousand receptors), Note: The star mark denotes the location of the Windsor West air quality station, and the circles are two receptors for hourly simulation.

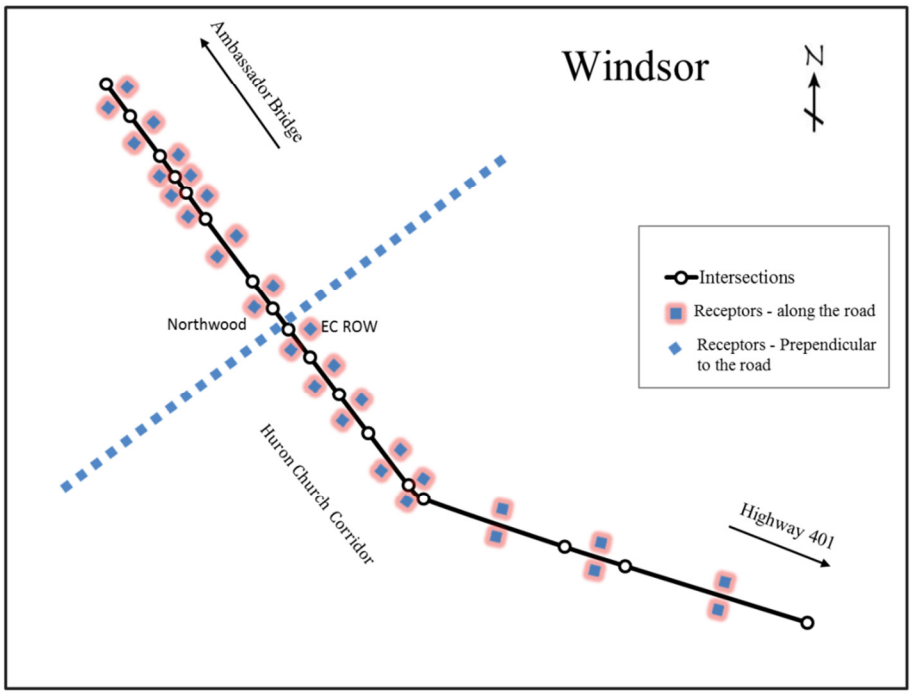

Figure 3.9: Sketch of the Huron Church Corridor and location of 50 receptors perpendicular to the road on a typical traverse with a spacing of 40 m and 32 receptors along the road located at the middle of road section and 40 m from the road.

Vehicular emissions

Traffic emissions were estimated by multiplying Vehicle Kilometer Traveled (VKT) by emission factor of vehicles (mass/VKT) from Mobile6.2. VKT at each road segment was estimated by multiplying vehicle counts (Section 3.4) by the length of the road segment.

Spatial and temporal emissions were required to model dispersion using the AERMOD. In this regard, one-hour base emission for all road sections and the ratio of emission in a given hour of day, day of week, and season to the one-hour base emission were used. Vehicle counts in the peak hour were used for calculation of the one-hour base emission (Section 3.4). The peak hours occurred in the AM and PM at the northbound and southbound roads, respectively. The temporal traffic profiles were required for calculation of temporal emission profiles. They were calculated as the ratio of hourly traffic to the peak traffic.

NOx and benzene emissions were estimated using 1) hour-of-day, day-of-week, and seasonal vehicle counts for each road segment by direction of travel (Section 3.4), and 2) hour-of-day emission factors of NOx and benzene by season from Mobile6.2 (Section 3.5). NOx and benzene emissions for 16 road sections between College and Howard intersections by direction of travel (e.g. northbound and southbound) were used for dispersion modeling.

Emission source parameters

Due to the curvature in some road sections, they were broken down into smaller line segments, called “line sources”. These line sources were differentiated either by having different emissions or having different bearings. As a result, there were 36 line sources in

each direction of the road. Coordinates of line sources were obtained from Google Earth (2010). Following ISCST3 (EPA, 1995) and AERMOD (EPA, 2004a), line sources were treated as a series of adjacent volume sources. For calculation of the initial lateral dimension (σy_0), the width of the volume source was assumed to be equal to the road width. The lengths of the volume sources were equal to or less than the road width. The road width in each direction was in the range of 10-15 m. The total numbers of volume sources was 1846. Other emission source parameters are listed in Table 3.10.

Meteorological inputs

Meteorological inputs included surface and upper air data in 2008. The AERMET was used for pre-processing the raw meteorological parameters for the use in AERMOD. A majority of the land use in the study area is low intensity residential. The site characteristics including albedo, Bowen ratio, and surface roughness for this land-use obtained from MOE (2009b) were used in AERMET. Since traffic data were collected in local time, meteorological data were shifted from EST to local time during the daylight saving period of March 9 – November 2, 2008. Details of the meteorological data source and processing can be found in Appendix A.

NOx to NO_2 conversion

For NOx to NO_2 conversion, there are two methods in AERMOD: Ozone Limiting Method (OLM) and Plume Volume Molar Ratio Method (PVMRM). Since the PVMRM option provides a more accurate estimate of NO_2 concentrations (Hanrahan, 1999), it was used for NO_2 simulation. NOx emissions and hourly background O_3 concentrations are required for NO_2 simulations. By default, the NO_2/NOx ratio in the plume is 0.1. In other words, 10% of the NOx emission in the plume is NO_2, and 90% is NO. It should be noted

that NO_2/NOx ratios in the exhaust emissions of cars and trucks are slightly different, but still around 0.1. For example, using a tunnel study, Boulter et al (2007) found the NO_2/NOx ratios of cars and trucks as 0.16 and 0.11, respectively. Thus, in this study the default value of 0.1 was used.

By moving away from the plume, the NO concentration decreased due to reacting with O_3 (Reaction 3.1). This reaction results in NO_2 formation called NOx titration. NO_2 concentration increased away from the plume.

$$NO + O_3 \rightarrow NO_2 + O_2 \qquad \text{(Reaction 3.1)}$$

The hourly O_3 concentrations in 2008, required for AERMOD NO_2 simulation, were obtained from the Windsor-West Station (MOE, 2009a). O_3 is a regional pollutant, and O_3 concentration does not vary much over the study domain of 10 km×11km. Thus, O_3 concentration at the Windsor-West Station which is 900 m away from the road can be used for NO_2 simulation over the study domain. AERMOD uses hourly O_3 concentrations for simulating NO_2 concentrations.

3.6.2 Analysis of simulation results

This section identifies the factors affecting hourly and annual mean NO_2 and benzene concentrations and predicts concentrations using regression models. For this purpose, spatial and temporal patterns of simulated NO_2 and benzene concentrations were observed.

Spatial patterns

The model simulated concentrations were imported to ArcGIS (ESRI, 2010) for visualization of spatial patterns. Annual mean and maximum hourly concentrations of NO_2 and benzene at receptors on the buffer distance of 100 0m from the road centerline (Figure 3.8) were plotted. Receptors located 0-20 m from the road were excluded because they are hotspots where the general public is not exposed.

Fall-off patterns of annual mean and maximum hourly concentrations were plotted for the 50 receptors perpendicular to the EC Row-Northwood road section (Figure 3.9). Fall-off equations of annual mean concentrations were estimated as a power function of distance to the road as shown in Equation 3.6.

$$\text{Fall-off}(x) = f_0\, x^{f_1} \tag{3.6}$$

where:

Fall – off (x): Ratio of concentration at distance x to the concentration at the location 40 m from the road. The 40 m was the distance for the closest receptor to the road [Fall – off (40) = 1]
x: Distance to the road (m) [≥40 m]
f_0, f_1: Constant and coefficients of the regression

Comparison of fall-off patterns of observed and simulated NO_2

Fall-off patterns of the simulated and observed NO_2 concentrations at a transect perpendicular to Huron Church Road were compared. NO_2 concentrations at 11 sites near the College-Giradot road section were collected, six sites in the east of the road and five sites in the west as shown in Figure 3.10. Passive Ogawa NO_2 samplers were used during

9-26 May 2010, with sampling intervals of 6-hr to 4-day. The average concentrations by site were used in the comparison. These data were provided by Health Canada.

For comparison during the same time period, NO_2 concentrations were simulated during May 1-31 2010. NOx emissions were the same as those in spring 2008, but meteorological data were for May 2010. The surface and upper air data in 2010 were obtained from Environment Canada (2012a) and NOAA (2012), respectively. Other setup parameters are the same as listed in Table 3.10.

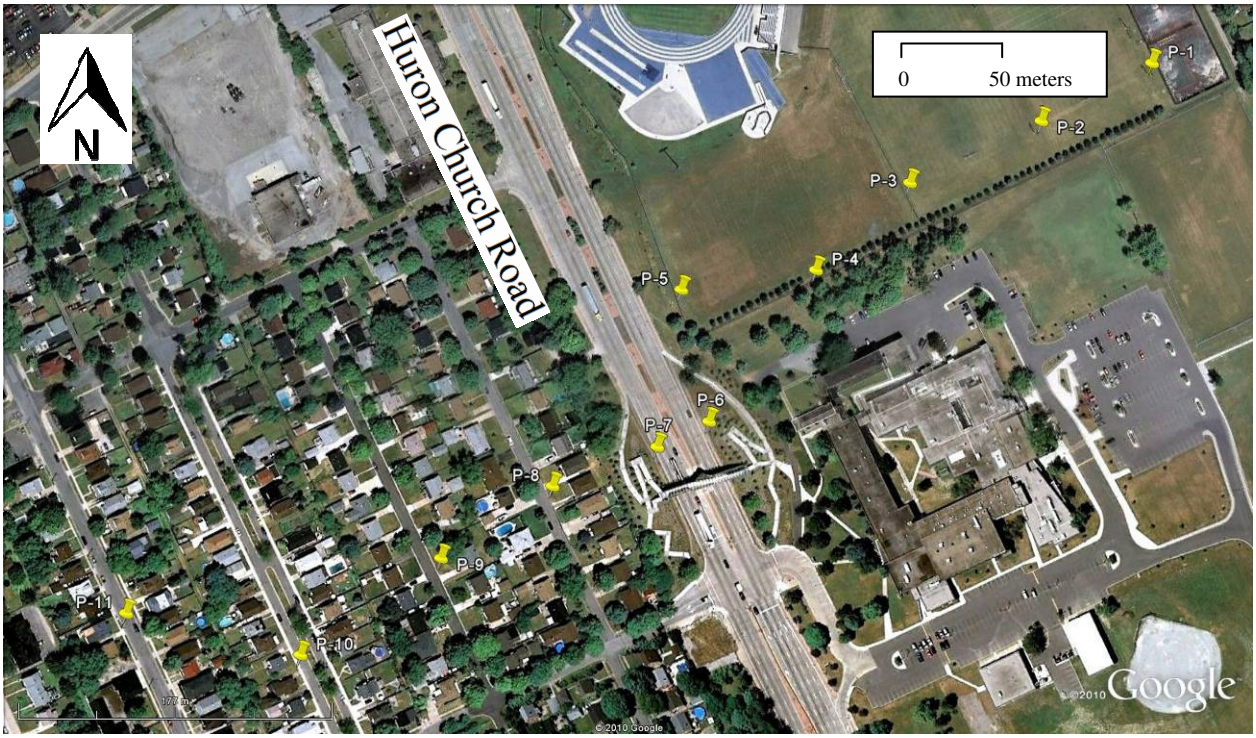

Figure 3.10: Map of passive monitoring sites (yellow pins) near the Giradot-College road section (Source of base map: Google Earth, 2010)

Hour-of-day and seasonal patterns

Hour-of-day and seasonal NO_2 and benzene concentrations were plotted for 40 m east and 40 m west of the EC Row N – Northwood road section, respectively (Figure 3.8).

Comparison of temporal patterns of observed and simulated concentrations

Hour-of-day patterns of simulated and observed NO_2 concentrations were compared at the Windsor-West Station located approximately 900 m west of the road (Figure 3.8). Hourly observed NO_2 concentrations the Windsor-West Station in 2008 were obtained from MOE (2009a). NO_2 concentrations were collected using "analyzers operating on the principle of chemiluminescence involving the gas phase reaction of NO with O_3" (Environment Canada, 2012b). As these instruments only measure NO, "NO_2 is measured by reducing it to NO using a catalytic converter" (Environment Canada, 2012b).

To identify separate effects of traffic and meteorological factors on NO_2 concentrations, three additional simulation scenarios of AERMOD were run for a receptor at the Windsor-West Station: unit emission, car only, and truck only. In the unit emission case, one unit emission was applied to all road segments and to all hours of the year, i.e. 1 g of NOx emission per 1 m of road section per 1 second. In the 'car only' and 'truck only' cases, only emissions from cars and trucks were considered, respectively. Those cases were to identify effects of car and truck counts on simulated concentrations.

Seasonal patterns of observed and simulated NO_2 and benzene concentrations at the Windsor-West Station in 2008 were compared. The observed hourly NO_2 and daily benzene concentrations in 2008 were used MOE (2009a). Daily VOC concentrations (24-hour average) including benzene were collected every six days. VOC samples were "analyzed for C_2 to C_{12} hydrocarbon species" in the laboratory (Environment Canada, 2012b). In this regard, "a combined gas chromatography/flame ionization detector

(GC/FID) system is used for quantification of C_2 hydrocarbons, while a combined gas chromatography/mass selective detector (GC/MSD) system operating in selected ion monitoring (SIM) mode is used for quantification of C_3 to C_{12} hydrocarbon" (Environment Canada, 2012b). Benzene concentrations were available for 42 days in 2008.

Analysis of variance (ANOVA)

The major factors affecting hourly NO_2 concentrations at the Windsor-West Station were identified. First, cross-correlation among potential factors and concentrations were investigated. Three groups of factors were determined: temporal factors (hour of day, day of week, and season), traffic (car counts, truck counts, and car-NOx-equivalent) and meteorological factors (wind speed, mechanical mixing heights, and convective mixing heights). The car-NOx-equivalent was used to represent emissions by both cars and trucks combined. In this regard, it was assumed that one truck is equal to 10 car-NOx-equivalent as the NOx emission factors of trucks were estimated to be 10 times that of cars. The wind speed was readily available in the observed meteorological data (Environment Canada, 2012a). However, mechanical and convective mixing heights were estimated using the AERMET.

The ANOVA method was used to quantify variations in simulated and observed hourly concentrations at the Windsor West explained by these factors. The angle between the wind direction and the perpendicular line from the road to receptor was calculated. If the angle was between -85º and 85º, it was assumed that the receptor is downwind of the road. Statistical analysis was performed only for these downwind hours to exclude effects of wind direction. In total, the receptor was downwind of the road for

33% of year (2870 hours of the year). Table 3.11 shows the statistical summary of data. It should noted that convective mixing heights were only available during the daytime (8:00-19:00)

Table 3.11: Descriptive statistics of concentrations, vehicle counts and meteorological factors

Variable	Number of hours	Number of missing	Mean	Standard Deviation	Minimum	25th	Median	75th	Maximum
Simulated NO_2(ug/m3)	2870	0	2.527	5.745	0	0.172	0.614	1.597	49.54
Observed NO_2(ppb)	2853	17	13.768	8.149	2	8	12	18	61
Car(veh/h)	2870	0	1153.1	590.7	150	531	1285	1572	2398
Truck(veh/h)	2870	0	337.86	146.84	40	217	321	476	606
Car-NOx-Equivalent(veh/h)	2870	0	4531.6	1977.1	561	2714.3	4380	6337	8187
Wind Speed(m/s)	2870	0	3.7785	2.1385	1.1	2	3.6	5.3	12.8
Mechanical Mixing Height(m)	2870	0	941.7	784.3	46	325.8	744	1403	4000
Convective Mixing Height(m)	1183	1687	705.1	499.2	1	303	604	1039	2446

Regression modeling of concentrations

It is worthwhile to obtain simplified relationships that potentially represent complex modeling approach by dispersion models and to predict ambient air concentrations with a reasonable accuracy. In this regard, the simulated concentrations have been used to develop regression models. For instance, Mölter et al. (2010) used the estimated concentrations by a dispersion model at multiple locations of Greater Manchester, UK, to develop a land-use regression model. Predictor variables were traffic intensity, emission, and land-use in different buffer distances from the receptors.

Hourly concentration models

Statistical analysis indicated that simulated concentrations by AERMOD are affected by car and truck counts, and wind speed. The relationship among ambient air concentration

(dependent variable), vehicle counts and meteorological factors is not linear. Thus, a logarithmic regression model was developed to estimate hourly concentrations of NO_2 and benzene as shown in Equation 3.7. NO_2 and benzene concentrations were estimated at a receptor 40 m east of the road (Figure 3.8).

$$C(t) = f_0 \, Car\_Eq(t)^{f_1} \, WindSpeed(t)^{f_2} \quad (3.7)$$

where:

C(t): Ambient air concentrations at hour t (µg/m3)
Car_Eq(t): Car-NOx-Equivalent (veh/h) and Car-Benzene-Equivalent, for NO_2 and benzene, respectively.
Windspeed: Wind speed at hour t (m/s)
f_0, f_1- f_2: Constant and coefficients of the regression, respectively

In order to make the models applicable in the other urban areas, the Car-NOx-Equivalent (veh/h) and Car-Benzene-Equivalent were used for NO_2 and benzene models, respectively. In this regard, one truck was assumed to be equal to 10 and 0.2 Car-NOx-Equivalent and Car-Benzene-Equivalent, respectively. This is because annual average NOx and benzene emission factors of trucks were 10 and 0.2 times those of cars, respectively. It should be noted that NOx and benzene emission factors of vehicles varied with seasonal temperature. However, here for simplification purposes, fixed numbers were used to represent trucks with car-emission-equivalent.

Concentrations were plotted versus wind speed, and distinct difference in concentrations was observed during the daytime (8:00-19:00) and the nighttime (1:00-7:00 and 20:00-00:00). This is because AERMOD considers the convective mixings during the daytime. Thus, different models were developed for daytime and nighttime.

Hourly concentrations in Equation 3.7 were developed for a receptor 40 m from the road. In order to estimate concentrations at the other location, fall-off patterns of concentrations in Equation 3.6 were used. Thus, concentration at a receptor x away from the road can be calculated as shown in Equation 3.8.

$$C(x,t) = \text{Fall - off}(x) \times C(t) \tag{3.8}$$

where:

C(x, t): Ambient air concentrations at x m way from the road at hour t (µg/m3)
Fall – off (x): From Equation 3.6
C(t): Concentration as a function of vehicle counts and wind speed in Equation 3.7

Annual mean concentration models

To examine spatial distribution of concentrations, receptors were classified into seven groups with respect to their distance to the road, i.e. 0-20 m, 20-50 m, 50-100 m, 100-200 m, 200-400 m, 400-600 m, and 600-1000 m as shown in Figure 3.11. As explained earlier, receptors located 0-20 m from the road were excluded from further analysis.

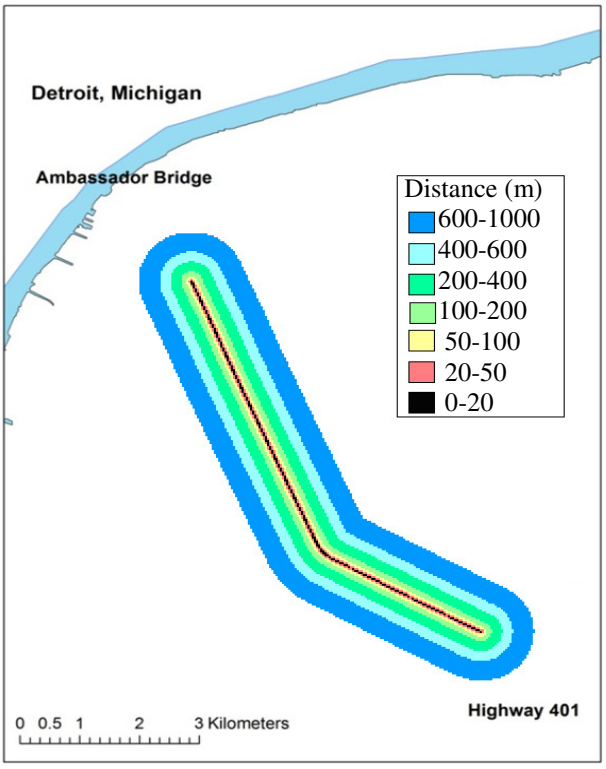

Figure 3.11: Classification of receptors with respect to the distance to the road

Car and truck counts at different distances from the receptors were used to predict concentrations at receptors. This concept is similar to that used by Land-Use Regression (LUR) models, where concentrations at each location are predicted using spatially distributed characteristics, e.g. vehicle counts in a buffer of 100 m. Table 3.12 shows the list of predictors used for prediction of concentrations.

Table 3.12: Predictor variables for estimation of annual mean concentrations

Variable	Buffer
Car-Eq[a] counts weighted by length of the segments	20-50 m 50-100 m 100-200 m 200-400 m 400-600 m 600-1000 m
West	-

[a] Car-NOx-Equivalent (veh/h) and Car-Benzene-Equivalent, for NO_2 and benzene, respectively.

A multinomial linear regression model was developed to investigate the effects of car and truck counts on concentrations. The counts were weighted with the length of the road segments. Due to the prevailing wind direction from the west, higher concentrations were observed east of the road. Therefore, a dummy variable "west" was used to capture the effect of wind direction. Separate regression models were developed for each group of the receptors.

3.6.3 Relationship between NO_2 /benzene and truck/car ratios

Given that meteorological inputs for simulating NO_2 and benzene concentrations were the same, it is expected that NO_2/benzene concentration ratio follows the NOx/benzene emission ratio. In addition, since trucks are high NOx emitters and cars are high benzene emitters, it is worthwhile to find a relationship between the NO_2/benzene concentration ratio and the truck/car counts ratio. A linear relationship was fitted between the ratio of NO_2 to benzene concentrations and the ratio of truck to car counts as shown in Equation 3.9. This relationship was developed based on simulated hourly NO_2/bezenene concentration ratio at the receptor 40 m east of the EC Row-Northwood road section, and the hourly truck/car counts ratio at this road section.

$$NO_2/\text{Benzene} = C_0 + C_1(\text{Truck/Car}) \qquad (3.9)$$

where:

NO_2/Benzene: ratio of NO_2 to benzene concentrations
Truck/Car: ratio of truck to car counts
C_0 and C_1: Constant and the coefficient of the regression

The ratio of annual mean NO_2/benzene concentrations was calculated for each of 16 receptors, located 40m east of the center of the road (Figure 3.9). A linear relationship was fitted between these 16 NO_2/benzene and truck/car ratios.

The ratio of annual mean NO_2/benzene concentrations was calculated and plotted for all receptors in the buffer distance of 1000 m (Figure 3.8). For further investigation, the ratio of annual mean NO_2/NOx and NOx/benzene concentrations was calculated and plotted.

The ratios of truck to car counts at different buffer distances from the receptors (Figure 3.11) were used to predict the NO_2/benzene concentration ratio at the receptors. The NO_2/benzene concentration ratio was predicted using a multinomial linear regression model. The explanatory variables used in the model are shown in Table 3.13.

Table 3.13: Explanatory variables for estimation of NO_2/benzene concentration ratio

Variable	Buffer distance from the road (circle)
Ratio of truck to car counts weighted by length of the segments	20-50 m 50-100 m 100-200 m 200-400 m 400-600 m 600-1000 m

3.7 Effects of input parameters on estimated emissions and concentrations

In this section, a sensitivity study was conducted to quantify the effects of various modeling options on the estimated vehicular NOx and benzene emissions, as well as NO_2 and benzene concentrations. The options involved in this investigation include more-refined input data in estimation of emission and concentration, different land use approaches in AERMOD, NO_2 simulation options in AERMOD, and stop-and-go movements of vehicles on emission and concentration.

3.7.1 Sensitivity of results to input data in a macroscopic level using Mobile6.2 and AERMOD

As listed in Table 3.14, nine scenarios were identified to estimate the effects of more detailed data on the estimation of emission factors using Mobile6.2 and ambient air concentrations of NO_2 and benzene using the AERMOD. In the Base Case, less detailed data, but more default values were used. Only one factor was changed at a time in Scenario 1-7 . In Scenario 8 all factors were changed simultaneously (Table 3.14). Then, the resultant emission factors of LDVs, HDVs, total emissions, and annual mean and maximum hourly concentrations were compared between each scenario and the Base

Case. The percentage difference between each scenario and the Base Case was calculated as shown in Equation 3.10.

$$\text{Percentage difference} = (\text{Scenario-Base Case})/\text{Base Case} \times 100\% \quad (3.10)$$

To estimate the effects of temporal variability of vehicular emission on concentrations using the AERMOD dispersion model, five scenarios out of nine were considered for dispersion modeling. In these scenarios, temporal resolution of input emission for dispersion modeling was different. Input emissions were a constant annual rate in the Base Case whereas emissions varied by season in Scenario 4, by hour of day in Scenario 6 and by hour of day, day of week and season in Scenario 7.

Table 3.14: Setup of scenarios – Effects of more-detailed input data

	Emission factors by Mobile6.2				Time resolution of vehicle counts	Time resolution of emission for dispersion modeling
	Changed parameters versus Base Case	Values in Base Case	Alternative values	Output format		
S0 – Base Case	None	-	-	Annual (1)	Annual (1)	Annual
S1 – Road Types & Average Speed	Road type & average speed	Arterial 50km/h	Arterial 40km/h	Annual (1)	Annual (1)	NA
			Arterial 60km/h	Annual (1)	Annual (1)	NA
			Arterial 80km/h	Annual (1)	Annual (1)	NA
			Freeway 60km/h	Annual (1)	Annual (1)	NA
			Freeway 80km/h	Annual (1)	Annual (1)	NA
			Local Road	Annual (1)	Annual (1)	NA
S2 – Local Vehicle Mile Traveled	Vehicle composition	Default	Local breakdown	Annual (1)	Annual (1)	NA
S 3- Ontario Vehicle Age Distribution	Vehicle age distribution	Default	Ontario vehicle registration	Annual (1)	Annual (1)	NA
S4 – Seasonal Temperature	Temperature & output format	Min/max of annual mean hour of day: 7/13 °C	Hour of day by season	Seasonal (4)	Seasonal (4)	Seasonal (4)
S5 – Seasonal Fuel	Fuel properties & output format	Ontario Annual average	Ontario values for two seasons (summer and winter)	Seasonal (4)	Seasonal (4)	NA
S6 – Hour of Day	Output format	-	-	Hour of day (24)	Hour of day (24)	Hour of day (24)
S7 – Hour-Day of Week – Season Temperature	Temperature & output format	Min/max of hour of day: 7/13 °C	Hour of day by season	Hour of Day by season (24*4)	Hour of day by day of week and by season (24*3*4)	Hour of day by day of week and by season (24*3*4)
S8 – Best Case	Vehicle composition	Default	Local breakdown	Hour of Day by season (24*4)	Hour of day by day of week and by season (24*3*4)	Hour of day by day of week and by season (24*3*4)
	Vehicle age distribution	Default	Ontario vehicle registration			
	Temperature	Min/max of hour of day: 7/13 °C	Hour of day by season			
	Fuel properties	Ontario Annual average	Ontario values for two seasons (summer and winter)			

Setup parameters of Mobile6.2 in the Base Case

Table 3.15 lists setup parameters of Mobile6.2 in the Base Case. Huron Church Road is an arterial road with 17 signalized intersections. The posted speed limits are 80 km/h for a 3.4-km section of the road, and 60 km/h for the remaining 6-km section. Due to stop-and-go traffic behavior on the road, the average speed is expected to be lower than the speed limits. According to a traffic survey by DRIC study (2008a), travel time and average speed in northbound direction were approximately 10 min and 55km/h, respectively, on weekdays of February 2006. However in the southbound direction, travel time was slightly longer in the afternoon peak period (13 min) compared to other hours of day (10 min). Daily average travel time (6am-8pm) was 11.5 min, which corresponds to average speed of 50 km/h. Thus, an average speed of 50 km/h was used for both directions.

Table 3.15: Setup parameters of Mobile6.2 in the Base Case

Parameters	Description and/or value
Road type and average speed	Arterial road and 50km/h, respectively, for the Huron Church Road.
Vehicle Mile Traveled (VMT) composition	Default composition in Mobile6.2
Vehicle age distribution	Default nation-wide profiles of Mobil6.2 of US in 1996
Ambient temperature	Minimum and maximum hour of day temperature in 2008 at Windsor Airport, as – 7 and 13 °C, respectively (Environment Canada, 2012a)
Fuel properties	Ontario annual average from DRIC (2008c)
Output format	Annual average
Vehicle activities	Default values

By default, 99.9% VMT (Vehicle Mile Traveled) of LDVs are for gasoline vehicles; 44% for LDGVs (Light Duty Gasoline Vehicles, e.g. Sedan) and 56% for LDGTs (Light Duty Gasoline Trucks, e.g. SUVs, Pickup trucks). VMT of HDVs is 70% for Heavy Duty Diesel Vehicles (HHDVs) and 30% for Heavy Duty Gasoline Vehicles (HDGVs).

Mobile6.2 requires either the minimum and maximum daily temperatures or the hour-of-day temperatures. When minimum/maximum temperatures are selected, the minimum and maximum temperatures are assigned to 6am and 3pm, respectively. Then a predefined hour-of-day temperature pattern is used for calculation of temperature in the remaining 22 hours (EPA, 2003). In this study, minimum/maximum temperatures were obtained from the hourly temperature in 2008 at Windsor Airport (Environment Canada, 2012a).

Mobile 6.2 reports running and cold-start exhaust emissions for both NOx and benzene. In addition, it reports evaporative emissions for benzene (as a VOC). However, for this analysis, evaporative benzene emissions were not considered since the majority of evaporative emissions are not on-road emissions - for example, hot soak, rest, and refueling evaporative emissions.

S1: Road type and average speed

In this scenario, instead of Arterial road type with an average speed of 50km/h, six relevant options were considered: 1) Local road, 2-4) Arterial roads with an average speed of 40, 60 and 80 km/h, and 5-6) Freeways with an average speed of 60 and 80 km/h.

Mobile6.2 is sensitive to the road type and average speed, as these parameters are used to represent the driving cycles of vehicles. Speed correction factors (SCFs) are

defined for specific pollutant types and vehicle types. The SCFs are used to take into account changes of emission factors for a particular road type. According to EPA (2001), SCFs of LDVs were estimated by emission tests of some LDVs under various driving cycles. A total of 12 driving cycles were used: six for the Freeway road type (average speeds of 63.2, 59.7, 52.7, 30.5, 18.6, 13.1 mile/h), one for freeway ramp (average speed of 34.6 mile/h), three for the Arterial road type (average speeds of 24.8, 19.2, and 11.6 mile/h), one for the Local road type (average speed of 12.9 mile/h) and one for the Non-freeway-Area-Wide-Urban-Travel (19.4 mile/h). Maximum speed and acceleration in each driving cycle are listed in Table C1 (Appendix C).In the case of HDVs, SCFs of NOx are described in a function of average speed (EPA, 2001). There are separate functions for Heavy Duty Diesel Vehicles (HDDVs) and Heavy Duty Gasoline Vehicles (HDGVs) as shown in Figure C1 (Appendix C). The SCF of HDDVs for NOx emissions has a U-Shape function where emissions are high in low and high average speeds, and emissions are lower at intermediate average speeds. On the other hand, SCFs of HDGV linearly increase with the average speed. Since emissions are different for different driving cycles for the same average speed, Mobile6.2 uses the Off-Cycle Correction Factors (OCCF) for NOx emissions of HDVs. OCCF are determined for each road type (EPA, 2002b).

S2: Local vehicle composition

In this scenario, instead of the use of default composition of the VMT, local compositions were used as listed in Tables 3.8 and 3.9. As explained in Section 3.5.4, four sets of data were used for calculation of local VMT compositions. The first set was composition of short and long trucks on the road from DRIC (2008b) counts in 2006-2007 - 10% and

90% respectively. The second set was the Ontario Light Duty Passenger Vehicles (LDPV) breakdown in 2006 from Transport Canada (2006) - 70% passenger cars and 30% passenger trucks. The third set was the fuel breakdown of vehicles from Transport Canada (2006). The fourth set were default values of VMT composition in Mobile6.2; which was used for further breakdowns among weight classes in Mobile6.2 (Table 3.7). More details can be found in Section 3.5.4.

S3: Ontario vehicle age distribution

In this scenario, Ontario vehicle age distribution was used instead of default values (US national means). Ontario vehicle registrations in 2008 by model year (1989-2008) for three weight classes were obtained from Statistics Canada (2008). The classes were vehicles up to 4.5 tonnes, trucks 4.5 tonnes to 14.9 tonnes, and trucks 15 tonnes or more. It should be noted that the number of vehicle model years earlier than 1989 was reported in the 1989 values. Vehicle registrations by model year were used to calculate vehicle age distributions. Alignment of vehicle classes in Mobile6.2 with age distribution categories is listed in Table 3.6. Figure 3.12 compares Ontario vehicle age distribution with default values in Mobile6.2 for two major classes of vehicles. Since average age of Ontario vehicles was lower than the default average age of vehicles, it is expected that the emission factor of vehicles be lower when the vehicle age distribution in Ontario is used.

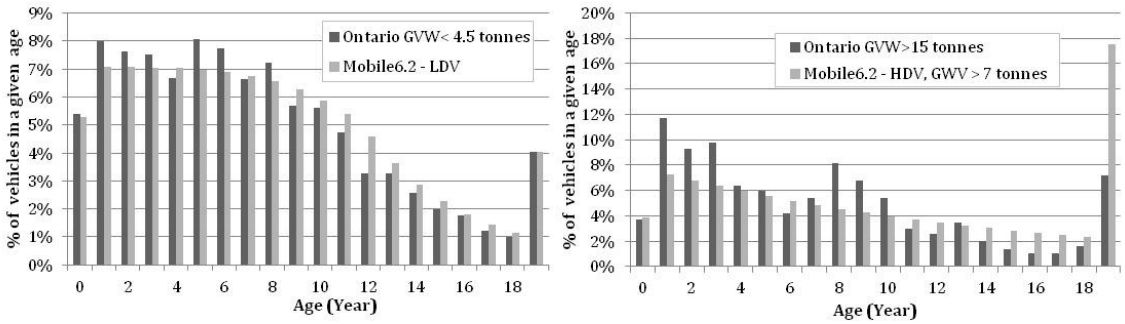

(a) LDVs (b) HDVs

Figure 3.12: A comparison of vehicle age distribution between Ontario and default values

Vehicle age distributions are likely to be different by location. Since vehicle age affects emissions, emission factors are different in different locations. Thus, the nation-wide distribution of vehicle age in Canada was compared with the distribution in Ontario and default Mobile6.2 as shown in Figure 3.13. It was observed that the average vehicle ages from Ontario sources were the lowest among the three cases.

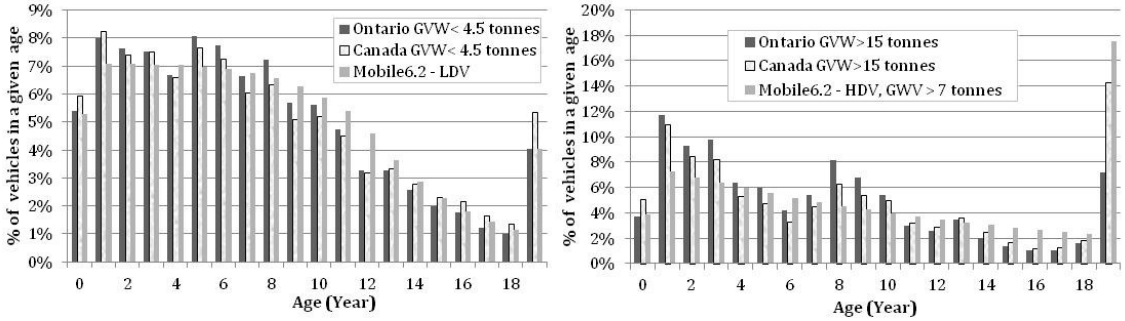

(a) LDVs (b) HDVs

Figure 3.13: Vehicle age distribution in Ontario, Canada, and default Mobile6.2

Table 3.16 shows the difference in emission factors between vehicle age distributions for Ontario and Canada, and the default vehicle age distribution in Mobile6.2 (US national means). It was found when the Canada vehicle age distribution was used, emission factors were not much different compared to the default values, e.g. 4% for

NOx and 6% for benzene. However, when Ontario vehicle age distribution was used, NOx and benzene emission factors were lower by 7% and 10%, respectively, than the default values.

Table 3.16: Difference in emission factors – vehicle age distributions versus default values in Mobile6.2.

	Vehicle Age Distribution	Light-duty vehicle Emission factor (g/km)	Heavy-duty vehicle emission factor (g/km)	Total emission
NOx	Ontario profile	-2.5%	-9.2%	-7.2%
	Canada profile	-1%	-5%	-4%
Benzene	Ontario profile	-10%	-13%	-10%
	Canada profile	-6%	-7%	-6%

S4: Seasonal temperature

In Scenario 4, hour-of-day temperature by season was used instead of annual average hour-of-day Minimum/Maximum temperatures. Mobile6.2 was separately run for each of the four seasons. Seasonal variations in temperature are important because cold-start emissions are higher in colder seasons. Seasonal emissions were estimated using seasonal emission factors of vehicles along with seasonal car and truck counts.

Seasonal mean of hourly temperatures were observed at Windsor Airport in 2008 (Environment Canada, 2012a). It is worthwhile to compare the seasonal variations in temperature in Windsor with the other locations to confirm that results are applicable to other study areas. As shown in Figure 3.1, seasonal variations in temperature were similar between Windsor and an average of 100 US cities. However, this comparison does not necessarily mean that seasonal temperatures are similar in all urban areas. Thus, results of

this study are applicable for locations with similar seasonal temperatures as Windsor, such as cities in northeastern US or southern Ontario.

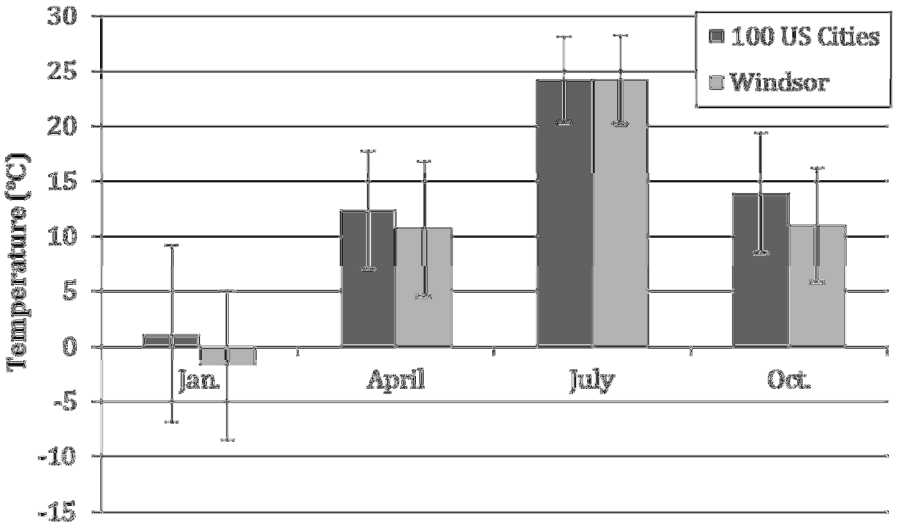

Figure 3.14: Comparison of seasonal variations in temperature between Windsor (Environment Canada, 2012a) and 100 U.S. cities (Infoplease.com, 2012)

S5: Seasonal fuel properties

In this scenario, different fuel properties were assumed in summer and winter instead of using annual average values of fuel properties. As listed in Table 3.17, some fuel properties are different across seasons. Seasonal variations in fuel RVP are higher than the variation in other fuel properties. In order to estimate effect of each factor, one factor of each of the fuel properties listed in Table 3.17 was changed at a time.

Table 3.17: Average fuel properties in Ontario in 2003 (DRIC, 2008c)

Season	RVP [a]	E200 [b]	E300 [c]	Aromatics	Olefins	Benzene	Ethanol
	PSI [d]	vol%	vol%	vol%	vol%	Vol%	vol%
Winter	14.6	53.9	84.4	25.1	9	0.73	1.92
Summer	9.7	47.9	82.4	28.8	9.7	0.73	1.92
Year	12.1	50.9	83.4	26.9	9.3	0.73	1.92
Difference (Winter vs Year)	20%	6%	1%	-7%	-3%	0%	0%
Difference (Summer vs Year)	-20%	-6%	-1%	7%	3%	0%	0%

[a] Reid Vapor Pressure

[b] Percentage of fuel that evaporates at 200 degrees Fahrenheit under 1atm

[c] Percentage of fuel that evaporates at 300 degrees Fahrenheit under 1atm

[d] Pounds per Square Inches

To check the applicability of results in other study areas, seasonal variations in fuel properties in Windsor and 23 US States were compared (Figure 3.15). Similar variations were observed.

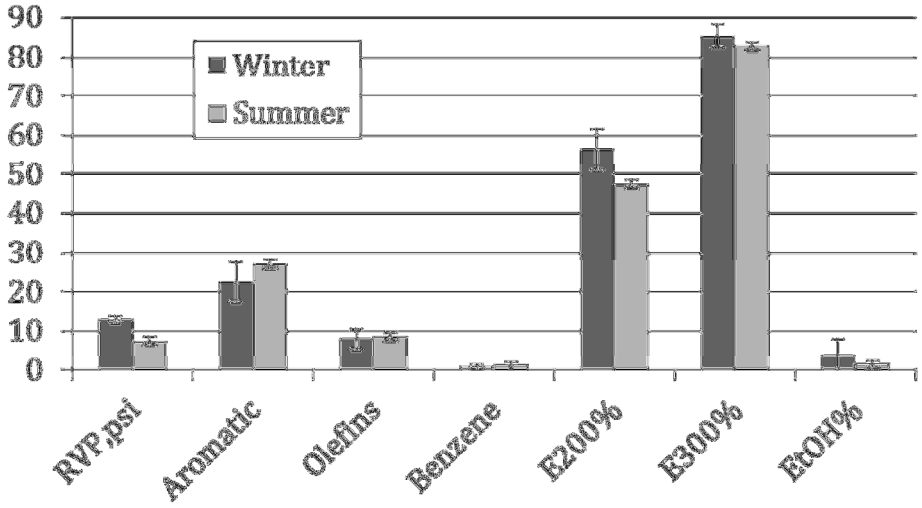

(a) 23 US States

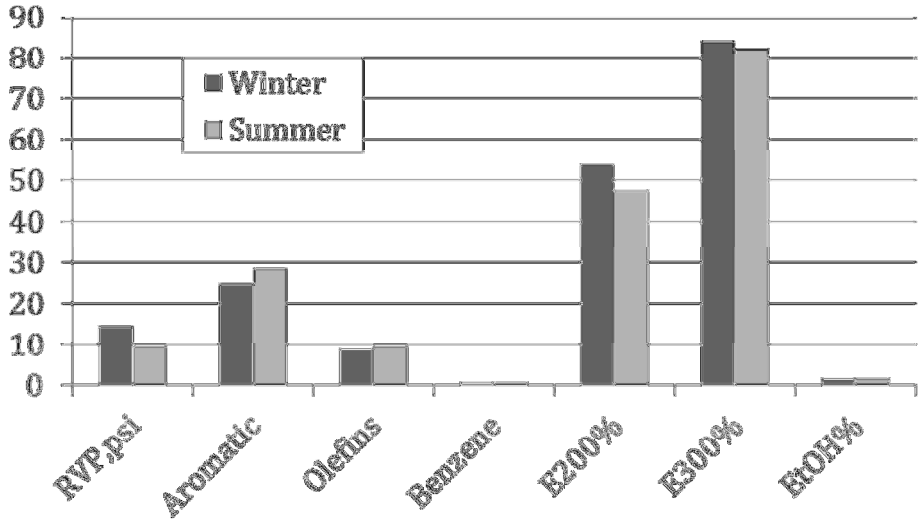

(b) Ontario

Figure 3.15: Seasonal fuel properties (a) average of 23 US States (EPA, 1999a) (b) Ontario (DRIC, 2008c)

S6: Hour-of-day emission factor

The Scenario 6 examined the effect of hour-of-day variations of emission factors. Due to hour-of-day variation in temperature, it is expected that emission factors vary with hour. Mobile6.2 was separately run for each hour using hourly temperature. Hour-of-day car

and truck counts and hour-of-day emission factors by Mobile6.2 were used to estimate hour-of-day emissions. As discussed earlier, this scenario was used for dispersion modeling using AERMOD.

It should be noted that hour-of-day variations in traffic emission is similar in all urban areas. For instance, as shown in Figure 3.16, hour-of-day pattern of vehicle counts on a US typical road with that on Huron Church Road 2008 are similar.

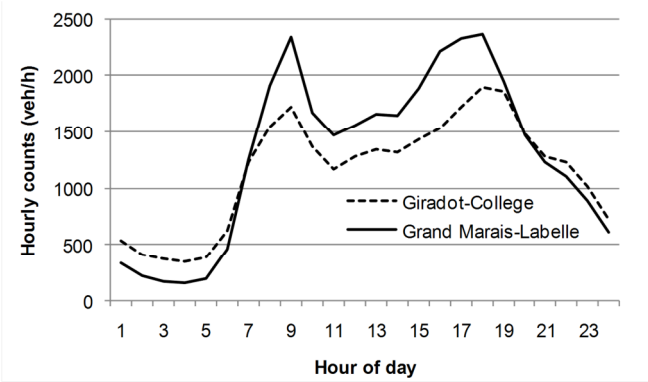

(a) Huron Church Road in 2008

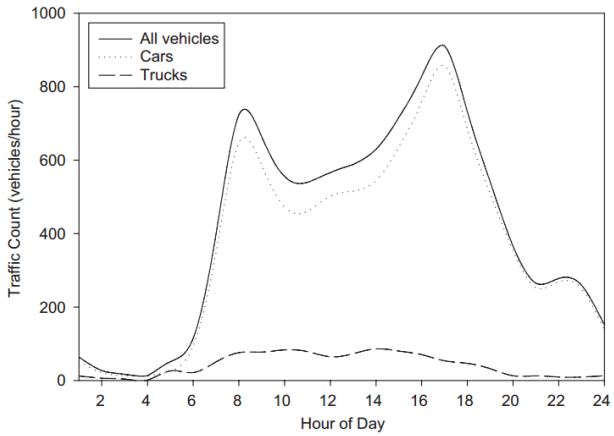

(b) Mid-town Manhattan area, US (Zhou and Levy, 2008) – Reprinted with permission (Appendix D).

Figure 3.16: Hour of day pattern of vehicle counts

S7: Simulation by hour of day, day of week and season

In Scenario 7, emission factors of vehicles are estimated by hour of day, day of week (weekday, Saturday, and Sundays) and season (winter, spring, summer, and fall). Mobile6.2 was run for each combination of hour of day, day of week and season. These emission factors along with hour of day car and truck counts by day of week and by season were used to estimate hour-of-day emissions by day of week and by season, and then these emissions were used in dispersion modeling.

S8: Best Case

Scenario 8 was the Best Case, in which changes in scenarios 2, 3, 5, and 7 of mentioned above were considered simultaneously. It was called the Best Case as the most detailed data was used in this case. This scenario was used to identify the overall effects of input parameters on estimation of emission factors using the Mobile6.2 and ambient air concentrations of pollutants using the AERMOD.

NO_2 and benzene concentrations

AERMOD dispersion model was used to estimate concentration of air pollutants. Maximum hourly and annual mean concentrations of benzene and NO_2 were estimated for the Base Case, and Scenario 4, 6, 7, and 8 at 50 receptors perpendicular to the road and 32 receptors parallel to the road (Figure 3.9). The average concentrations at 32 receptors were calculated for each scenario; the percentage difference between the Base Case and each scenario was calculated (Equation 3.10).

Hourly concentrations were estimated at the two receptors 40 m from the road, one in the east and one in the west of the EC Row-Northwood road section (Figure 3.8). From

simulated hourly concentrations at these two receptors, hour-of-day and seasonal average concentrations were calculated. The box plot, histogram, and probability plot of hourly concentrations were drawn using Minitab (2011). Results were used to compare the percentile distribution of concentrations among different scenarios. Other setup parameters are listed in Table 3.10.

3.7.2 Options in AERMOD

Site characteristics

Mixing heights and therefore simulated concentrations are strongly affected by the site characteristics including albedo, Bowen ratio, and surface roughness. Site characteristics are determined based on land use of the study area. Thus, the objective of this section is to choose an appropriate choice for land-use for our study domain, and to investigate effects of land-use choices on annual mean and hour-of-day concentrations.

Site characteristics were used in AERMET (EPA, 2004b) to compute atmospheric stability and sensible heat flux. The albedo is the fraction of sunlight reflected by surface back to the space. The Bowen ratio is "an indicator of surface moisture" (EPA, 2004b). The surface roughness length is known as the height at which the horizontal wind speed is zero (EPA, 2004b). AERMOD is sensitive to the surface roughness (Faulkner et al., 2008).

Site characteristics of the study domain can be represented by a weighted average of typical values provided for different land-use types. In this regard, MOE (2009b) suggested considering land-use types for both the study domain and a 1-km buffer. To account for spatial distribution of the site characteristics, different values of site

characteristics can be used for different wind-direction sectors in AERMET. A wind direction sector is the chop of the circle, e.g. 1-30 degrees.

Recommended values for site characteristics for 24 typical land-use types are provided by MOE (2009b). Among these, there are two residential land-use types: high intensity residential and low intensity residential. The high intensity residential is described as "highly developed areas with apartment complexes and row houses" whereas low intensity residential is described as "areas with a mixture of constructed materials and vegetation" (Wulder & Nelson, 2003).

Five scenarios of site characteristics were considered as listed below and site characteristics for each scenario were obtained from MOE (2009b):

- Scenario 1: Land-use is high intensity residential, called 'Urban'.
- Scenario 2: Land-use is low intensity residential, called 'Suburb'.
- Scenario 3: Site characteristics are weighted over the study area according to the fraction of different land-use types, called 'Land-Use Ave'.
- Scenario 4: Site characteristics are weighted over the study area according to the fraction of different land-use types in different eight wind direction sectors, called 'LU by Wind Direction'. The wind direction sectors were 1-45, 46-90, 91-135, 136-180, 181-225, 226-270, 271-315, and 316-360 degrees.
- Scenario 5: Mixing heights by the meteorological pre-preprocessor PCRAMMET (EPA, 1999c) in ISCST3 (EPA, 1995). ISCST3 was the U.S. regulatory atmospheric dispersion model before replacing AERMOD in 2006 (EPA,2004b). There are two land use options in ISCST3: urban and rural. The urban option was considered in this study.

Site characteristics in Scenarios 1 and 2 were obtained from MOE (2009b). Site characteristics in Scenarios 3 and 4 were calculated using land use of the study area. Unlike in Scenarios1-3, the site characteristics were determined for eight wind direction sectors in Scenario 4. At any given hour, one of them will be used in dispersion simulation of AERMOD based on the wind direction on that hour.

A land-use GIS layer from DMTI (2002) and a land-cover GIS layer from Geobase (2000) were used to classify the land-use of the study area into one of 32 USGS reference. Land-use within 2 km from the Huron Church Road were estimated as cropland and pasture (36%), followed by residential (34%), deciduous forest (10%), and commercial and industrial (11%), park and recreational (4%), water (3%), and government and recreational (2%). In Scenario 3, site characteristics for above-listed land-use types were obtained from MOE (2009b). The site characteristics were averaged based on the fraction of land-uses. Alternatively, average site characteristics can be calculated using AERSURFACE (EPA, 2013b). AERSURFACE uses US "national land cover datasets and look-up tables of surface characteristics that vary by land cover type and season".

Table 3.18 lists site characteristics in Scenarios 1-3. In all scenarios, albedo is the the highest in winter due to less vegetation and snow cover and therefore higher reflectivity of the earth. Surface roughness is the highest in Scenario 1, almost double that in other scenarios. This is because the height of obstacles (e.g. buildings) is larger in the urban areas compared to the other land-use types. Site characteristics in Scenarios 2 and 3 were similar as the suburb land-use (Scenario 2) may be rephrased as a mixture of constructed materials and vegetation (Scenario 3).

Table 3.18: Site characteristics in Scenarios 1-3

Scenarios	Season	albedo (A)	Bowen ratio (Bo)	Surface roughness (Zo, m)
Sceanrio 1 Urban (MOE, 2009b)	Winter	0.35	0.5	1
	Spring	0.18	1.5	1
	Summer	0.18	1.5	1
	Fall	0.18	1.5	1
Scenario 2 Suburb (MOE, 2009b)	Winter	0.45	0.5	0.5
	Spring	0.16	0.8	0.52
	Summer	0.16	0.8	0.54
	Fall	0.16	1	0.54
Scenario 3 Land-Use Average within 2 km from the road	Winter	0.49	0.54	0.32
	Spring	0.15	0.66	0.39
	Summer	0.18	0.70	0.48
	Fall	0.18	0.92	0.48

Site characteristics in Scenario 4 were different by the wind direction sector as shown in Figure 3.17. Distribution of Surface roughness was not even. It was higher in the wind direction sectors with a higher share of urban land use, e.g. 250-65 degree.

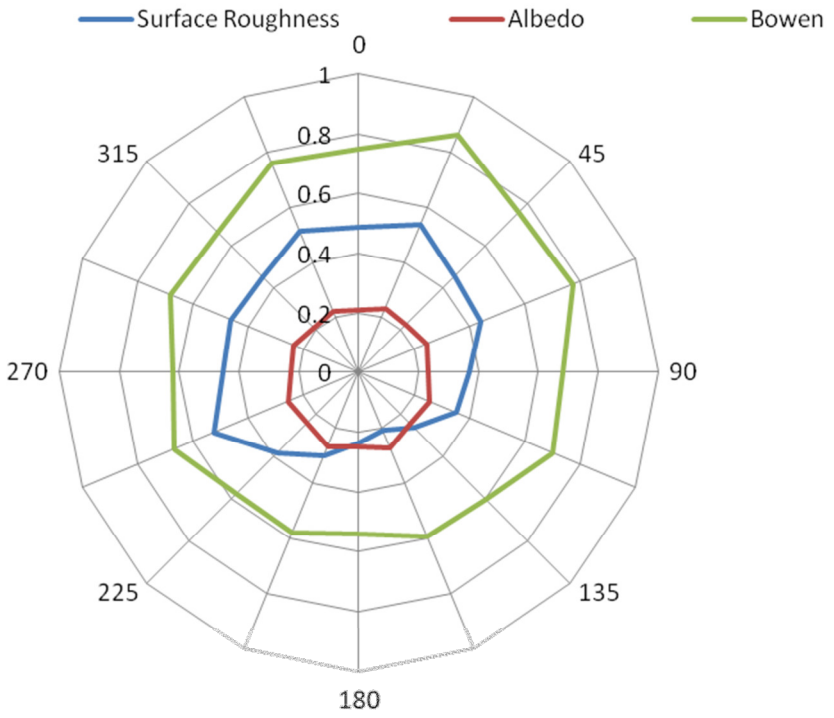

Figure 3.17: Site characteristics in Scenario 4, average of four seasons.

Meteorological data in 2008 were processed for each scenario. Their corresponding site characteristics for each Scenario were used in AERMET (2004b). NO_2 concentrations from traffic on Huron Church Road in 2008 were estimated using AERMOD for two receptors, 40m east and west of the EC Row-Northwood road section (Figure 3.8). Setup parameters are listed in Table 3.10

Hour-of-day convective and mechanical mixing heights estimated by AERMET were calculated. For the purpose of quality control, mixing heights estimated by AERMET were compared with those by MOE (2010) which were simulated for London, Ontario during 1996-99. Figure 3.18 compares hour-of-day pattern of mixing heights in Windsor (this study) and those in London. The mechanical mixing for Windsor-Urban option was slightly lower than those for London. This is because of slightly higher temperature and

wind speed in Windsor (annual means of 10 °C and 4.4 m/s, respectively) compared to those in London (annual means of 8 °C and 3.7 m/s), respectively. On the other hand, convective mixing heights were lower in Windsor than London. The mixing heights in the Windsor-Suburb option were the lowest.

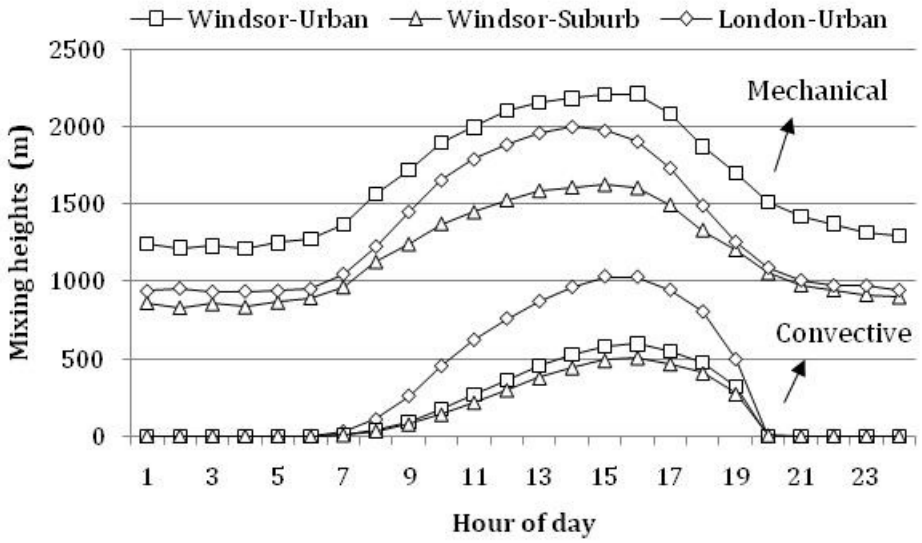

Figure 3.18: Comparison of mixing heights between Windsor (estimated using AERMET) and London (source of data: MOE, 2010)

NO_2 simulation

AERMOD simulates NOx concentrations using the NOx emissions. However, if NO_2 concentration is desired, there are two methods for NO_2 simulation in the AERMOD: Ozone Limiting Method (OLM) and Plume Volume Molar Ratio Method (PVMRM) (EPA, 2004a). Both methods are developed in the basis of the Reaction 3.1. Both methods assume that 10% of NOx in the plume is NO_2, and 90% is NO. The molecular weights of NOx and NO_2 were assumed to be equal in both methods, i.e. 42 g/mole.

The OLM utilizes a simplified approach for the reaction chemistry. The basic assumption in OLM is NO_2 concentrations (Reaction 3.1) are proportional to ground-level concentrations of NO and O_3 in units of parts per million (ppm) (Hanrahan, 1999). In other words, if O_3 concentration is less than NO concentration of the plume:

$$NO_{2\ plume}\,(ppm) = NO_{2\ initial}\,(ppm) + O_3\,(ppm) \qquad \text{(Hanrahan, 1999)} \qquad (3.11)$$

Reprinted with permission (Appendix D)

and if O_3 concentration is greater than or equal to NO concentration of the plume:

$$NO_{2\ plume}\,(ppm) = NOx_{\ initial}\,(ppm) \qquad \text{(Hanrahan, 1999)} \qquad (3.12)$$

Reprinted with permission (Appendix D)

It should be noted that initial NO and NO_2 concentrations are calculated using the ratio of NO_2/NOx emissions in the vehicle exhaust gas, provided by user, e.g. with a ratio of NO_2/NOx=0.1, the initial NO and NO_2 concentrations are 90% and 10% of NOx concentrations, respectively.

The OLM is limited for the use of only one emission source. The other drawback of OLM is that the formation of NO_2 in the NOx titration (Reaction 3.1) is not proportional to the moles of each reactant, but the concentration of reactants in ppm (Hanrahan, 1999).

In contrast to OLM, the PVMRM assumes that the NOx titration (Reaction 3.1) is proportional to the number of moles of reactants (Hanrahan, 1999). The PVMRM method calculates the NO_2/NOx ratio in the following four steps. First, the plume volume at a given receptor is calculated using dispersion coefficients, i.e. σ_y and σ_z. Second, number

of NOx moles in the plume volume is calculated using molecular weight of NOx (assumed as NO_2=46), ambient temperature, and ambient pressure. Third, the number of O_3 moles is calculated using O_3 concentrations. Fourth, the NO_2/NOx ratio is calculated using Equations 3.13 and 3.14, i.e. by assuming an initial NOx/NO_2 ratio of 0.1 in the exhaust and increasing the ratio by the value of moles O_3/moles NOx in the path to the receptor. The equilibrium ratio of NO_2/NOx is assumed to be 0.9.

NO_2/NOx = (moles O_3/moles NOx) + 0.1 (Hanrahan, 1999) (3.13)
Reprinted with permission (Appendix D)

$NO_2/NOx \leq 0.9$ (Hanrahan, 1999) (3.14)

Both OLM and PVMRM options in AERMOD were considered for NO_2 simulation. Spatial and temporal distribution of NO_2 concentrations in each option was observed. The hourly background O_3 concentrations were obtained from the Windsor West Station (MOE, 2009a). NOx and NO_2 concentrations by OLM and PVMRM methods were simulated using the AERMOD. Annual mean concentration was estimated at 50 receptors (Figure 3.9), and fall-off patterns of NO_2/NOx ratios were observed. Hourly concentrations were estimated at the receptor 40 m east of the EC Row – Northwood road section (Figure 3.8). Other simulation parameters are listed in Table 3.10.

3.7.3 Effect of stop-and-go movement in a microscopic level

This section explains the method used to:

- Identify effects of stop-and-go movement on vehicular NOx emissions and ambient air concentrations of NO_2

- Develop an analytical model for obtaining stop-and-go profiles of vehicles near signalized intersections
- Compare spatial distributions of NOx vehicular emissions estimated by the Micro-emission model (Panis et al., 2006) and a macro-emission model, Mobile6.2.
- Develop NOx correction factors for Mobile6.2 near signalized intersections, based on the spatial distributions of NOx emissions by the Micro-emission model and Mobile6.2.

3.7.3.1 Study area

Effects of stop-and-go were studied during morning peak of traffic (9:00-10:00). High levels of air pollution usually occur during this time, when traffic emission is high and dispersion factors including wind speed and atmospheric mixings are relatively low.

A 5.3 km section of Huron Church Road between College Avenue and Pulford Street was used for this study (Figure 3.2), as signalized intersection counts and timing plans were available only for the 12 signalized intersections along this road section. The morning peak hour (one busiest hour in 8-10 am) signalized intersection counts including number of cars and trucks at each approach were used. A detailed method for estimation of vehicle counts can be found in section 3.3.

Road geometries including the coordinates of intersections and lane configurations were obtained from Google Earth (2010). All the left-turn lanes in the northbound and southbound road are exclusive lanes (i.e. no shared left-turn and through lane). Signal timing plans including the durations of green, red and yellow intervals by approach at each signalized intersection and offset time for signal coordination were obtained from

the City of Windsor. The cycle time of all intersections is 120 seconds. The durations of intervals for through movement at each signalized intersection are shown in Figure 3.19. All signalized intersections were coordinated using a progression speed of 37 km/h.

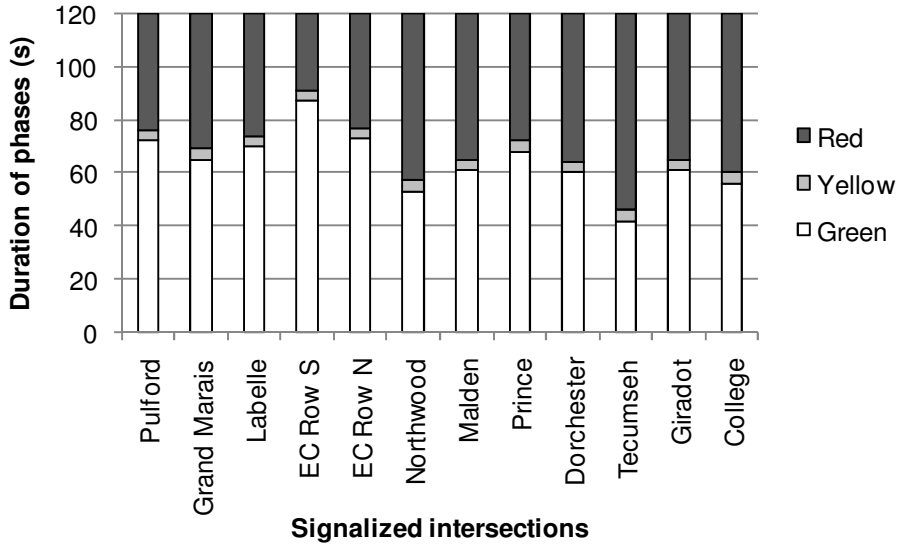

Figure 3.19: Duration of intervals for through movement at each signalized intersection

3.7.3.2 Description of Scenarios

To evaluate effects of stop-and-go traffic condition on NOx emission and NO_2 concentrations, seven scenarios were considered as listed in Table 3.19. Mobile 6.2 and the Micro-emission model were used for estimation of NOx emissions. The AERMOD was used for estimation of NO_2 concentrations. Mobile6.2 estimates emissions based on the average speed of vehicles and the road type while the Micro-emission model uses the speed and acceleration of the vehicles.

Table 3.19: Scenarios used to investigate effects of stop-and-go

	Speed profiles	Method for estimation of average speed and SAFD	Emission Model
S1	Base Case - Cruise 50km/h	-	Micro-emission model (Panis et al., 2006)
S2	Link-specific SAFD [a]	Analytical approach	
S3	Link-specific SAFD	Traffic simulation	
S4	Correction factors	-	
S5	Base Case-Arterial Road 50km/h	-	Macro-emission model, Mobile6.2 (EPA, 2003)
S6	Arterial Road and Link-specific average speed	Analytical approach	
S7	Arterial Road and Link-specific average speed	Traffic simulation	

[a] Speed and Acceleration Frequency Distribution

To estimate average speed, and the Speed and Acceleration Frequency Distribution (SAFD) at each link (≤10 m), two methods were used: 1) an analytical method and 2) a traffic simulation model. In the analytical method, a queue estimation model from the Canadian Capacity Guide by ITE (2008) along with some typical acceleration and deceleration profiles of vehicles from Akçelik and Besley (2001) was used. For the traffic simulation model, VISSIM (PTV AG, 2012) was used. The VISSIM traffic simulation model simulates individual movements of vehicles; thus, this method is more complex and requires more input data and processing work.

Scenarios 1 (Cruise 50 km/h) and 5 (Arterial 50 km/h) were assumed as the Base Case in the Micro-emission model and Mobile6.2, respectively (Table 3.19). In Scenarios 2 and 3, SADF at each link was estimated using the traffic simulation and the analytical approach, respectively. Similarly in Scenarios 6 and 7, the average speed at each link was calculated using the traffic simulation and the analytical approach, respectively. In

Scenario 4, NOx correction factors for Mobile6.2 were developed based on emission profiles by the Micro-emission model.

In Scenarios 1-3 and 5-7, the average speed and the SAFD estimated by the analytical approach and the traffic simulation were compared. In addition, the NOx emission and NO_2 concentration between the cases with and without consideration of stop-and-go movement were compared. For instance, to determine effects of stop-and-go movement using the Micro-emission model, results for the analytical method and the simulation (Scenario 2 and 3) were compared with those from cruising at50km/h (Scenario 1). On the other hand, results using the Mobile6.2 were compared to those from an arterial road 50 km/h (Scenario 5). It should be noted that this comparison does not quantify real effects of stop-and-go, as on the road, not all vehicles experience stop-and-go movements. In addition, the "Arterial 50 km/h" in Mobile6.2 already has the stop-and-go traffic condition, and it is not cruise only.

3.7.3.3 Spatial distribution of average speed and SAFD

To examine spatial variability in average speed and SAFD, the road sections were broken down into smaller pieces with a length less or equal to 10 m, called "links". The length of 10m was chosen to be consistent with the emission treatment into the atmospheric dispersion model, AERMOD (Table 3.10). In AERMOD, volume emission sources have a length equal or less than that of the width of the road, which is approximately 10 m. In total, there were 550 links in each direction of the road.

It is expected that the average speed of trucks be lower than that of cars, as average deceleration and acceleration of trucks are lower than those of cars. However, the result of a paired t-test indicates that the simulated average speeds of cars and trucks at links

were not statistically different at a 95% confidence interval (mean speed of cars: 43.4km/h and mean speed of trucks: 43.2km/h, $p > 0.05$). Therefore, the average speed and SAFD at each link was collected for cars only and were used for both cars and trucks.

Traffic simulation using VISSIM

The VISSIM traffic simulation model (PTV AG 2008) was used to capture instantaneous speed and acceleration of vehicles and to estimate average speed of vehicles at each link. In VISSIM, different vehicle lengths and acceleration/deceleration are used for cars and trucks separately. The model simulates individual vehicle movements based on cars following techniques and pre-specified vehicle operational characteristics. Entry volumes at each intersection were set to car and truck counts upstream of that road section. The volumes in each approach were estimated based on the proportions of left-turn, through and right-turn movements from Huron Church Road as observed in the intersection vehicle counts (Section3.2). Desired speed distribution of vehicles was set to the range of 55-65 km/h with an 85th percentile of 60 km/h which is the speed limit on the road. Since most trucks on the road were truck trailers with the approximate length of 22 m, their length was entered as 22 m. For cars, six default lengths–one for each of six classes – and their default proportions of total car traffic as in VISSIM (PTV AG 2008) were used.

Car and truck counts were collected in the middle of each road section and turning lanes. The simulation was run for 1 hour in the morning peak periods on weekdays (9:00-10:00). For the calibration purposes, the observed numbers of cars and trucks in the simulation were compared to the adjusted car and truck counts. They were similar; the

differences between the two mean counts were less than 5% for both cars and trucks in each direction.

The average speed of cars at each link was estimated using the link evaluation method in VISSIM. For estimation of SAFD, second-by-second speed and acceleration of cars were collected in the middle of each link. Data were collected in the middle lane and for a duration of 30 minutes, after a 10-minute warm-up of traffic simulation. It should be noted that traffic simulation starts with an empty network. The middle lane was selected because a majority of through traffic uses this lane.

The second-by-second speed and acceleration were categorized in the same format as the SAFD format used for development of driving cycles in Mobile6.2. This format includes 10 speed categories and 15 acceleration categories. The speed bins are in the range of 0-45mph with a step of 5 mph (i.e. 0 mph, 0.1-5 mph…. 40.1-45 mph), and the acceleration bins are in the range of -7.5 ~7.5 mph/s with a step of 1 mph/s (i.e. -7.5~-6.5 …. 6.5~7.5 mph/s). It should be noted that 1 mph is equal to 1.6 km/h and 1 mph/s is equal to 0.447 m/s^2.

Analytical approach

The analytical method was developed based on the assumption that when vehicles face red or yellow lights, they decelerate, stop, and then accelerate to reach to the cruise speed after the signal turns to green. Figure 3.20 depicts the movement of one vehicle in a space-time diagram. In order to determine the location of each accelerating and decelerating vehicle, the number of stopped vehicles at the end of the red phase needsto be estimated.

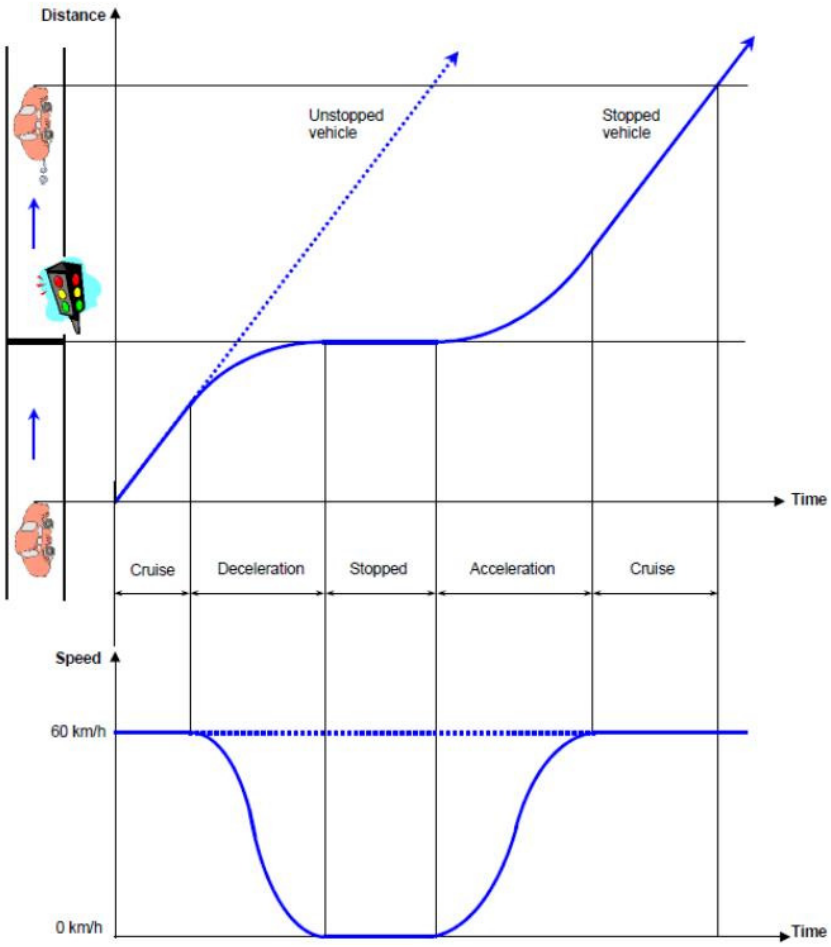

Figure 3.20: Space and time diagram for a vehicle approaching a signalized intersection (Source: Akçelik & Besley, 2001) – Reprinted with permission (Appendix D).

The number of stopped vehicles at the end of the red phase of signalized intersections was calculated using the "liberal estimate of average queue reach" by the Canadian Capacity Guide (ITE, 2008) as shown in Equation 3.15.

$$Q_{reach} = q\,(c - g_e) / [3600\,(1 - y)]\,K_f \qquad (3.15)$$

where:

Q_{reach} = number of stopped vehicles at the end of red interval (pcu)
q = lane-by-lane arrival flow (pcu/h)
c = cycle time (s), (i.e. 120s for Huron Church Road)

g_e = effective green interval (s)
y = lane flow ratio = q/S, where the S is saturation flow (pcu/h) (=1728 for the City of Windsor (ITE, 2008))
K_f = adjustment factor for the effect of the quality of progression

It should be noted that this method is more appropriate for a less-saturated condition where a majority of queued vehicles are discharged during the green interval, with less overflow to the next cycle. The method was deemed valid because the level of service for signalized intersections on Huron Church Road was in the range of A to C (DRIC, 2008a).

The lane-by-lane arrival flows at signalized intersections were estimated by converting all vehicles into passenger car units (pcu). Based on the Canadian Capacity Guide (ITE, 2008), each truck is equivalent to 2.5 pcu. An adjustment factor for quality of progression due to signal coordination was used. This factor is a function of green interval and the level of progression. Since all signals on the road are coordinated, the level of progression was assumed to be favorable. The adjustment factors were calculated using the green time of the signal. They were in the range of 0.3 - 0.8 for different signals.

After calculation of the number of stopped vehicles in the unit of pcu (Equation 3.15), the number of stopped cars and trucks were calculated as shown in Equations 3.16 and 3.17.

$$Q_{cars} = Q_{reach} / (1 + 2.5 \text{Truck/Car}) \quad (3.16)$$

$$Q_{trucks} = Q_{cars} \times \text{Truck/Car} \quad (3.17)$$

where:

Q_{reach}: number of stopped vehicles at the end of red interval (pcu) from Equation 3.15
Q_{cars} and Q_{trucks}: the number of stopped cars and trucks at the end of red interval (pcu), respectively
Truck/Car: the ratio of truck counts to the car counts

The physical length of the queue depends in the number of stopped vehicles and the spacing between vehicles, which is equal to the physical length of the vehicles plus the gap. For passenger cars, spacing is reported as 6 m (4 m length plus 2m gap). For trucks, spacing is assumed as 25 m because majority of trucks on Huron Church Road are truck trailers with a physical length of 22 m plus a 3m assumed gap. The physical length of the queue of the vehicles was calculated using Equation 3.18.

$$L_{que} = Space_{cars}Q_{cars} + Space_{trucks}Q_{trucks} \quad (3.18)$$

where:

L_{que}: physical length of the queue of the vehicles (m)
Q_{cars} and Q_{trucks}: number of stopped cars and trucks from Equations 3.16 and 3.17), respectively
$Space_{cars}$ and $Space_{trucks}$: spacing of cars and trucks (=6 m and 25 m for cars and trucks, respectively

It was assumed that only stopped vehicles are decelerate and accelerate. All other vehicles travel at the speed of 60 km/h, the speed limit of the road. The deceleration and acceleration profiles were obtained from a study by Akçelik & Besley (2001). These profiles, shown in Figure 3.21, are for a light-duty vehicle: acceleration from zero to the speed of 60 km/h (Figure 3.21a) and deceleration from 60 km/h to zero (Figure 3.21b). It

should be noted that these profiles were used for both cars and trucks although trucks are expected to have different acceleration and deceleration profiles.

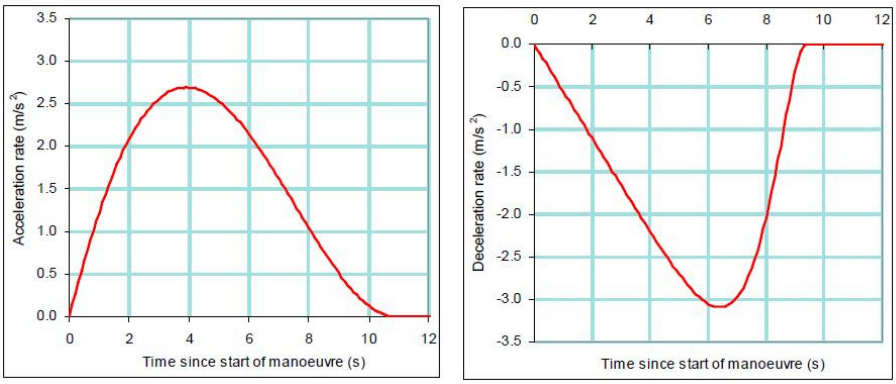

a) Accelerating from 0km/h to 60km/h b) Decelerating from 60km/h to 0km/h

Figure 3.21: Typical acceleration and deceleration profiles of vehicles near signalized intersections (Source: Akçelik & Besley, 2001) – Reprinted with permission (Appendix D).

A third-degree polynomial regression was fitted to the profiles ($p<0$, $R^2=0.98$) as shown in Equation 3.19.

$$a(t) = f_0 + f_1 t + f_2 t^2 + f_3 t^3 \quad (3.19)$$

where:

a(t): acceleration/deceleration of the vehicle at the time t (m/s^2)
t: time (s)
f_0 and f_1-f_3: constant and polynomial coefficients as listed in Table 3.20

The acceleration and deceleration functions were integrated to derive speed functions of accelerating and decelerating vehicles (Equation 3.20).

$$v(t) = \int a(t)dt = v_0 + f_0 t + \frac{1}{2} f_1 t^2 + \frac{1}{3} f_2 t^3 + \frac{1}{4} f_3 t^4 \quad v(t) = \int a(t)dt = c + \sum_{i=1}^{4} f_i t^i$$

(3.20)

where:

$v(t)$: Speed of the vehicle at the time t

v_0 : Speed of the vehicle at the time 0, i.e. 0 km/h for accelerating and 60 km/h for decelerating vehicles

The space-time functions of accelerating and decelerating vehicles were obtained by integrating the speed functions (Equation 3.21).

$$x(t) = \int v(t)dt = x_0 + v_0 t + \frac{1}{2} f_0 t^2 + \frac{1}{6} f_1 t^3 + \frac{1}{12} f_2 t^4 + \frac{1}{20} f_3 t^5 \quad (3.21)$$

where:

$x(t)$: Position of the vehicle at the time t

x_0 : Initial position of the vehicle

Table 3.20: constant and polynomial coefficients of acceleration and deceleration profiles in Figure 3.21

Coefficients	f_0	f_1	f_2	f_3
Acceleration	0.000	1.560	-0.269	0.012
Deceleration	0.000	-0.170	-0.198	0.023

Acceleration and deceleration distances were calculated to estimate the number of accelerating and decelerating vehicles and furthermore average speed on the link. From Equations 3.19-3.21, the time and distance for a vehicle accelerating from zero to 60 km/h were estimated as 10.4 s and 102 m, respectively. Similarly, the time and distance for a vehicle decelerating from 60 km/h to zero were estimated as 9 s and 90 m, respectively.

The average speed and SAFD at the middle of each link "M" were estimated in the following steps:

1) Stopped number of vehicles in the queue, estimated using Equation 3.15, was placed behind the stop line, with a spacing equivalent of cars and trucks. The

spacing equivalent was calculated by dividing the physical length of the queue (Equation 3.18) by the number of stopped vehicles (Equation 3.15). Figure 3.22 shows a sketch of stopped vehicles behind the stop line of a signalized intersection at the end of the red interval.

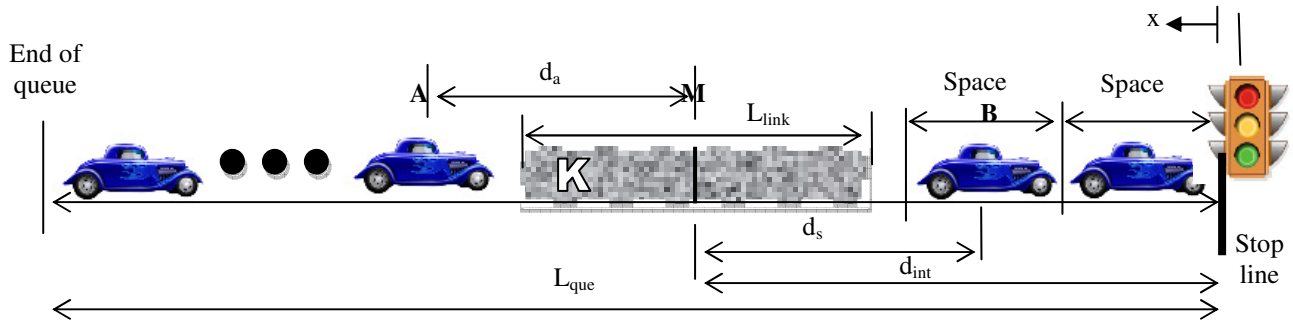

Figure 3.22: Sketch of stopped vehicles behind the stop line at the end of the red interval

2) Coordinates of each stopped vehicle (X_V) and the middle of link (X_M) with respect to the stop line were calculated; then, for each stopped vehicle, the difference 'X_V- X_M' was calculated.

3) If $0<X_V-X_M<102$ m (e.g. vehicle A in Figure 3.22), it means that this stopped vehicle will accelerate while crossing point M. This is because the point M is located before the stopped vehicle, and its distance from the stopped vehicle is less than the acceleration distance of 102 m. Acceleration and speed of such a stopped vehicle while crossing point M were estimated by solving Equations 3.19-3.21.

4) If $-90<X_V-X_M<0$ (e.g. vehicle B in Figure 3.22), it means that this stopped vehicle has decelerated while crossing point M. This is because the point M is located after the stopped vehicle, and its distance to the stopped vehicle was

less than the stopping distance for deceleration (90 m).Deceleration and speed of such a stopped vehicle while crossing point M were estimated by solving Equations 3.19-3.21.

5) For calculation of idling time, it was assumed that the queue is formed linearly, in which the first stopped vehicle idles for the whole yellow and red intervals and the last vehicle decelerates but does not idle. This assumption is based on assumption of a constant flow of incoming vehicles. Thus, the idling time was calculated if the middle of the link was located within the queue zone, between the stop line and the tail of queue. In other words, if $0<X_M< L_{que}$ (Figure 3.22). The idling time at each link was calculated as shown in Equation 3.22.

$$Time_{idle} = Time_{idle\ of\ veh} \times N_{idle} \quad (3.22)$$

$$Time_{idle\ of\ veh} = (1-d_{int}/L_{que}) \times (\text{Red time} + \text{yellow time})$$

$$N_{idle} = L_{link}/Space_{equ}$$

where:

$Time_{idle}$: Total idling time at each link (s)
$Time_{idle\ of\ veh}$: Idling time for one vehicle (s/pcu)
N_{idle} : Average number of idling vehicles at each link (pcu)
d_{int}: Distance from point M (middle of link) to the stop line (m) (Figure 3.22)
L_{que}: Length of queue (m) (Figure 3.22)
L_{link}: Length of link (~10 m) (Figure 3.22)
$Space_{equ}$: Spacing equivalent of cars and trucks ($=L_{que}/Q_{reach}$; Q_{reach} from Equation 3.15; m/pcu) (Figure 3.22)

The number of cruising vehicles at each link was estimated by subtracting lane-by-lane arrival flow during each cycle of intersection (i.e. $q \times 3600/120$) from the number of vehicle accelerating and decelerating at the middle of the link.

6) The average speed at each link was calculated by dividing total distance traveled by total time lapsed as shown in Equation 3.23:

$$Avg\ Speed = \frac{L_{seg} \times (N_{cruise} + N_{acc} + N_{dec})}{N_{cruise} \times \frac{L_{seg}}{V_{cruise}} + L_{seg} \sum_{i=1}^{N_{acc}} \frac{1}{V_{acc}(i)} + L_{seg} \sum_{i=1}^{N_{dec}} \frac{1}{V_{dec}(i)} + Time_{idle}} \quad (3.23)$$

where:

N_{cruise}, N_{acc}, and N_{dec}: Numbers of cruising, accelerating, and decelerating vehicles passing the midsection, respectively (Figure 3.22)
V_{cruise}: Speed of the cruising vehicles, i.e. 60km/h
$V_{acc}(i)$: Speed of accelerating vehicle i while passing the midsection
$V_{dec}(i)$: Speed of decelerating vehicle i while passing the midsection
$Time_{idle}$: Total idling time at each link from Equation 3.22

7) Speed and acceleration frequency distribution (SAFD) at each link was estimated by categorizing the time spent in each specific acceleration and speed category. Similar to traffic simulation method, the category was a table composed of 10 columns of speed bins and 15 rows of acceleration bins.

For display of results, SAFD were summarized to four vehicle operational modes as Cruise (-0.447 m/s^2<acceleration<0.447 m/s^2), Idle (speed=0 and acceleration=0), Acceleration (acceleration>0.447 m/s^2), and Deceleration (acceleration<-0.447 m/s^2). It should be noted that acceleration of 0.447 m/s^2 is equal to 1 mile/hr/s.

3.7.3.4 Vehicular emission

As discussed earlier, two methods for calculation of emission were considered: the Micro emission model and Mobile6.2. These methods are described in detail below.

Micro-emission Model

A micro-emission model developed by Panis et al. (2006) was used to estimate emission rates of cars and trucks under different speed and acceleration conditions. This model was developed using observed instantaneous speed, acceleration, and emission of vehicles

under urban traffic conditions. Equation 3.24 (Panis et al., 2006) shows the non-linear multiple regression model.

$$NOx(t) = \max(E0, f_1 + f_2 v(t) + f_3 v(t)^2 + f_4 a(t) + f_5 a(t)^2 + f_6 v(t) a(t) \quad (3.24)$$

(Panis et al., 2006) – Reprinted with permission (Appendix D)

where:

NOx(t): NOx emission rate at time t in g/s
v(t) and a(t): Instantaneous speed (m/s) and acceleration of vehicles (m/s^2) at time t, respectively
E0: Lower limit of emission (g/s) specified for each vehicle type
f_1-f_6 : Regression coefficients listed in Table 3.21.

Table 3.21: Regression coefficients and lower limit of emission (Source: Panis et al., 2006)

	E0	f_1	f_2	f_3	F_4	F_5	f_6
Gasoline car ($a \geq -0.5$ m/s^2)	0	6.19E-04	8.00E-05	-4.03E-06	-4.13E-04	3.80E-04	1.77E-04
Gasoline car ($a < -0.5$ m/s^2)	0	2.17E-04	0	0	0	0	0
Heavy Duty Vehicle	0	3.56E-02	9.71E-03	-2.40E-04	3.26E-02	1.33E-02	1.15E-02

Using the Micro-emission model (Equation 3.24), emission rates of light-duty and heavy-duty vehicles were calculated for 10 categories of speeds and 15 categories of acceleration. This lookup table was used for estimation of emissions using the Micro-emission model. Figure 4.23 shows these emission rates. As expected, higher emissions were observed in higher accelerations.

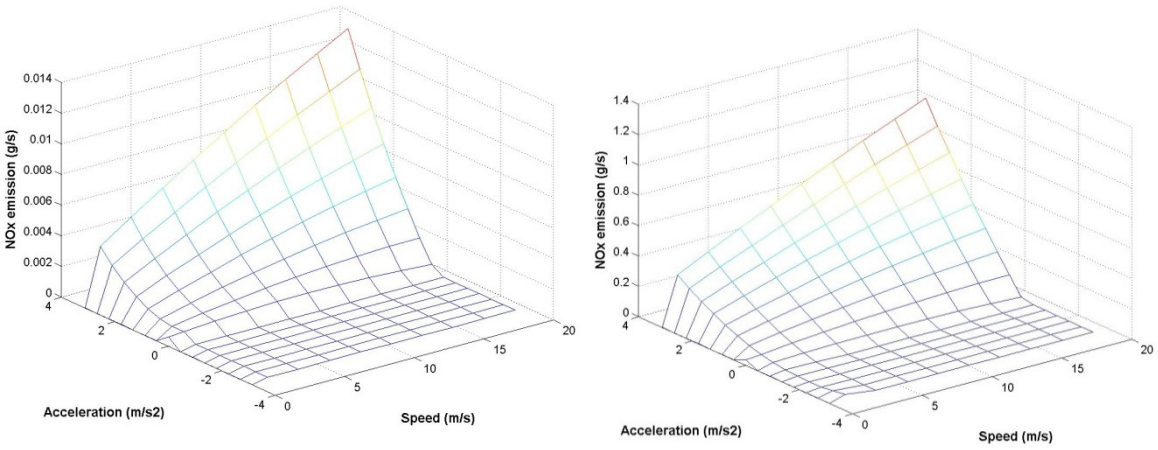

(a) LDVs (b) HDVs

Figure 3.23: NOx emission rate of vehicles versus speed and acceleration (Source of data: Panis et al., 2006)

Idling emission at each link was calculated for cars and trucks separately using Equation 3.25. It was assumed that vehicle composition in the queue is the same as vehicle composition in the arrival flows.

$$NOx_{idle} = Time_{idle} \times N_{idle} \times ER_{idle} \quad (3.25)$$
$$N_{idle} = L_{link} / Space \times Composition$$

where:

NOx_{idle}: Idling NOx emission of vehicles (g)
$Time_{idle}$: Total idling time at each link (s) from Equation 3.22
N_{idle}: Total number of idling vehicles for all lanes (veh)
ER_{idle}: Idling emission rate of vehicles (g/s/veh)
$L_{linkveh)}$: Length of link (~10 m)
Space: Space occupy by each vehicle, i.e. 25 m for trucks and 6m for cars
Composition: Traffic composition of vehicles, i.e. for cars is car% and for trucks is truck %.

Emissions during non-idling modes (acceleration, deceleration, and cruise) were calculated using the speed of vehicles and the length of the link. Emissions were

calculated for cars and trucks separately. For each link, emissions for given speed-acceleration categories were calculated and they were summed over all categories (10 Speed × 15 Acceleration) as shown in Equation 3.26.

$$NOx = \sum_{v=1}^{10} \sum_{a=1}^{15} L_{link} ER(a,v) \times N(a,v) / Speed(a,v) \tag{3.26}$$

where:
NOx: Total NOx emissions of vehicles at each link (g/h)
L_{Link} : Length of link (~10 m)
ER(a,v): Emission rate of vehicles at the specific acceleration (a) speed (v) category (g/s/veh) (Figure 4.23)
N(a,v): Vehicle counts (veh/h)
Speed (a,v): Speed of vehicles (m/s) at the specific acceleration (a) and speed (v) categories

Mobile6.2

Average speed and road type are the two parameters used by Mobile6.2 to represent driving cycles. Average speed of vehicles at each link was already estimated using the traffic simulation and the analytical approach. To determine the proper road type in this study, the modal distributions of driving cycles in different road types of Mobile6.2 were examined. The three road types in Mobile6.2: arterial, freeway, and local are explained below. The local road is only specific to the average speed of 20.1 km/h. In other words, if the local road is chosen, Mobile6.2 uses a default speed of 20.1 km/h instead of requiring an average speed input. Figure 3.24 compares the SAFD of driving cycles at the three particular road types with similar average speeds in the range of 18 to 21 km/h. It was observed that the majority of freeway driving at average speed of 21 km/h is spent in cruising at a low speed (5-35 km/h; Figure 3.24(a)). Contrarily, the majority of arterial

driving is in idling or cruising in high speeds (40-60km/h; Figure 3.24(b)). Overall, local driving (Figure 3.24(c)) is similar to arterial driving.

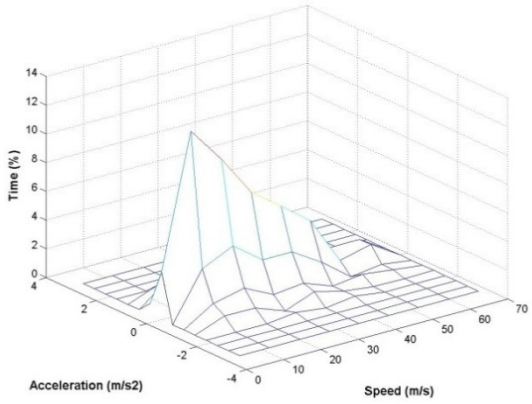

(a) Freeway – Average speed: 21km/h

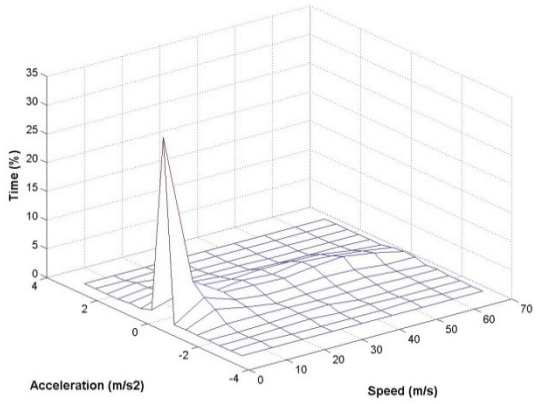

(b) Arterial – Average speed: 18.5km/h

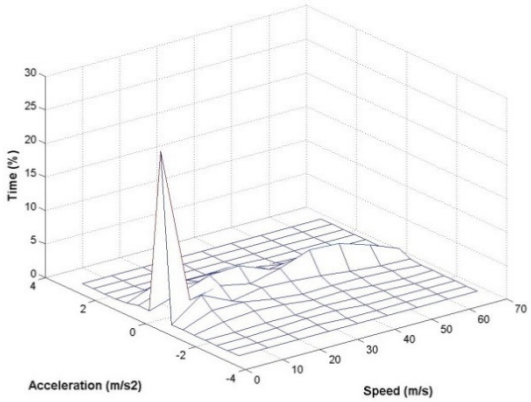

(c) Local – Average speed: 20.1km/h

Figure 3.24: Time distribution of speed and acceleration at three selected driving cycles (Source of data: EPA, 1997).

Figure 3.25 shows the time distribution of vehicle operational modes at the three driving cycles of the arterial road. It was observed that as the average speed in arterial road increases, the time in idling linearly decreases whereas the time in cruising linearly increases. For instance, in the average speed of 40 km/h, the time in idling is 15% lower compared to the average speed of 20 km/h. It was estimated that at the average speed of

50 km/h, which is close to the average speed on Huron Church Road, approximately 70% of vehicles are cruising, 6% idling, and the other 24% accelerating and decelerating.

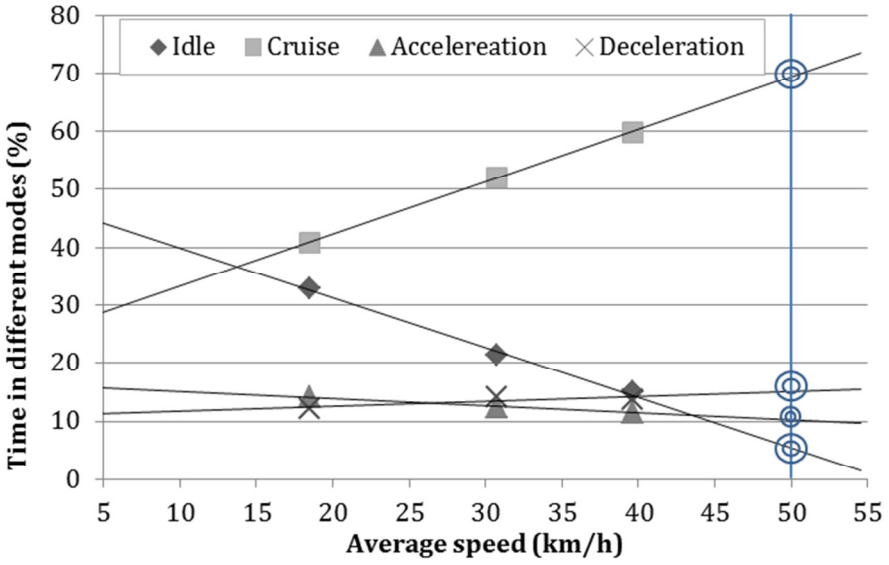

Figure 3.25: Three driving cycles of the arterial road by driving modes (EPA, 1997)

Among the three road types, the Arterial Road reflects the stop-and-go movements more reasonably for this study. This is because Huron Church Road driving is similar to the arterial driving (Figure 3.24b) where average speed of vehicles is mainly affected by idling, acceleration, and deceleration. The cruise speed on the road is also similar to that in arterial driving 40 to 60 km/h.

NOx emission at each link was calculated using default input parameters of Mobile6.2. The maximum/minimum temperature was set to 7/13 °C, and Ontario annual average fuel properties were used. The arterial road was selected.

3.7.3.5 Correction factors for NOx emissions by Mobile6.2 near signalized intersections

As discussed in Section 2.5.2, Mobile6.2 tends to underestimate emissions near

signalized intersections where a large portion of vehicles stop and go. Correction factors were derived to adjust vehicular emissions near the signalized intersections. These factors were developed using NOx emissions estimated by the micro-emission model using the analytical approach (Scenario 3 in Table 3.19).

Driving modes of vehicles in areas near signalized intersections were classified into deceleration, queue, and acceleration zones as shown in Figure 3.26. In the deceleration zone, vehicles start to decelerate at red intervals. In the queue zone, vehicles may cruise, decelerate, stop, or accelerate. In the acceleration zone, the stopped vehicles start to accelerate at green intervals.

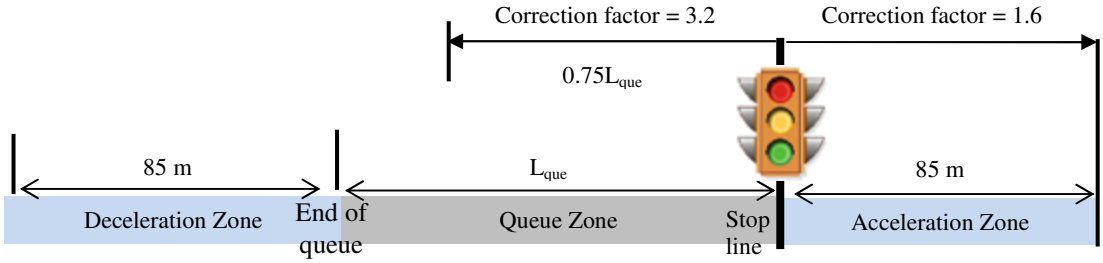

Figure 3.26: Sketch of driving modes of vehicles near signalized intersections

Correction factors for NOx emission were developed in the following steps:

1) NOx emissions at each link (≤10 m) by the Micro-emission model (Scenario 3) were normalized based on NOx emissions for a cruise speed of 60 km/h on that link. In other words, they were normalized based on emissions upstream of the intersection, where all vehicles cruise at 60 km/h.
2) Average normalized emissions in the deceleration, queue, and acceleration zones, were calculated, and were approximately 0.75, 3.9, and 1.6, respectively. This means that there were 25% less emissions in deceleration zone than the emissions

for a constant speed of 60 km/h while emissions in the queue zone are 3.9 times higher than the emissions for a constant speed of 60 km/h. The length of deceleration and acceleration zones was calculated, and was approximately 85 m for each (Figure 3.26).

3) To reduce the number of correction factors, the reduced emissions in the deceleration zone were combined with a portion of the queue zone. It was found that amount of reduced emission in deceleration zone was approximately equal to the increased emission at the 25% of the queue zone immediately downstream of the deceleration zone (Figure 3.26). Finally, two correction factors were estimated. First, the factor for upstream of signalized intersections was calculated as 3.2, which should be applied to the 75% of the physical queue length behind the stop line (Figure 3.26). Second, the factor for downstream of signalized intersections was 1.6. This should be applied to the acceleration zone, 85m downstream of signalized intersections.
4) Separate correction factors were developed for LDVs (cars) and HDVs (trucks) by repeating steps one to three for car and truck NOx emissions, separately.

3.7.3.6 NO_2 simulation

NO_2 concentration was estimated using the AERMOD. Meteorological parameters in 2008 at the hour 9:00 (9:00-10:00 in the local time) were used. Discreet receptors were placed with a spacing of 40 m in both parallel and perpendicular to the road up to 1000 m away from the centerline of the road (Figure 3.8). Other setup parameters are listed in Table 3.10. NO_2 concentrations in Scenarios 1-4 (Table 3.19) were estimated. Two transit lines parallel to the road are located 40m and 200m from the center of the road. NO_2

concentrations were compared among scenarios at these transit lines. The percentage differences in concentrations between cases of stop-and-go (Scenarios 2 and 3) and the cruise 50km/h were calculated and plotted.

CHAPTER IV

4. RESULTS OF PART I: SPATIAL AND TEMPORAL DISTRIBUTIONS OF VEHICLE COUNTS, EMISSIONS AND CONCENTRATIONS

4.1 Vehicle counts

4.1.1 Long-term variations in vehicle counts

As explained in Section 3.3, monthly and annual variations in Windsor-Detroit Border Crossing were used to adjust the vehicle counts at each intersection of Huron Church Road. Figure 4.1 shows the annual car and truck counts at the Windsor border crossing from Canada to US. The number of border crossing cars consistently decreased during 2004 to 2008. On the other hand, truck counts were approximately constant during 2004 to 2007, and decreased by 17% in 2008 due to the economic crisis experienced in this region. The annual adjustment factor for each year was the ratio of counts on that year by the year 2008 counts.

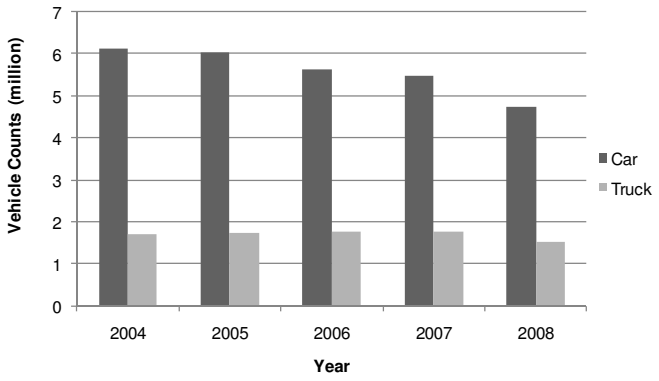

Year		
	Adjustment factor	
	Car	Truck
2004	0.774	0.888
2005	0.786	0.865
2006	0.842	0.853
2007	0.867	0.852
2008	1.000	1.000

Figure 4.1: Annual car and truck counts at Windsor border crossing from Canada to U.S. (Data source: BTS (2009))

Monthly variation in truck counts during 2004-2008 is shown in Figure 4.2. Except for 2008, monthly variations during 2004 - 2007 were similar. Truck count were low during cold months of December, January and February and high during warm months of May, June, and August – November. However, truck counts were the lowest in July as two weeks of this month is the shut-down time of automotive industries in Windsor and Detroit. It should be noted that a majority of cross-border trucks carry loads for the automotive industries.

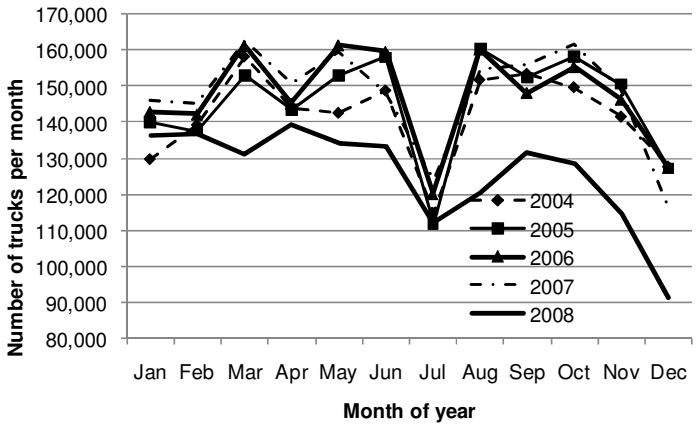

Month	Truck adjustment factor
Jan	1.019
Feb	1.010
Mar	0.924
Apr	0.981
May	0.944
Jun	0.947
Jul	1.215
Aug	0.948
Sep	0.955
Oct	0.940
Nov	1.008
Dec	1.202

Figure 4.2: Monthly truck counts at Windsor border crossing from Canada to U.S. in 2004-2008. (Source: BTS (2009))

Figure 4.3 shows monthly variations in car counts at two traffic count stations along the Huron Church Road (Figure 3.2). Monthly variations at both stations were similar. The counts were high in April and September and low in the other months. Monthly adjustment factors, the ratio of annual average counts to the count in a given month, were

in the range of 0.93 – 1.07. This indicates that monthly car counts varied only 7% compared to the annual average counts.

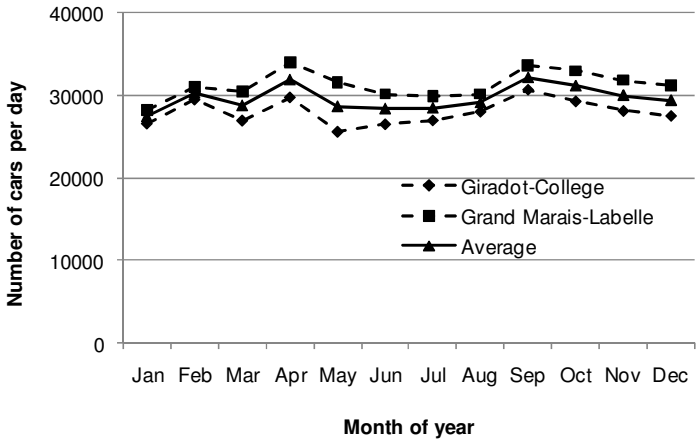

Month	Car Adjustment factor
Jan	1.071
Feb	0.994
Mar	1.060
Apr	0.931
May	1.011
Jun	1.030
Jul	1.022
Aug	0.996
Sep	0.940
Oct	0.941
Nov	0.996
Dec	1.030

Figure 4.3: Daily car counts on Huron Church Road by month in 2008 at two traffic count stations.

4.1.2 Spatial patterns of vehicle counts

Figure 4.4 shows the adjusted car and truck counts, and truck percentages (i.e. the number of trucks divided by the sum of the numbers of cars and trucks) in 2008 on northbound road during the morning peak period and southbound road during the afternoon peak period. As explained in Section 3.4, the morning peak period at Huron Church Road occurred on the northbound road and the afternoon peak period on southbound road. In the northbound direction, car counts generally increased towards the exit ramp to the eastbound EC Row Expressway (a major urban highway that runs across the city in the east/west direction), decreased in the section between the exit ramp and the entrance ramp, and increased again immediately north of the entrance ramp. This reflects

that a substantial portion of cars leaves and enters Huron Church Road at the junctions with the Expressway. Figure 4.4(a) also shows that car counts gradually decreased towards the border crossing north of the Expressway. This is expected since local car traffic leaves Huron Church Road at the cross streets before the border crossing. However, there was no significant variation in truck counts across different road sections.

The afternoon peak on Huron Church Road was in the southbound road, where most U.S. commuters return home by car and a high number of trucks travel from the U.S. to Canada. Car counts increased towards the Expressway due to merging cars from the cross streets and the Expressway (Figure 4.4(b)). However, car counts gradually decreased south of the Expressway due to diverging cars to the cross streets. Similar to the spatial pattern in the northbound road, truck counts did not vary significantly in the southbound road. This reflects that a majority of trucks that cross the border continue travelling along Huron Church Road towards Highway 401 (a major truck route to central and southwestern Ontario) without diverging to the cross streets.

On average, truck percentages on the northbound and southbound roads were 17% and 19%, respectively (Figure 4.4). Truck percentages were slightly higher in the road sections between Howard Ave and HC line road, as the car counts were lower in these road sections.

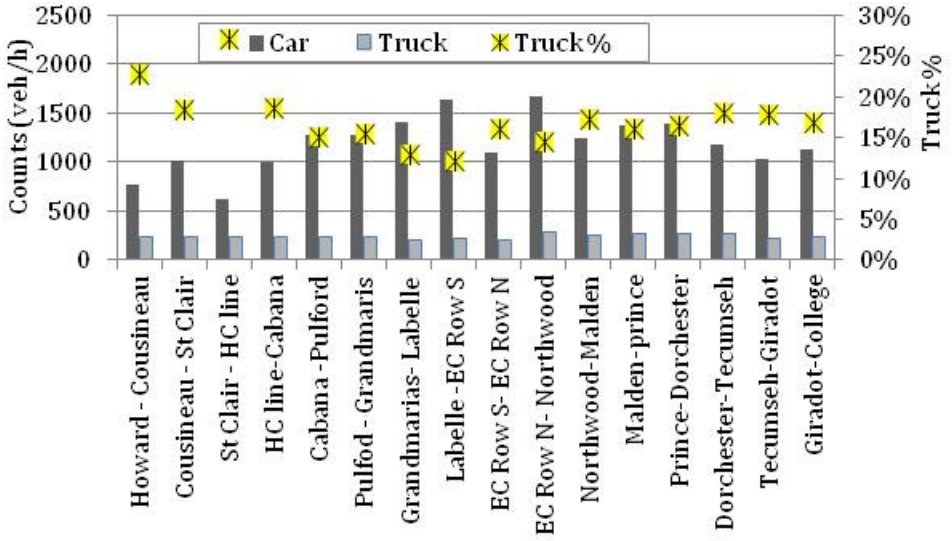

(a) Morning peak period in northbound direction

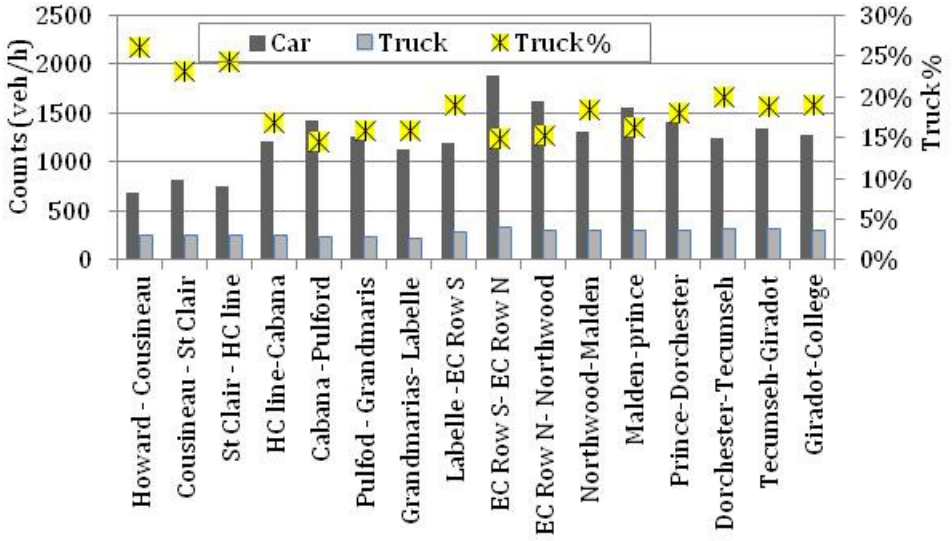

(b) Afternoon peak period in southbound direction

Figure 4.4: Adjusted car and truck counts in 2008 during peak hours on Huron Church Road

Figure 4.5 shows spatial distribution of annual total car and truck counts in 2008 across road sections on Huron Church Road. In comparison to car counts, truck counts varied less among road sections. Truck and car counts were higher between EC Row and College Ave. Car and truck counts were similar in northbound and southbound roads.

Truck percentages were much higher in annual average counts (in the range of 18%-37% with an average of 24%) than peak hour counts (in the range of 12%-27% with an average of 18%) (Figure 4.4). Since trucks produce more emissions than cars, particularly for PM and NOx, the use of peak hours for investigation of vehicular emission and air quality may not reflect the worst case scenario.

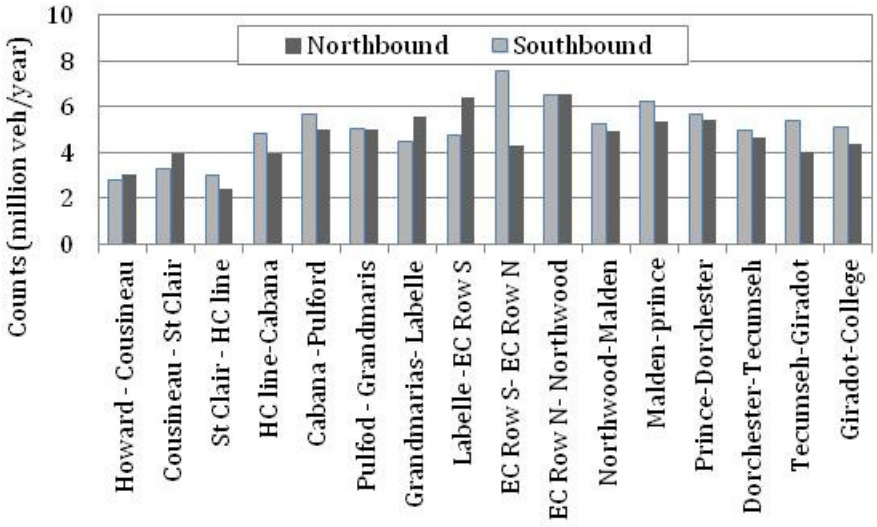

(a) Car counts

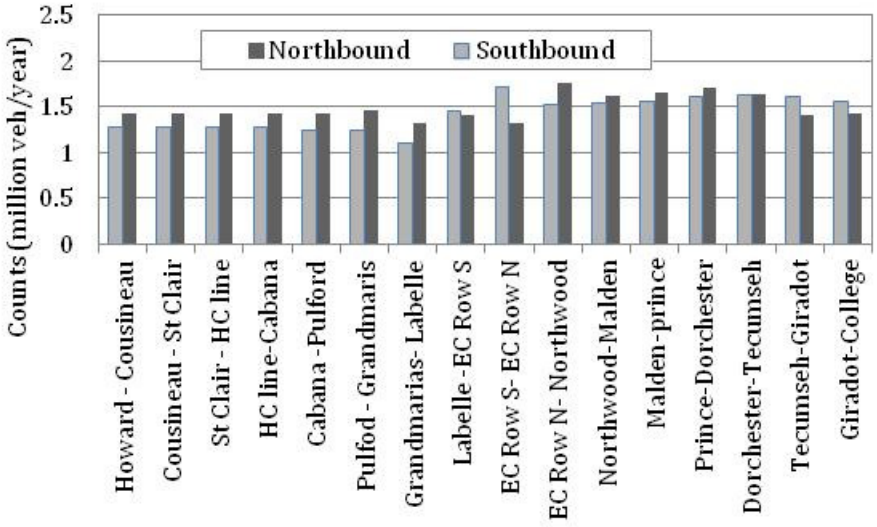

(b) Truck counts

Figure 4.5: Annual vehicle counts by road segment in 2008

Figure 4.6 shows spatial distribution of unidirectional annual vehicle counts. Truck counts were slightly higher in the section between EC Row Expressway and College Ave as a portion of trucks enter or exits Huron Church Road through EC Row Expressway. Car counts were the lowest in the section between Howard Ave and Cabana Road.

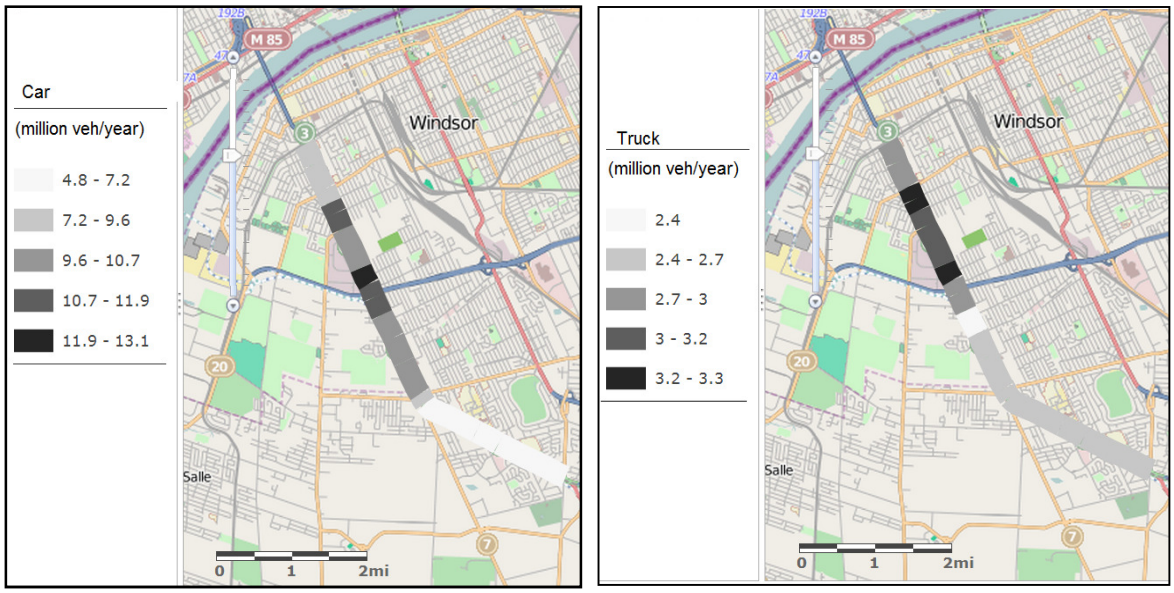

(a) car counts (b) truck counts

Figure 4.6: Spatial distribution of unidirectional annual vehicle counts in 2008

4.1.3 Temporal patterns of vehicle counts

Figure 4. 7 shows hour-of-day variations in car and truck counts by traffic station, direction of travel, day of week, and season. Hour-of-day patterns of vehicle counts were similar at both stations (Figure 3. 2).

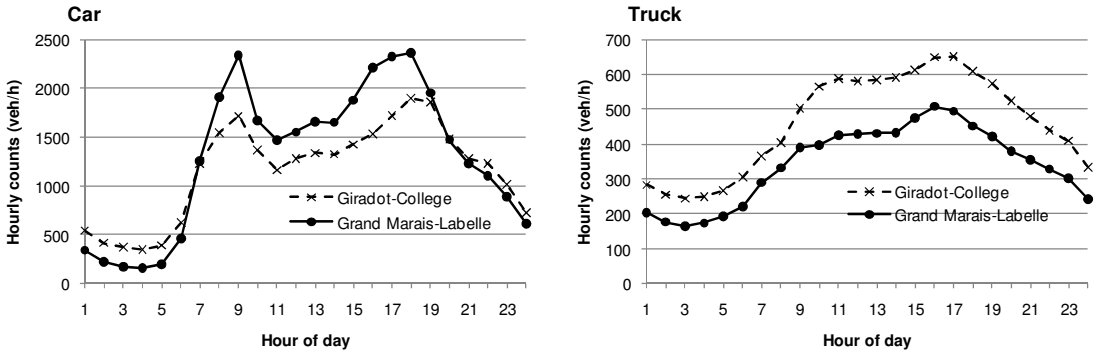

(a) Hour-of-day variation at the two traffic count stations

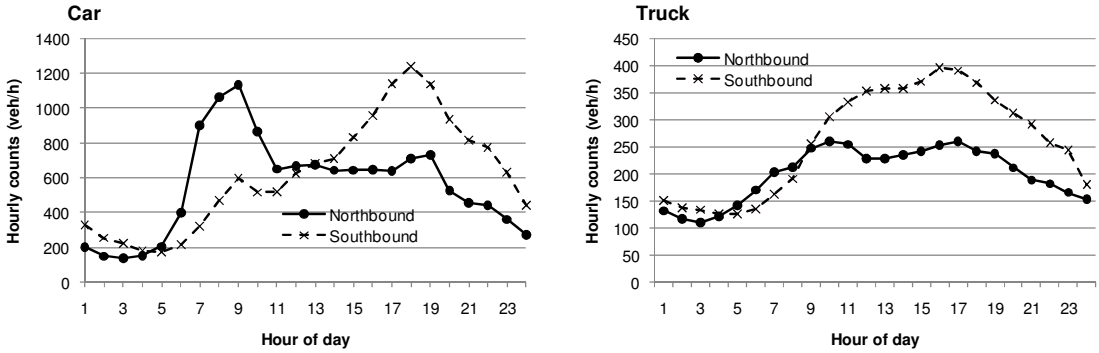

(b) Hour-of-day variation by direction at Giradot - College road section

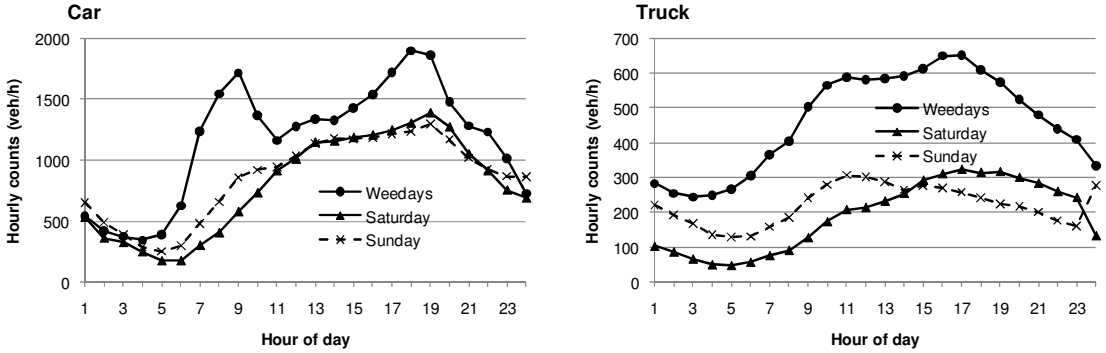

(c) Hour-of-day variation at Giradot - College road section by day of week

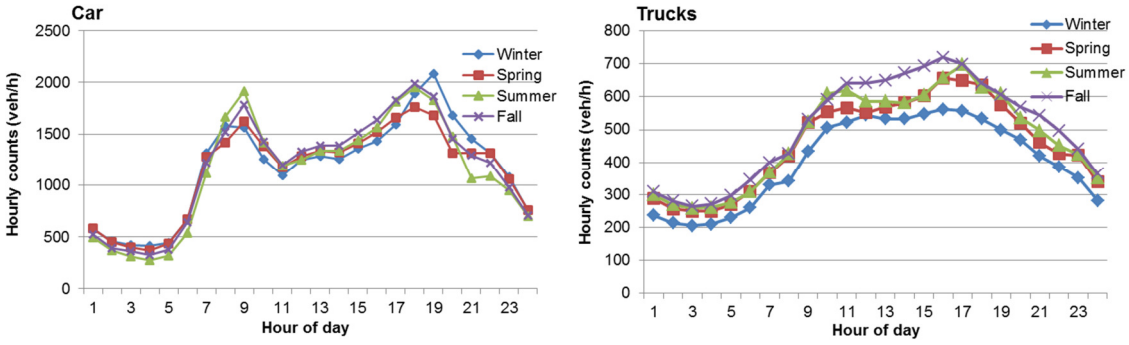

(d) Hour-of-day variation at Giradot - College road section by season

Figure 4.7: Hour-of-day variations of vehicle counts in 2008

It was observed that car and truck counts increased in the morning (1:00-8:00). Two distinct peaks of car counts were observed in the morning peak hour at 9:00-10:00 and afternoon peak at 17:00-18:00. These peaks reflect work trips including between Canada and the US. Truck counts slightly increased during 9:00-17:00. After 17:00, both car and truck counts decreased.

Overall, hour-of-day variability was significant for both car and truck counts ($p < 0.05$). The results of one-way ANOVA showed that a mean vehicle count for at least one hour among 24 hours is significantly different from the mean vehicle counts for the other hours. To identify the hours during which vehicle counts are significantly different from the counts in the other hours, the Scheffe test was performed. The results of the Scheffe test showed that the northbound car counts during the morning peak period (9:00-10:00) and the southbound car counts during the afternoon peak period (17:00-18:00) were significantly higher than the car counts in the other hours at both stations ($p < 0.05$).

Hour-of-day variations in hourly counts on the Giradot – College section were also different between northbound and southbound directions as shown in Figure 4.7(b). It was found that hour-of-day southbound truck counts were significantly higher than the northbound counts ($p < 0.05$).

Day-of-week variations in hourly vehicle counts on the Giradot – College section are shown in Figure 4.7(c). Both car and truck counts were higher on weekdays than weekends. Moreover, truck counts were higher in the morning and lower in the afternoon on weekends. The results of the paired t-tests showed that three pairs of hour-of-day car counts, weekdays – Saturday, weekdays – Sunday, and Saturday – Sunday, were all

significantly different ($p < 0.05$). But hour-of-day truck counts were not significantly different between Saturday and Sunday.

Seasonal variations in hourly car counts on the Giradot – College section are shown in Figure 4.7(d). The results of the paired t-tests showed that hour-of-day car counts were significantly different between summer and fall ($p = 0.02$). On the other hand, truck counts were lower in winter than spring, summer and fall. The results of the paired t-test showed that all 6 pairs of hour-of-day truck counts between the four seasons (spring, summer, fall, and winter) were significantly different ($p < 0.05$).

4.2 Temporal patterns of NOx and benzene emission factors

Benzene emission factors of cars fueled in Michigan were 29% higher than benzene emission factors of cars fueled in Ontario (20.1 vs. 15.6 mg/VKT). This is because most of cars are gasoline (98.5%, Table 3.8), and the benzene content of Ontario gasoline is half of Michigan gasoline (Table 3.4). Also, it was estimated that 76% of cars on Huron Church Road use Ontario fuel (Section 3.5).

Figure 4.8 shows hour-of-day benzene emission factors of cars and trucks by season. For both cars and trucks, the trends were similar in spring and fall. The colder the season is, the higher the emission is. This is due to higher cold start emissions in colder months. In warmer seasons (spring, summer and fall), higher emission factors were observed for cars during the daytime due to higher evaporative emissions.

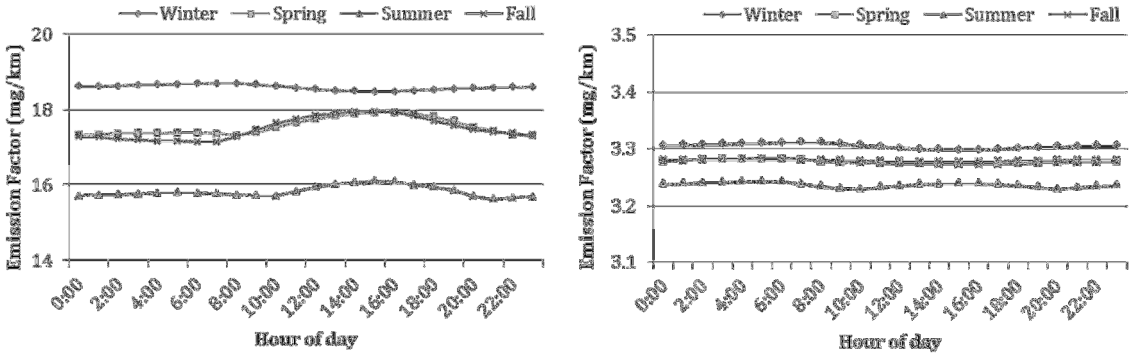

(a) Cars (b) Trucks

Figure 4.8: Hour of day benzene emission factor by season from Mobile6.2

In comparison with cars (Figure 4.8 (a)) for which the changes in benzene emissions factor were up to 20% from season to season and up to 10% from hour to hour, the changes for truck emission factor (Figure 4.8(b)) were negligible (2%). This is because a majority of trucks were diesel and benzene emission factors of diesel vehicles are low and slightly vary with ambient temperature in Mobile6.2.

NOx emission factors of cars using Ontario and Michigan fuels were equal (0.46 g/VKT) reflecting little effect of gasoline properties in Mobile6.2 on NOx emissions. Figure 4.9(a) shows hour-of-day variation in NOx emission factor by season. Similar to benzene emission factors, the emission was higher in colder seasons due to higher cold start emissions. In spring and fall, lower NOx emission was observed for cars during the daytime due to lower cold start emissions. In summer, higher emission was observed during the daytime. This is because in the calculation of NOx emission factor in Mobile6.2, two different equations are used (EPA, 1999b). When temperature is below 75°F (20°C), the NOx emissions decrease as the temperature increases. In contrast, when temperature is above 75°F, the NOx emissions increases as the temperature increases due

to air-conditioner use. There are no significant seasonal and hour-of-day variations in NOx emission factors of trucks (Figure 4.9(b)). This is because trucks are HDVs and Mobile6.2 does not use any temperature correction factor for HDVs (EPA, 1999b).

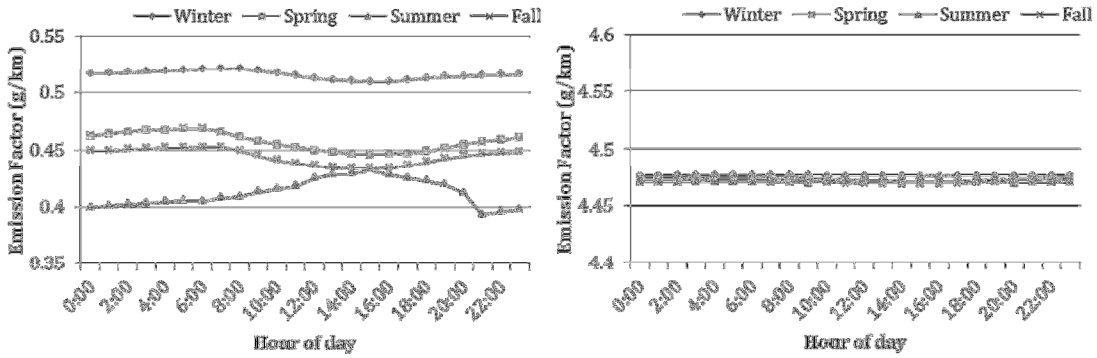

(a) Cars (b) Trucks

Figure 4.9: Hour of day NOx emission factor by season from Mobile6.2

4.3 NOx and benzene emissions

4.3.1 Spatial patterns of emissions

Figure 4.10 shows simulated benzene and NOx emissions at each road segment. NOx emission is generally higher toward the Bridge where truck traffic volume is high (Figure 4.5(b)). This is because the NOx emission factor of trucks (4.5 g/km-veh) is 10 times that of cars (0.45 g/km-veh). Benzene emission is high on the road section between Cabana and Tecumseh where car traffic volume is high (Figure 4.5(a)). The benzene emission factor of cars (17.4 mg/km-veh) is five times that of trucks (3.3 mg/km-veh) (Figure 4.8(a)). In comparison to NOx emissions, benzene emissions vary more among road sections. The coefficient of variance (ratio of standard deviation to mean) of NOx and benzene emissions among road sections were 12% and 21%, respectively.

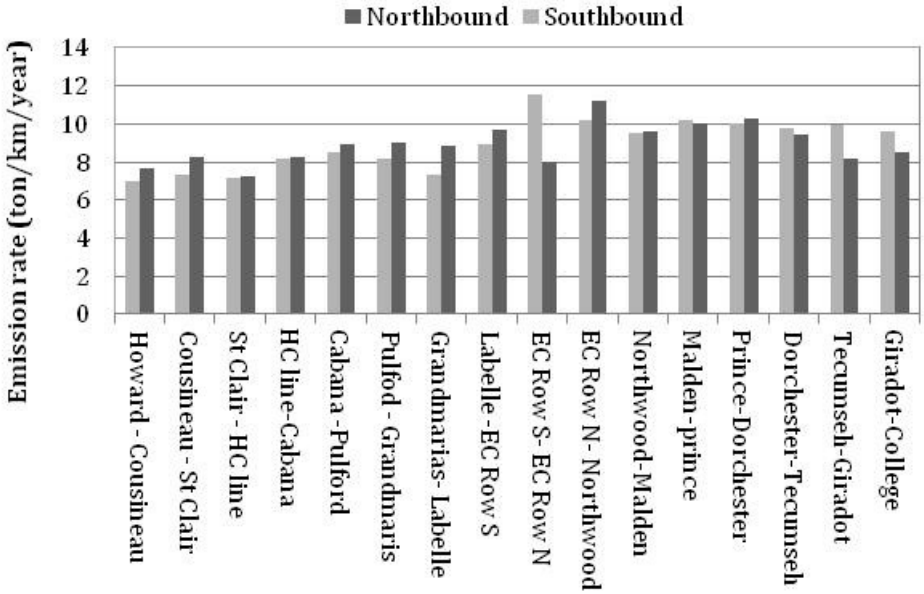

(a) NOx emission

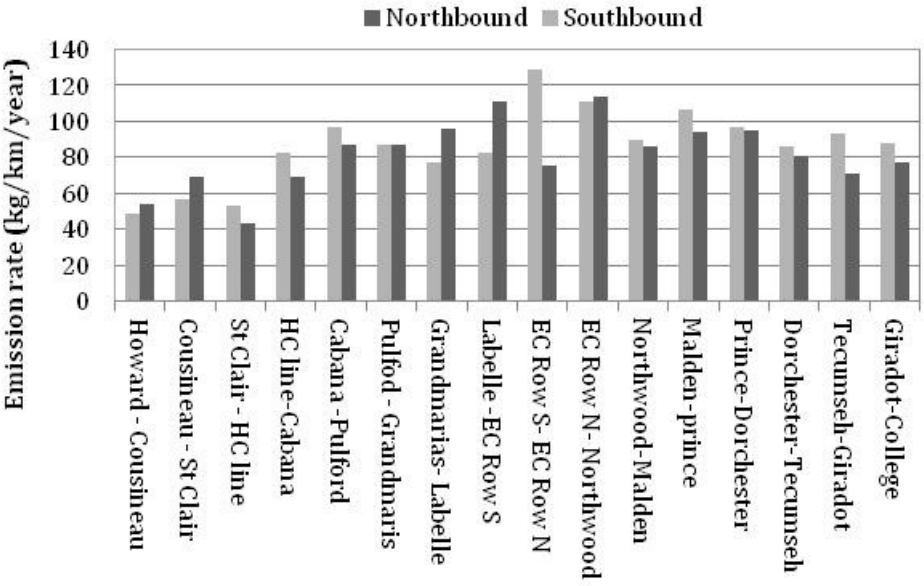

(b) Benzene emission

Figure 4.10: Spatial distribution of vehicular emissions in 2008

4.3.2 Temporal patterns of emissions

Hour-of-day variations in car and truck counts and NOx and benzene emissions at the Giradot - College road section are shown in Figure 4.11. NOx emissions increased in the morning due to an increase in traffic volumes, reached its maximum at 17:00-18:00 (peak hour of truck traffic volume) and decreased afterward. This pattern is similar to that of truck counts, as NOx emissions are mainly affected by truck traffic. Hour-of-day benzene emission had morning and afternoon peaks, when car traffic volume was high.

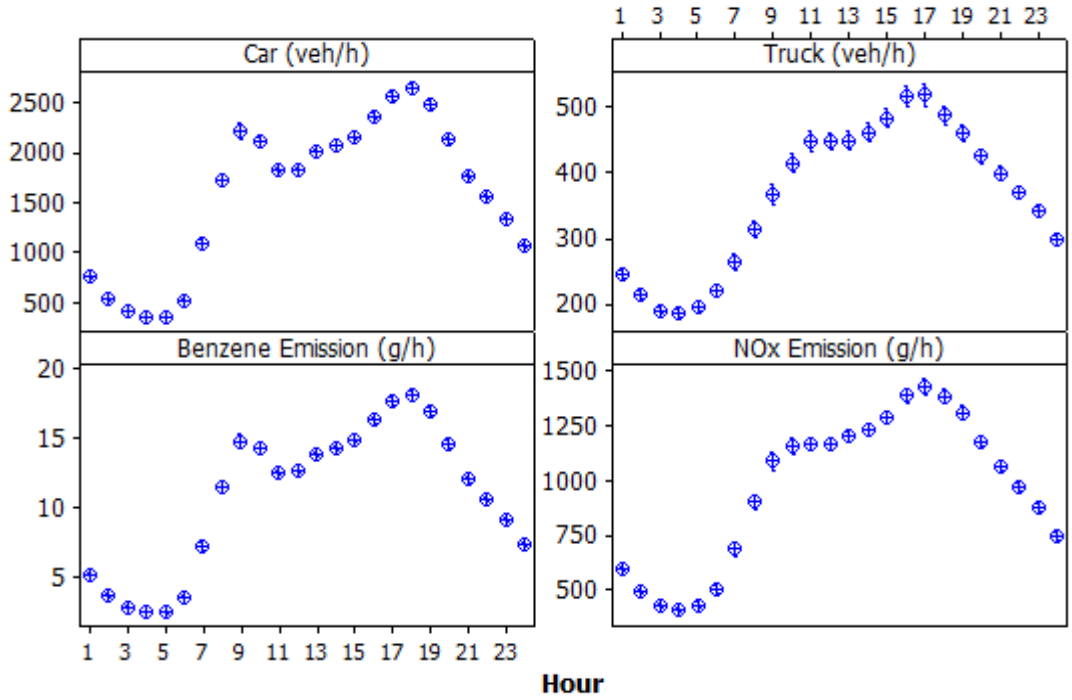

Figure 4.11: Hour-of-day variations in vehicle counts, and NOx and benzene emissions at the Giradot - College road section in 2008

As for seasonal variations, NOx and benzene emissions were high during fall when both car and truck traffic volumes were high (Figure 4.12). NOx emissions were low during winter and summer. This is because in winter, truck counts were low (Figure 4.7(d)) while in summer both car counts (Figure 4.7(d)) and NOx emission factors of cars were low (Figure 4.9(a)). The lowest benzene emission occurred during summer when

both car counts and benzene emission factor of cars were low (Figure 4.8(a)). Despite the low car and truck counts in winter, benzene emission was high, because of high benzene emission factors of cars due to cold starts (Figure 4.8(a)).

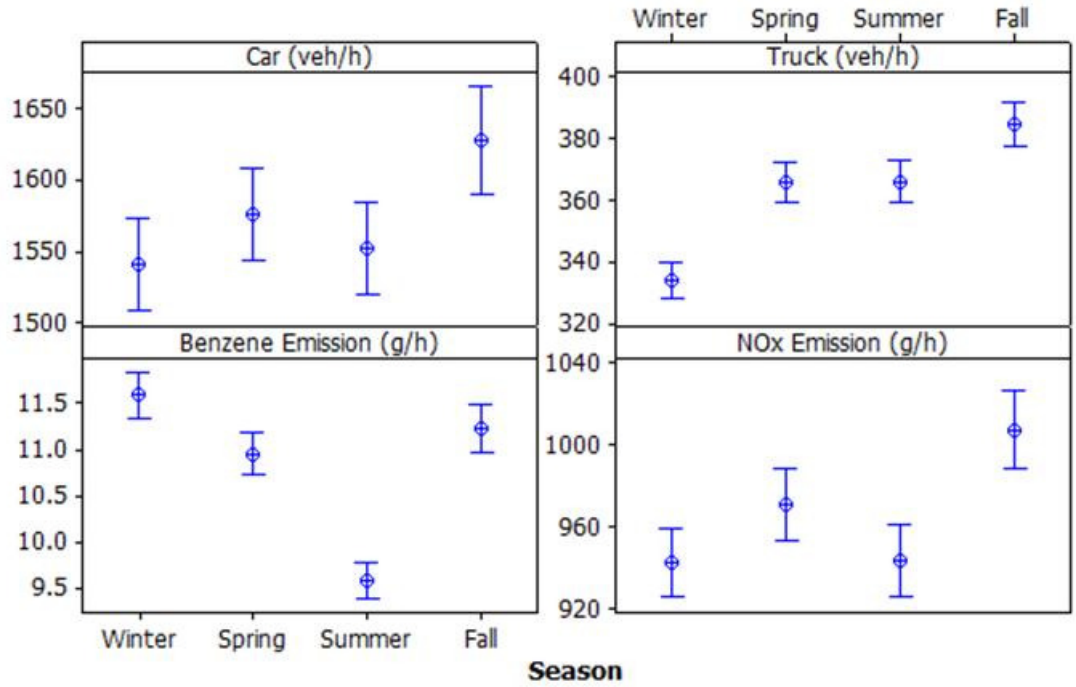

Figure 4.12: Seasonal variations in vehicle counts, and NOx and benzene emissions at the Giradot - College road section in 2008

4.4 Patterns of meteorological factors

4.4.1 Annual and seasonal wind-roses

Figure 4.13 shows the wind-rose at the Windsor Airport in 2008. Prevailing wind direction occurred in the south-west quadrant.

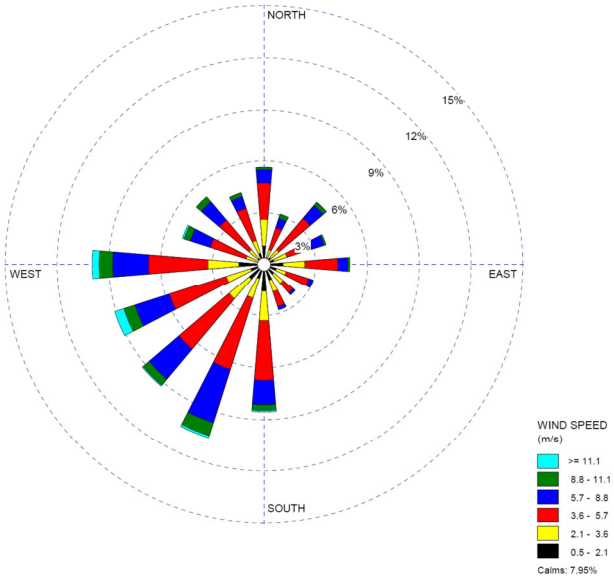

Figure 4.13: Wind-rose at Windsor Airport in 2008

Figure 4.14 shows the wind-rose at Windsor Airport in 2008 by season. The prevailing wind during the winter and summer is from the south-west quadrant (Figure 4.14(a) and Figure 4.14(c)). The prevailing wind directions during the spring is from both south-west and north-east quadrants (Figure 4.14(b)). During the fall, the prevailing wind is from the west (Figure 4.14(d)).

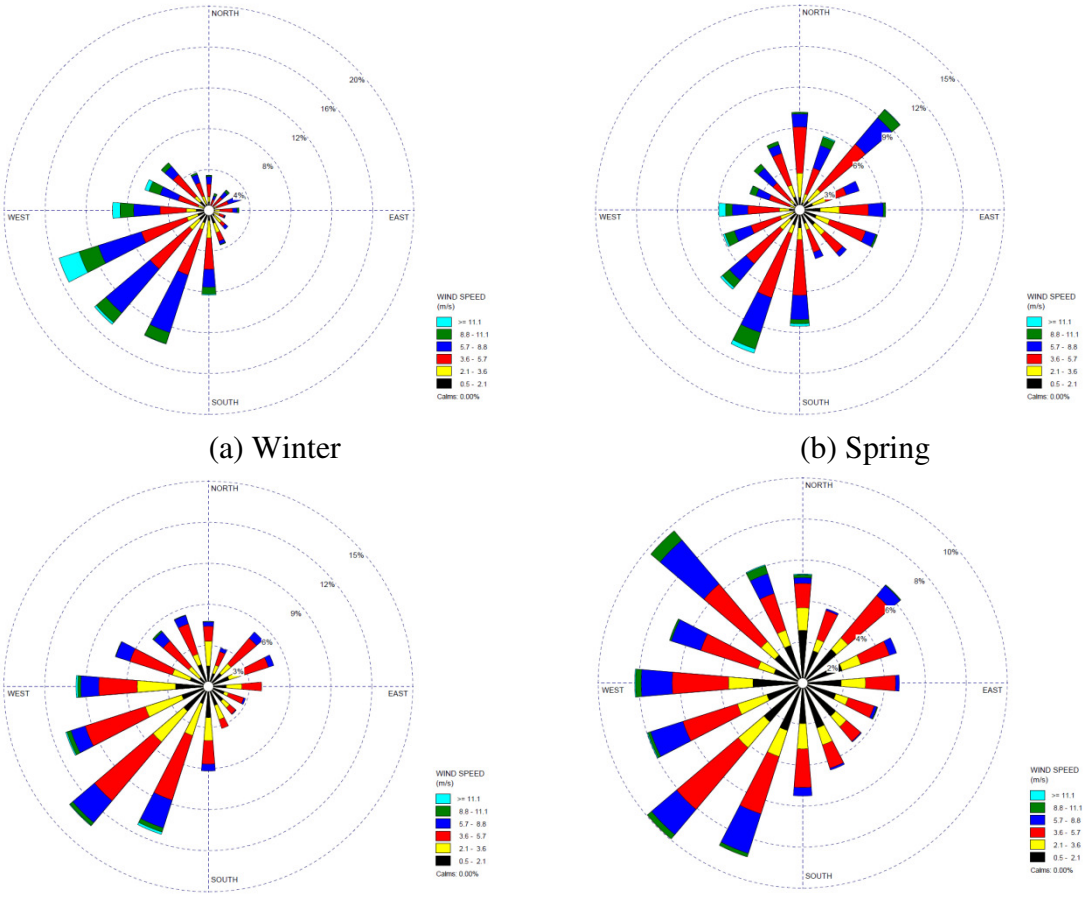

(a) Winter (b) Spring

(c) Summer (d) Fall

Figure 4.14: Wind-roses at Windsor Airport in 2008 by season

4.4.2 Hour-of-day patterns of wind speed and mixing heights by season

Figure 4.15 shows hour-of-day variations in wind speed, mechanical mixing heights, and convective mixing heights by season. Similar temporal variations were observed for wind speed and mechanical mixing heights; they were high during the daytime. This reflects the fact that mechanical mixing heights were a function of wind speed (EPA, 2004a). Convective mixing heights were higher during warmer seasons due to higher temperature which induces convections. The convective mixing height is only available during daytime. It continuously increased after the sunshine till the peak value in the evening (17:00 - 19:00). This increase is more pronounced for warmer seasons.

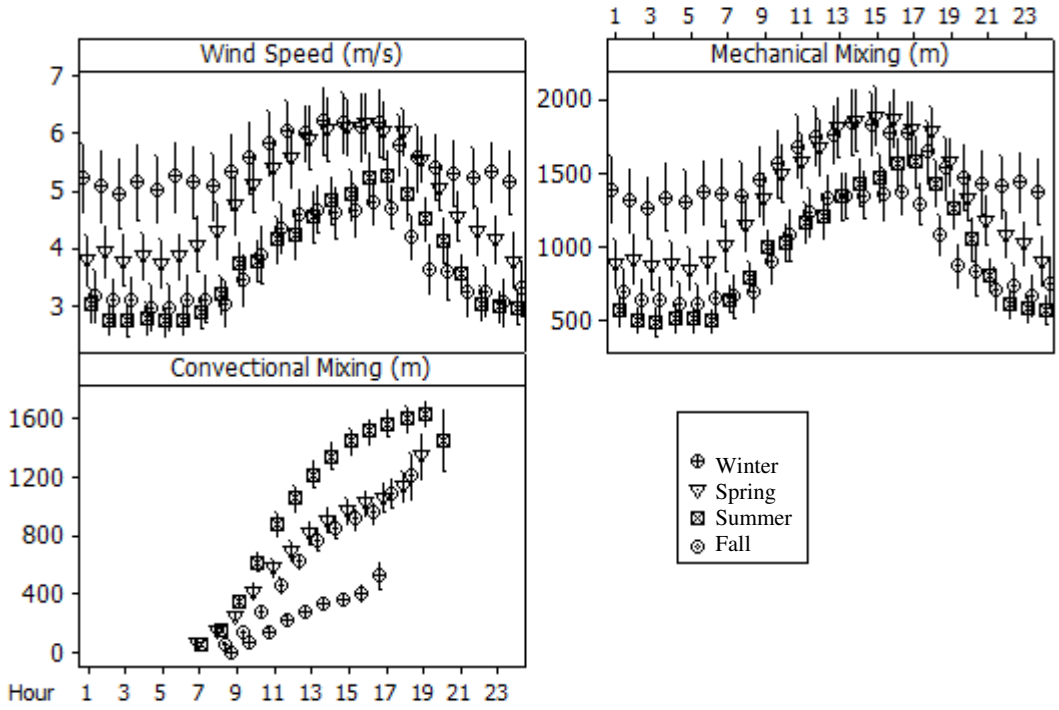

Figure 4.15: Hour-of-day variation in wind speed and mixing heights by season (local time)

4.5 Spatial and temporal patterns of NO_2 and benzene concentrations

4.5.1 Spatial patterns of concentrations

Figure 4.16(a) shows annual mean concentrations of NO_2 in the study domain, which were in the range of 0.43 $\mu g/m^3$ – 46 $\mu g/m^3$. Concentrations decreased further away from the road. Annual benzene concentrations were in the range of 0.0033 $\mu g/m^3$ – 0.47 $\mu g/m^3$ (Figure 4.16(b)). Spatial distribution of NO_2 and benzene were similar. As expected, patterns at east and west sides are affected by the wind direction. The overall pattern is affected by emission and wind speed.

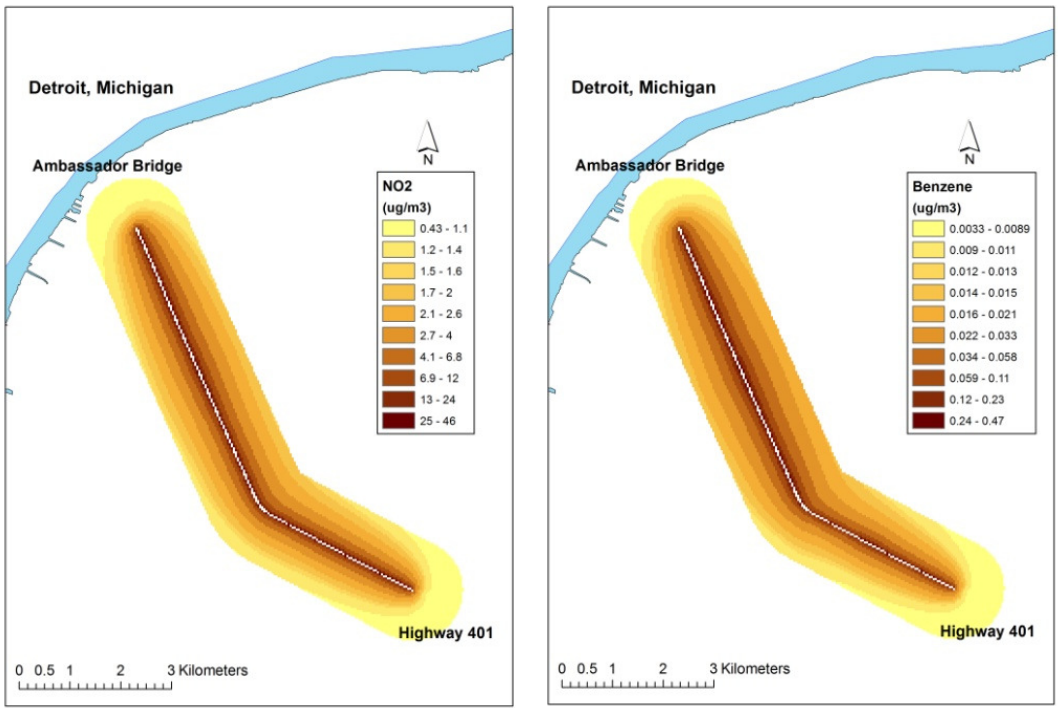

a) NO_2 b) Benzene

Figure 4.16: Annual mean NO_2 and benzene concentrations in 2008

Similar patterns of maximum hourly concentrations were observed for NO_2 and benzene (Figure 4.17). In comparison to the annual mean concentration patterns in Figure 4.16, maximum hourly concentrations did not decrease away from the road with a uniform fashion, especially at west side of the road curvature (marked area) where e.g. concentrations of 110 $\mu g/m^3$ extended up to 500m from the road. This is because maximum hourly concentration at each receptor occurred in a specific hour during the year, and multiple factors could contribute to this high concentration, e.g. low wind speed and mixing, high emission, wind directions from road towards the receptors, or a combination of these factors.

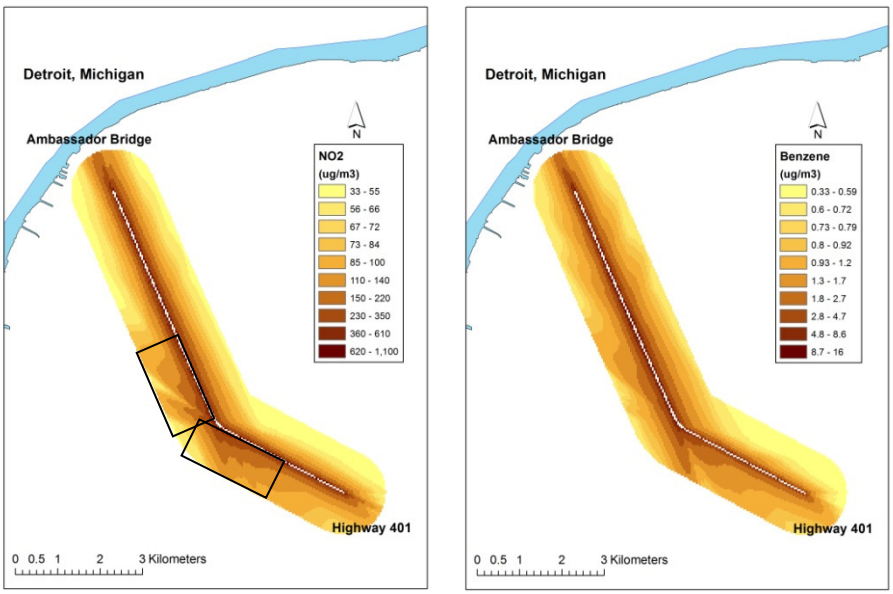

a) NO_2 b) Benzene

Figure 4.17: Maximum hourly concentrations of NO_2 and benzene

4.5.2 Falloff patterns of concentrations

Figure 4.18 shows the falloff patterns of annual mean and maximum hourly of NO_2 and benzene concentrations from the centerline of the road at a transit line perpendicular to the EC Row – Northwood road section (Figure 3.8). Falloff patterns of NO_2 and benzene concentrations were similar. Concentrations sharply decreased with distance from the road. At distances of 200, 400, and 600 m from the road, the annual mean concentrations were 24%, 13%, and 9% of the concentration at a distance of 40 m from the road. Using a paired t-test, it was observed that annul mean concentration was significantly higher \ the east of the road than west ($p<0.05$). The mean NO_2 in the east and west were 5.05 $\mu g/m^3$ and 4.35 $\mu g/m^3$, respectively. At receptors located 40m from the road centerline, annual mean concentrations in the east and west of the road were 27 $\mu g/m^3$ and 24 $\mu g/m^3$, respectively. This is due to prevailing winds from the south-west quadrant (Figure 4.14).

Maximum hourly NO_2 concentrations were not significantly different between the east and west sides of the road ($p<0.05$). On the other hand, maximum hourly benzene concentrations were significantly higher west of the road ($p>0.05$).

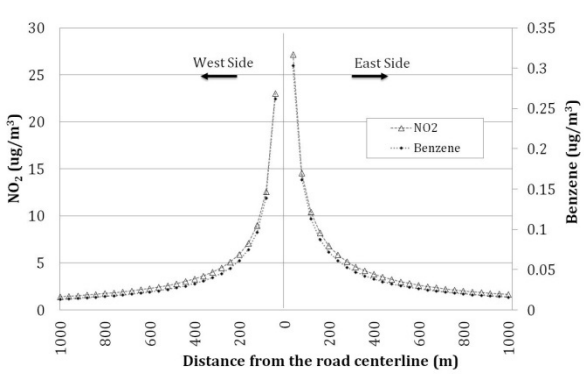

(a) Annual mean concentration

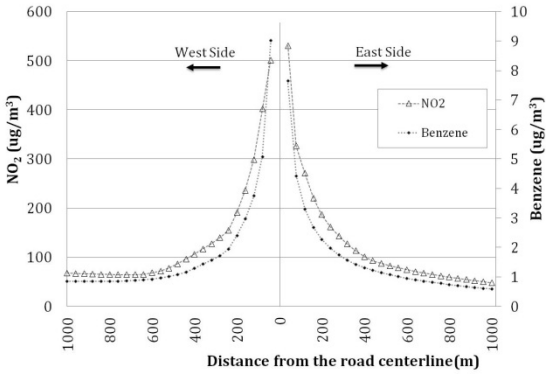

(b) Maximum hourly concentration

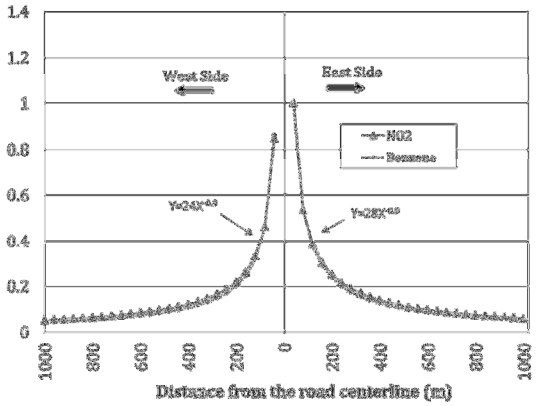

(c) Normalized annual mean

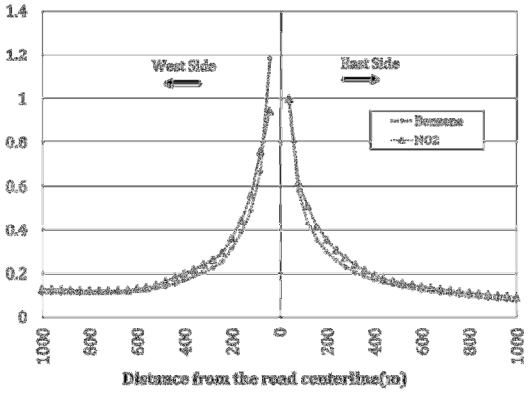

(d) Normalized maximum hourly

Figure 4.18: Fall-off pattern of annual and maximum hourly concentrations from the road centerline – at (c) and (d), concentrations were normalized to those at 40m east of the road

Falloff patterns of observed and simulated NO_2 concentrations at a transit line perpendicular to the Giradot - College road section (Figure 3.10) in May 2010 were compared in Figure 4.19.

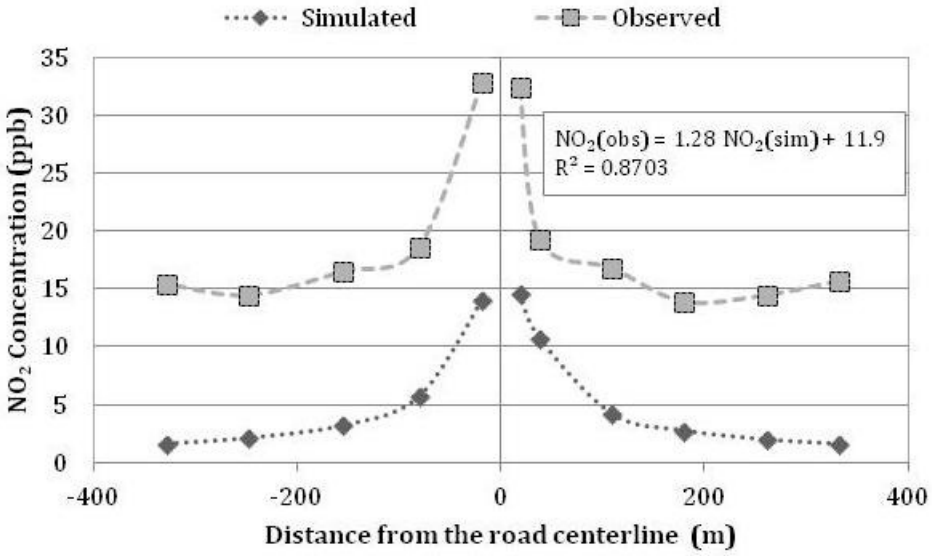

(a) Concentrations

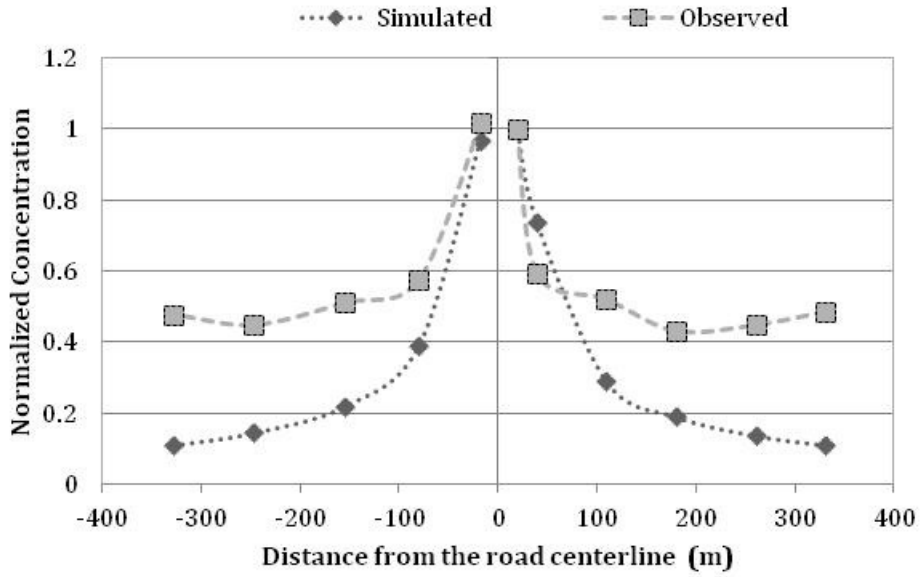

(b) Normalized concentrations

Figure 4.19: Falloff patterns of simulated and observed NO_2 concentrations at a transit line perpendicular to the Giradot - College road section in May 2010 – Observed concentrations were provided by Health Canada

Observed concentrations were consistently higher than simulated concentrations, as the background concentration was not considered in simulation. Falloff patterns were

similar. Both observed and simulated concentrations abruptly dropped within 100 m from the centerline of the road. In the distance up to 200 m from the road, simulated concentrations continued to decrease compared to the observed concentrations. This is because the simulated concentrations only include the emissions from traffic on Huron Church Road, but not the concentrations due to other roads and the background. At the receptors 200 m away from of the road, the observed concentrations leveled off at 15 ppb, suggesting a very small impact of Huron Church Road traffic emissions. In other words, at approximately 200m away from the road, the observed concentrations were approaching the background values. For model predicted concentrations, this distance is at least 350 m.

A linear relationship was fitted between observed and simulated concentrations (R^2 = 0.87, $p < 0.05$). The slope of the regression line which reflects the ratio of the observed concentrations to the simulated concentrations was close to one (1.28). The intercept of 11.9 ppb reflects the background concentration. Falloff patterns of the observed concentrations (Figure 4.14) were consistent with previous studies (Beckerman, 2008). Similarly, falloff patterns of simulated concentrations were similar to findings by Batterman et al. (2010) using the CALINE4 dispersion model.

4.5.3 Temporal patterns of concentrations

Figure 4.20 shows hour-of-day variation in NO_2 and benzene concentrations at a receptor 40 m east and a receptor 40 m west of the road (Figure 3.8). Similar patterns were observed for receptors east and west of the road. NO_2 concentrations slightly varied during 1:00-7:00 am, and rapidly decreased after 7 am although car and truck counts were high during this time period (Figure 4.11). This is due to higher wind speed and

mixing height during the daytime (Figure 4.15) leading to strong dispersion. NO_2 concentrations were low till 18:00, and increased afterward due to lower wind speed and mixing heights (Figure 4.15). Hour-of-day patterns of benzene concentrations were similar to those of NO_2 concentrations with the exception of 1:00-7:00. During 1:00-7:00, the increase in concentrations was more pronounced for benzene than NO_2. This is because NO_2 concentrations were mainly affected by the truck counts and benzene concentrations by car counts, and during this time period an increase in car counts was more apparent than truck counts (Figure 4.11). Concentrations were the highest during 19:00-0:00 when traffic counts were not the highest (Figure 4.11).

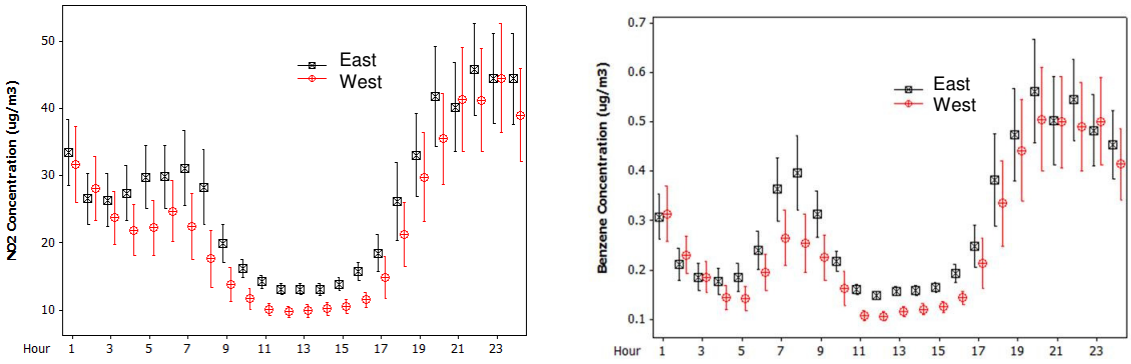

a) NO_2 b) Benzene

Figure 4.20: Hour of day NO_2 and benzene concentrations at a receptor 40 m east and a receptor 40 m west of the road

Figure 4.21 shows seasonal variations in NO_2 and benzene concentrations. Similar patterns were observed for both pollutants. Among the four seasons, concentrations were the highest in fall because of high car and truck counts (Figure 4.12) and low wind speed in this season (Figure 4.15). Concentrations were significantly higher in the east of the road during winter and summer due to prevailing winds from the south-west quadrants in these seasons (Figure 4.14(a) and Figure 4.14(c)). Factors that would contribute to lower

benzene concentrations in winter include high wind speeds (Figure 4.15) and low car vehicle counts (Figure 4.12). However, benzene concentrations in winter were higher than in spring and fall due to cold start effects, thus higher benzene emissions (Figure 4.12).

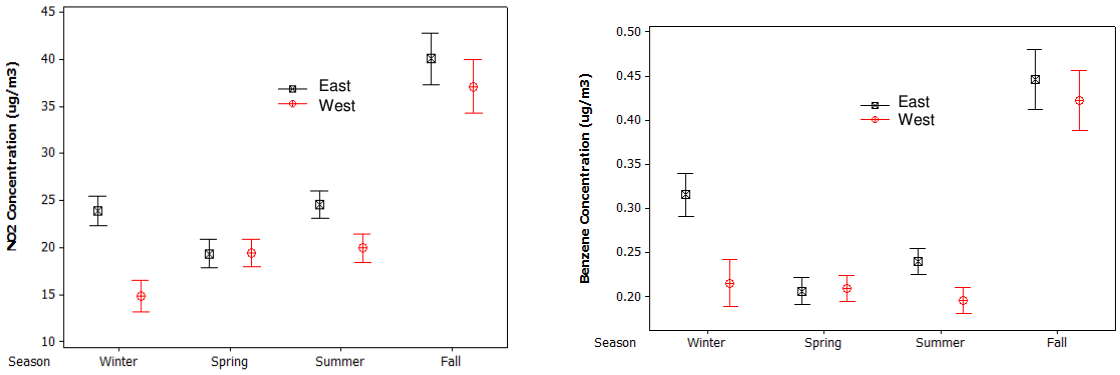

a) NO_2 b) Benzene

Figure 4.21: Seasonal mean NO_2 and benzene concentrations at a receptor 40 m east and a receptor 40 m west of the road

4.5.3.1 Effects of meteorological parameters and vehicle types on hour-of-day concentrations

As explained in Section 3.6.2, three cases of the AERMOD simulation, namely Unit Emission, Car Emission, and Truck Emission, were conducted to identify effects of meteorological parameters and vehicle types on hour-of-day concentrations. In the Unit Emission Case, emissions were constant for all hours of the year with a value of 1g/m/s per direction (Section 3.6.2). This resulted in high emission and concentration for the Unit Emission Case. Thus, for side-by-side comparison of concentrations by the Unit Emissions and by the Total Emission, a secondary axis was used. The Total Emission was the actual emission from both cars and trucks. It varied with hour. Figure 4.22

compares hour-of-day patterns of concentrations from the Unit Emission case with the total emission case and hour-of-day reciprocal of wind speed. It was observed that when a unit emission is applied to all hours, concentrations are low during the daytime. Hour-of-day concentrations of the Unit Emission case were high during 1:00-7:00 and 18:00-24:00 and low during 8:00-17:00 (Figure 4.22(a)). As the emission is invariable with time of day in the Unit Emission case, concentrations are only affected by the meteorological parameters. Also, it is expected that the concentration pattern be similar to the reciprocal of wind speed. This is true for the time periods of 1:00-7:00 and 18:00-24:00 (Figure 4.22(b)). However, during 8:00-17:00, the reciprocal of wind speed decreased whereas concentrations from the Unit Emission case varied little. This is because strong dispersion by convective mixings in AERMOD leading to low concentrations.

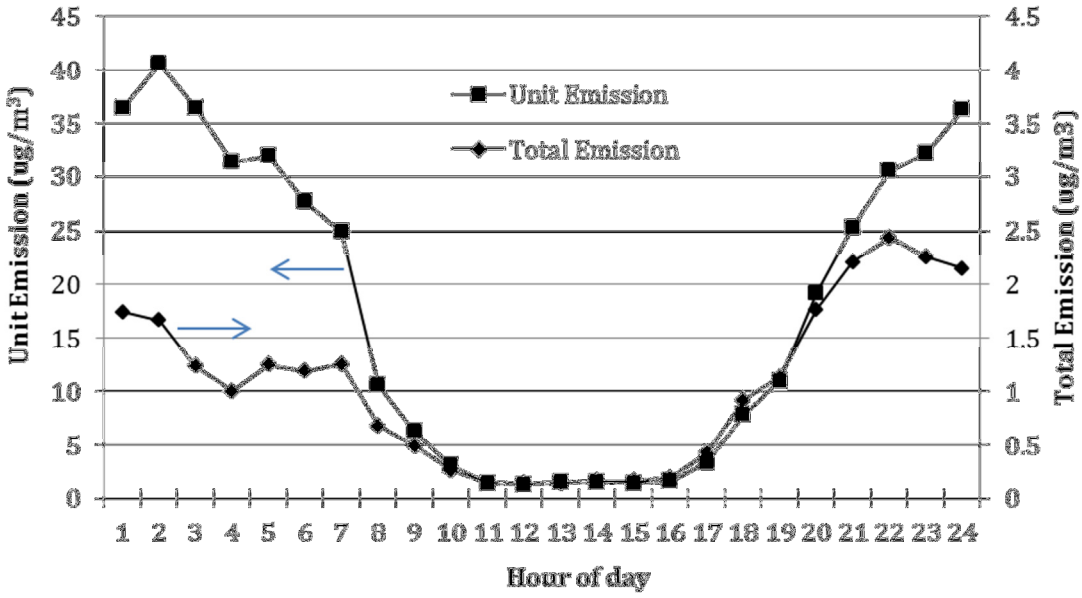

(a) Concentrations by unit emission and total emission

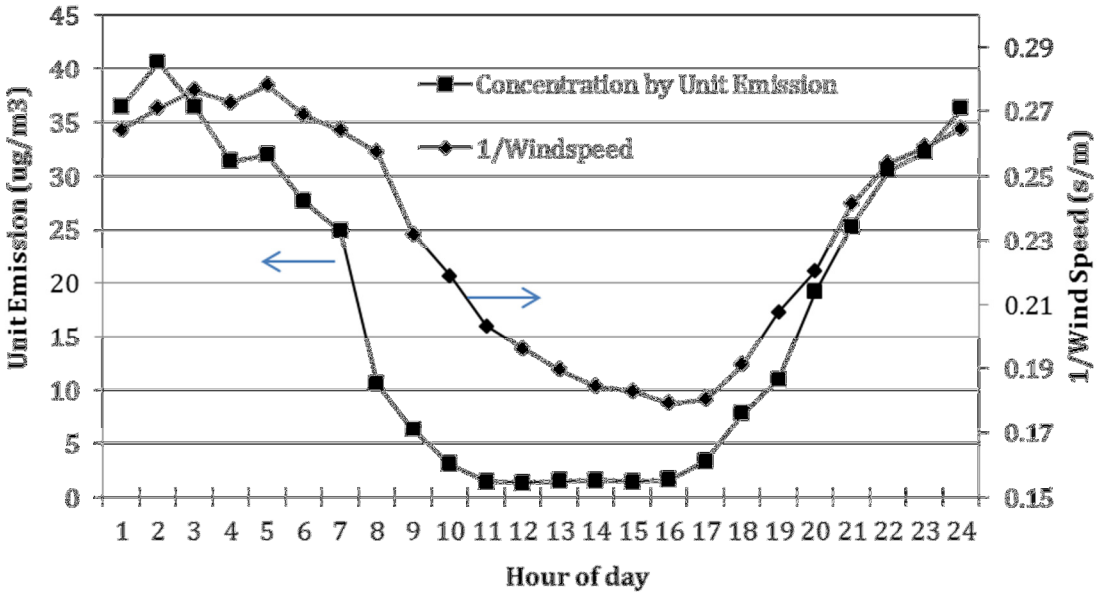

(b) Concentrations by unit emission and reciprocal of wind speed

Figure 4.22: Hour-of-day concentrations at the Windsor-West Station by a unit emission and total emission

Difference in concentrations between the Unit Emission and the Total Emission reflects the effects of vehicle counts on the simulated concentrations. As shown in Figure 4.22(a), similar concentrations were observed during 8:00-21:00. This means that traffic

emissions have a smaller impact on air quality in term of change in absolute concentration values during this time period due to strong dispersion (higher wind speeds and mixing heights). On the other hand, during 1:00-7:00 and 21:00-24:00, concentrations from the Unit Emission case were relatively higher than the Total Emission case. This reflects that effects of vehicle counts on concentrations are more pronounced during these time periods when the atmosphere is stable and wind speed is low.

Figure 4.23(a) compares hour-of-day concentrations among Car Emission, Truck Emission, and Total Emission cases at the Windsor-West Station. It was observed that hour-of-day patterns of concentrations for the Total Emission and the Truck Emission were similar. This is because trucks produce more NO_2 emissions than cars. Unlike the Total Emission, the concentrations for the Car Emission case increased after 4:00 and reached to a peak in the morning at 7:00.

Hour-of-day concentrations from one-vehicle emission (Figure 4.23(b)) were calculated by dividing the hour-of-day concentrations (Figure 4.23(a)) to the hour-of-day vehicle counts (Figure 4.7). It was observed that hour-of-day patterns of one-car and one-truck emissions were similar to the hour-of-day pattern of the Unit Emission Case (Figure 4.22(a)). As the NOx emission factor of trucks was approximately 10 times that of cars, the concentrations from the one-truck emissions were approximately10 times those from one-car emissions.

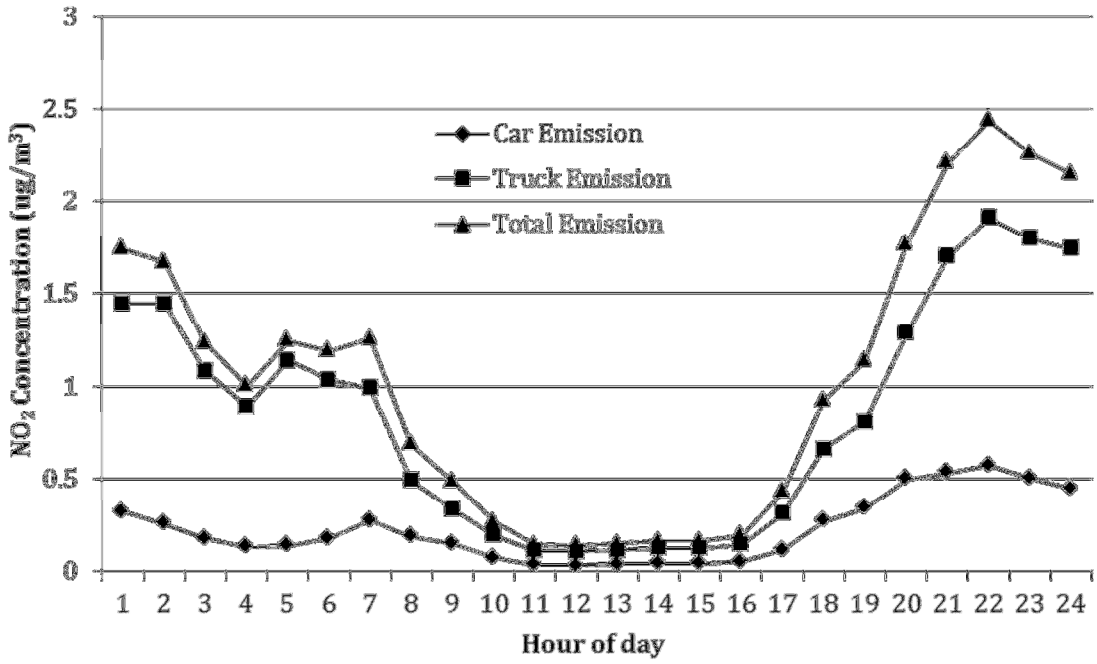

(a) Concentration by vehicle type

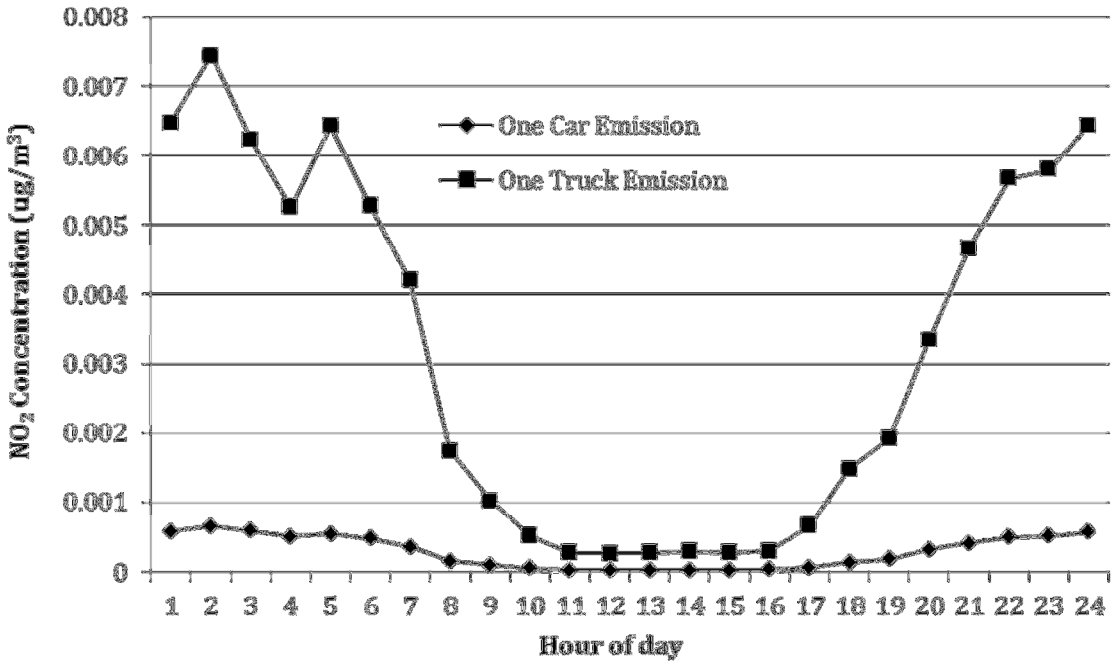

(b) Concentrations from one car and one truck

Figure 4.23: Hour-of-day concentrations at the Windsor-West Station by vehicle type

Results from the above-listed cases (Figure 4.23(b)) can be used to estimate hour-of-day variations in concentrations. In particular, results from one-car and one-truck emissions (Figure 4.23(b)) could be used to estimate hour-of-day concentrations for vehicle counts with various truck percentages.

Variance in simulated concentrations

As the magnitudes of the concentration levels were different among Unit Emission, Total Emission, Car Emission, and Truck Emission, NO_2 concentrations were normalized to the annual mean value of each case. Table 4.1 shows mean, standard deviation, and variance of NO_2 concentrations and standard deviation and variance of the normalized concentrations in the four simulation cases.

Table 4.1: Mean, standard deviation, and variance of NO_2 concentrations

	NO_2 concentrations ($\mu g/m^3$)			Normalized NO_2 concentrations	
Variable	Mean	Standard Deviation	Variance	Standard Deviation	Variance
Car Emission	0.2230	0.7837	0.6141	3.514	12.351
Truck Emission	0.8327	2.8072	7.8803	3.371	11.365
Total Emission	1.0422	3.5036	12.2752	3.362	11.302
Unit Emission	17.6580	59.8170	3578.0690	3.388	11.475

The statistical "Test for Equal Variance" was performed with normalized NO_2 concentrations. Figure 4.24 shows paired comparison of standard deviations among four simulation cases. Variation in normalized NO_2 concentrations by Unit Emission (SD=3.39) and Total Emission cases were not significantly different from each other (SD=3.36) Figure 4.24(a)). As the emission is invariable in the Unit Emission case, concentrations are only affected by the meteorological parameters. Thus, this comparison

indicated that variation in concentrations was mainly due to variations in meteorological parameters. Variation in the concentrations due to Car Emission (SD=3.52) was slightly higher than the variation due to Truck Emission (SD=3.37) (Figure 4.24(b)); however, the difference is statistically significant. This is because car counts had higher variability with time of day than truck counts (Figure 4.24). Variations in concentrations due to Truck Emission and Total Emission were not significantly different from each other. This reflects that a majority of NOx emissions were from truck traffic. In conclusion, variations in NO_2 concentrations were mainly due meteorological parameters and less due to traffic as they did not vary with hour-of-day as much as atmospheric dispersion. However, variation in NO_2 due to Car Emission was statistically significantly higher than the variation in the other cases, "Unit Emission", "Total Emission" and "Truck Emission".

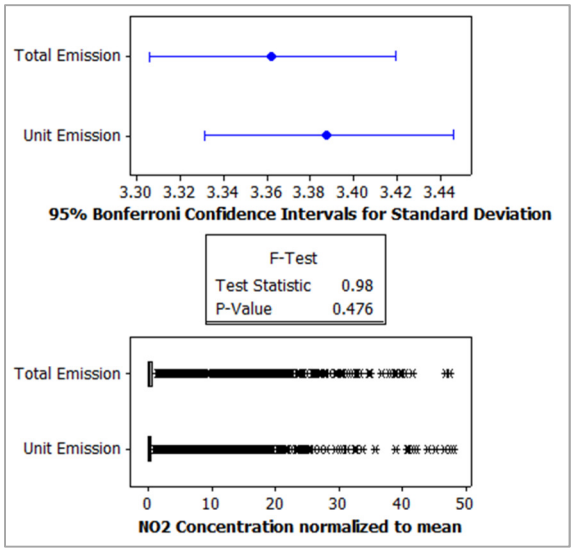

(a) Total Emission vs Unit Emission

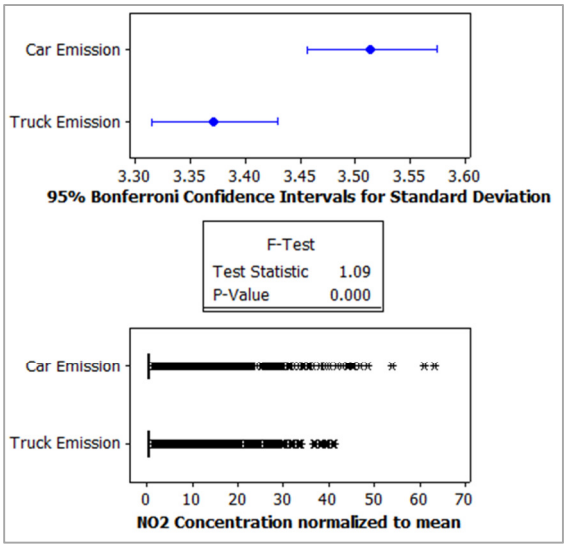

(b) Car Emission vs Truck Emission

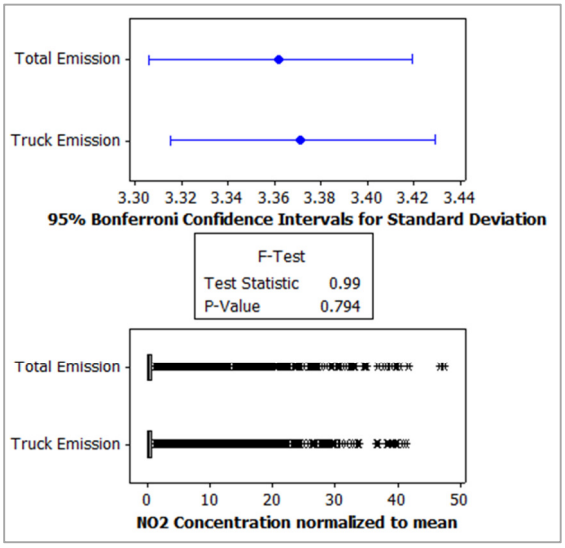

(c) Total Emission vs Truck Emission

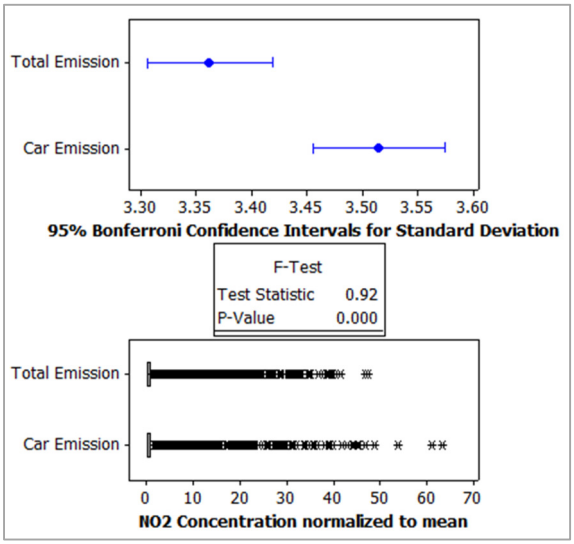

(d) Total Emission vs Car Emission

Figure 4.24: Paired comparison of standard deviations among four simulation cases – Hourly NO_2 concentrations were normalized to corresponding annual mean

4.5.3.2 Comparison of simulated and observed concentrations

Figure 4.25 shows hour-of-day patterns of simulated and observed NO_2 concentrations at the Windsor-West station. As expected, observed NO_2 concentrations at the Windsor-

West Station located 1 km from the Huron Church Road were much higher than simulated concentrations. This is because the station is approximately 900 m away from the road, where simulated concentration was low. However, observed concentrations were high as the station is more affected by the local traffic and background concentration which were not considered in the simulation. Hour-of-day patterns of observed and simulated concentrations were similar. Concentrations were lower during the daytime (10:00-17:00) than at night (18:00-24:00). However, in comparison to simulated concentrations, observed concentrations are highest during the morning peak hour of car traffic (8:00).

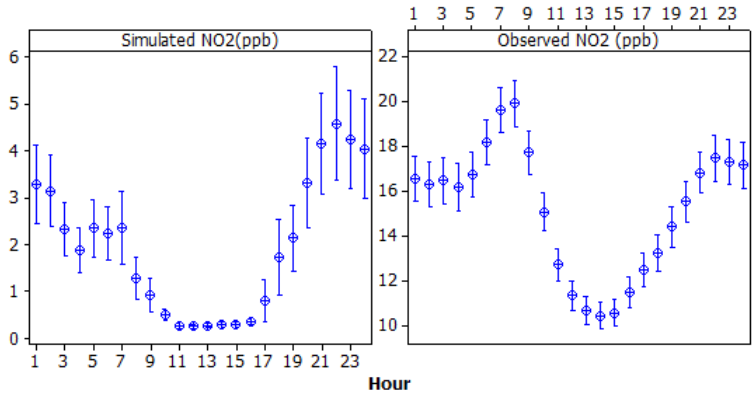

Figure 4.25: Comparison of hour-of-day simulated and observed concentrations at the Windsor-West Station in 2008

This discrepancy is because the majority of simulated NO_2 concentrations at the Windsor-West Station were from trucks (Figure 4.23(a)) while cars are the dominant vehicle type in local traffic near the Windsor West station. In other words, the hour-of-day car traffic profile is expected to have more effects on the observed concentrations at the receptor. Assuming that the local car count profile is similar to that of the Huron Church Road, hour-of-day concentrations of the Car Emission Case were compared with

hour-of-day of observed concentrations as shown in Figure 4.26. Similar to the observed pattern, concentrations by the Car Emission Case increased after 4:00 and it reached to a peak in the morning. However, in comparison to the observed pattern, morning peak of Car Emission Case occurred one hour earlier (7:00) and it is less sharp. This is because of consideration of convective mixings by the AERMOD after 7:00 (Figure 4.15). In other words, overestimation of mixing during the daytime resulted in lower than actual concentrations by AERMOD during 7:00-18:00.

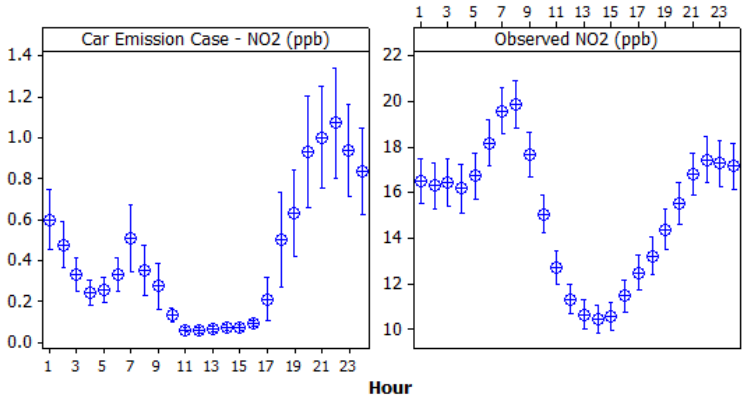

Figure 4.26: Comparison of hour-of-day concentrations by the Car Emission Case with observed concentrations at the Windsor-West Station in 2008

Figure 4.27 shows the scatter plot of simulated and observed hour-of-day concentrations at the Windsor-West Station. It was observed that simulated and observed concentrations were moderately correlated (R^2 = 42.8%, p = 0.001). However, as denoted in Figure 4.27, observations at hours 6:00-9:00 were far from the regression line, which indicate large differences between observed and simulated concentrations during this time period. Observed concentrations were highest during morning peak hour of car traffic (8:00) whereas simulated concentrations decreased after 7:00. This reflects effects of convective mixing heights which lowered the simulated concentrations (Figure 4.25).

As shown in Figure 4.22, after 7:00 concentrations from the Unit Emission Case sharply dropped.

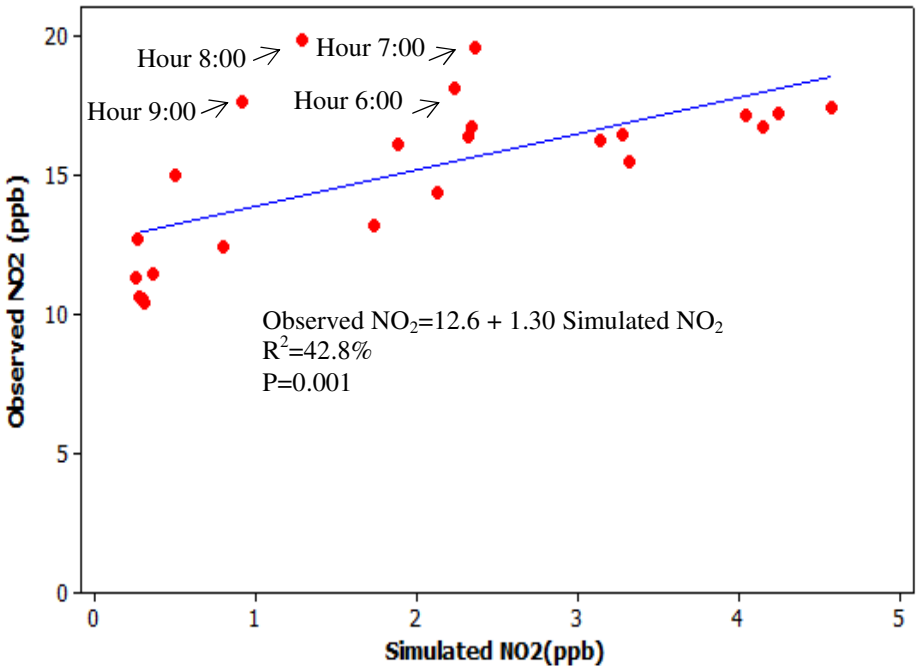

Figure 4.27: Scatter plot of hour of day simulated and observed NO_2 concentrations at Windsor-West station in 2008 - Simulated concentrations were in $\mu g/m^3$, which were converted to ppb assuming 25°C and 1 atm thus 1 ppb=1.88 $\mu g/m^3$

A linear relationship was fitted between observed and simulated hour-of-day concentrations at the Windsor-West station (Observed NO_2=12.6 + 1.30 Simulated NO_2). It was observed that this relationship was similar to that predicted by the 10 receptors at the transit line perpendicular to the Giradot - College road section (Figure 4.14) (Observed NO_2=11.9 + 1.28 Simulated NO_2). In particular, the intercept which reflect the background concentrations were approximately 12 ppb.

Seasonal variations in observed and simulated NO_2 concentrations were compared in Figure 4.28. Using one-way ANOVA, it was found that both observed and simulated

concentrations were significantly different by season. Also, season explained 9% and 4% of the variations in observed and simulated concentrations, respectively. However, orders by season were quite different for observed and simulated concentrations. The observed concentrations were the highest in winter whereas simulated concentrations were the highest in fall. This discrepancy could be due to the fact that the station was far from the road, and seasonal patterns of traffic and emissions could be quite different at Huron Church Road and the local traffic near the station.

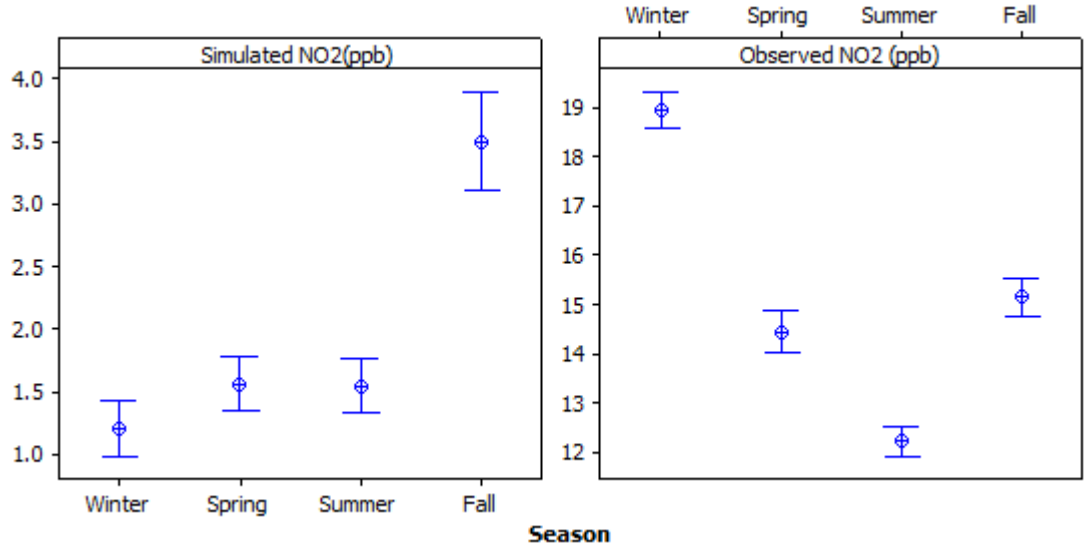

Figure 4.28: Seasonal mean of all hourly observed and simulated NO_2 concentrations at the Windsor-West Station in 2008 - Simulated concentrations were in $\mu g/m^3$, which were converted to ppb assuming 25°C and 1 atm thus 1 ppb=1.88 $\mu g/m^3$

Seasonal variations in daily observed and simulated benzene concentrations were compared in Figure 4.29. The result of one-way ANOVA shows that seasonal variations in both observed ($p = 0.978$) and simulated ($p = 0.176$) concentrations were not significant. Mean of all daily values were statistically the same, and there was no seasonal trend. Simulated concentrations were lower than the observed concentrations as

the station is 1 km away from the road, and also background concentration were not considered.

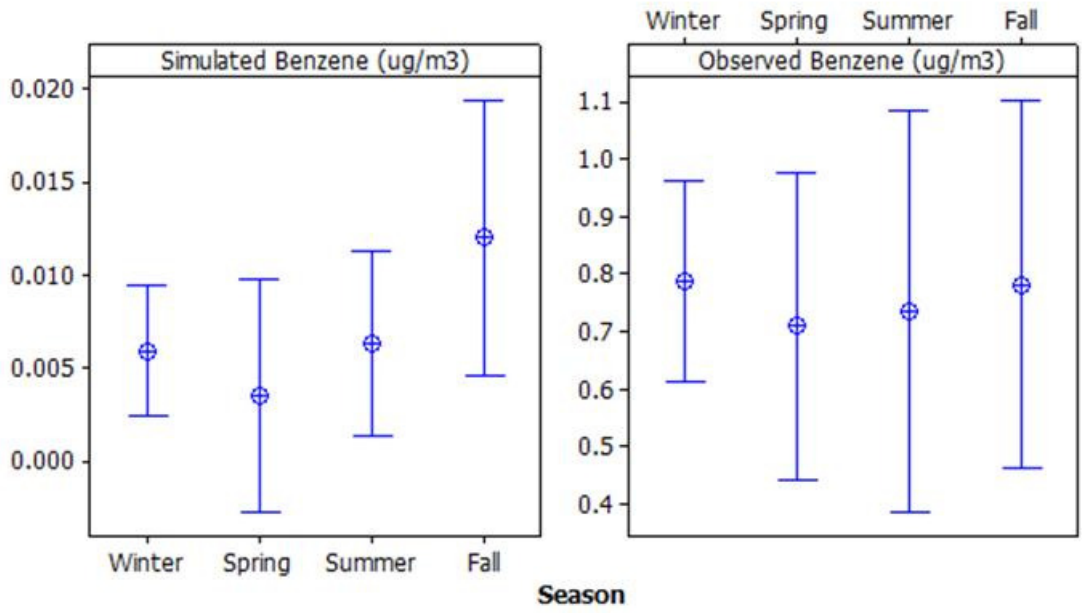

Figure 4.29: Seasonal means of daily observed and simulated benzene concentrations at the Windsor-West Station in 2008

Figure 4.30 compares day-of-week patterns of simulated and observed concentrations at the the Windsor-West Station in 2008. Both simulated and observed concentrations were significantly higher during the weekdays than Saturdays and Sundays due to higher traffic (Figure 4.7c). Simulated concentrations were slightly higher during the Sundays than Saturdays due to higher truck counts (Figure 4.7c). On the other hand, the observed concentrations were higher during Saturdays than Sundays potentially due to higher car counts at local roads near the Windsor-West. Car counts were higher during Saturdays than Sundays on Huron Church Road (Figure 4.7c). As mentioned earlier, observed NO_2 concentrations were affected by local car traffic.

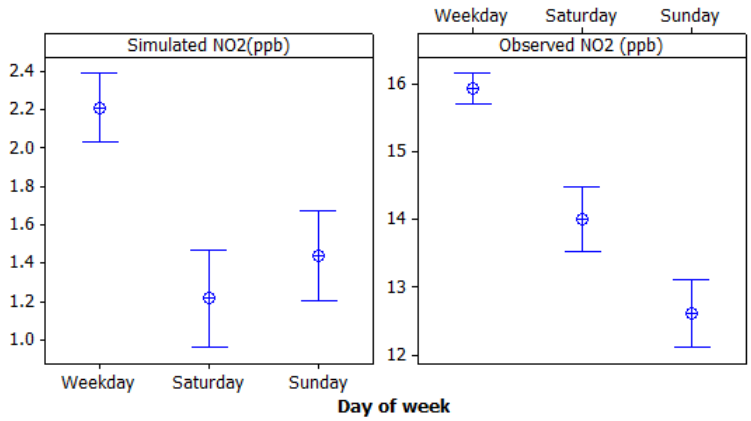

Figure 4.30: Comparison of day-of-week patterns of simulated and observed concentrations at the Windsor-West Station in 2008

4.5.4 Major factors affecting NO_2 concentrations

In this section, major factors affecting simulated and observed concentrations were identified. The receptor was at the Windsor West Station, and the hours were those in which the receptor was downwind of Huron Church Road, approximately 33% of the year. The matrix plot among concentrations and all factors is shown in Figure 4.31.

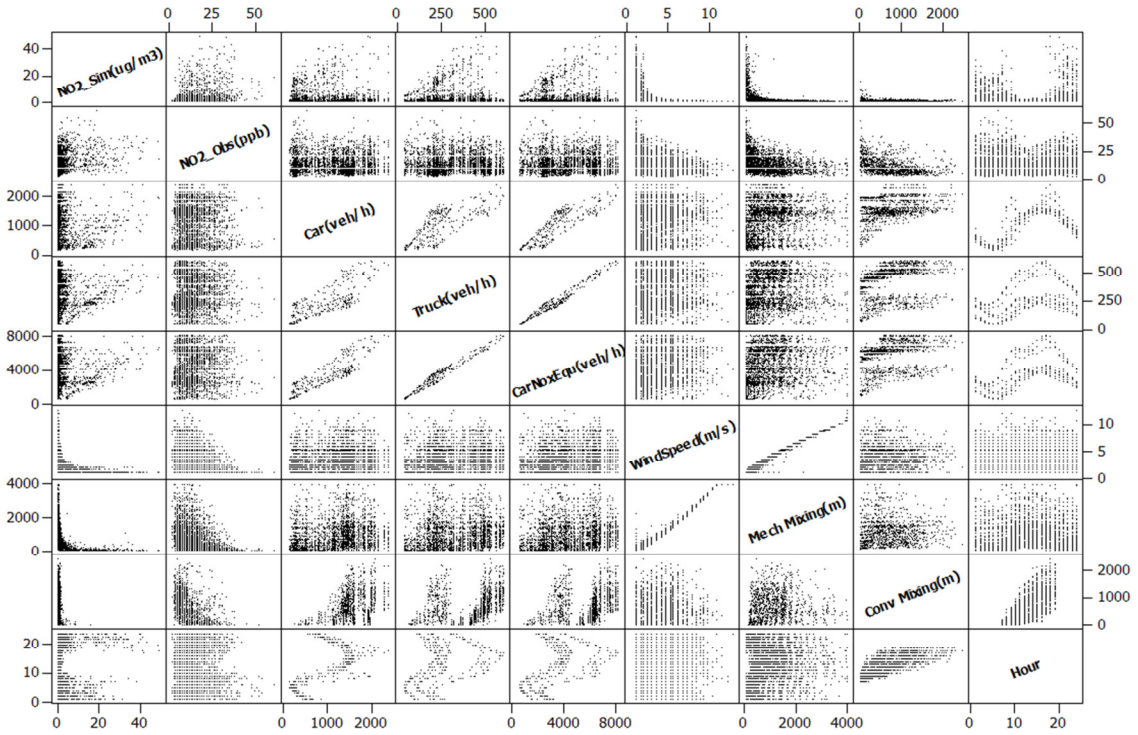

Figure 4.31: Correlation of NO_2 concentrations with hour of day, traffic counts, and meteorological factors (wind speed and mixing heights)

It was observed that NO_2 concentrations were correlated with traffic counts (car, truck, and car-NOx-equivalent) and meteorological parameters (wind speed and mechanical mixing heights) (Figure 4.31). However, simulated concentrations were stronger correlated with other factors. Both observed and simulated concentrations were lower during the daytime than night. However, simulated concentrations were very low suggesting underestimation by the AERMOD during the daytime.

Figure 4.31 suggests that the relationship between traffic counts and concentrations could vary for daytime and nighttime observations, i.e. high concentrations and strong correlation with traffic counts during the nighttime and low concentrations and weak correlation with traffic counts during the daytime. As a result, the linear correlations between concentrations (both observed and simulated) and traffic counts (car, truck and

car-NOx-equivalents) were weak (Figure 4.31 and Table 4.3). As for the three meteorological parameters: wind speed, mechanical mixing heights, and convective mixing heights, each was inversely correlated with both observed and simulated NO_2 concentrations.

Simulated concentrations were low during the daytime when wind speed was high and convective mixing effects were considered in the AERMOD (Figure 4.31). Effects of time of day on simulated concentrations were further investigated by plotting concentrations versus truck counts and wind speed during nighttime and daytime, as shown in Figure 4.32.

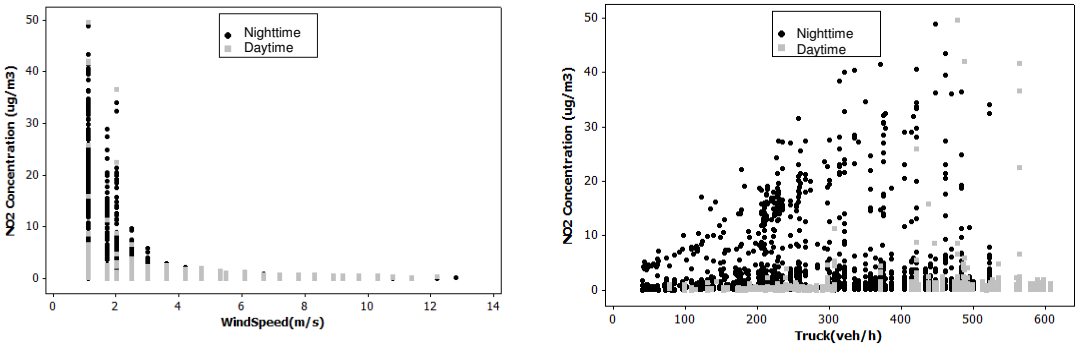

(a) Simulated NO_2 versus wind speed (b) Simulated NO_2 versus truck counts

Figure 4.32: Scatter plot of hourly simulated NO_2 concentrations during daytime and nighttime versus (a) wind speed and (b) truck counts

Two distinctive relationships between concentrations and wind speed were observed during the daytime and nighttime (Figure 4.32(a)). For the same wind speed, NO_2 concentrations were much higher and more scattered during nighttime than the daytime. Similarly, for the same truck counts, NO_2 concentrations were much higher and more

scattered during nighttime than the daytime (Figure 4.32(b)). This is due to higher mixings during the daytime.

The one-way ANOVA of simulated and observed NO_2 concentrations at the Windsor-West Station was performed (Table 4.2). Results showed that traffic counts explained more variations in observed (12-13%) than in simulated concentrations (15-19%). As for meteorological factors, when one was considered at a time, wind speed explained 32% of variations in simulated concentrations, followed by mechanical mixing heights (13%) but little by the convective mixing heights (0%). For observed concentrations, a similar amount of variability was explained by each of the three meteorological factors (17% to 22%).

Table 4.2: One-way ANOVA (R^2) of simulated and observed NO_2 concentrations with respect to temporal factors, traffic counts, and meteorological conditions at the Windsor-West Station

Factors		Simulated NO_2 concentrations			Observed NO_2 concentrations		
		R^2	R^2 (adj)	P	R^2	R^2 (adj)	P
Temporal factors	Hour of day (1, 2..24)	10%	9%	<0.001	8%	7%	<0.001
	Day of week (Weekday, Saturday, and Sunday)	1%	1%	<0.001	1%	1%	0.001
	Season (Winter, Spring, Summer, Fall)	4%	4%	<0.001	9%	8%	<0.001
Traffic	Car (veh/h)	21%	13%	<0.001	25%	17%	<0.001
	Truck (veh/h)	18%	12%	<0.001	21%	15%	<0.001
	Car-NOx-Equivalent. (veh/h)	21%	12%	<0.001	27%	19%	<0.001
Meteorological conditions	Wind speed (m/s)	33%	32%	<0.001	23%	22%	<0.001
	Mechanical mixing heights (m)	58%	13%	<0.001	62%	20%	<0.001
	Convective mixing heights (m)	48%	0%	0.999	76%	17%	0.003

The one-way ANOVA results (Table 4.2) showed that hour-of-day, day-of-week and seasonal variations of both simulated and observed concentrations were significant. Among these temporal factors, hour of day (9%) explained the most variations in simulated concentrations followed by season (4%), and day of week (1%). For observed concentrations, the season (8%) explained more variations than hour of day (7%) and day of week (1%). The large difference in percentage explained by season, 8% in observed versus the 4% in simulated, is somewhat consistent with the greater difference in observed seasonal means than in simulated as shown in Figure 4.33.

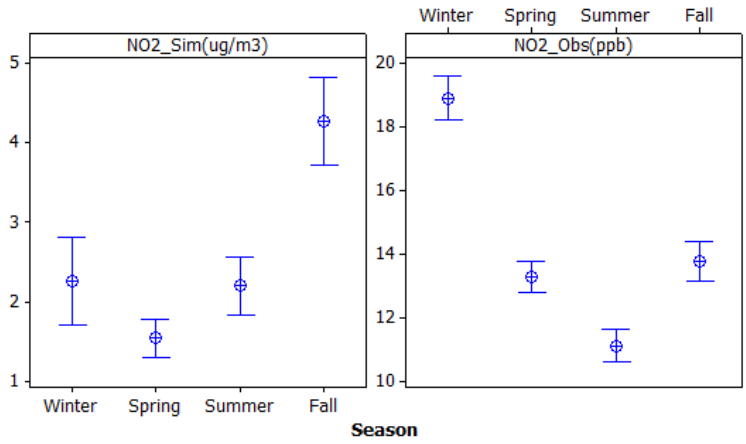

Figure 4.33: Seasonal mean of hourly observed and simulated NO_2 concentrations at the Windsor-West Station in 2008 – Only downwind hours were used.

The multi-factor ANOVA was used to partition variability in concentrations with respect to traffic counts, meteorological parameters, and temporal factors. In this analysis, it is essential that factors not be strongly correlated with each other. Table 4.3 lists cross correlation between factors. There were strong correlations among traffic counts: truck, car and car-NOx-equivalent ($r \geq 0.809$, $p < 0.001$). Similarly, there was a strong correlation among wind speed and mechanical mixing heights ($r = 0.89$, $p < 0.05$). It

was also observed that traffic counts and hour of day were strongly correlated ($r \geq 0.45$, $p<0.05$). Thus, among traffic counts and among meteorological factors, only one factor should be considered at a time for the multi-factor ANOVA. Overral, the linear R^2 was low between factors and concentrations (maximum of r was 0.39). This suggests that the relationship between concentrations and factors is not linear.

Table 4.3: Pearson linear correlation coefficients between hourly NO_2 concentrations at the Windsor West Station, and other factors, sample size of all factors was 2870

	Simulated NO_2 (ug/m3) (n=2870)	Observed NO_2 (ppb) (n=2853)	Car (veh/h)	Truck (veh/h)	Car-NOx-Equi (veh/h)	Wind speed (m/s)	Mechanic. mixing (m)	Conv. mixing (m) (n=1183)	Hour of day	Day of week
Observed NO_2 (ppb)	0.337*									
Car (veh/h)	-0.113*	-0.058*								
Truck (veh/h)	-0.041*	-0.057*	0.809*							
Car-NOx-Equi	-0.064*	-0.06*	0.9*	0.984*						
Wind speed	-0.41*	-0.385*	0.224*	0.157*	0.184*					
Mechanical mixing (m)	-0.381*	-0.376*	0.26*	0.183*	0.213*	0.98*				
Convective mixing (m)	-0.126*	-0.39*	0.354*	0.278*	0.31*	0.032 NA	0.039 NA			
Hour of day	0.076*	-0.06*	0.554*	0.45*	0.5*	0.131*	0.13*	0.691*		
Day of week	-0.063*	-0.071*	-0.212*	-0.598*	-0.507*	-0.023 NA	-0.014 NA	0.001 NA	-0.022 NA	
Season	0.149*	-0.164*	0.03**	0.071*	0.062*	-0.304*	-0.274*	0.215*	0.038*	0.057*

* $p<0.05$

NA Not significant ($p>0.05$)

After examining cross correlations between factors, the multi-factor ANOVA was carried out using factors with low cross-correlation coefficients. The ANVOA was started with all factors including traffic counts (car-NOx-equivalent), meteorological parameters (wind speed), and temporal factors (hour, day of week, and season). When all factors were considered, the ANOVA was not performed due to potential correlation among the factors. Thus, one temporal factor was removed at a time, and different combinations of temporal factors were used in ANOVA. Only the factor "season" worked with traffic

counts (car-NOx-equivalent) and meteorological parameters (wind speed) to explain the variations in concentrations, but the percentage explained by season was less than 1%. It was observed that the combination of traffic counts with mechanical mixings also did not work. Table 4.4 lists the multi-factor ANOVA models used for portioning of variability in observed and simulated concentrations.

Table 4.4: Multi-factor ANOVA partitioning (R^2 (adj)) of simulated and observed NO_2 concentrations at the Windsor-West Station (all factor in the models are significant at $p<0.05$)

Adjusted Sum of Squares	ANOVA	Traffic counts			Meteorological factors		Temporal factors			R^2
		Car (veh/h)	Truck (veh/h)	Car-NOx-Equivalent (veh/h)	Wind speed (m/s)	Mechanical Mixing height (m)	Hour of day	Day of week	Season	(adj)
Simulated NO_2 (ug/m^3)	Model 1	14	-	-	27	-	-	-	-	41
	Model 2	-	12	-	28	-	-	-	-	39
	Model 3	**-**	**-**	**15**	**28**	**-**	**-**	**-**	**-**	**40**
	Model 4a	-	-	-	29	-	6	1	1	40
	Model 4b	-	-	-	29	-	7	-	0	39
	Model 5a	-	-	-	-	54	4	0	1	22
	Model 5b	-	-	-	-	54	4	-	0 (p=0.1)	20
Observed NO_2 (ppb)	Model 1	24	-	-	22	-	-	-	-	40
	Model 2	-	21	-	22	-	-	-	-	39
	Model 3	**-**	**-**	**25**	**21**	**-**	**-**	**-**	**-**	**42**
	Model 4a	-	-	-	24	-	4	1	13	40
	Model 4b	-	-	-	24	-	4	-	13	40
	Model 5a	-	-	-	-	58	4	0	5	35
	Model 5b				-	58	4	-	5	35

It was observed that wind speed and traffic counts combined explained 39% or more of variations in concentrations (Models 1-3 in Table 4.4). For traffic, the use of car, truck, and car-NOx-equivalent were similar when they were combined with wind speed to explain variations in concentrations. In particular, the car-NOx-equivalent and wind speed explained 15% and 28% of variations in simulated concentrations, respectively. In comparison to simulated concentrations, less percentage variations in observed

concentrations was explained by wind speed (21%), but more by car-NOx-equivalent (22%).

It was observed that wind speed combined with hour of day, day of week, and season explained 40% of the variations in both observed and simulated concentrations. The wind speed explained the most: 29% in simulated and 24% in observed. Among the three temporal factors, hour of day (6% in simulated and 4% in observed) and season (1% in simulated and 13% in observed) explained the most. However, the percentages explained by these factors were quite different between multi-factor and one-way ANOVA methods (Table 4.2). Also, there was a large discrepancy in percentage explained by season, 13% in observed versus 1% in simulated concentrations, once again suggesting a lack of seasonal variability when wind speeds is considered in the analysis. Model 4 indicates that those three temporal factors combined with wind speed explain as much visibilities in concentrations as traffic and wind speed combined (Models 1-3). This is not unexpected because traffic is correlated with hour of day and day of week (Table 4.3). In Model 5, mechanical mixing heights combined with hour of day and season only explained 22% and 35% of variations in simulated and observed concentration, respectively.

Among the five models listed in Table 4.4, Model 3 was preferred, as it explained most variations in both observed and simulated concentrations. The predictors in Model 3 were car-NOx-equivalent and wind speed. The use of the car-NOx-equivalent makes the model applicable to other urban areas with a different truck percentage. This model also includes the wind speed, which is readily available while the mixing heights need to be estimated using models such as the AERMET.

In summary, the ANOVA shows very good agreement between observed and simulated concentrations in terms of major factors and the percentage of variability explained by each of those factors. This indicates that the simulation model did a good job in representing the effects of the driving force of dispersion and concentrations, which is rarely reported in the literature. The ANOVA results could be used for developing regression concentration models. Traffic counts and wind speed are the two main factors which should be considered (Model 3). As hour-of-day explained 9% of variations in observed concentrations, and concentrations were lower during the daytime (8:00-19:00) due to strong mixing, it might be necessary to develop separate daytime and nighttime models. When hourly traffic data is not available, temporal factors could be used (Model 4).

4.6 Regression models of concentrations

In this section, results of regression models, which were developed to estimate hourly and annual mean concentrations, are presented. Hourly concentrations were predicted for the receptor 40m east of the road. Annual mean concentrations were predicted for all receptors at the study domain.

4.6.1 Hourly concentration models

As the relationship among concentration (dependent variable), vehicle counts and meteorological factors is not linear (Figure 4.31), log-linear regression models were developed to estimate NO_2 and benzene concentrations at a receptor 40 m east of the road (Figure 3.8). Table 4.5 lists the constant and coefficients of the regression models (Equation 3.7). The log-linear model fit was good (R^2 = 72-90) and all variables were

significant at a 95% confidence level. Thus, daytime and nighttime concentrations can be predicted based on equivalent car counts, and wind speed. Details of the regression results can be found in Appendix B. The constant term was lower in the daytime concentration model than the nighttime model (Table 4.5) by a factor of 5 and 8 for NO_2 and benzene, respectively. The constant term (Equation 3.7) reflects effects of factors other than vehicle counts and wind speed such as atmospheric mixings and emission factors. The main difference between nighttime and daytime observations is the consideration of convective mixings by the AERMOD during the daytime. This implied that convective mixing increased dispersion of pollutants and lowered air pollutant concentrations during daytime.

Table 4.5: Hourly concentration models at the receptor 40m east of the road (Equation 3.7) ($p<0.001$)

C		N	f_0	f_1	F_1	f_2	R^2 (adj)
Concentration ($\mu g/m^3$)	Time period	# of records	Constant	Car-NOx-Equivalent counts (veh/h)	Car-Benzene-Equivalent counts (veh/h)	Wind speed (m/s)	
NO_2	Night time	3186	0.0882	0.91	NA	-1.50	89%
	Day time	2339	0.0167	0.92	NA	-0.75	77%
Benzene	Night time	3186	0.0032	NA	0.90	-1.50	90%
	Day time	2339	0.0004	NA	0.97	-0.74	72%

Effects of wind speed on concentrations were lower during the daytime than nighttime. For instance, a 10% increase in wind speed decreased the concentrations during daytime and nighttime by 13% ($[1+10\%]^{-1.5}$-100%) and 7% ($[1+10\%]^{-0.75}$-100%), respectively. This is because convective mixings are only considered in the AERMOD during daytime, and in turn strong mixings lead to lower effects of wind speed during daytime. As

expected, coefficients of vehicle counts and wind speed were positive and negative, respectively.

The coefficients of regression models were similar for benzene and NO_2 during both nighttime and daytime. This reflects the same effect of factors (vehicle counts and wind speed) on both benzene and NO_2 concentrations. For instance, a 10% increased in wind speed lowered the nighttime NO_2 and benzene concentrations by 13%. Similarly, a 10% increase in car counts increased the benzene and NO_2 concentrations by 9%.

Based on Gaussian equations used in AERMOD, the relationship between emission (input) and concentration (output) is linear (EPA, 2004a). However, the power of car-emission-equivalents in Table 4.5 was in the range of 0.9-0.97. Thus, the hourly concentration models were developed again by assuming the power of car-emission-equivalents equal to 1. Results are listed in Table 4.6. After the power of car-emission-equivalent was set to 1, it was observed that 1) the model fits slightly decreased 2) the constant term decreased, and 3) the power of wind speed remained similar.

Table 4.6: Hourly concentration models at the receptor 40m east of the road assuming the power of Car-NOx-Equivalent and Car-Benzene-Equivalent equal to 1 (Equation 3.7) ($p<0.001$)

C		N	f_0	f_1	F_1	f_2	R^2 (adj)
Concentration ($\mu g/m^3$)	Time period	# of records	Constant	Car-NOx-Equivalent counts (veh/h)	Car-Benzene-Equivalent counts (veh/h)	Wind speed (m/s)	
NO_2	Night time	3186	0.0442	1	NA	- 1.51	87%
	Day time	2339	0.0085	1	NA	- 0.737	68%
Benzene	Night time	3186	0.0017	NA	1	- 1.52	87%
	Day time	2339	0.0003	NA	1	- 0.747	65%

There was a strong correlation between traffic counts and hour of day (Table 4.3). Thus, hourly concentration models at the receptor 40m east of the road were developed using the hour-of-day normalized car counts and wind speed as shown in Equation 4.1.

$$C(t) = f_0 \times Car\_Norm(hour-of-day) \times Windspeed(t)^{f_2} \quad (4.1)$$

where:

C(t): Ambient air concentration at hour t
Car_Norm (hour-of-day): Hour-of-day car count normalized to the car counts during 17:00-18:00 as shown in Figure 4.34.
Windspeed: Wind speed at hour t (m/s)
f_0 *and* f_2: Constant and coefficient of the regression

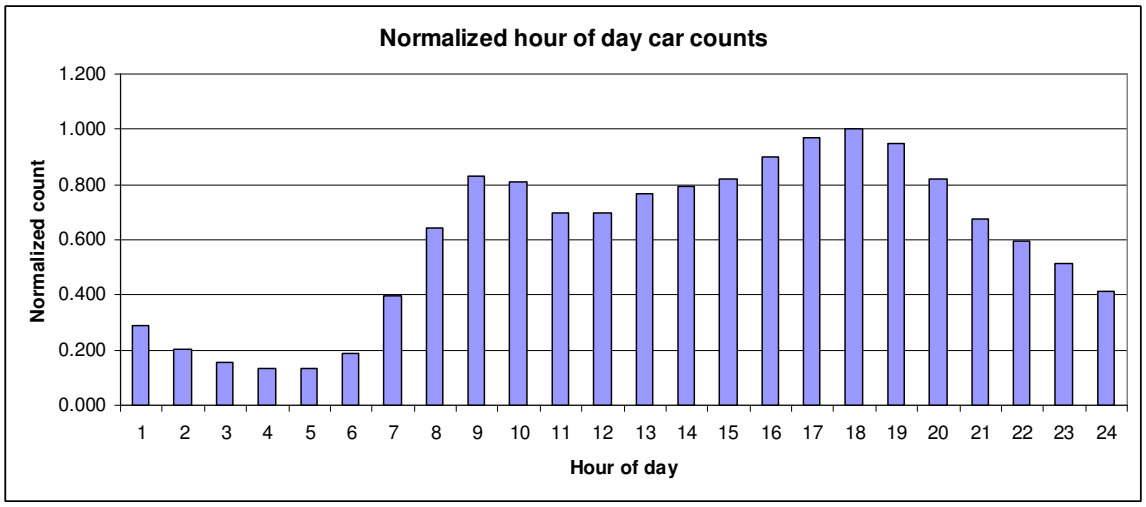

Figure 4.34: Hour-of-day car counts at Huron Church Road in 2008 normalized to the car count during 17:00-18:00

Table 4.6 lists the constant and the coefficient of the regression models developed to estimate hourly concentration using the normalized hour-of-day car counts and wind speed. In this model instead of hourly traffic counts, a 24-hour profile was used (Figure 4.34). However, the model fit was moderate ($R^2 \geq 52\%$, $p<0.05$). This indicates that the use of a 24-hour profile yields similar results as the use of hourly counts for regression

modeling. In comparison to the models developed using hourly counts (Table 4.6), the model fit were lower for the models developed using the 24-hour profile (Table 4.7).

Table 4.7: Hourly concentration models at the receptor 40m east of the road using normalized hour-of-day car counts (Equation 4.1) ($p<0.001$)

C		N	f_0	f_2	R^2 (adj)
Concentration ($\mu g/m^3$)	Time period	# of records	Constant	Wind speed (m/s)	
NO_2	Night time	3186	473	- 1.6	70%
	Day time	2339	67	- 0.75	52%
Benzene	Night time	3186	4.4	- 1.5	81%
	Day time	2339	0.88	- 0.77	59%

Logarithmic regression models were also developed to estimate NO_2 (observed and simulated) and benzene (simulated) concentrations at the Windsor-West Station. The constant and coefficients of regression models are listed in Table 4.8. In comparison to those at the receptor 40m east of the road (Table 4.5), the model fit for the hourly models at the Windsor-West Station was lower, as the station was 1 km away from the road. This was more pronounced for the daytime models. For both observed and simulated NO_2 models, the coefficient of wind speed was higher for the nighttime models. On the other hand, the absolute value of coefficients (f_1 and f_2) was much higher for the simulated NO_2 model than the observed model. This is expected as the observed concentrations include both background and traffic-related concentrations. In other words, per 10% increase in car counts, the observed and simulated concentrations during the nighttime increased by 1.3% and 10%, respectively.

Table 4.8: Hourly concentration models at the Windsor-West Station using Car-NOx-Equivalent counts and wind speed (Equation 3.7) ($p<0.001$)

C		N	f_0	f_1	f_1	f_2	R^2 (adj)
Concentration ($\mu g/m^3$)	Time period	# of records	Constant	Car-NOx-Equivalent counts (veh/h)	Car-Benzene-Equivalent counts (veh/h)	Wind speed (m/s)	
Simulated NO_2	Night time	1697	2.50E-03	1.01	NA	-2.17	60%
	Day time	1150	3.04E-05	1.18	NA	-0.858	16%
Observed NO_2	Night time	1693	6.69E+00	0.136	NA	-0.43	22%
	Day time	1160	3.03E+00	0.185	NA	-0.293	10%
Simulated Benzene	Night time	1697	1.62E-04	NA	0.929	-2.14	59%
	Day time	1150	2.78E-08	NA	1.71	-0.857	16%

The regression models presented in Table 4.5-7 could be used to predict NO_2 and benzene concentrations during nighttime and daytime. Models require the car-equivalent counts and wind speed. For example, 100 cars per hour with a wind speed of 2m/s yields a NO_2 concentration of 16$\mu g/m^3$ and 2 $\mu g/m^3$ during nighttime and daytime, respectively. These simple models could help researchers and policy makers in estimation of traffic-related air quality. The regression models predict concentrations for a receptor 40m east of the road. To estimate concentrations at any other location, they should be adjusted by the normalized falloff pattern of concentration in Figure 4.18. For example, concentrations at 200 m east of the road are 24% those at 40 m east of the road.

4.6.2 Annual mean concentration models

Table 4.9 lists the estimated parameters of multinomial linear regression models for annual mean NO_2 concentrations at different receptors. A strong relationship ($R^2 \geq 75\%$, $p<0.05$) between concentrations at receptors and car-NOx-equivalent counts within a distance from the receptors was observed. Concentrations in the west of the road were lower due to prevailing wind from the southwest quadrant (Figure 4.13). As expected, the constant term and coefficients decreased for the receptors away from the road (Figure 4.16). Both constant term and coefficients were positive as expected.

Table 4.9: Estimated parameters of multiple linear regression models - NO_2 concentration. All coefficients and models were statistically significant ($p < 0.001$).

Group of receptors (Figure 3.11)		Group 1	Group 2	Group 3	Group 4	Group 5	Group 6
Buffer		20-50 m	50-100 m	100-200 m	200-400 m	400-600 m	600-1000 m
N (# of records)		362	608	1231	2587	2748	5950
C (regression constant)		9.3	6.5	3.44	1.76	1.3	0.76
West		-3.7	-1.7	- 0.93	- 0.52	-0.34	-0.22
Car_NOx_	20-50 m	2.6					
Equivalent [a]	50-100 m		0.54				
	100-200 m			0.15			
	200-400 m				0.05		
	400-600 m					0.02	
	600-1000 m						0.008
R2		83%	75%	78%	81%	75%	84%

[a] Annual Average Daily Car-NOx-Equivalent Counts times the length of road segments (m) /106

Table 4.10 lists the estimated parameters of the regression models for benzene annual mean concentrations. A strong relationship ($R^2 \geq 79\%$, $p < 0.05$) between concentrations at receptors and car-benzene-equivalent counts within a distance from the receptors was observed.

Table 4.10: Estimated parameters of multiple linear regression models - Benzene concentration.All coefficients and models were statistically significant ($p < 0.001$).

Group of receptors (Figure 3.11)		Group 1	Group 2	Group 3	Group 4	Group 5	Group 6
Buffer		20-50 m	50-100 m	100-200 m	200-400 m	400-600 m	600-1000 m
N (# of records)		362	608	1231	2587	2748	5950
C (regression constant)		0.078	0.048	0.026	0.014	0.011	0.007
West		-0.036	-0.017	-0.009	-0.005	-0.003	-0.002
Car_Benzene	20-50 m	0.106					
_Equivalent [a]	50-100 m		0.025				
	100-200 m			0.007			
	200-400 m				0.002		
	400-600 m					0.001	
	600-1000 m						0.0003
R^2		87%	80%	82%	85%	79%	87%

[a] Annual Average Daily Car-Benzene-Equivalent Counts times the length of road segments (m) /10^6

Regression models in Table 4.9 and Table 4.10 predict NO_2 and benzene concentrations at each receptor using car and truck counts in different buffer distances from the receptor. These models are suitable for estimation of annual mean concentrations from road networks, where concentrations at each receptor are likely to be affected by multiple roads. For this purpose, geospatial tools such as Arc GIS (ESRI, 2010) could be used for estimation of vehicle counts at different buffer distances from the receptors (predictors), and consequently, calculation of concentrations.

4.7 Ratio of NO_2 to benzene concentrations

This section presents the results for spatial and temporal distribution of the NO_2/benzene concentration ratio. In addition, relationships between NO_2/bezene concentration ratio and truck/car counts ratio were investigated. At the end of this section, observed and modelled ratios of NO_2/benzene were compared.

4.7.1 Spatial distribution of NO_2/bezene concentration ratios

Since trucks are high NOx emitters and cars are high benzene emitters, spatial distribution of NO_2/benzene concentration ratio is affected by the truck/car count ratio in each road section. Figure 4.35 shows side-by-side comparison of NO_2/benzene ratios at receptors and truck/car ratio at road sections. Higher NO_2/benzene ratios were observed near road sections with higher truck/car count ratios (Figure 4.35(b)). However, it was observed that NO_2/benzene ratio decreases with the distance from the road at the road sections with higher truck/car ratio and it increases with the distance from the road at the road sections with lower truck/car ratio (Figure 4.35(a)).

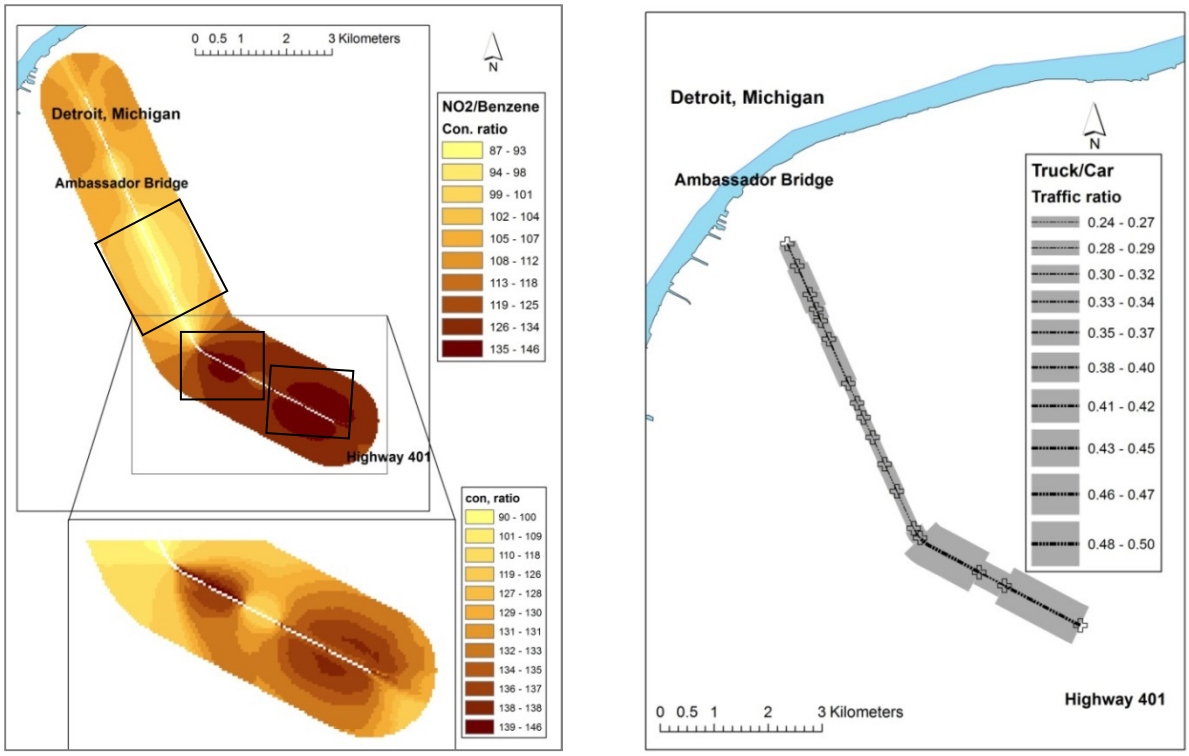

(a) NO_2/Benzene (b) Truck/car ratio

Figure 4.35: Spatial distribution of (a) NO_2/benzene and (b) truck/car ratios

The NO_2/benzene ratio can be expressed as a product of NO_2/NOx and NOx/benzene ratios. To analyze spatial variations in NO_2/benzene ratio, spatial distribution of NO_2/NOx and NOx/benzene ratios were investigated as shown in Figure 4.36. It was observed that the NO_2/NOx ratio increased in a uniform fashion near all the road sections from 0.84 close to the road to 0.9 at 400 m away from the road. The increase in NO_2/NOx concentration ratio with the distance from the road was also observed by Minoura & Ito (2010). This is because as NO moves away from the road, a portion of NO is converted to NO_2 due to reaction with O_3; this process is known as NOx titration (Reaction 3.1). Spatial distributions of NOx/benzene (Figure 4.36(b)) and NO_2/benzene (Figure 4.35(a)) ratios were similar. The ratios decreased with distance from the road at the road sections with higher truck/car ratio (Figure 4.35(b)) and increased with distance from the road at

the road sections with lower truck/car ratio (Figure 4.35(b)). This is potentially because concentrations at receptors are affected by emissions from multiple road sections.

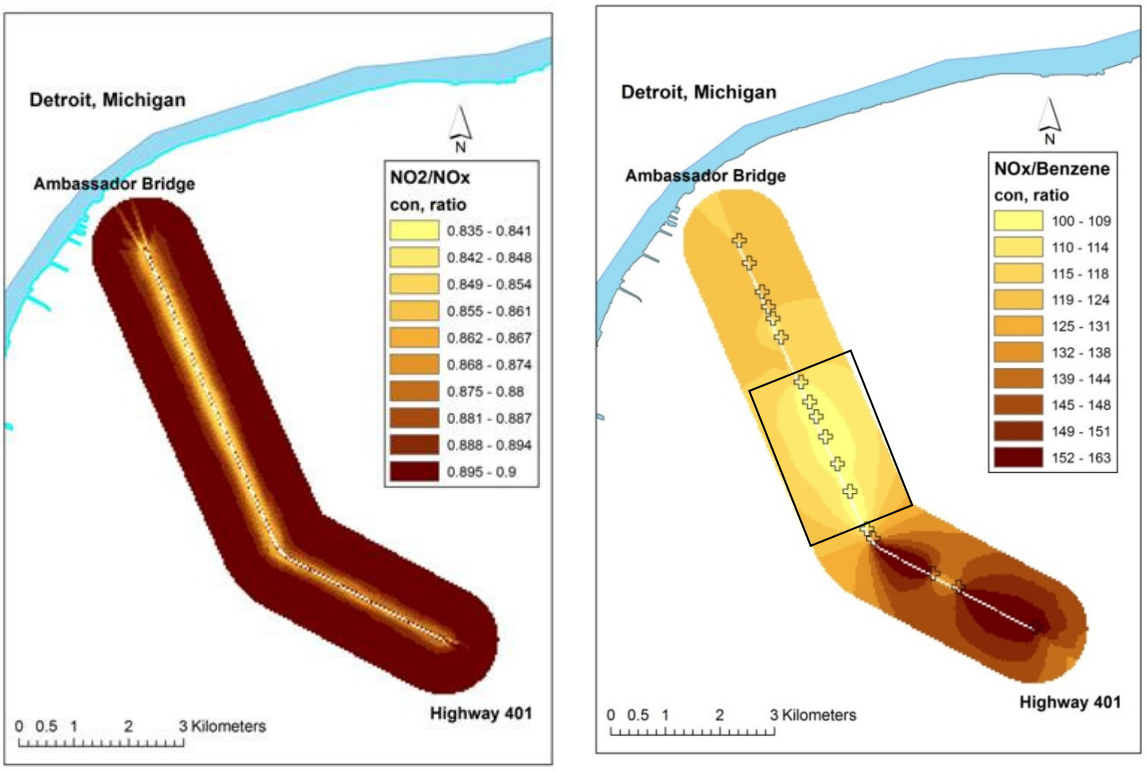

(a) NO_2/NOx (b) NOx/Benzene

Figure 4.36: Spatial distribution of (a) NO_2/NOx and (b) NOx/benzene ratios

To further examine this reasoning, a straight road section with similar values of truck/car ratios was considered: the Cabana-Northwood road section with truck/car ratios of 0.24-0.27 as marked in Figure 4.36(b). It should be noted that near this road section, NOx/benzene ratio increased with distance from the road. The NOx/benzene is the lowest near this road section due to the lowest truck/car ratio at this road section (Figure 4.35(b)). However, it is desired to find whether the increase in NOx/benzene ratio with distance from the road is to an effect of emissions from other road sections with higher truck/car ratios or not. As a result, the NOx/benzene ratios near the Cabana-Northwood

road section was modeled under two conditions: 1) emissions from the Cabana-Northwood road section only and, 2) emissions from all road sections. The first condition is not realistic. However, the idea is that whether increase in NOx/benzene near this road section is due to effects from other road sections or not?

It was found that in the simulation case where emission is produced from the Cabana-Northwood road section only, the NOx/benzene ratio did not change with the distance from the road (Figure 4.37(a)). However, in the simulation case where emission is produced from all road sections (Figure 4.37(b)), the NOx/benzene ratio increased with the distance from the road. This is potentially due to higher truck/car ratios at nearby road sections.

Overall, NO_2/benzene ratio increased with the distance from the road due to conversion of NO to NO_2 near the road. Away from the road, the NO_2/benzene ratio is affected by truck/car ratios at multiple road section. Thus, this could lead to increase or decrease in NO_2/benzene ratios with distance from the road.

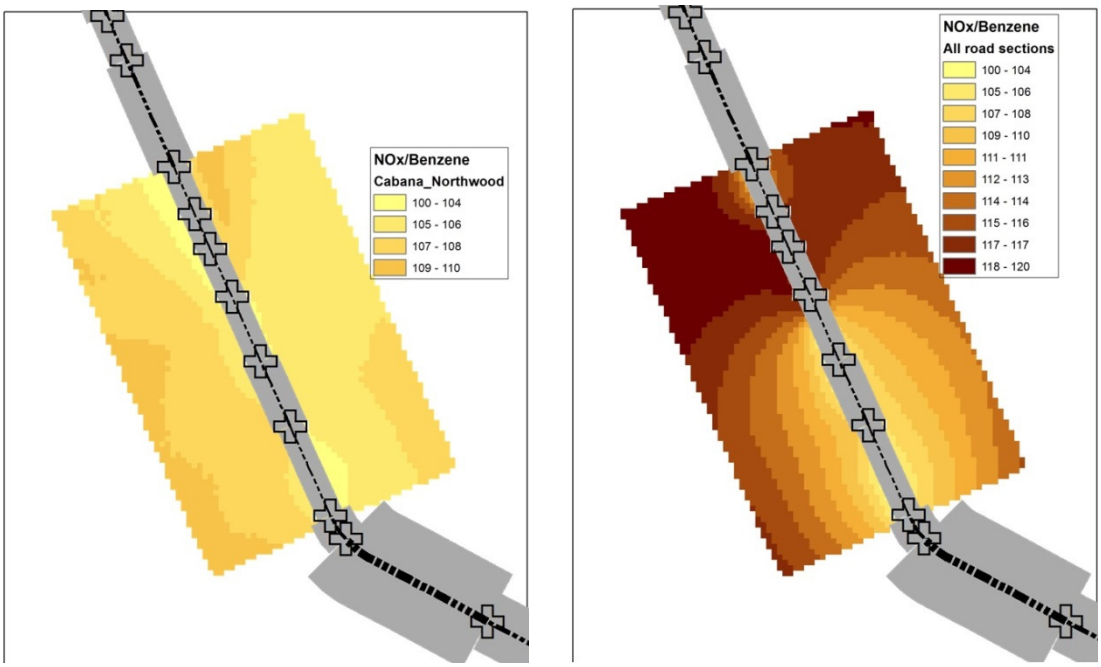

(a) Emissions from the Cabana – Northwood road section (b) Emissions from all road sections

Figure 4.37: Spatial distribution of NOx/benzene ratio – Gray colors indicate relative magnitude of truck/car ratios

4.7.2 Relationship between ratio of simulated NO_2/benzene and truck/car ratio

A significant linear relationship between the ratio of hourly NO_2 to benzene concentrations and the ratio of hourly truck to car counts was observed (Figure 4.38). The slope of the regression line (= 238) reflects the marginal increase in NO_2/benzene ratio per unit increase in truck/car ratio. For instance, for every 0.1 unit increase in the truck/car counts ratio, NO_2/benzene concentration ratio increases by 238×0.1=23.8. The intercept reflects the NO_2/benzene concentration ratio for cars only (= 30.5). This ratio is similar to the ratio of NOx/benzene emission factors of cars (= 27, Figure 4.8 and Figure 4.9). Also, the intercept is similar to the observed NO_2/benzene ratios by Modig et al. (2008) and Wheeler et al. (2008).

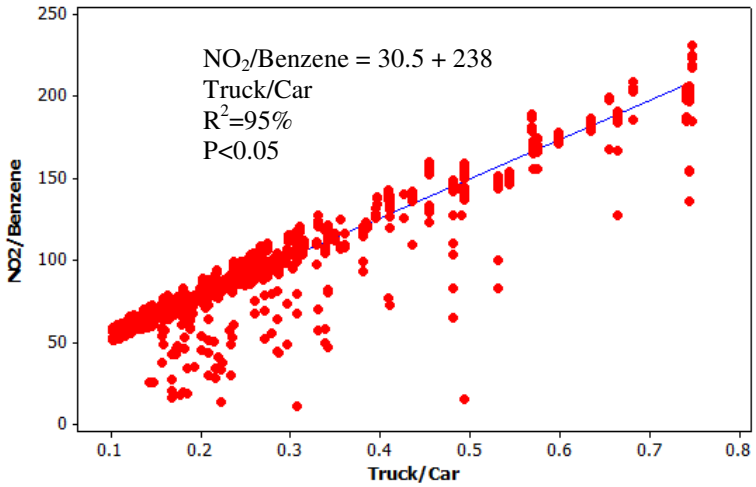

Figure 4.38: Scatter plot of NO_2/benezene concentration ratio at a receptor 40m east of the road versus truck/car counts ratio at the nearest road section, the EC Row-Northwood

This indicates that truck/car traffic ratio can be used to estimate NO_2/benzene concentrations ratio, which can be used in turn to predict the concentration of one compound when the other one is known. However, this relationship is valid only for traffic-related NO_2 and benzene concentrations. Thus, when using observed concentrations, the background concentrations of both NO_2 and benzene should be considered. In this regard, the background contributions, which vary by location, can be estimated using the ratio of observed concentrations at a nearby rural station to those at an urban station. Examples of background contribution for benzene and NO_2 are 0.13 (McCarthy et al., 2006) and 0.5 (Modig et al., 2004), respectively. Equation 4.2 shows how traffic-related concentration can be calculated using observed concentrations and the background contribution.

$$C_{traffic}=(1-R)\times C_{obs} \quad (4.2)$$

where:

$C_{traffic}$, C_{obs} : traffic-rated and observed concentrations, respectively.

R: background contribution, ratio of concentrations at a rural nearby station to that in an urban station

Figure 4.39 shows annual average NO_2/benzene concentration ratio at 16 receptors 40m east of the road (Figure 3.9) and truck/car counts ratio on the road sections. A linear relationship was fitted between NO_2/benzene and truck/car ratios. Similar to hourly observations in Figure 4.38, this relationship was significant (R^2 = 0.98, $p<0.05$). The intercepts and the slope of the regression lines were also similar (Figure 4.38 and Figure 4.39).

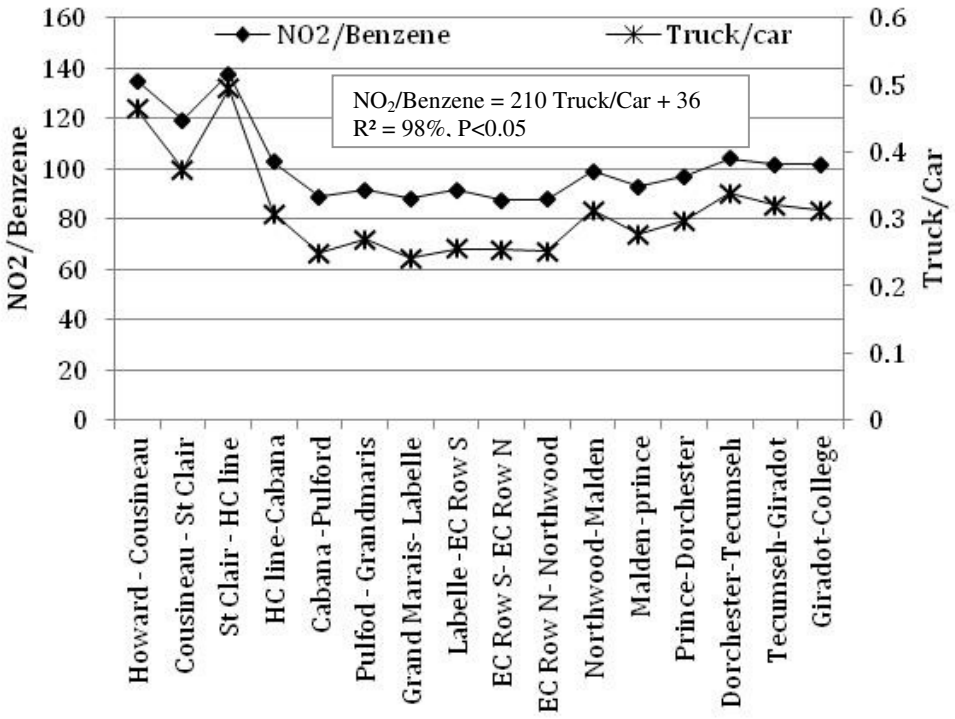

Figure 4.39: Spatial distribution of annual NO_2/benzene concentration ratio at receptors 40m east of the road and truck/car counts ratio on road sections

Table 4.11 lists constants and coefficients of multinomial linear regression models used for estimation of NO_2/benzene concentration ratio at groups of receptors located at buffer distance of 20-50 m, 50-100 m, 100-200 m, 200-400 m, 400-600 m, and 600-1000 m from the road. Predictors were truck/car ratios at buffer distances from the receptors. A significant relationship was observed between the NO_2/benzene concentration ratio and truck/car counts ratio in different distances from the receptors. The slope of the regression line decreased with the distance from the road, e.g. from 206 for the receptors 20-50 m from the road to 132 for receptors 600-1000m from the road. Contrarily, intercept of the regression models increased with the distance from the road. This implies that effects of truck/car ratio on the NO_2/benzene concentration ratios decreases with the distance from the road. This could be because the NO_2/benzene ratio far from the road is affected by truck/car ratios at multiple road sections (Figure 4.35(a)). In other words, if all road sections had the same truck/car counts ratios, the intercept and slope would be similar for all groups.

Table 4.11: Constant and coefficients of multinomial linear regression models – NO_2/Benzene concentration ratio versus truck/car counts ratio (for all models $p < 0.001$)

Groups of receptors		Group 1	Group 2	Group 3	Group 4	Group 5	Group 6
Models		Model 1	Model 2	Model 3	Model 4	Model 5	Model 6
Receptors at buffer distances from the road		20-50 m	50-100 m	100-200 m	200-400 m	400-600 m	600-1000 m
N (number of receptors)		362	608	1231	2587	2748	5950
c (constant)		41.6	43.9	48.8	56.3	63.4	67.9
Truck/Car ratio at buffer distances from the receptors (predictors)	Coefficients 20-50 m	196					
	50-100 m		188				
	100-200 m			180			
	200-400 m				164		
	400-600 m					146	
	600-1000 m						133
R^2(adj)		94%	94%	95%	93%	90%	90%

Field observations of NO2/benzene and truck/car ratio

Seasonal mean NO_2 and benzene concentrations at a station 40m west of the St. Clair – Cousineau Road section (Figure 3.2) along with car and truck counts at this road section during 2006-2007 were obtained from DRIC (2008b). As shown in Figure 4.40(a), the NO_2/benzene concentration ratio was positively correlated with the truck/car traffic ratio. Contrarily, there was negative correlation between NO_2 and benzene concentrations (Figure 4.40 (b)). This observation contradicts the priori expectation that near-road benzene and NO_2 concentrations are positively correlated because both are from traffic. However, the inverse relationship between seasonal NO_2 and benzene is due to inverse relationship between seasonal truck and car counts (Figure 4.40(c)); given that truck are high NOx emitters and cars are high benzene emitters. It should be noted that hourly car and truck counts were positively correlated, but seasonal mean counts were inversely correlated.

Based on the relationship between NO_2/benzene concentration ratio and truck/car counts (Figure 4.40(a)), NO_2/benzene ratio increased by 212 per one unit increase in truck/car traffic ratio. This observed concentration ratio was similar to the simulated concentration ratio as 238 for hourly simulations at a receptor 40m east of the road (Figure 4.27) and 206 for the group of receptors at the buffer distance of 20-50m from the road (Table 4.11). This comparison indicates that the simulated NO_2/benzene ratios are fine although background concentrations were not considered. Also, the multi-model method used in this study (Mobile 6.2 and AERMOD) predicts the NO_2/benzene concentration ratio close to the observation.

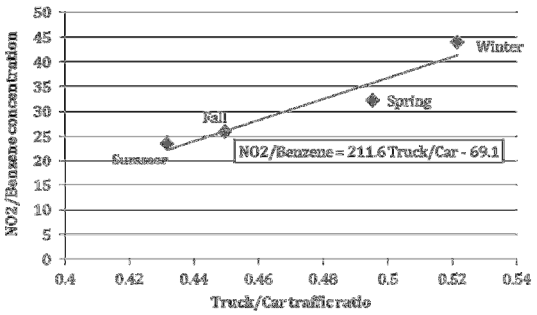

(a) NO_2/benzene versus truck/car

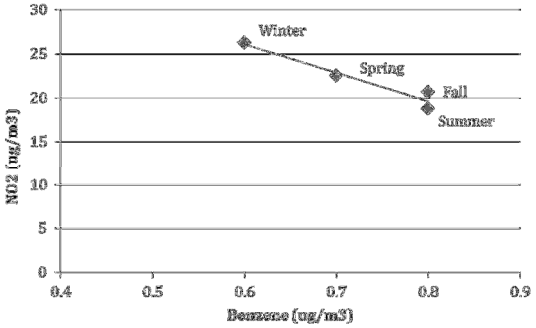

(b) NO_2 versus benzene

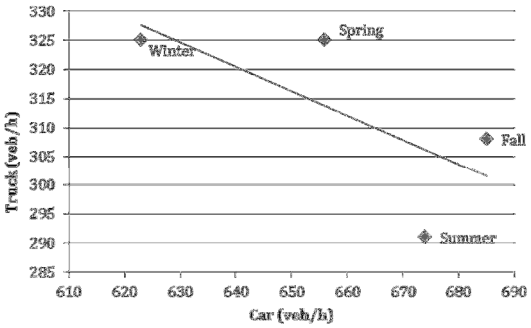

(c) Truck versus car

Figure 4.40: Seasonal mean concentrations and vehicle counts (Data source: DRIC, 2008b)

4.8 Comparison of simulated and observed NO_2/NO_x and NO_2/benzene ratios

For comparison of simulated and observed ratios NO_2/NOx and NO_2/benzene concentration ratios, background concentrations of NO_2, NOx, and benzene were estimated.

Background concentration

Background concentrations are the concentrations that are not from nearby sources. Thus, they are expected to be low and independent from wind direction in urban areas (Kumar et al., 2011). Kumar (2013, personal communication) suggested a method for estimation

of background concentrations: arrange the observed concentrations in a descending order and perform wind direction analysis. Figure 4.41 shows hourly NO_2 concentrations at the Windsor-West Station in 2008 in a descending order. Background concentration should be approximately the value near the tail of the data. It was assumed that the 25th percentile of observed NO_2 concentrations is the background concentration. However, the condition is that the lowest quartile of concentrations should be independent of wind direction. This condition was examined by plotting and comparing pollution roses of "all hours" versus the "lowest quartile" of data as shown in Figure 4.42. The pollution rose represented average concentrations in different wind direction sectors. From the pollution rose of "all hours", it was found that the highest concentrations are associated with winds from the southwest quartile. This indicates the existence of a strong source in the southwest of the station. However, the pollution rose for the lowest quartile was uniform. This satisfied the earlier condition that background concentration should be independent of the wind direction.

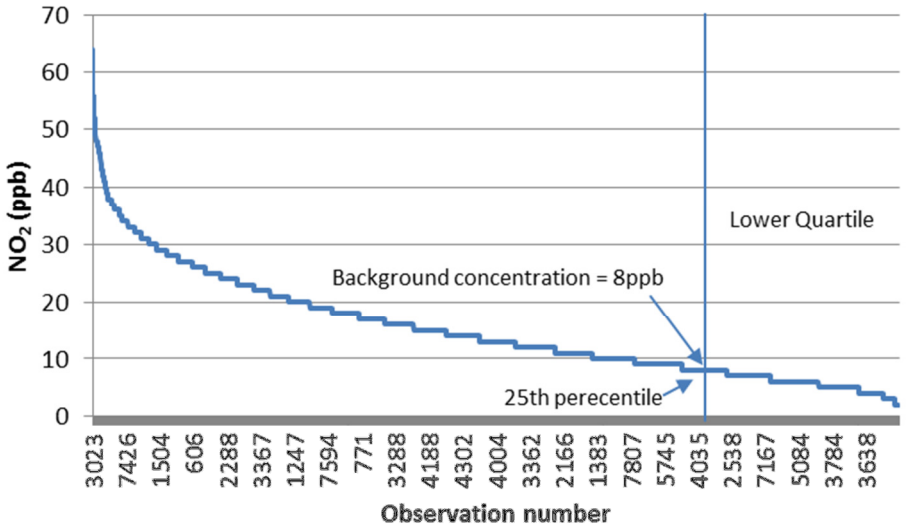

Figure 4.41: Hourly observed NO_2 concentrations in 2008 at Windsor-West Station in a descending order

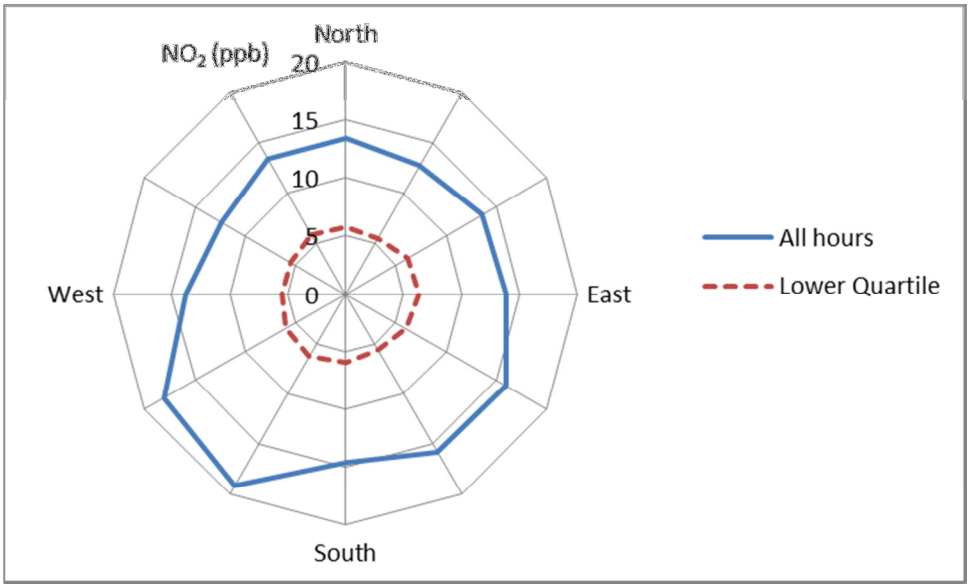

Figure 4.42: Pollution roses of NO_2 concentrations in 2008 at the Windsor-West Station Station

Similar method was used for NOx concentrations at the Windsor-West Station. Hourly NO_2 and NOx concentrations were collected in two stations 40m from the road during October 2006- September 2007 and they were obtained from DRIC (2008). Background concentrations ofNO_2 and NOx concentrations at these two stations were calculated using the same method used for the Windsor-West station. For benzene concentrations, there were 44 daily observations in 2008. The 25th percentile of daily benzene concentrations was 0.5 µg/m^3. This value was close to the lowest observed benzene concentrations across Windsor in 2004 (Wheeler et al., 2008). Table 4.12 lists estimated background concentrations of NO_2, NOx, and benzene at three air quality stations in Windsor.

Table 4.12: Estimated background concentrations of NO_2, NOx, and benzene at three air quality stations in Windsor

Station	Source	Distance to the road	Year	Background concentration		
				NOx (ppb)	NO_2 (ppb)	Benzene ($\mu g/m^3$)
OPHL	DRIC (2008b)	40 m	October 2006-September 2007	10.4	7.1	0.5 *
St. Clair	DRIC (2008b)	40 m	October 2006-September 2007	6.0	5.4	0.5 *
Windsor-West	MOE (2009a)	900 m	2008	11	8	0.5

* Background concentration of Benzene was assumed to be the same as concentration at the Windsor-West station as the annual mean concentrations were similar.

Table 4.13 compares the observed and simulated NO_2/NOx and NO_2/benzene concentration ratios at the two receptors 40 m (OPHL and St. Clair Stations) and one receptor 900m (Windsor West Station) from the road – with and without considering background concentrations. Observed ratios at the DRIC station and the Windsor-West were collected during October 2006-September 2007 and 2008, respectively. As the ratio of annual mean concentrations is not much different by year, this comparison is valid. It was found that when background concentrations are considered, the simulated NO_2/benzene ratio at all three stations and NO_2/NOx ratio at the Windsor-West Station become close to observed ratios.

Both observed and simulated (without background) NO_2/NOx concentration ratios were higher at the receptor 900 m from the road (Windsor-West: 0.75) than those at the receptors 40 m from the road (OPHL: 0.5 and St. Clair: 0.56). This is because NO_2 is formed at the locations away from the road. However, the magnitude of simulated

(without background) NO_2/NOx ratio (0.84-0.89) was much higher than the observed ratio (0.5-0.75). This is because a single road was considered in this study, and there is low amount of NOx emissions, which have been titrated with an excessive amount of O_3. It should be noted that the observed O_3 were used in AERMOD.

When background concentrations were added, the modeled NO_2/NOx ratios got closer to the observed ratios at the OPHL and Windsor-West stations. This is because background concentrations at the St. Clair station were lower than the other two stations (Table 4.12).

Table 4.13: Observed and simulated NO_2/NOx and NO_2/benzene concentration ratios

	Station	Source	Distance to the road	Year	Time resolution	Observed ratio	Simulated in 2008 without background	Simulated in 2008 with background from Table 4.12
NO_2/NOx (ppb/ppb)	OPHL	DRIC (2008b)	40 m	Oct 2006-Sep 2007	1 annual	0.5 (14/28)	0.86 (8.7/10.1)	0.77 (15.8/20.5)
	St. Clair	DRIC (2008b)	40 m	Oct 2006-Sep 2007	1 annual	0.56 (12/21)	0.84 (6.5/7.7)	0.87 (11.9/13.7)
	Windsor-West	MOE (2009a)	900 m	2008	1 annual	0.75 (15.2/20.4)	0.89 (1.1/1.2)	0.74 (16.1/21.9)
NO_2/ benzene (mass/ mass)	OPHL	DRIC (2008b)	40 m	Oct 2006-Sep 2007	1 annual	37.6 [(14×1.88)/0.7]	90 (16.2/0.18)	43.7 (29.7/0.7)
	St. Clair	DRIC (2008b)	40 m	Oct 2006-Sep 2007	1 annual	31.4 [(12×1.88)/0.7]	122 (1.1/.009)	37.9 (22.6/0.6)
	Windsor-West	MOE (2009a)	900 m	2008	39 Daily	39.8 [(16.2×1.8)8/0.76]	103 (0.81/.0077)	33.9 (15.9/0.508)

The increase in observed NO_2/NOx concentration ratio with the distance from the road was also reported by Minoura & Ito (2010). Minoura & Ito (2010) reported that the NO_2/NOx ratios were 0.53 and 0.65 at 20m and 100m from the road.

Overall, the observed and simulated ratios of NO_2/benzene concentrations were similar. Also, the NO_2/benzene concentrations ratios in Table 4.13 (31.4-43.7) were consistent with observations in previous studies (25.2-39.2) (Table 2.4). However,

simulated ratios were higher than observed at two stations near the road (OPHL and St. Clair) due to high a NO_2 formation in simulation.

4.9 Summary

This chapter investigated spatial and temporal variations in NO_2 and benzene concentrations and identified factors affecting such variations. The City of Windsor vehicle counts and emission factors of vehicles from Mobile6.2 were used to estimate vehicular emissions. Then, ambient air concentrations of NO_2 and benzene were estimated using the AERMOD air dispersion model. It was observed that annual mean concentrations were significantly higher in the east of the road than the west of the road, due to the prevailing wind from the southwest quadrant. Concentrations decreased sharply away from the centerline of the road. In terms of seasonal patterns, concentrations were high in fall due to high vehicle counts and low wind speed. Statistical analysis was performed to examine temporal variations of the concentrations. The result of ANOVA showed that vehicle counts and wind speed explained more than 40% of variations in simulated and observed concentrations. From the comparison between the Unit Emission Case (constant emission rate) and the actual case (hourly variable emission rate), it was found that variations in simulated NO_2 concentrations were mainly due to meteorological parameters rather than traffic as it did not vary with hour of day as much as atmospheric dispersion. Hour-of-day patterns of simulated and observed NO_2 concentrations were similar at the Windsor-west station, approximately 1 km west of the road. Fall-off patterns of simulated and observed NO_2 concentrations were also similar at 11 sites on a transit line perpendicular to the road. It was observed that nighttime concentrations from one-vehicle emission were five times higher than daytime

concentrations. In addition, effects of wind speed on concentrations were much higher in nighttime than daytime.

It was found that simple logarithmic regression models with predictors of vehicle counts, and wind speed can reasonably predict modeled hourly concentrations. Also, concentrations at each receptor can be predicted by car and truck counts in different buffer distances from the receptor.

Comparisons with observed patterns suggest that AERMOD reasonably replicates the hour-of-day and falloff pattern of concentrations. However, it tends to underestimate concentrations during the daytime, specifically after 7:00 due to consideration of convective mixings.

Spatial distributions of NO_2/benzene concentration ratios were investigated. It was found that NO_2/benzene ratio is strongly correlated with truck/car count ratio. Generally, the NO_2/benzene concentration ratio increased with the distance from the road because NO_2 forms away from the road. Results show that the NO_2/benzene concentration ratio can be predicted using truck/car count ratios at nearby road sections. However, if the observed concentrations are used, background concentrations of both NO_2 and benzene should be considered. In particular, it was found that per unit increase in truck/car ratio, both simulated and observed NO_2/benzene concentration ratios increased by approximately 200. Thus, the concentration of NO_2 or benzene can be predicted using the ratio if the other pollutant is known. Background concentrations of NO_2, NOx and benzene concentrations at the three stations near the road were estimated by examining observed concentrations. The simulated (with background) NO_2/benzene concentration ratios were similar to observed ratios.

CHAPTER V

5. RESULTS OF PART II: EFFECTS OF INPUT DATA ON EMISSIONS AND CONCENTRATIONS

5.1 Effects of more-detailed input data in a macroscopic level

This section presents the sensitivity of the estimated vehicular emissions and air pollutant concentrations to the details of the input data. Emission factors were estimated by Mobile6.2 and air pollutant concentrations by AERMOD.

5.1.1 Emission factors and total emission

NOx and benzene emission factors and total vehicle emissions were estimated in the Base Case and all other eight scenarios listed in Table 3.14. The percentage difference in emissions between each scenario and the Base Case was calculated.

Base Case

NOx and benzene emission factors of LDVs and HDVs in the Base Case are listed in Table 5.1. NOx emission factor of HDVs was almost eight times higher than that of LDVs whereas benzene emission factor of HDVs was one-third of that of LDVs.

Table 5.1: NOx and benzene emission factors of LDVs and HDVs in the Base Case

Emission factor	LDV	HDV
NOx (g/km/veh)	0.5	3.8
Benzene (mg/km/veh)	18.6	5.4

Scenario 1 – Road type and average speed

Figure 5.1 shows the changes in emission factors when different road type and average speed were selected rather than the arterial road with an average speed of 50 km/h. NOx emission factors of LDVs were not greatly affected by the choice of road types and average speed. On the other hand, NOx emission factors of HDVs changed considerably when a different road type was selected, particularly for Local road, Arterial road 80km/h and the Freeways 60 and 80 km/h. It was also observed that selecting an average speed higher or lower than 50km/h increases the NOx emission factors of HDVs; this is consistent with the pattern of Speed Correction Factors (SCFs) of HDVs shown in Figure C1. However for the same average speed of 60km/h (or 80km/h), NOx emission factor of HDVs was higher when the Freeway option was selected rather than the Arterial road option. This is because for the average speed of 60km/h, proportions of acceleration are higher in freeways than arterial roads (EPA, 1997).

Benzene emission factors of vehicles decreased as the average speed increased. This means choosing an average speed less than 50km/h will increase the emission factors. This pattern is more pronounced for HDVs. The Local road option increased the benzene emission factors by 37% in total, but 158% for HDVs. Detail calculation of emission factor by road type and average speed are reported in Appendix D. It should be noted that changes in annual total emissions are high for Huron Church Road due to high average truck percentage (24%). In most urban areas, where truck percentage is low, changes in total emission are expected to be similar to changes in emission factors of LDVs.

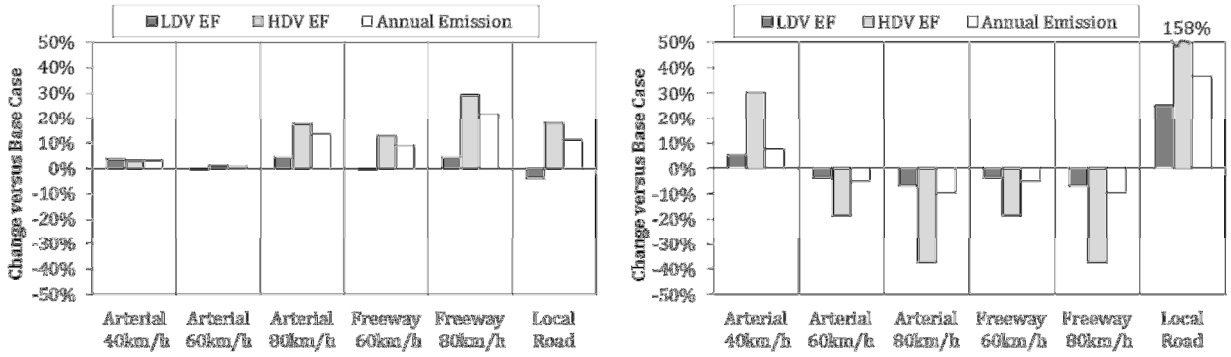

(a) NOx (b) benzene

Figure 5.1: Change in emission factors (Scenario 1-Base Case) – Effect of road type and average speed

Figure 5.2 shows the percentage change in emission factors and annual total emissions versus the Base Case. Overall, the use of local VMT composition results in the most change in total annual emission, 23% increase in NOx emissions and 15% decrease in benzene emissions.

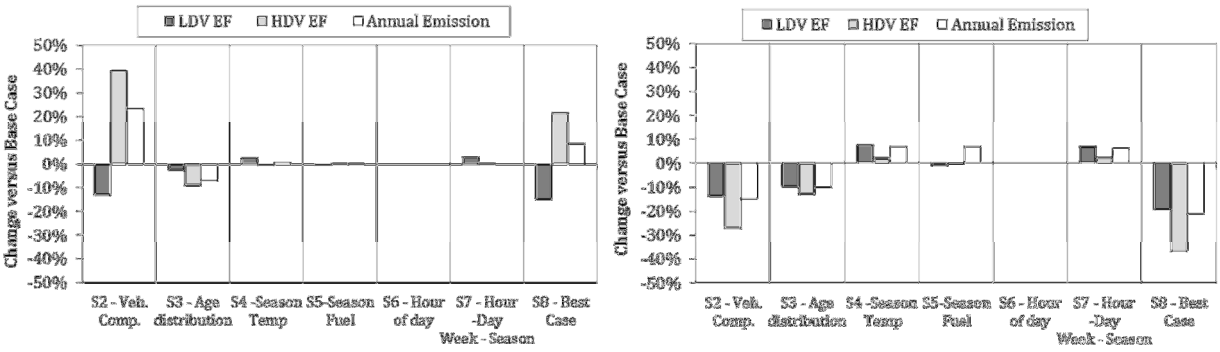

(a) NOx (b) benzene

Figure 5.2: Change in emission factors (Scenario - Base Case)

Scenario 2 – Local VMT composition

Use of local VMT composition over default values of Mobile6.2 highly affected the emission factors. Both NOx and benzene emission factor of LDVs decreased by 13% because of a lower VMT share of passenger trucks in total LDVs in Ontario (30%) compared to default values in Mobile6.2 (56%); given that passenger trucks are high emitters compared to passenger cars. Use of local VMT composition increased NOx emission factors for HDVs by 39% and decreased benzene emission factors of HDVs by 27%. This is because a majority of HDVs (90%) on Huron Church Road are truck trailers (classes HDV8a and HDV8b) where only 2% of them use gasoline (EPA, 2003). Lower share of HDGV in total HDVs resulted in decrease in benzene emission and, higher share of HDDV resulted in increase in NOx emission.

Scenario 3 – Ontario vehicle age distribution

When Ontario vehicle age distributions were used instead of default values of Mobile6.2, NOx and benzene emission factors decreased by 7% and 10%, respectively. This is because Ontario vehicles were younger than the average U.S. vehicles in Mobile6.2 (Figure 3.7) and emission factor of vehicles increases with age.

Scenario 4 – Seasonal temperatures

When seasonal temperatures were used instead of an annual average temperature, NOx and benzene emission factors of vehicles in winter increased by 6% and 28%, respectively. There was a little change in other seasons. The increase in winter was because cold-start emissions increased in lower temperatures. This is less pronounced for HDVs because a majority of HDVs are assumed as HDDV (70%) in Mobile6.2, and there is no temperature correction factor for HDDVs (EPA, 1999b).

Scenario 5 – Seasonal fuel properties

When seasonal fuel properties were used instead of annual average values, NOx emission factors of vehicles changed little, i.e. less than 1%. On the other hand, benzene emission factors of vehicles in winter and summer changed by -10% and 6%, respectively.

Figure 5.3 shows the effect of each fuel parameter on the emission factors. In winter, a higher RVP of 14.6 compared to annual average value of 12.1 resulted in a reduction of benzene emission factors of LDVs by 10%. This is consistent with findings from Tang et al. (2005) who reported a 6% decrease. However, a lower fuel RVP of 9.7 in summer compared to annual average resulted in negligible change in benzene emission factors of both LDVs and HDVs. Although E200 seasonally varies by 6% (Table 3.17), it did not affect benzene emission factors of both LDVs and HDVs. Effects of E300 and Olefin content of fuel were low due to less seasonal variability of these parameters. Aromatic content of fuel affected the benzene emission factors. Lower Aromatic content in winter by 7% (compared to annual average) resulted in a 4% reduction in emission factors.

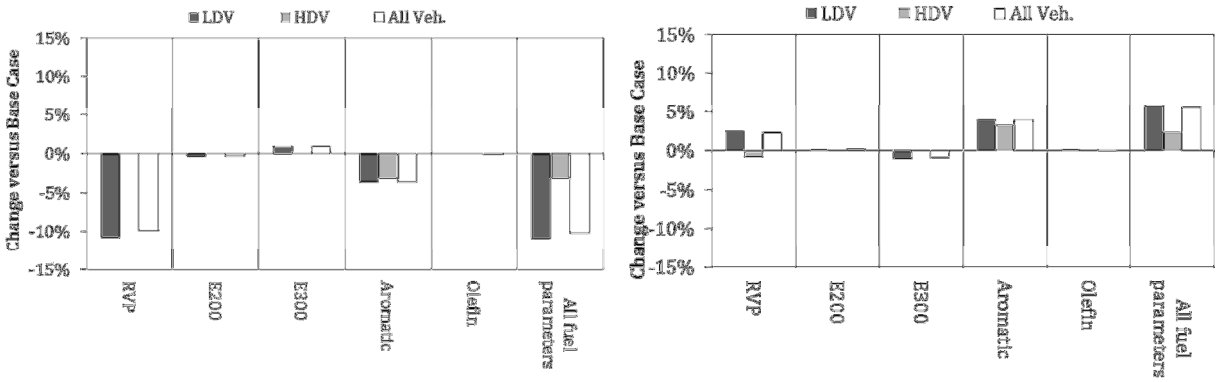

(a) Winter (b) Summer

Figure 5.3: Change in emission factors (S5-Base Case) – Effect of seasonal fuel properties

Scenario 6 – Hour-of-day emission factors

Figure 5.4 shows changes in emission factor of vehicles in 24 hour-of-day simulations versus the Base Case of annual emission factors. Hour-of-day variations in both NOx and benzene emission factors were negligible, i.e. less than 2%. This is due to little variations in hour-of-day temperature, i.e. 5°C (Figure 3.6). Hour-of-day NOx emission is higher during colder hours, e.g. early morning due to cold start leading to higher NOx emissions. However, benzene emission factors of LDVs were lower in colder hours, as the exhaust benzene emission of LDVs increases with temperature (EPA, 1999b).

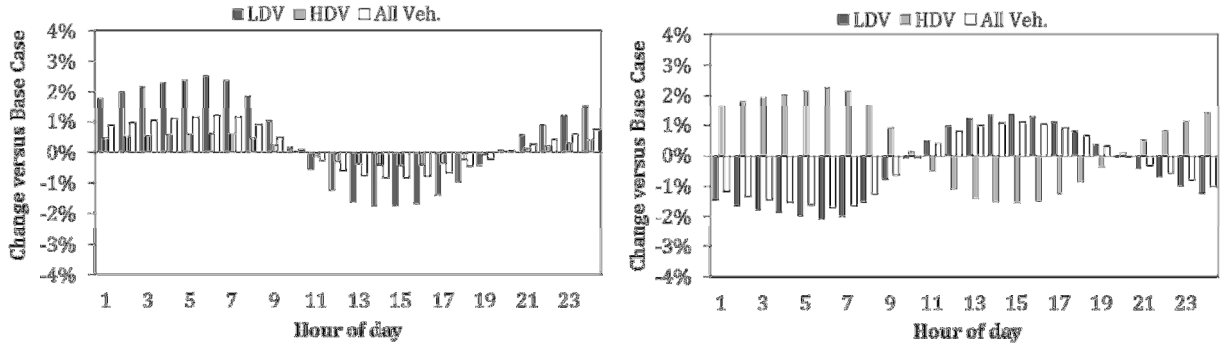

(a) NOX (b) Benzene

Figure 5.4: Change in hour of day emission factors (S6-Base Case)

Scenario 8 – Best Case

The differences between NOx and benzene emissions in the Best Case compared to the Base Case were 11% and -21%, respectively. In other words, when all options in Scenarios 2-7 were considered, NOx emission for all vehicles was 11% higher, and benzene emission was 21% lower compared to the Base Case. Changes in NOx emission for cars and trucks were -15% and 22%, respectively, and changes in benzene emission for cars and trucks were 19% and 37%,

respectively. It should be noted that effects of some factors may be additive whereas effects from some others may cancel out each other. For instance, effects of local VMTs (+39%) and Ontario vehicle age distribution (-9%) on NOx emission factors of HDVs were canceled out. Contrarily, effects of these two factors on benzene emission factors of HDVs were additive.

Spatial distribution of emissions

Figure 5.5 shows spatial distributions of NOx and benzene emissions in the Base Case. Since NOx emission factor of trucks is higher than those of cars, NOx emissions are higher where truck counts are high, e.g. between EC Row and College Ave (Figure 4.6(b)). On the other hand, benzene emissions are higher where car counts are higher. In comparison to NOx emissions, benzene emissions varied in a larger range over the road sections because of higher variations in car counts across the road sections compared to truck counts (Figure 4.6).

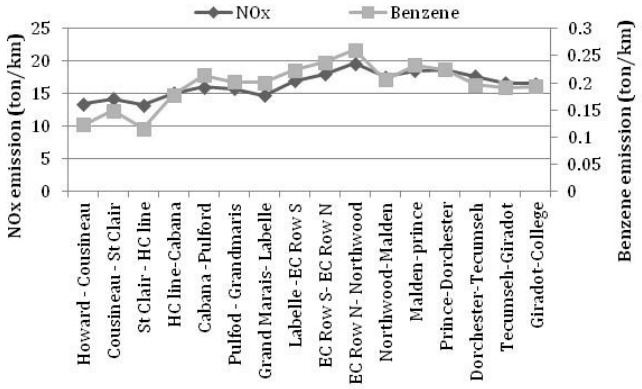

Figure 5.5: Annual emissions by road section in the Base Case

Temporal distribution of emissions

Temporal variations in emissions affect simulated concentrations. In particular, occurrence of maximum hourly is expected to be associated with peak hour emissions. Figure 5.6 shows hour-of-day variations in emissions in the Base Case, and Scenarios 6, 7 and 8 during weekdays.

Emissions in the Base Case and Scenario 4 did not vary by hour. On the other hand, emissions in Scenarios 6, 7 and 8 were higher during the daytime than nighttime as the emissions are described in a function of traffic volume. In comparison with Scenario 6 (Figure 5.6), peak hour emissions were higher in Scenario 7. This is because emissions in Scenario 7 varied by day of week unlike Scenario 6, where emissions were not different by day-of-week. Hour-of-day variations in NOx emissions in Scenarios 6, 7, and 8 (Figure 5.6(a)) were similar to those in truck counts (Figure 4.11), as trucks are high NOx emitters. On the other hand, hour-of-day variations in benzene emissions (Figure 4.26(b)) were similar to those in car counts (Figure 4.11), as cars are high benzene emitters.

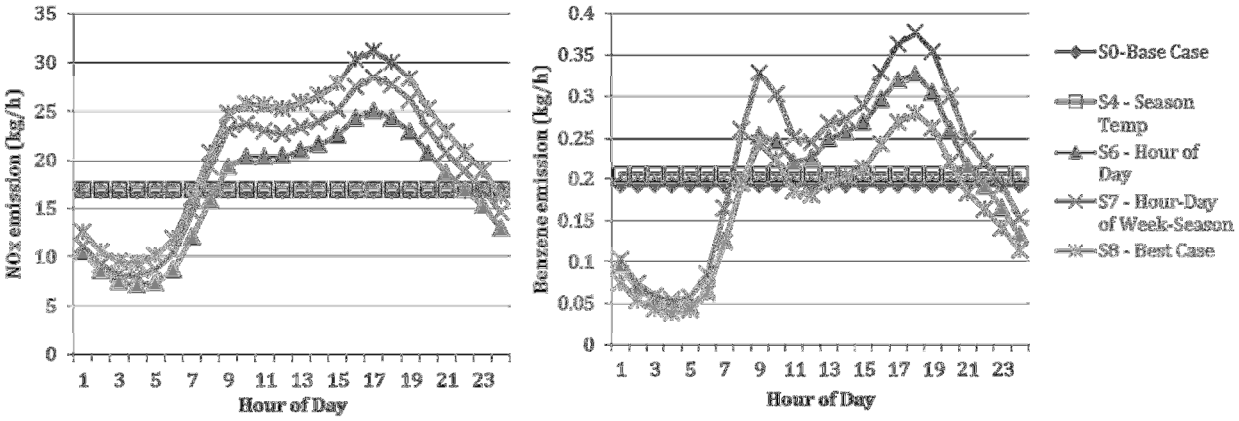

(a) NO_x (b) Benzene

Figure 5.6: Hour-of-day emissions in the Base Case and Scenarios 4, 6, 7 and 8

Seasonal variations of NOx emissions were lower than those of benzene emissions, as shown in Figure 5.7. This is because seasonal variability of NOx emission factor was much lower than that of benzene emission factor. Although car and truck counts were lower in the winter compared to other seasons, benzene emissions were the highest. This is because benzene

emission factors of cars were higher in the winter than other seasons by 28% due to cold start emissions (Figure 4.8).

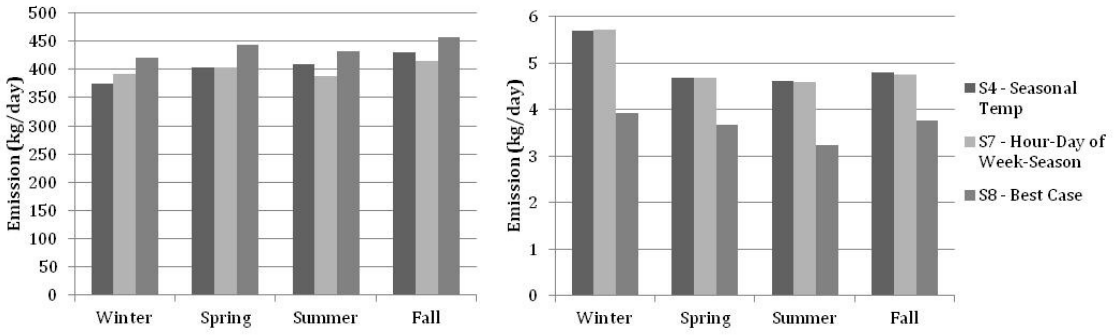

(a) NO_2 (b) Benzene

Figure 5.7: Seasonal variation of emissions in Scenarios 4, 7, and 8

5.1.2 Spatial distribution of concentrations

Figure 5.8 shows spatial distribution of change in annual mean and maximum hourly concentrations along the road in Scenarios 4, 6, 7 and 8 versus the Base Case. Spatial patterns of changes in annual mean concentrations were similar in all scenarios. In addition, annual mean concentrations in the Scenario 4 were not much different than the Base Case whereas annual mean concentrations in Scenarios 6, 7, and 8 were consistently lower than the Base Case (20%). In contrary with annual mean concentrations, maximum hourly concentrations in Scenarios 6, 7 and 8 were higher than the Base Case.

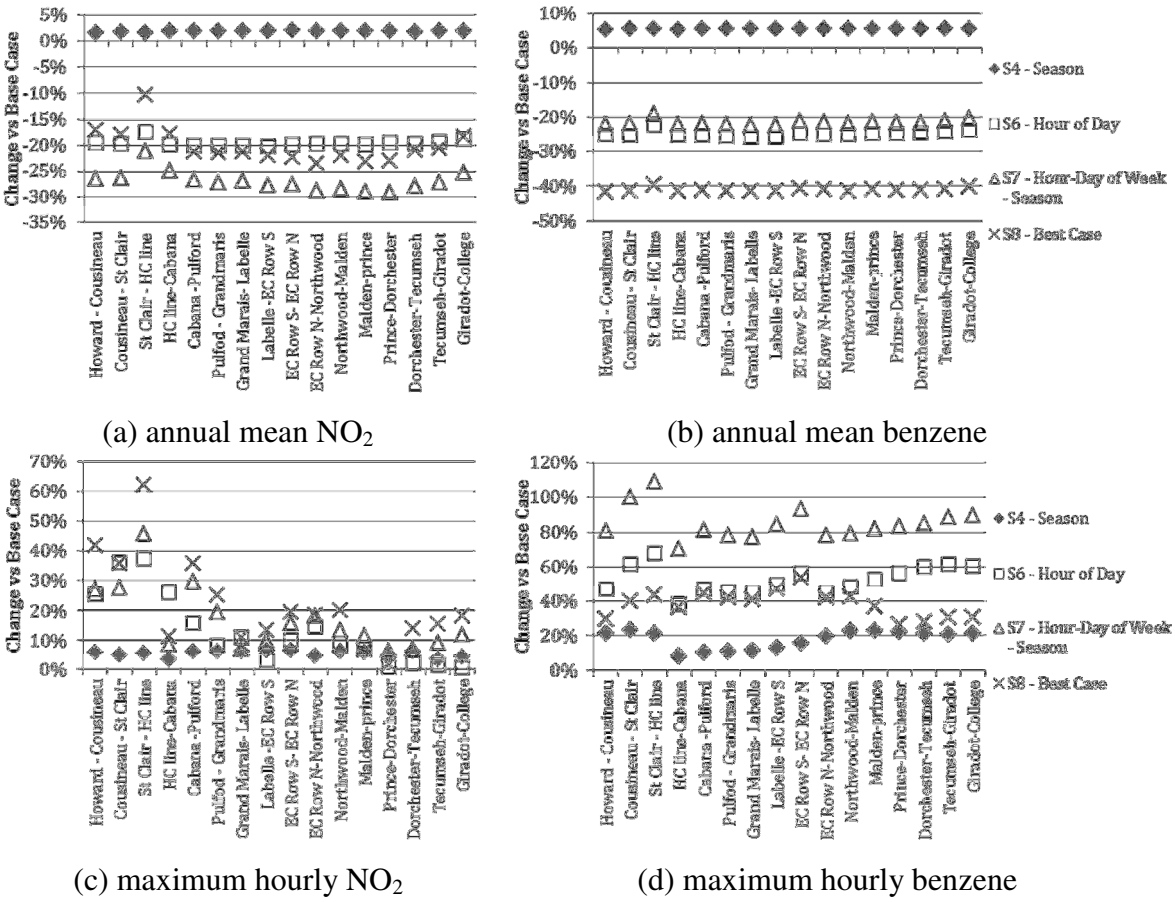

(a) annual mean NO_2 (b) annual mean benzene

(c) maximum hourly NO_2 (d) maximum hourly benzene

Figure 5.8: Spatial distribution of change in NO_2 and benzene concentrations versus the Base Case at 16 receptors, 40m east of the road

Figure 5.9 shows falloff patterns of normalized NO_2 and benzene concentrations in the five scenarios. As expected, Falloff patterns of annual mean and maximum hourly concentrations in all scenarios were similar.

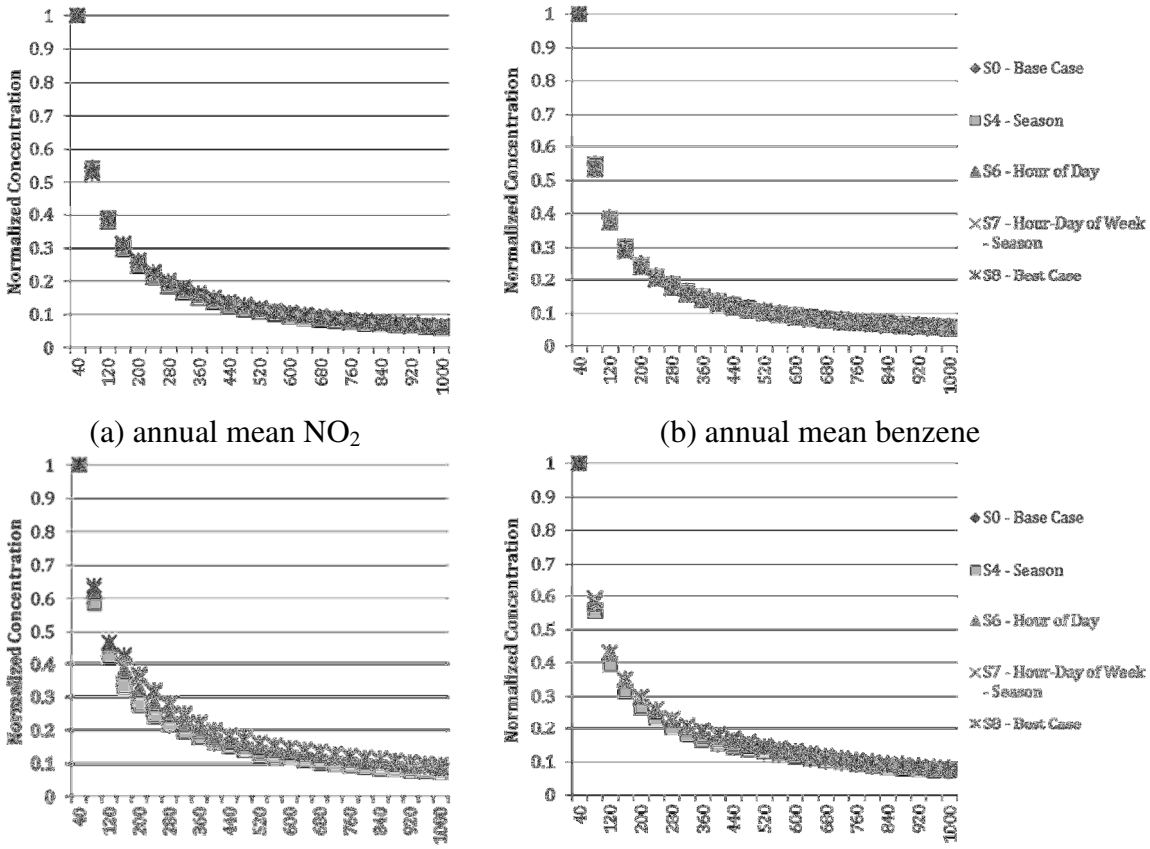

(a) annual mean NO_2 (b) annual mean benzene

(c) maximum hourly NO_2 (d) maximum hourly benzene

Figure 5.9: Normalized concentrations at 25 receptors perpendicular to the road – east of the road near EC Road

Figure 5.10 shows changes in annual mean and maximum hourly concentration in different scenarios versus the Base Case at 32 receptors along the road (Figure 3.9). Except for Scenario 4, annual mean concentrations in all other scenarios were lower by more than 20% compared to the Base Case. For instance, although total emission in the Base Case and Scenario 6 were similar, annual mean benzene concentration in Scenario 6 was 24% lower than those in the Base Case. On the other hand, maximum hourly concentrations in all scenarios were higher than those in the Base Case. This was more pronounced for scenarios with hourly variations in emission input (Scenarios 6, 7, and 8).

These results indicate when a constant hourly rate of emission instead of one with temporal variations, e.g. in Scenarios 6 (hour of day) or 7 (hour of day, day of week, and season) is applied for dispersion modeling, annual mean concentrations are overestimated and maximum hourly concentrations are underestimated.

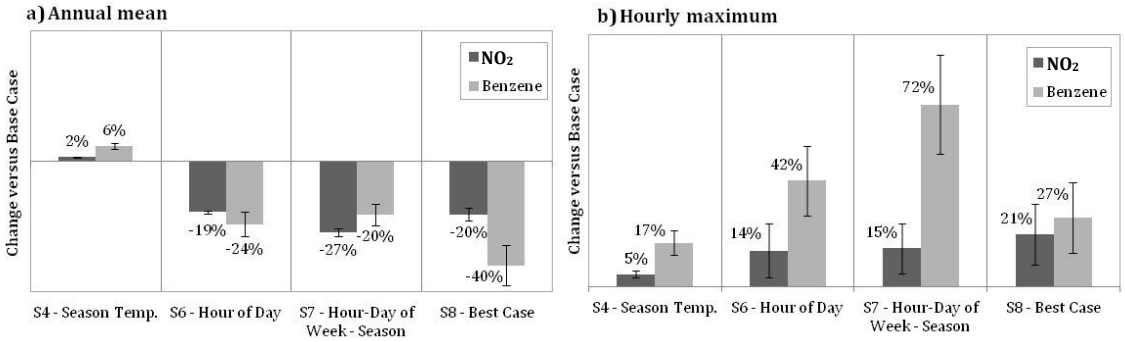

Figure 5.10: Changes in concentrations in different scenarios versus the base Case at 32 receptors along the road – bars are the standard deviation.

5.1.3 Temporal distribution of concentrations

Similar concentration patterns were observed at receptors 40m east and west of the road. Thus, results for the receptor at 40m east of the road are presented. Figure 5.11 shows hour-of-day concentrations of NO_2 and benzene. Similar patterns were observed for the Base Case and Scenario 4, where concentrations were higher during the nighttime (22:00-0:00 and 0:00-7:00) than the daytime. On the other hand, hour-of-day patterns of concentrations in Scenarios 6, 7 and 8 were similar, but different from those in the Base Case and Scenario 4. This discrepancy indicates that when hour-of-day variation of emission factor is not considered, concentrations are overestimated during the nighttime. In other words, hour-of-day concentration patterns reflect the combined effects of meteorological parameters and emission. During the nighttime, atmosphere is stable, and wind speed and temperature are low. Thus, a higher emission in the

Base Case during the nighttime (Figure 5.6) will result in high concentrations. On the other hand during the daytime, due to high wind speed and low stability of atmosphere, concentrations are likely to be low and they are less affected by the emissions. This is consistent with the finding from Figure 4.22, where daytime concentrations for two cases of the Total Emission and the Unit Emission were similar. In conclusion, the results suggest that during the nighttime, effects of emissions are more pronounced, and during the daytime, effects of meteorological parameters are more dominant. As a result of overestimations of hourly concentrations during the nighttime, annual mean concentrations in the Base Case and Scenario 4 were also overestimated (Figure 5.10 and Figure 5.11).

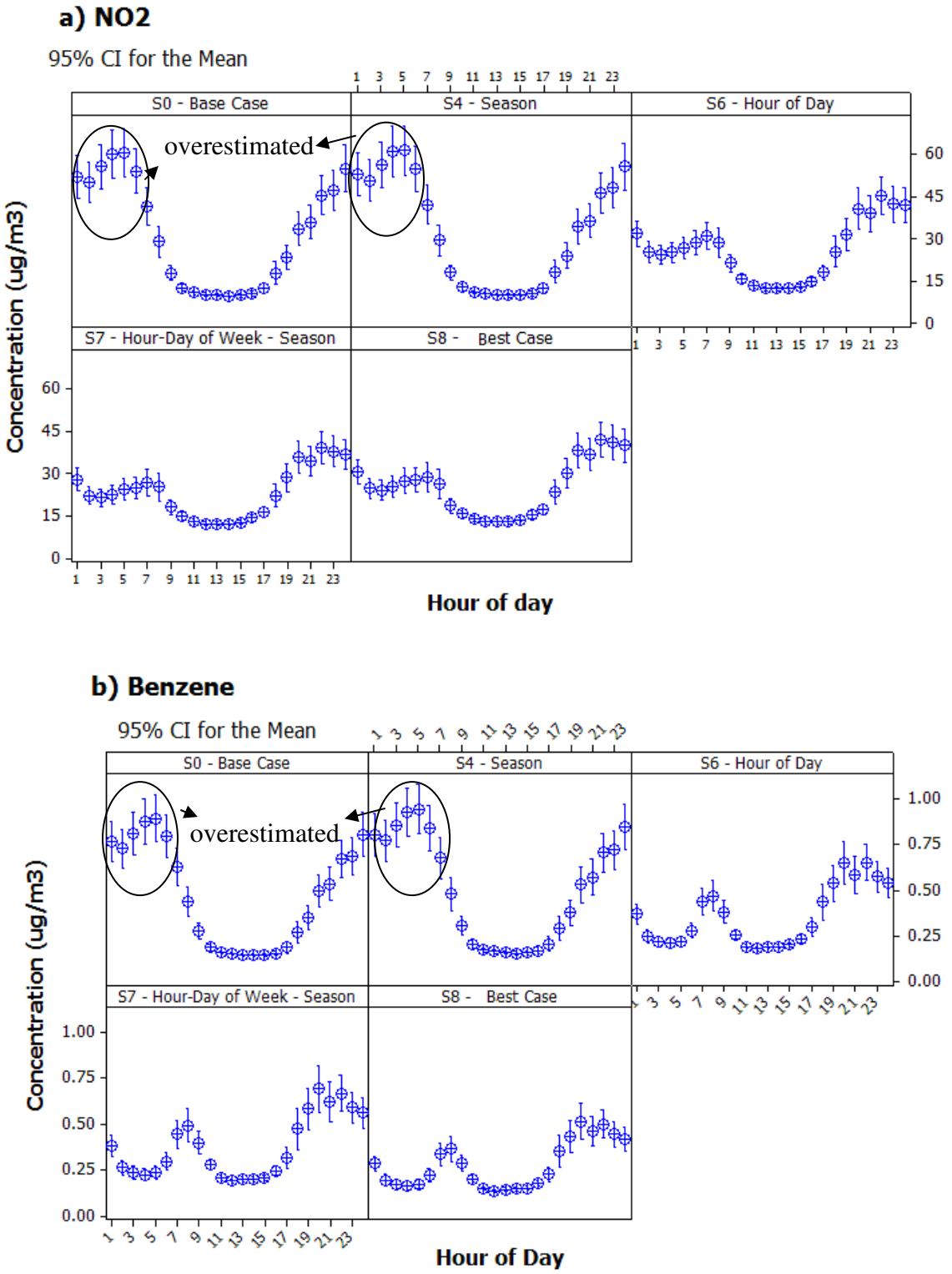

Figure 5.11: Hour of day concentrations in different scenarios at a receptor 40m east and of the road

As shown in Figure 5.12, mean concentrations in all scenarios are much higher than the median values. In other words the mean value is affected by the high concentrations. This is more pronounced for the Base Case and Scenario 4 where hour-of-day variations of emission were not considered for dispersion modeling. The median, 25^{th}, and 75^{th} percentiles of NO_2 concentration values were similar in all scenarios. Annual mean concentrations in Scenarios 6 and 7 were similar. In other words, the improvement of accuracy of the estimated annual mean concentrations by adding day-of-week and seasonal emissions (Scenario 7) is marginal over hour–of-day variations of emissions (Scenario 6). Distributions for all five scenarios and for both pollutants are skewed to the right, i.e. high concentrations occurred occasionally.

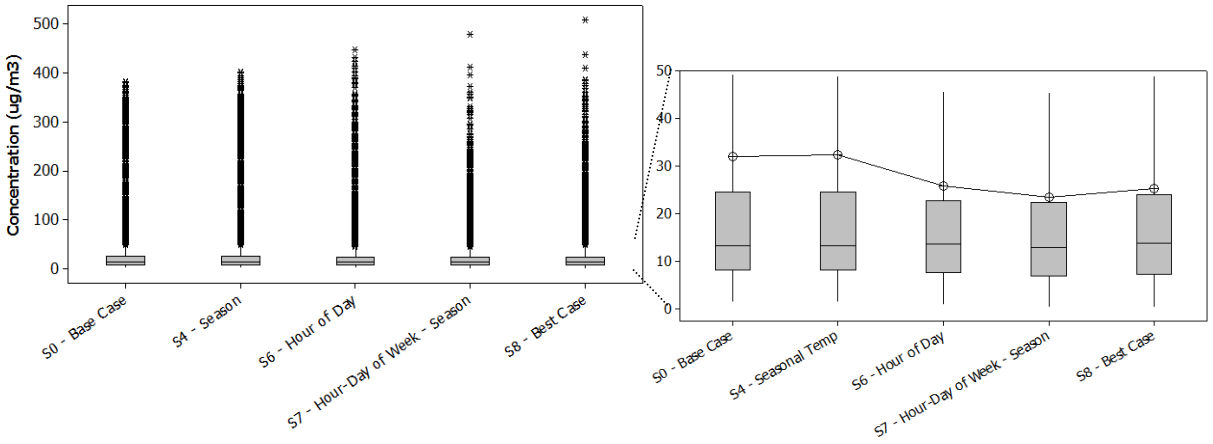

(a) NO_2

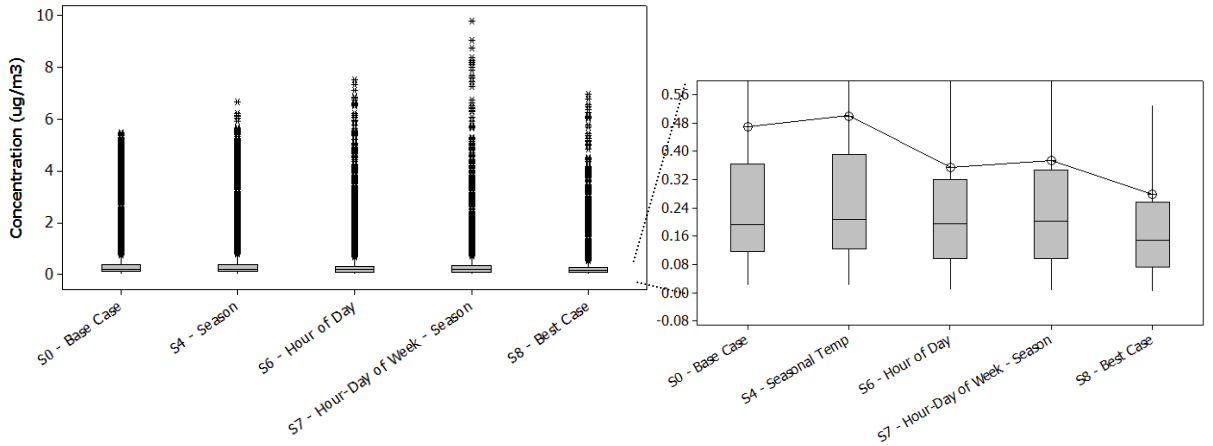

(b) Benzene

Figure 5.12: Box plot distribution of concentrations at a receptor 40 m east of the road, the lower edge of box is 25th percentile, the mid-line is median, top edge of box is 75th percentile, the circle with cross inside is the mean, and the stars are outliers.

In Figure 5.13, three distinctive patterns were observed in the percentile distribution of hourly concentrations at a receptor 40 m east of the road in the five scenarios. First, concentrations under 70th percentiles were similar in all five scenarios, as these low concentrations usually occurred during the daytime when effects of meteorological parameters are more dominant compared to the effect of emissions (Figure 4.22). Second, concentrations between 70th and 99th percentiles were consistently overestimated in the Base case and Scenario

4, where hour-of-day variation of emissions where not considered for dispersion modeling. For these scenarios, high concentrations usually occurred during the nighttime (Figure 5.11) when effects of meteorological parameters were less pronounced (wind speed was low and atmosphere was stable). This resulted in an overestimation of annual mean concentrations in the Base Case and Scenario 4 (Figure 5.12). Third, for concentrations above 99th percentiles, a distinctive separation was observed in the five scenarios because of different maximum hourly emissions (Figure 4.26). NO_2 concentrations above 99th percentile were the highest in Scenario 8 followed by Scenario 7, Scenario 6, Scenario 4, and the Base Case. The order was the same as the order of peak hour emissions in Figure 5.6. This indicates that high concentrations are associated with higher peak hour emissions. For concentrations above 99^{th} percentile, separations between scenarios were more obvious for benzene than NO_2. This is because the peak hour benzene emissions were more different by scenarios than NO_2 (Figure 5.6). Similar to NO_2 concentrations, order of benzene concentrations above 99^{th} percentile was the same as peak hour emissions.

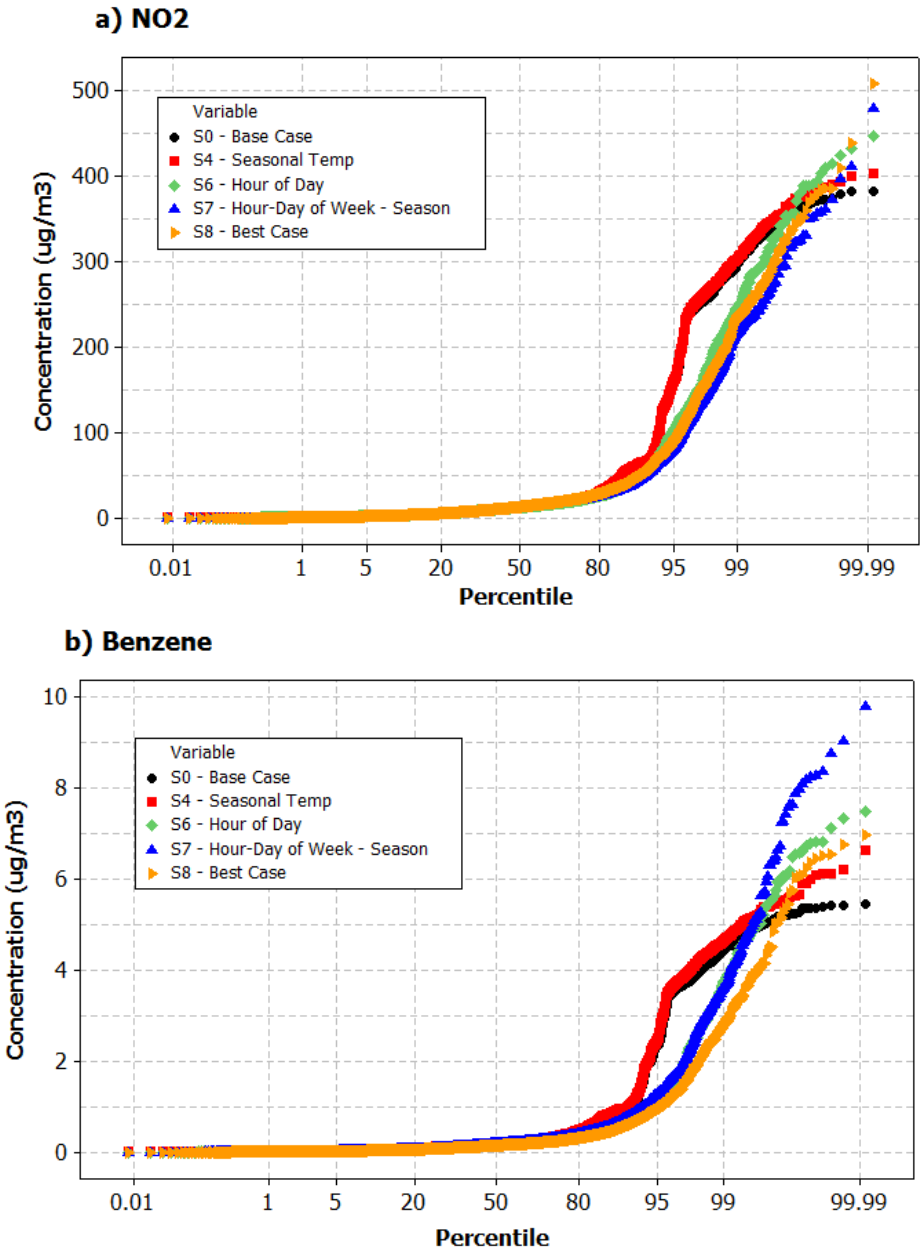

Figure 5.13: Percentile distribution of hourly concentrations at a receptor 40 m east of the road

Figure 5.14 shows seasonal average NO_2 and benzene concentrations at a receptor 40m east of the road. Overall, variations in concentrations by season were similar. However, the difference between the Base Case and the other Scenarios is less during winter compared to the other seasons. NO_2 concentrations in Scenarios 6 and 7 were similar in all seasons. This is because

NOx emissions did not greatly vary by season (Figure 5.7(a)). On the other hand, benzene concentrations were higher during winter in Scenario 7 than Scenario 6 due to higher benzene emissions (Figure 5.7(b)).

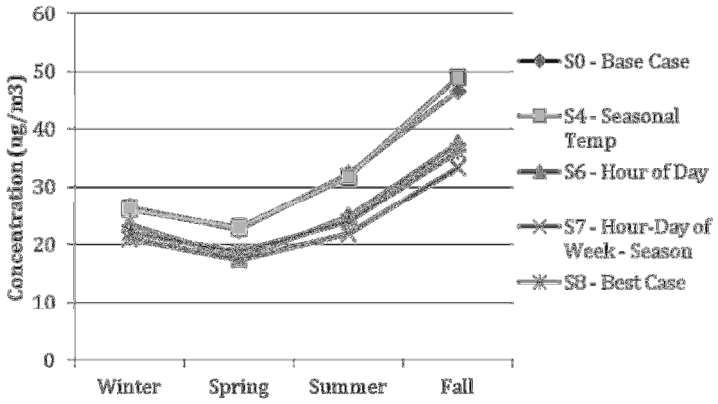

(a) NO_2

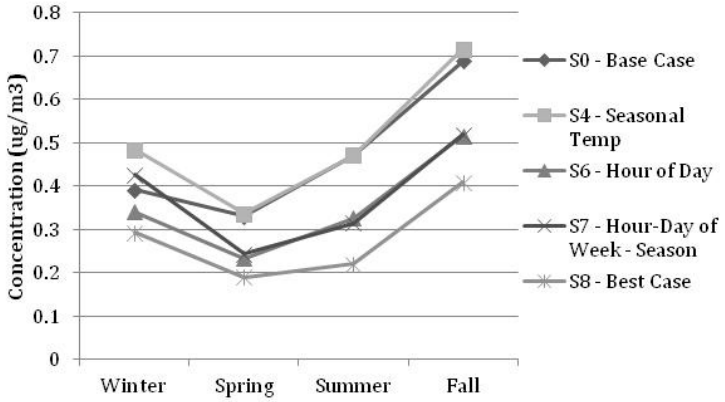

(b) benzene

Figure 5.14: Seasonal average concentrations at a receptor 40m east of the road

5.1.4 Summary

This section investigates effects of level of details in input data on emission factors estimated by Mobile6.2 and ambient air concentrations by AERMOD. In this regard, the Base Case was considered where vehicle composition and vehicle age distribution were default values of Mobile6.2, vehicle counts, temperature, and fuel properties were annual average values, road

type and average speed were Arterial 50km/h and the input emission factor was a constant annual rate. In addition to the Base Case, eight more scenarios were considered, and one input parameter changed at a time in each scenario (Table 3.14). Different temporal resolution of input emission for dispersion modeling was considered, i.e. by hour-of-day and day-of-week and season. The results of the sensitivity analysis are summarized in Table 5.2 including changes in emission factors, emissions and ambient concentrations versus the Base Case. The changes were categorized into four groups: negligible (change ≤ 5%), low (5-10%), intermediate (10-20%) and high (> 20%). It was found that choice of road type and average speed could change the estimated of NOx emissions by 10-20% when Local road, Arterial road 80km/h, and the Freeways 80 km/h were selected compared to choice of Arterial road 50km/h (in the Base Case). On the other hand, benzene emissions were less sensitive to the choice of road type and average speed, except for the choice of Local road (+20%). Use of local vehicle composition over default values of Mobile6.2 changes the estimated NOx emission by more than 20%. It was observed that annual mean and maximum hourly concentrations are highly sensitive to consideration of hour-of-day variability of input emission for dispersion modeling (Scenarios 6 and 7), e.g. it decreased the annual mean concentration by more than 20% and increased the maximum hourly concentration by more than 20%. It was found that results from the Best Case (Scenario 8), where all changes in Scenarios 1 to 7 were considered, were quite different from the Base Case..

Findings from this study suggest that detailed input data are needed for estimation of emissions and ambient air concentrations. Overall, the detailed information on road type, average speed, and vehicle composition are recommended for estimation of emissions using Mobile6.2 (Scenarios 1 and 2). Also, consideration of hour-of-day emission is suggested for dispersion modeling (Scenario 6).

Table 5.2: Summary of results - change in emission factors, emissions, and ambient concentrations versus the Base Case [(scenario-base case)/base case*100]

		NOx					Benzene				
		Emission factor		Emission	NO_2 Concentration [a]		Emission factor		Emission	Benzene Concentration [a]	
		LDV [b]	HDV [c]	Annual total	Annual mean	Maximum hourly	LDV	HDV	Annual total	Annual mean	Maximum hourly
S1 – Road Types & Average Speed	Arterial 40km/h	**O**	**O**	**O**	NA	NA	↑	↑↑↑	↑	NA	NA
	Arterial 60km/h	**O**	**O**	**O**	NA	NA	**O**	↓↓	**O**	NA	NA
	Arterial 80km/h	**O**	↑↑	↑↑	NA	NA	↓	↓↓↓	↓	NA	NA
	Freeway 60km/h	**O**	↑↑	↑	NA	NA	**O**	↓↓	**O**	NA	NA
	Freeway 80km/h	**O**	↑↑↑	↑↑↑	NA	NA	↓	↓↓↓	↓	NA	NA
	Local Road	**O**	↑↑	↑↑	NA	NA	↑↑↑	↑↑↑	↑↑↑	NA	NA
S2 – Local VMT		↓↓	↑↑↑	↑↑↑	NA	NA	↓↓	↓↓↓	↓↓	NA	NA
S3 – Ontario Vehicle Age Distribution		**O**	↓	↓	NA	NA	↓	↓↓	↓	NA	NA
S4 – Seasonal Temp		**O**	**O**	**O**	**O**	↑	↑	**O**	↑	↑	↑↑↑
S5 – Seasonal Fuel		**O**	**O**	**O**	NA	NA	**O**	**O**	↑	NA	NA
S6 – Hour of Day		**O**	**O**	**O**	↓↓	↑↑	**O**	**O**	**O**	↓↓↓	↑↑↑
S7 – Hour-Day of Week – Season		**O**	**O**	**O**	↓↓↓	↑↑↑	↑	**O**	↑	↓↓↓	↑↑↑
S8 – Best Case		↓↓	↑↑↑	↑	↓↓↓	↑↑↑	↓↓	↓↓↓	↓↓↓	↓↓↓	↑↑↑

Base case:

O : Negligible change, ≤ 5%
↑ : Low change, 5- 10%
↑↑ : Intermediate change, 10- 20%
↑↑↑: High change, > 20%
↑ Positive change, ↓ Negative change

a) Concentration change at a receptor, 40m east of the road
b) Light Duty Vehicles
c) Heavy Duty Vehicles

5.2 Effects of options in AERMOD

5.2.1 Effects of site characteristics

Figure 5.15 shows hour-of-day mixing heights in different scenarios of site characteristics. Hour-of-day patterns of mixing heights were similar in all scenarios. However, the mechanical and convective mixing heights were greater in the 'Urban 'scenario because of a higher surface roughness (Table 3.18). Mixing heights were similar for three scenarios of 'Suburb', 'Land-use Ave, and 'LU by Wind Direction'.

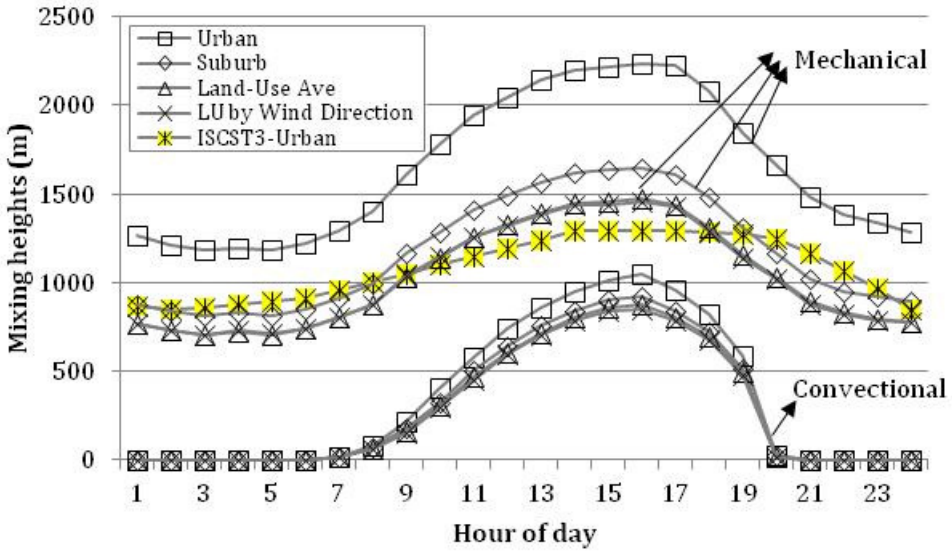

Figure 5.15: Hour of day mixing heights in different site scenarios

Figure 5.16 shows hour-of-day NO_2 concentrations at a receptor 40m east of the road under different scenarios of the site characteristics. NO_2 concentrations in the urban scenario were the lowest. This is because higher surface roughness in urban option (Table 3.18) increases atmospheric mixings (Figure 5.15). This difference is more pronounced during the nighttime, when there were weak atmospheric mixings. In comparison to the

urban scenario by AERMOD, the urban scenario by ISCST3 has slightly higher concentrations during the daytime. This reflects the effects of convective mixings during the daytime, which is not considered in ISCST3. Convective mixings lead to more dispersion of air pollutants in addition to the mechanical mixings.

Because of prevailing wind direction from the west, NO_2 concentrations in the east of the road were higher than the west of the road in all scenarios. However, ratios of the east to west concentrations were much higher in 'Suburb', 'Land-Use Ave', and 'LU by Wind Direction' Scenarios as shown in Figure 5.17. It suggests that higher ratio of east to west concentrations is associated with lower surface roughness. In other words, with increased surface roughness, there are stronger vertical mixings, and consequently the effects of wind direction on the simulated concentrations decreased.

Among all scenarios, ISCST3-Urban had the highest ratio of east to west concentrations. In other words, ISCST3 is more sensitive to wind direction than AERMOD. This is because under the same atmospheric conditions, AERMOD tends to be more dispersive where both mechanical and convective mixings were considered,

Estimated concentrations by 'Suburb', 'Land-Use Ave', and 'LU by Wind Direction' Scenarios were similar (Figure 5.16 and Figure 5.17). The 'Land-Use Ave' and 'LU by Wind Direction' approaches require land use data and more processing time for geospatial analysis of site characteristics. Thus, the use of Suburb Scenario was selected in this study. It is also recommended for future studies as less effort is needed and results are similar to more sophisticated and time consuming approaches.

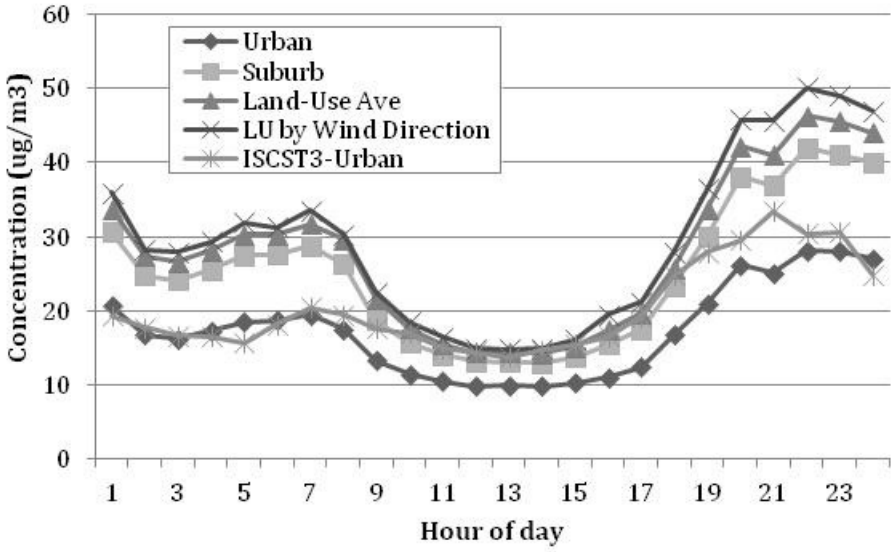

Figure 5.16: Hour of day NO_2 concentrations at a receptor 40m east of the road under different scenarios of site characteristics

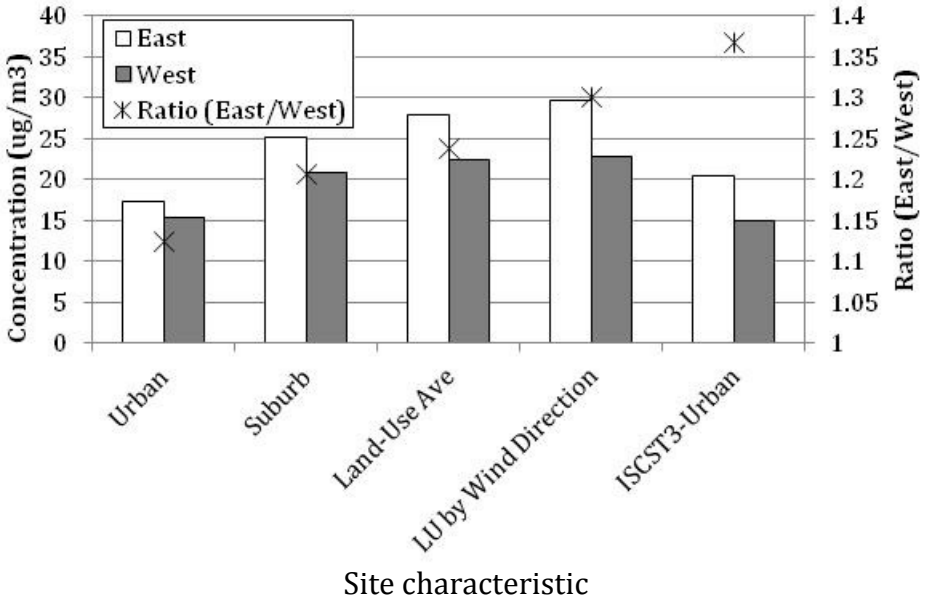

Figure 5.17: Annual mean NO_2 concentrations at receptor 40m east and west of the road under different scenarios of site characteristics

Lateral and vertical turbulence coefficients

In calculation of vertical (σ_{wT}) and lateral (σ_{vT}) turbulence coefficients in AERMOD, two velocities are used: surface friction velocity (u*) and convection velocity scale (w*). The first variable represents the strength of wind speed and the latter variable represents strength of convective mixings. Both these variables are calculated by AERMET, the preprocessor of AERMOD. Figure 5.18 shows diurnal pattern of these variables in 2008 for Windsor. Surface friction velocity was higher during the daytime than nighttime by up to a factor of two. The convective velocity only exists during the daytime.

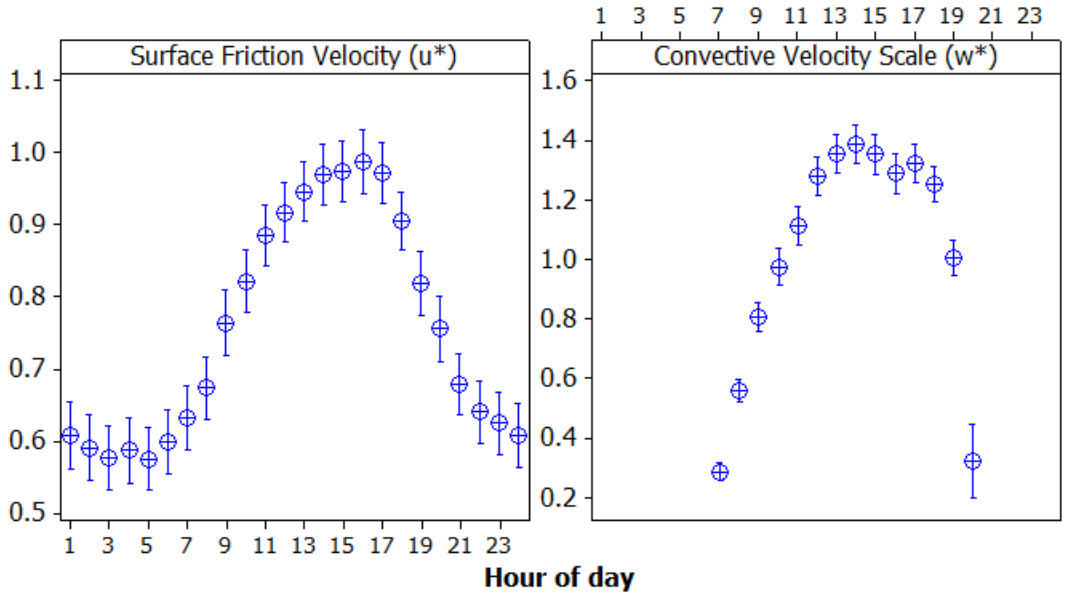

Figure 5.18: Estimated hour-of-day pattern of u* and w* in 2008 in Windsor - 'Suburb' option

Both vertical (σ_{wT}) and lateral (σ_{vT}) turbulence coefficients have two components: 1) mechanical mixing and 2) convective mixing. The convective mixing is additive to the mechanical mixing during the daytime, when the earth-surface heat flux is positive (EPA, 2004). This is called the CBL (Convective Boundary Layer) condition. During the nighttime, when the earth-surface heat flux is zero or negative, only mechanical mixing is

considered. This is called SBL (Stable Boundary Layer) condition. Model formulations for estimation of turbulences in AERMOD were obtained from EPA (2004d). Details equations can be found in Appendix D.

For a receptor at the nose height (i.e. z=1.5 m), mechanical and convective components of the lateral and vertical turbulence coefficients were calculated using Equations D1-D6 and were plotted (Figure 5.19). The convective mixing contributed to approximately 20% of lateral turbulence coefficient during the daytime and had little contribution on vertical turbulence coefficient. The mechanical portion of vertical and lateral turbulence coefficients is almost two times higher during daytime than nighttime. Thus, the high numerical values of atmospheric turbulence close to the ground computed by the AERMOD model during the daytime may be partially/fully responsible to lower concentrations during the day than night. However, the actual reason needs further investigation by examining the AERMOD formulation for calculation of dispersion coefficients.

It should be noted that the convective component of the vertical turbulence coefficient was near zero (Figure 5.19(b)) because the height of the receptor was low (z=1.5m). For receptors located in a height greater than 10% of the convective mixing height, contribution of convective component will be considerable – same as the convective component of the lateral (Figure 5.19(a) and Equation D6).

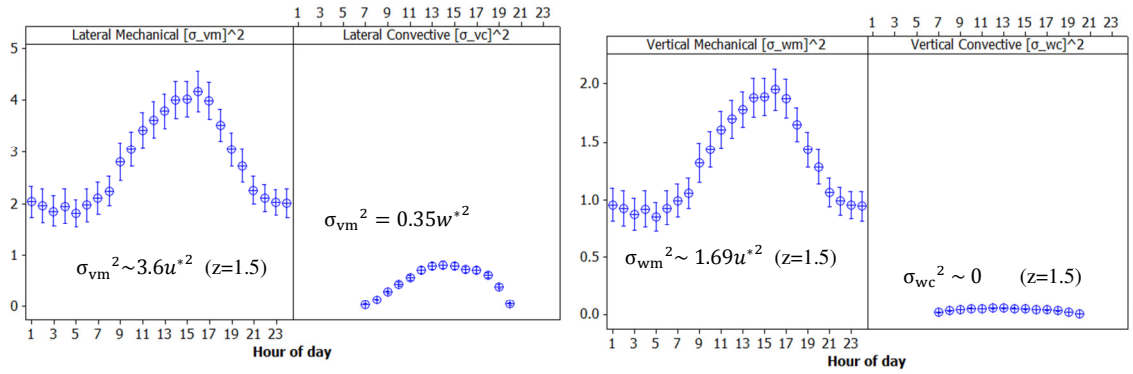

a) Lateral b) Vertical

Figure 5.19: Mechanical and convective components of the lateral and vertical turbulence coefficients in Windsor – 'Suburb' option

5.2.2 Options for NO_2 simulation

Figure 5.20 shows falloff patterns of NO_2 /NO_X concentration ratios by OLM and PVMRM options. The NO_2 concentrations in OLM option are similar to NO_X concentrations. This is because of the underlying assumptions in OLM method as shown in Equations 3.11 and 3.12. In the OLM method, it is assumed that when the O_3 concentrations are higher than NO concentrations, NO_2 concentrations are equal to the NOx concentrations (Equation 3.12). In comparison to the OLM option, the NO_2/NO_X ratio in PVMRM option increased from 0.8 near the road to the equilibrium ratio of 0.9 (Equation 3.14) away from the road. Normalized falloff patterns of NOx and NO_2 by both PVMRM and OLM methods were identical (Figure 5.20(b)).

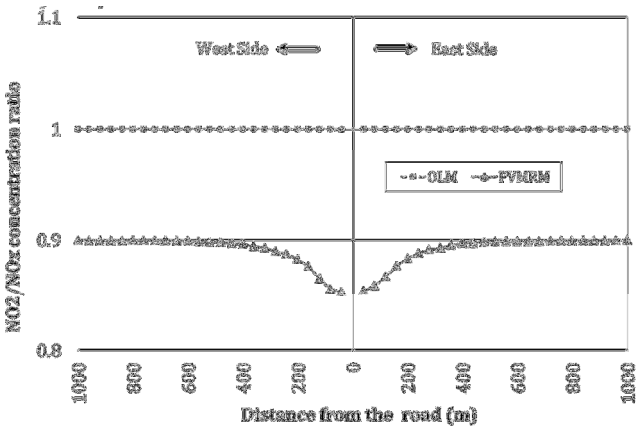

(a) NO_2/NOx ratio

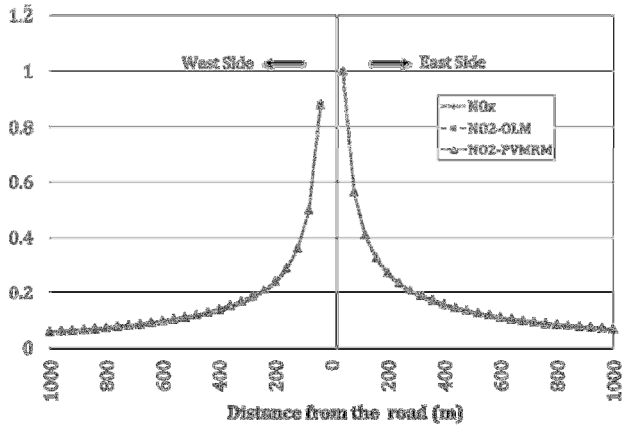

(b) Normalized concentrations

Figure 5.20: Distribution of (a) NO_2/NOx ratio and (b) normalized concentrations with distance from the road

Figure 5.21 shows the hour-of-day NO_X and NO_2 concentrations at a receptor 40m east of the road. In the OLM option, NO_2 and NO_X concentrations are similar, with the exception of hours 8:00, 9:00 and 22:00. During these hours, NOx concentrations were relatively high and O_3 concentrations were relatively low, which led to less amount of NO_2 formation (Equations 3.11 and 3.12). However, NO_2 concentrations in PVMRM option are apparently lower than NO_X concentrations for all hours, as the maximum ratio of NO_2/NOx was set to 0.9 (Equation 3.14).

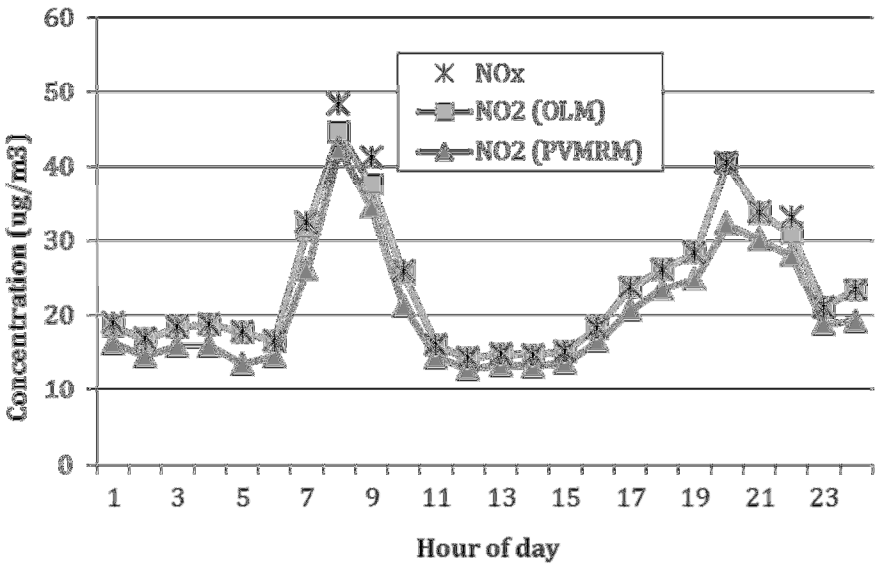

Figure 5.21: Hour of day NOx and NO_2 concentrations at a receptor 40m east of the road.

Among the two options for NO_2 simulation, the PVMRM option in AERMOD is recommended for NO_2 simulation because it represents the chemistry of NO_2 formation more accurately, e.g. NO_2/NO_X ratio in PVMRM option increased with the distance from the road whereas in OLM option, this ratio was almost one, and it did not change with the distance from the road. This is due to the fact that only one road section was considered in this study. Thus, low amount of NOx emissions under an excessive amount of O_3 leads to nearly 100% of NO being converted to NO_2 instantly. These have potentially resulted in high NO_2 concentration under the OLM option. To further investigate this reasoning, the road emissions were doubled and quadrupled, and NO_2 and NOx concentrations were simulated. Figure 5.22 shows distribution of NO_2/NOx ratios with the distance from the road under the OLM and PVMRM methods and the cases of double and quadruple emissions. It was observed when emissions were doubled or quadrupled, the NO_2/NOx ratios at receptors near the road decreased compared to the case of regular emissions for both the OLM and PVMRM methods. This is because higher NOx emissions and NO

emissions, and the same amount of O_3 lowered the conversion of NO to NO_2 (Equations 3.11 and 3.12). In the OLM method, when emissions were doubled, the NO_2/NOx ratio increased from 0.95 near the road to 1.0 at 150m from the road. Similarly in the PVMRM method with doubled emissions, the NO_2/NOx ratio increased from 0.6 at 40 m from the road to 0.9 at 600m away from the road. The ratio of 0.6 for NO_2/NOx at near road was close to the observed ratio of 0.56 at 40m away from the road at the DRIC station. These results indicate that the higher NOx emissions could lower the NO_2/NOx ratios which are closer to the observed values. These also reflect the limitation of this study where emissions are limited to one road only leading to overestimation of NO_2/NOx ratio.

Although PVMRM method resulted in a more realistic pattern of NO_2/NOx ratio than OLM in this study, a recent study by Hendrick et al. (2012) identified major limitations of this method. The authors evaluated the performance of PVMRM and OLM method against an air quality field survey dataset. Based on their investigations, the turbulence coefficients of the plume volume in PVMRM method should be improved by considering other atmospheric conditions rather than convective such as neutral and stable. Also, it was suggested to consider an interpolation method to avoid discontinuities when plums of different sources are merged.

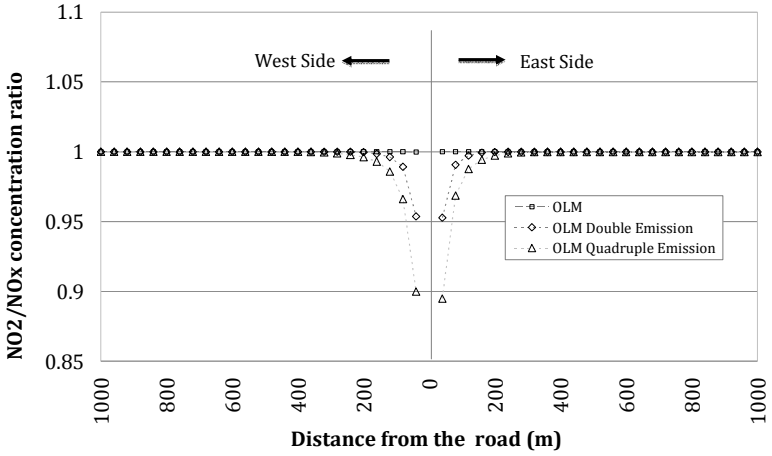

(a) OLM

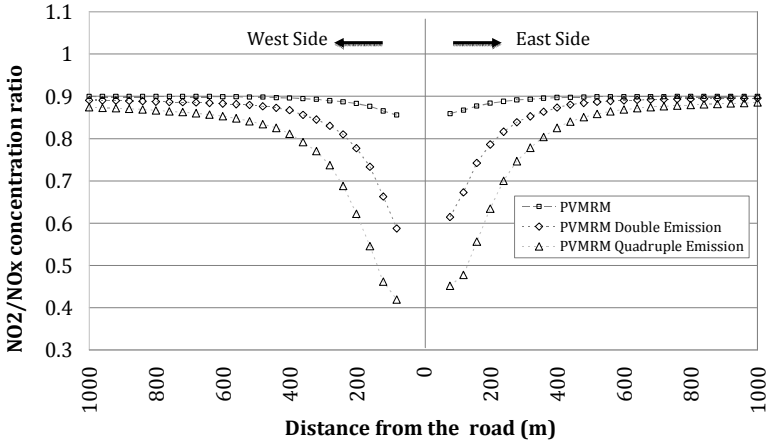

(b) PVMRM

Figure 5.22: Distribution of NO_2/NOx ratios with distance from the road

5.2.3 Comparison of volume and area sources

For this comparison, the release height (1.25m) and width were the same for both area and volume sources. In total, there were 72 sources in the simulation for area source, and 1840 sources in the simulation for volume source. The total NOx emissions were the same for both methods of area and volume sources (8.81 g/s).

Figure 5.23 compares hour-of-day NOx concentrations by the methods of area and volume sources at locations 40, 200, 400, and 1000 m away from the road. Similar patterns were observed for both methods at different locations.

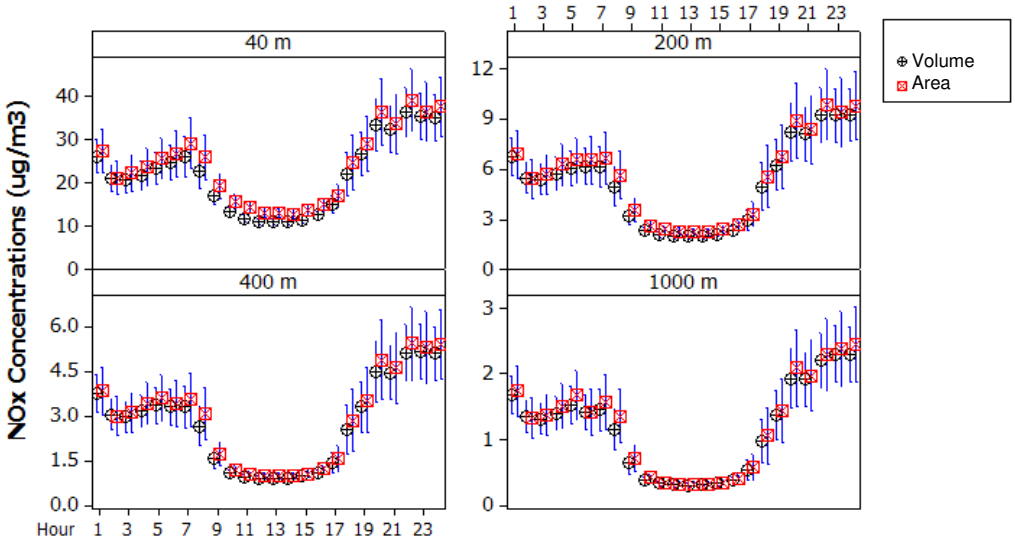

Figure 5.23: Hour-of-day NOx concentrations by two methods of area and volume sources at locations 40, 200, 400, and 1000 m away from the road.

However, the hour-of-day mean concentration was generally higher by the area source than the volume source (up to 22%), as shown in Figure 5.24 which shows the percentage difference [(area-volume)/volume×100]). This effect was more pronounced during the daytime (10:00-17:00) for the receptors closer to the road (15%-20%). This suggests that there is less dispersion when the area source is used for simulation than the volume source.

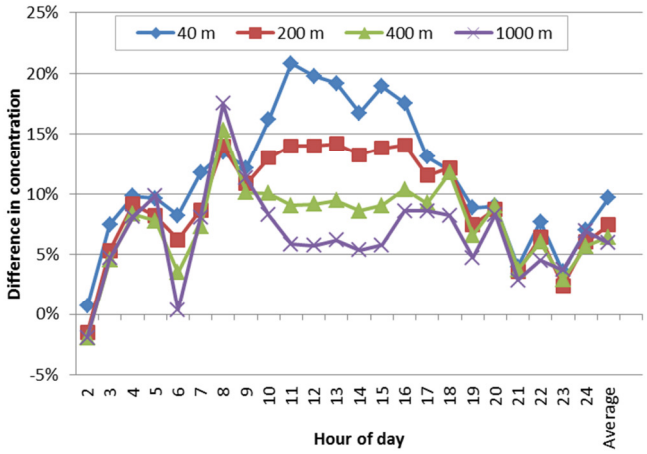

Figure 5.24: Hour-of-day difference in NOx concentrations between the area and volume sources at locations 40, 200, 400, and 1000m away from the road.

5.2.4 Summary

In this section, effects of site characteristics and NO_2 options on simulated concentrations by the AERMOD were investigated. It was found that choice of land-use for defining site characteristics: surface roughness, aledo, and Bowen ratios could highly affect estimated concentrations. In particular, choice of the 'Urban' land-use for the site characteristics lowered the simulated concentrations by 45% compared to the choice of the Suburb land-use, as the surface roughness in urban areas (1m) was two times that in suburb areas (0.5m). In addition, it was observed that the estimated concentrations by three cases of suburb land-use, the land-use average, and the land-use average by wind direction sector were similar. Thus, the use of Suburb Scenario is suggested for future studies, as less effort is needed, and results are similar to more sophisticated and time consuming approaches. Results suggested the importance of land-use choice for determining site characteristics in simulations by AERMOD.

AERMOD equations for calculation of lateral and vertical turbulence coefficients were examined, and it was found that high mixing during the daytime leads to high

values of turbulence coefficients during the daytime. In particular, the convective mixing contributed to approximately 20% of lateral turbulence coefficient during the daytime and had little contribution on vertical turbulence coefficient when the receptor is near ground level, but for receptors located in a height greater than 10% of the convective mixing height, the convective mixing contributed to approximately 50% of vertical turbulence coefficient during the daytime.

The NO_2 simulation methods in AERMOD, OLM and PVMRM, were investigated. It was observed that the NO_2/NOx ratio in the PVMRM method increased from 0.85 near the road to 0.9 away from the road due to NOx titration and conversion of NO to NO_2 whereas in the OLM method, the NO_2/NOx ratio was 1.0 and it did not change with the distance from the road due to low NOx emission which resulted in 100% conversion of NO to NO_2 instantly under excessive amount of O_3. NO_2 concentrations were simulated using the methods of volume and area sources. It was observed that concentrations were generally higher for the area source method than the volume source method – especially during 10:00-17:00 by up to 22%.

5.3 Effects of stop-and-go traffic movements in a microscopic level

5.3.1 Stop-and-go profiles

Table 5.3 lists percentages of times in different driving modes and average speed in both directions of the road during morning peak hour of 9:00 to 10:00. Overall, average speed of vehicles was lower in the northbound direction than the southbound direction, e.g. 43km/h and 51km/h for traffic simulation. This is because car and truck counts were much higher (by 120%, 60%) in the northbound than the southbound direction (Figure 4.7). It should be noted that the northbound road carries outbound work trips from

residential areas to workplaces in the US or Windsor downtown during morning peak hours. Given that higher traffic caused more severe congestion, average speed in northbound was lower than that in southbound.

Table 5.3: Time in different driving modes and average speed on the road

	Method	Time in different mode				Average speed (km/h) Minimum-Maximum (Mean)
		Cruise	Acceleration	Deceleration	Idle	
Northbound	Traffic simulation	44%	14%	19%	23%	2.2-57(43)
	Analytical approach	47%	11%	10%	32%	5.4-60 (51)
Southbound	Traffic simulation	55%	14%	13%	18%	1.2-58(51)
	Analytical approach	54%	9%	10%	27%	3-60(55)

Between the two methods, the northbound average speed by the analytical method was higher than the traffic simulation. This is because both the time percentage and speed of cruise were higher for the analytical method than the traffic simulation. However, average speed in southbound was similar in both methods.

In both northbound and southbound directions, the following results were observed. First, the time percentages of idling were higher for the analytical approach than the traffic simulation. Second, the time percentages of acceleration and deceleration were lower for the analytical approach than traffic simulation.

Vehicle counts were lower in the southbound direction than the northbound direction. As a result, different distributions of driving modes were observed for both directions and both methods (Table 5.3). As expected, time percentage in cruise was higher and time percentages in other modes (acceleration, deceleration, and idle) were lower in the southbound direction with lower traffic than the northbound direction. It was observed that the difference in time percentage of cruise between the analytical method and traffic simulation were smaller in the southbound direction with lower traffic.

Figure 5.25 shows the spatial distribution of time percentage in different driving modes along the road. Similar patterns were observed for both traffic simulation and analytical approach. Vehicles cruise between the signalized intersection, decelerate before the signalized intersections and accelerate after intersections. These similarities were more pronounced in the southbound direction with lower traffic volume. However, distinct differences were observed in time percentages in different modes between the two methods in northbound direction. Time percentage in idling was generally lower in the traffic simulation than the analytical approach. This could be because in traffic simulation, traffic signal coordination which is supposed to lower traffic delays at consequent signals, were considered. On the other hand, time percentages in acceleration and deceleration were higher in the traffic simulation. This is because the traffic simulation can capture interactions between vehicles and can take into consideration accelerations and decelerations due to lane changing or vehicle following. Between the two methods, although the simulation models speed profiles and time distributions of driving modes more realistically, it requires an extensive amount of data for validation. On the other hand, analytical method is simple and can provide comparable results with the traffic simulation.

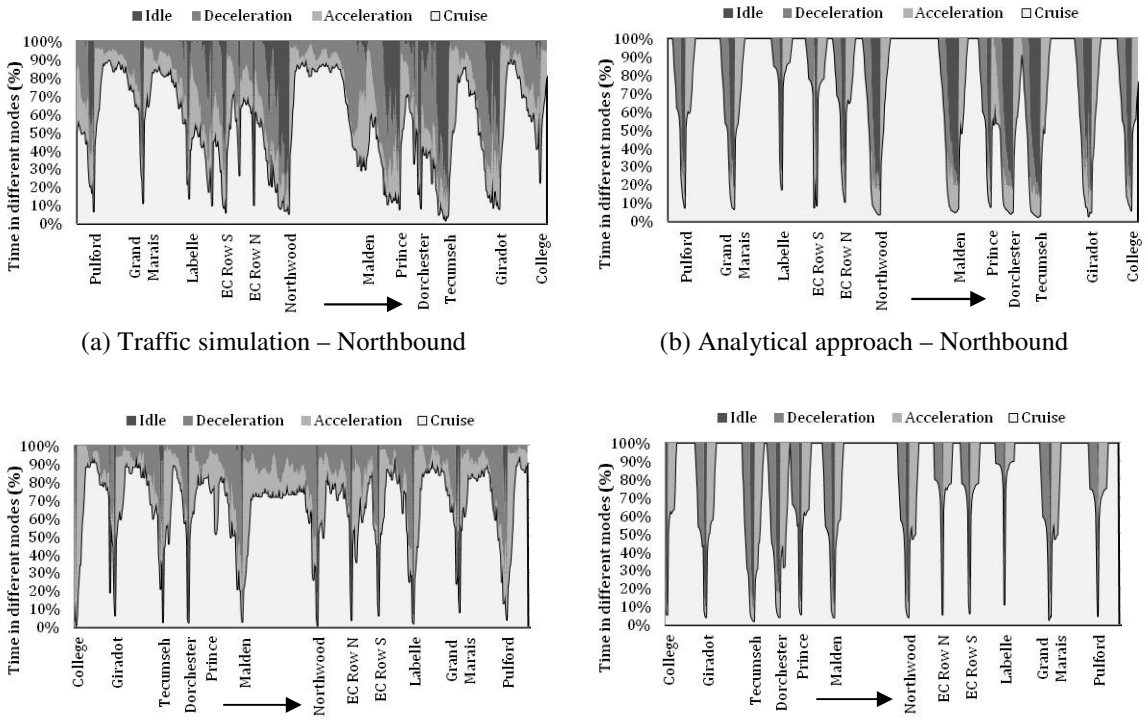

(a) Traffic simulation – Northbound

(b) Analytical approach – Northbound

(c) Traffic simulation – Southbound

(d) Analytical approach – Southbound

Figure 5.25: Spatial distribution of time percentage in different driving modes

Figure 5.26 shows spatial variation in average speed along the road modeled by analytical method and traffic simulation. As expected, average speed of vehicles decreased before the signalized intersections where vehicles decelerate and idle, and it increased after the intersections, where vehicles accelerated to reach a cruise speed. Spatial variation in average speed was similar in both methods. This is more pronounced in the southbound direction where vehicle counts were lower and vehicles are less likely to interact.

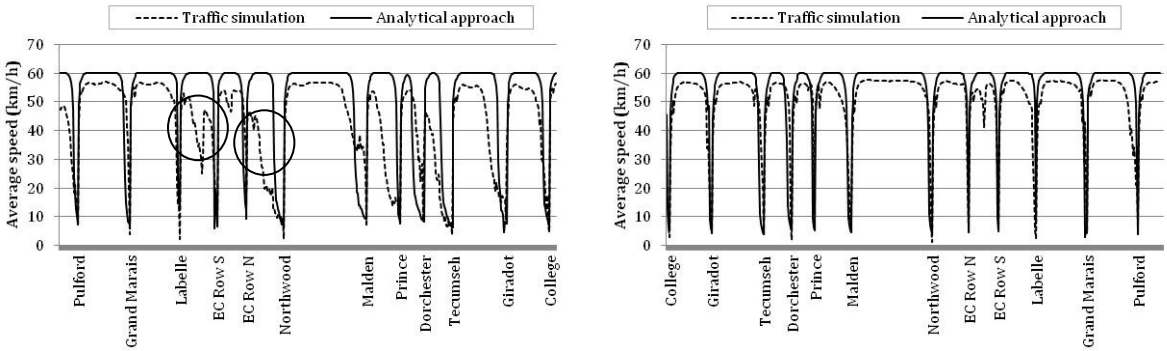

(a) Northbound (b) Southbound

Figure 5.26: Spatial variation of fleet average speed

In the northbound direction, distinct differences in average speeds between both methods were observed (Figure 5.26(a)). For instance, as marked (circle) in Figure 5.26(a), average speeds of vehicles before the exit to the EC Row (Labelle – EC Row S road section) and after the entrance from the EC Row (EC Row N – Northwood road section) were lower by traffic simulation method. This is because unlike the analytical approach, the traffic simulation method traces the movements of individual vehicles and it can capture interactions between vehicles. When a portion of vehicles merges from the EC Row exit, frequent acceleration, deceleration, and lane-changing occur; this could contribute to lower average speeds. Similarly, high volume of merging traffic from the EC Row entrance mingles with the vehicles on Huron Church Road and causes frequent acceleration and deceleration. Average speed of vehicles in the road segment between intersections was higher in the analytical approach, as it is assumed to be the speed limit on the road as 60km/h. In the northbound direction, average speed by the traffic simulation was lower than the analytical method due to higher percentage in acceleration and deceleration modes (Figure 5.25).

5.3.2 Vehicular emissions

5.3.2.1 Micro-emission model

Figure 5.27 compares emission factors of vehicles during deceleration, acceleration, and cruise using the micro-emission model (Panis et al., 2006). As expected, vehicles produced more emissions per distance-traveled when they accelerate than cruise, e.g. 6 and 4 times higher for LDVs and HDVs, respectively. Also, deceleration emissions were lower than cruise emissions.

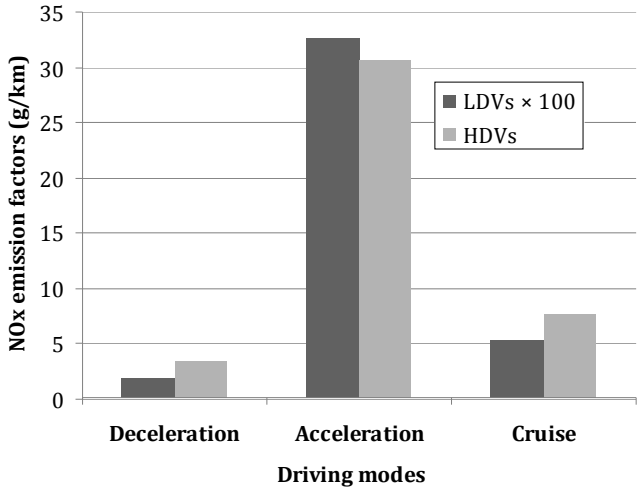

Figure 5.27: NOx Emission factors of LDVs and HDVs by driving modes using the Micro-emission model – For conversion of time-based emission rates to distance-base emission factors, average speeds of 60km/h, 40km/h and 40km/h were used for cruise, acceleration, and deceleration, respectively.

Table 5.4 lists total emission estimated using the micro-emission model by direction, method, and driving mode. It was found when the spatial variations in speed and acceleration were considered, the total emission was 10% - 27% higher than when all vehicles cruise at 50 km/h as used in AERMOD base case simulation. This increase was more pronounced in the northbound direction where proportions of acceleration and

idling were higher (Table 5.3) compared to the southbound direction. NOx emissions were higher in the traffic simulation because of a higher proportion of the accelerating vehicles (Table 5.3). As expected, deceleration emissions were very low due to lower emission factors (Figure 5.27).

Table 5.4: Total emission over the 9.5km road using the-micro emission model by direction, method, and driving modes

Direction	Method	Percentage of total emission				Total emission (kg)	Difference vs cruise 50km/h
		Cruise	Acceleration	Deceleration	Idle		
Northbound	Cruise 50km/h	100%	0%	0%	0%	12.1	-
	Traffic simulation	46%	48%	4%	2%	15.3	27%
	Analytical approach	62%	31%	2%	5%	14.2	18%
Southbound	Cruise 50km/h	100%	0%	0%	0%	7.6	-
	Traffic simulation	56%	41%	2%	1%	8.8	16%
	Analytical approach	70%	25%	1%	4%	8.3	10%

Figure 5.28 shows the spatial distribution of NOx emission by driving modes using the micro-emission model. It was observed that acceleration and cruise emissions account for the majority of emissions. This reflects high emission factors of accelerating vehicles and high time percentage in cruise (more than 44%, Table 5.3). Deceleration and idling emissions were low and occurred before the signalized intersections. In comparison to emissions estimated using the traffic simulation, those by analytical approach composed of less acceleration emissions due to less time percentage in accelerating mode (Figure 5.25).

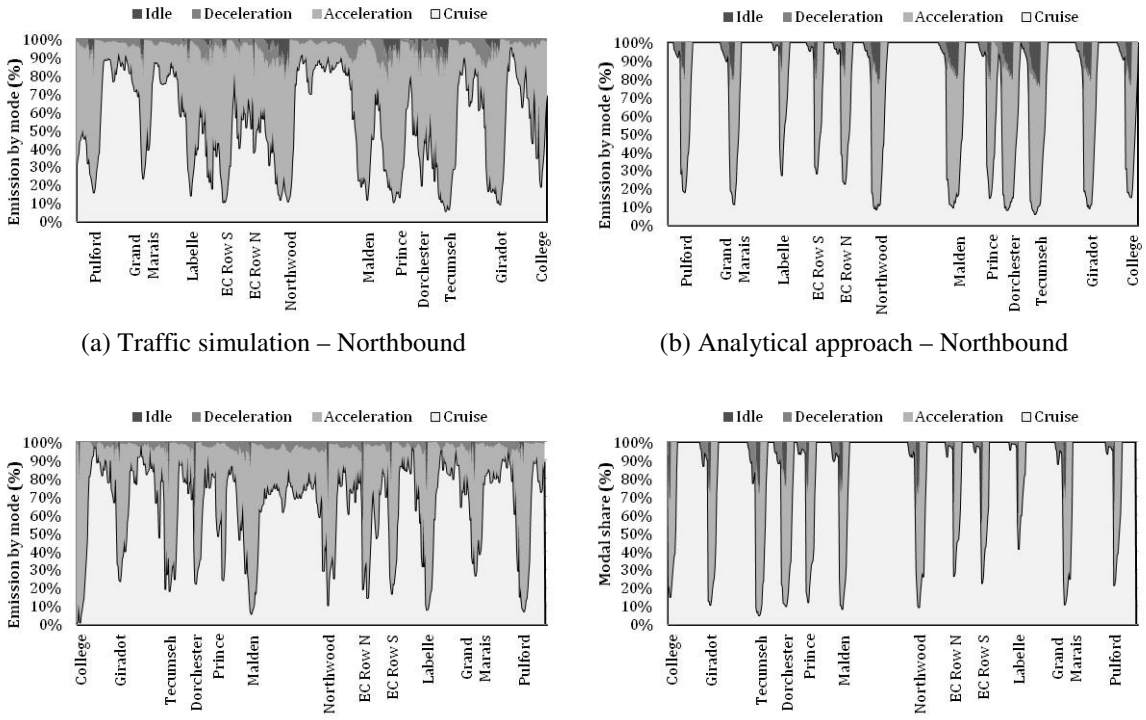

(a) Traffic simulation – Northbound

(b) Analytical approach – Northbound

(c) Traffic simulation – Southbound

(d) Analytical approach – Southbound

Figure 5.28: Spatial distribution of emission by driving mode - estimated using a micro-emission model

Figure 5.29 shows spatial variations in emission estimated by the micro-emission model. NOx emissions were higher, up to a factor of four, near the signalized intersection compared to the road segment between the signalized intersections. Emissions before and after the signalized intersections were high due to the idling emission and the acceleration emissions, respectively. Spatial distributions of NOx emission estimated using the traffic simulation and the analytical approach were similar. This was expected since speed profiles were similar (Figure 5.26). This similarity is better reflected in the southbound road due to lower traffic and consequently less interaction between vehicles, and given that analytical approach cannot capture interaction between vehicles.

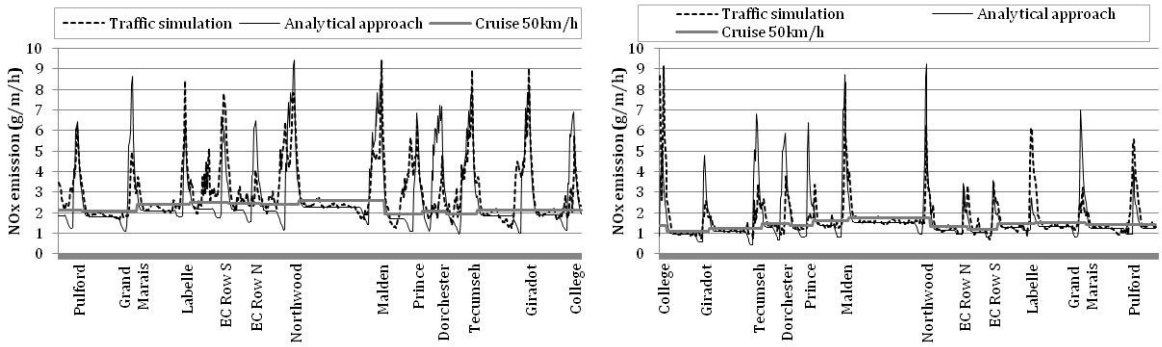

(a) Northbound (b) Southbound

Figure 5.29: Spatial distribution of emission estimated by the micro-emission model

5.3.2.2 Mobile6.2

Table 5.5 lists the total emission estimated using the Mobile6.2. It was observed that when different average speed is used for each link of the road (10m or less in length), total emissions in the northbound and southbound directions were higher by 7% and 2%, respectively, compared to those in the Base Case of Arterial 50km/h.

Table 5.5: Total emission over the 9.5km road estimated using Mobile6.2 by direction and method

	Northbound		Southbound	
Method	Total emission (kg)	Difference in emission vs Arterial 50km/h	Total emission (kg)	Difference in emission vs Arterial 50km/h
Arterial 50km/h	9.0	-	5.14	-
Link-specific average speed by traffic simulation	9.8	8%	5.25	2%
Link-specific average speed from analytical method	9.6	7%	5.34	4%

Figure 5.30 shows spatial variation in NOx emissions estimated using Mobile6.2. In the northbound direction, it was observed that when average speed was different for each

link (=10m or less), emissions near signalized intersections were two times higher than the emissions estimated using the Arterial 50km/h. This is because average speed of vehicles was lower near the signalized intersections (Figure 5.26). In addition, the emissions at road segments were not different among the three cases of traffic simulation, analytical approach, and Arterial 50km/h as Mobile6.2 is not sensitive to speeds in the ranges of 50-60/km/h (Figure 5.1).

In comparison to the emission estimated using the micro-emission model, spatial variations in emission estimated using Mobile6.2 was lower. This is because Mobile6.2 only used the average speed of vehicles for calculation of emissions whereas the micro-emission model used the instantaneous speed and acceleration of vehicles.

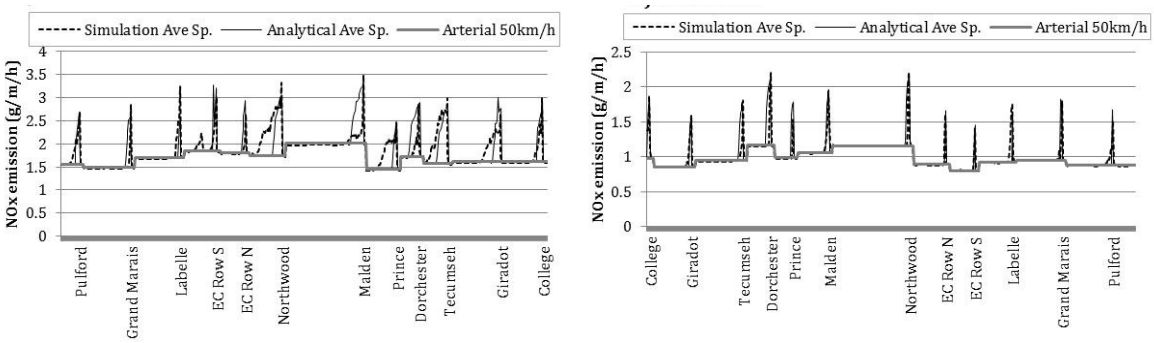

(a) Northbound (b) Southbound

Figure 5.30: Spatial variation of NOx emission estimated using Mobile6.2

5.3.3 Mobile6.2 NOx correction factors near signalized intersections

Figure 5.31 shows spatial distribution of normalized emissions estimated by the micro-emission model and the Mobil6.2 in the northbound direction using stop-and-go profiles determined by the analytical method. Both micro-emission model and Mobil6.2 estimated high emissions near signalized intersections. However, peak emissions were much higher

for the micro-emission model, as this model considers emissions of different driving modes.

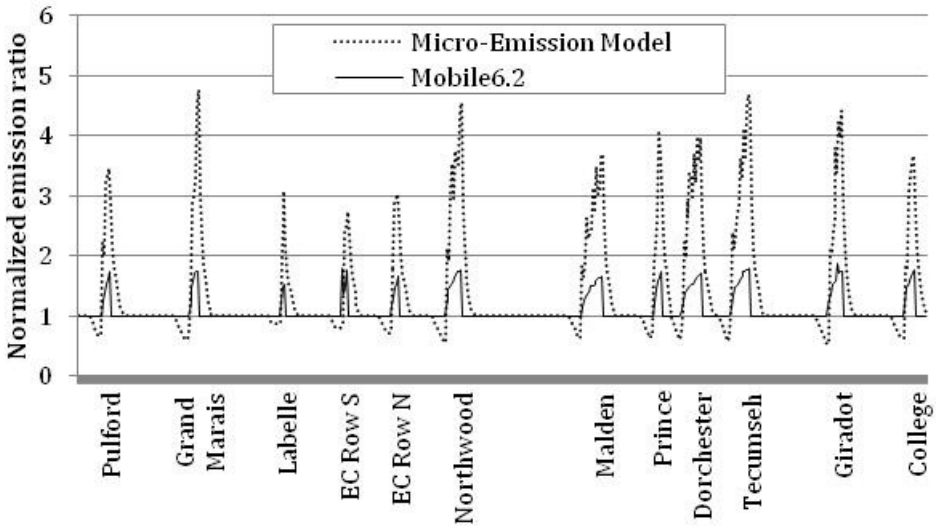

Figure 5.31: Spatial distribution of normalized emissions by Mobile6.2 and micro-emission model.

Because Mobile6.2 cannot sufficiently capture the effects of stop-and-go movements on vehicular NOx emissions due to the use of an average speed, correction factors were derived to adjust vehicular emissions near the signalized intersections. Correction factors were found to be 3.2 for 75% of the length of queued vehicles upstream of signalized intersections, and 1.6 for 85m downstream of the signalized intersections on Huron Church Road (Figure 3.26). Table 5.6 lists correction factors for upstream and downstream of the signalized intersections by vehicle type. It was found that upstream correction factors for LDVs (7.9) were 2.6 times higher than those of HDVs (3.0). This is because the ratio of acceleration to cruise emissions was much higher for LDVs (4.1) than HDVs (2.7) in the micro emission model (Figure 5.27).

Table 5.6: Mobile6.2 NOx correction factors near signalized intersections by vehicle type

	Upstream		Downstream	
	Correction Factor	Distance	Correction Factor	Distance
LDV	7.9	83% Queue length	2.0	85
HDV	3.0	72% Queue length	1.5	85
Combined for Huron Church Road with 20% truck	3.2	75% Queue length	1.6	85

For the use of correction factors listed in Table 5.6, it is suggested to adjust car and truck NOx emissions with the correction factors of LDVs and HDVs, respectively. These correction factors should not be weighted with car and truck counts.

Figure 5.32 shows the spatial distribution of emissions for different driving mode zones by the micro-emission model, Mobile6.2, and the derived corrections factors at the Northwood intersection. The micro-emission model showed lower emission in the deceleration zone, higher emissions in the queue and acceleration zones, in which emissions reach to a peak at the stop-line and decrease afterward. Mobile6.2 shows smaller changes in emissions of deceleration and acceleration zones.

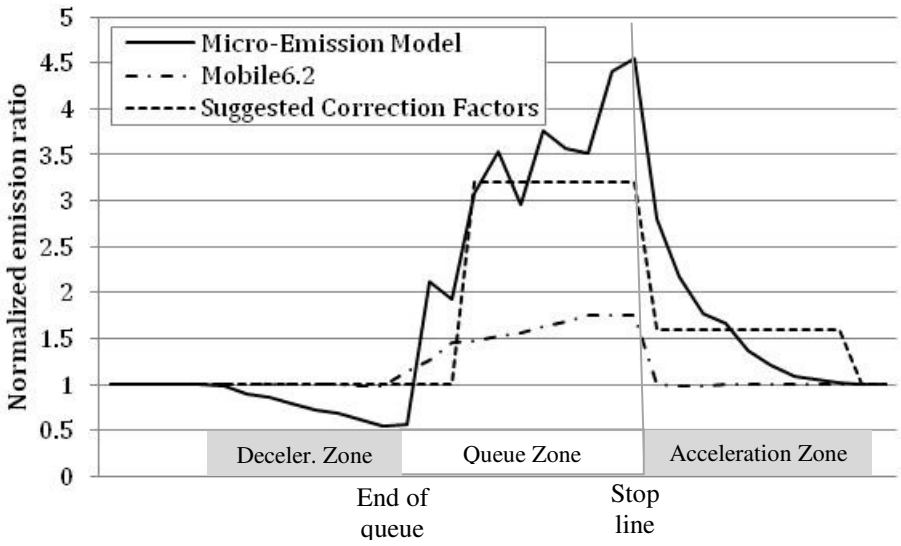

Figure 5.32: Spatial distribution of normalized emission near the Northwood intersection, northbound approach

Figure 5.33 compares NOx emissions by the micro-emission model using the analytical method with emission estimated using the derived correction factors. It was observed that correction factors sufficiently replicate variations in emissions using the micro-emission model. Thus, the use of correction factors overcomes deficiencies of Mobile6.2 in estimations of emissions near signalized intersections. The difference between total emissions by the micro-emission model and those by correction factors was less than 2%.

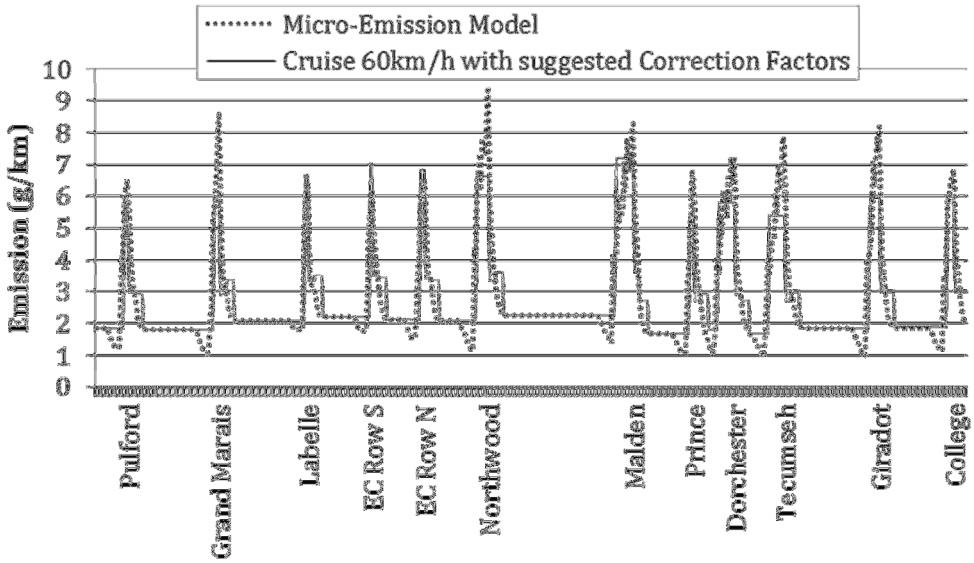

Figure 5.33: NOx emissions by the micro-emission model using the analytical method and by cruise 60km/h with suggested correction factors

In this study, correction factors were developed for cars, trucks, and all vehicles based on morning peak traffic (Table 5.6). The correction factors upstream of the signal were described in a function of queue length of vehicles. As a result, these factors are expected not to change with the change in vehicle counts, as higher counts increase the queue length. However, the downstream correction factors are expected to change with the vehicle counts, as the change in number of accelerating vehicles could affect the magnitude of the correction factor for the acceleration zone. It should be noted that the correction factors in this study were developed using the emission profiles at 12 signalized intersections where the queue ratio (number of queued vehicles to the vehicle counts) was in the range of 15% to 77% (mean: 49%). Thus, for the use of these correction factors in other study areas, this fact should be considered that this correction factors were developed based on morning peak vehicle counts (9:00-10:00) and the specific traffic condition on Huron Church Road.

5.3.4 NO_2 concentration

Figure 5.34 shows NO_2 concentrations at 40m and 200m east and west of the road when emissions were estimated using the micro-emission model. It was observed that NO_2 concentrations were higher near signalized intersections when stop-and-go movement was considered. Spatial variations in NO_2 concentrations were more apparent at the receptor 40 m from the road than 400m from the road. This is because away from the road, NO_2 concentrations are more likely to be affected by NOx emissions at multiple road sections. It was observed that despite small variations, spatial distributions of concentrations estimated by analytical approach and traffic simulation are comparable. Table 5.7 lists the range and average of concentrations at the receptors 40 m and 200m away from the road. As the higher emissions result in higher concentrations, NO_2 concentrations were higher in the analytical approach and the traffic simulation compared to those for cruise speed 50km/h. It was observed when stop-and-go movement was considered, concentrations at the receptor 40m to the road were higher by up to a maximum of 96% (on average 20%).

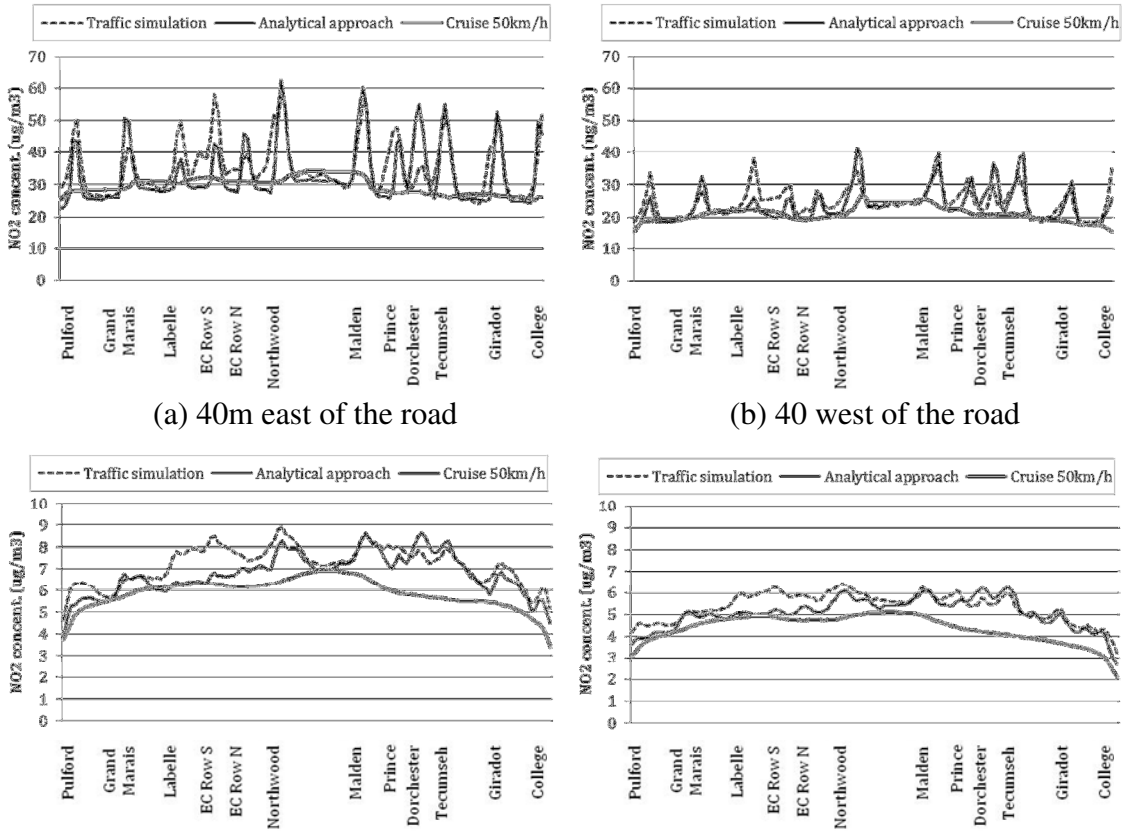

(a) 40m east of the road (b) 40 west of the road

(c) 200m east of the road (d) 200 west of the road

Figure 5.34: NO_2 concentrations using emission by the micro-emission model at the receptors 40 and 200m east of the road during morning peak hours (9:00-10:00) of 2008

Table 5.7: Range and average of concentrations ($\mu g/m^3$) among 550 receptors 40 m and 200 m during morning peak hours (9:00-10:00) of 2008, minimum – maximum (mean)

	40m east of the road		200m east of the road	
	Concentration	Difference in concentration vs Cruise 50km/h	Concentration	Difference in concentration vs Cruise 50km/h
Cruise 50km/h	25.3 ~ 34.2 (29.7)		3.4 ~ 6.9 (5.9)	
Traffic simulation	22.6 ~ 62.6 (33.6)	-12% ~ 108% (14%)	3.9 ~ 8.6 (6.8)	-4% ~ 51% (16%)
Analytical approach	24.2 ~ 58.1 (35.7)	-15% ~ 97% (21%)	4.6 ~ 8.9 (7.2)	2% ~ 52% (23%)

Figure 5.35 shows spatial distribution of difference in NO_2 concentrations between the cases of stop-and-go movement and the Cruise 50km/h. It was observed that at the receptors up to 1000 m from the road, the difference was in the range of -20% and 80%.

In the areas close to midsections, a majority of vehicles cruise at speeds higher than 50km/h; as a result, emissions and concentrations were lower by up to 10%. The positive difference was observed in the areas close to the signalized intersections where emissions were higher due to high acceleration and idling emissions generated by frequent stop-and-go movement (Figure 5.25). Overall, at the receptors up to 200m away from the road, the difference was in the range of 10%-50% (mean: 30%) near the signalized intersections. This indicates that when stop-and-go movement was not considered, the simulated concentrations at the receptors close to signalized intersections could be underestimated by up to 50%. Away from the road, the difference between stop-and-go movement and cruise 50km/h decreased, i.e. it was in the range of 20% to 50%. Near the College Ave, the percentage difference was the highest, as the southbound emission were very high near the College Ave (Figure 5.29).

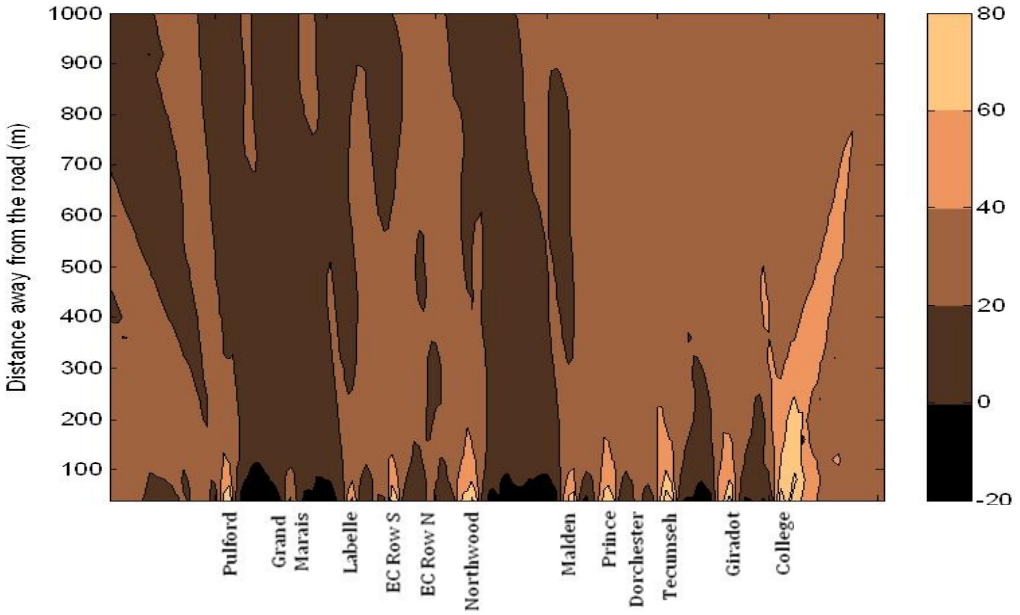

a) Traffic simulation

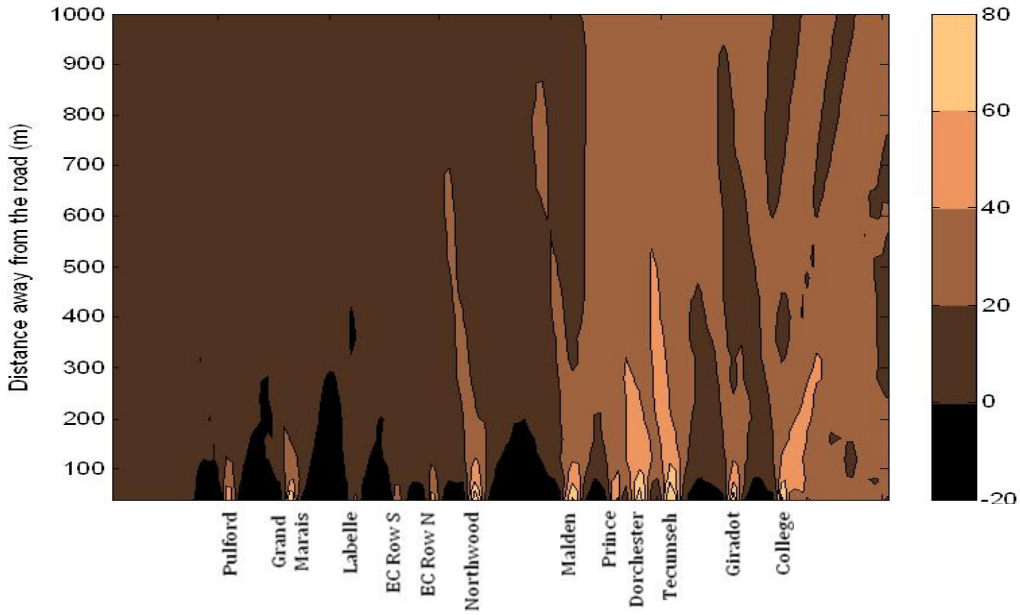

b) Analytical method

Figure 5.35: Spatial distribution of percentage difference in NO_2 concentration compared to the case of Cruise 50km/h – East of the road

NO_2 concentrations by the analytical method and correction factors

To examine whether correction factors replicate the emission as estimated by the micro-

emission model, the NO_2 concentrations by the cruise 60km/h with correction factors were compared to those by the micro-emission model (Figure 5.36). It was observed that spatial variations in concentrations were similar for both methods at the receptors 40m and 200m from the road. On average, the difference in concentrations between the two methods was less than 1%.

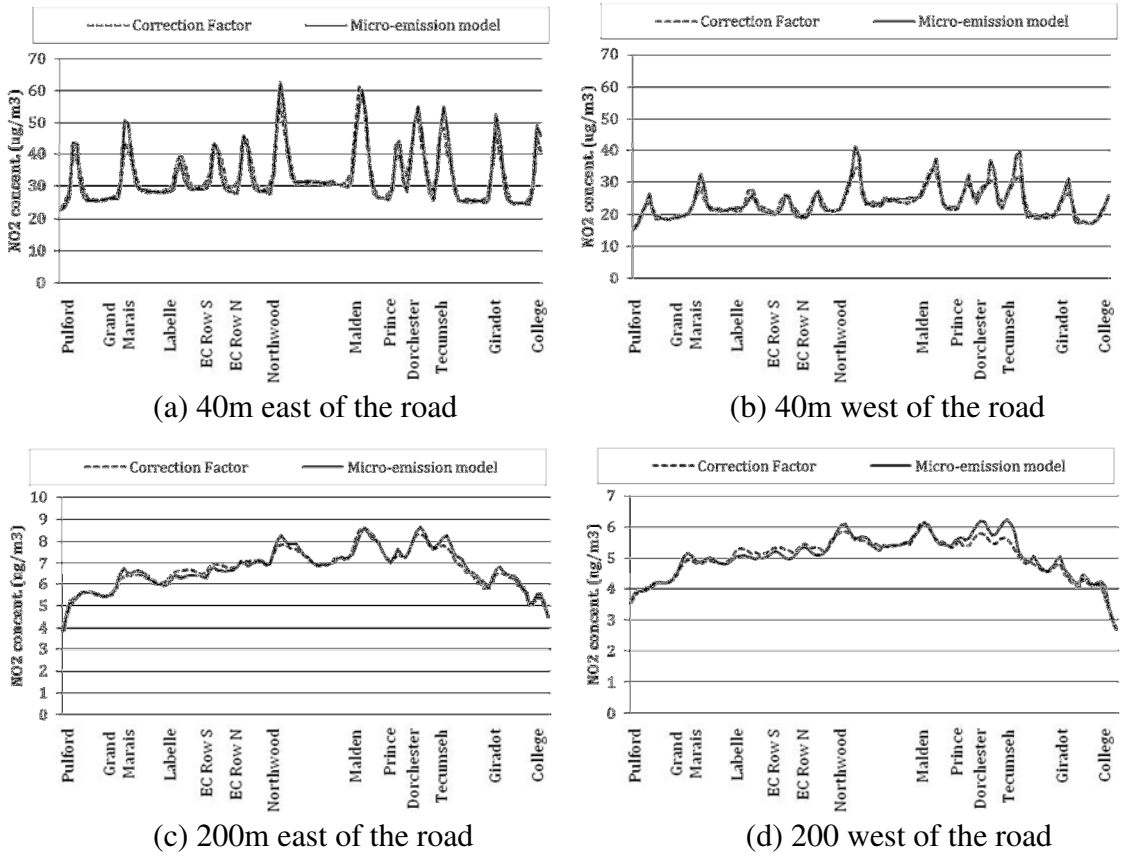

(a) 40m east of the road

(b) 40m west of the road

(c) 200m east of the road

(d) 200 west of the road

Figure 5.36: Spatial distribution of NO_2 concentration using the Micro-emission model and the cruise 60 km/h with correction factors

Figure 5.37 shows spatial distribution of percentage difference in NO_2 concentrations between the micro-emission model and the correction factors in the east of the road. It was observed that the difference was in the range of ±5%. These results indicate that the

use of correction factors can sufficiently reflect the variations in emissions and concentrations near signalized intersections due to stop-and-go.

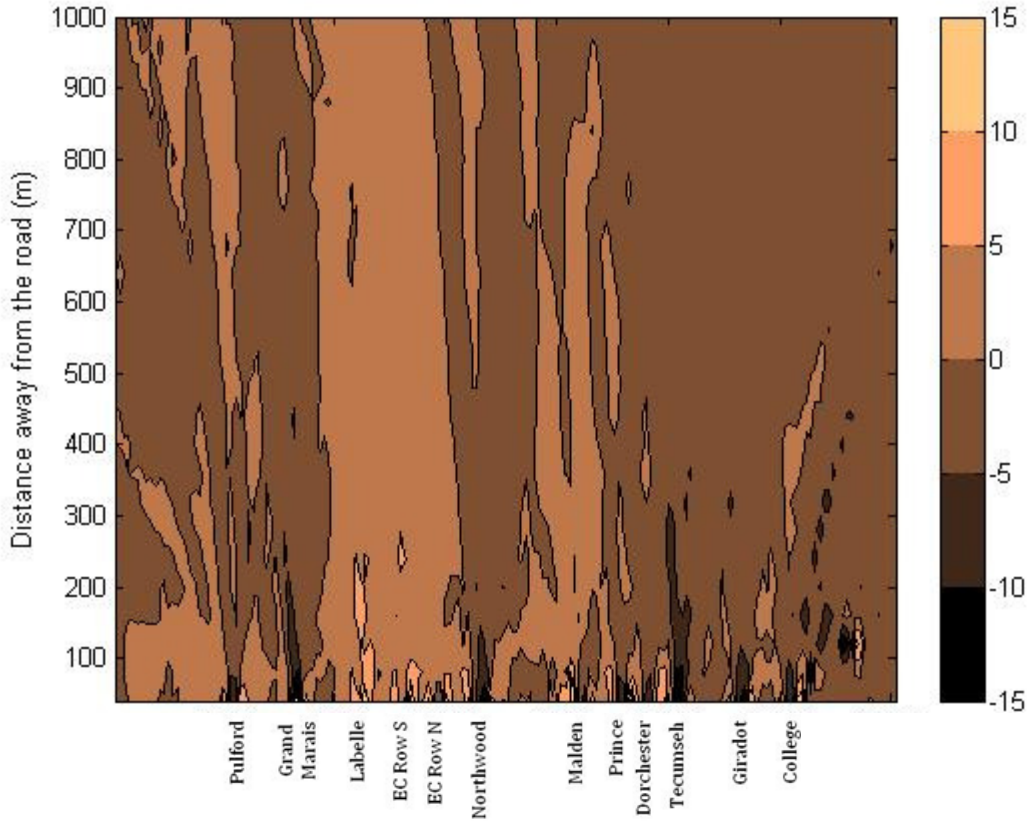

Figure 5.37: Spatial distribution of percentage difference in NO_2 concentration between micro-emission model and correction factors – East of the road

5.3.5 Summary

This section investigated effects of stop-and-go movement on vehicular NOx emission and ambient air concentration of NO_2 on Huron Church Road in Windsor, Ontario during the morning peak hour (9:00-10:00). Results indicate that the analytical method developed based on a queue estimation function with some typical acceleration and deceleration profiles of vehicles can be used to determine stop-and-go speed profiles. Also, despite some variations, spatial distributions of emissions and concentrations

estimated using the analytical and traffic simulation were similar. Both methods showed high emissions and concentrations near signalized intersection and low at road segments between intersections. When using the micro-emission model, total emissions estimated by traffic simulation and the analytical method were higher by 22% and 15%, respectively, than the case of cruise speed of 50km/h.

It was observed when different average speeds were used for each link of the road (10m or less in length) for calculation of emission factors using Mobile6.2, total emissions were higher by 7% compared to the Arterial 50km/h. Emissions were particularly high for the links near signalized intersections – they were higher by 32% than the Arterial 50km/h.

Because Mobile6.2 cannot sufficiently capture the effects of stop-and-go movements on vehicular NOx emissions due to the use of an average speed, correction factors were derived to adjust vehicular emissions near the signalized intersections. Correction factors were found to be 3.2 for 75% of the length of queued vehicles upstream of signalized intersections, and 1.6 for 85m downstream of the signalized intersections on Huron Church Road. It should be noted that these correction factors were estimated based on morning peak hour vehicle counts with a truck percentage of 24%. Separate correction factors were also developed for cars and trucks (Table 5.6). Correction factors could be used for different traffic composition by adjusting car and truck emissions with correction factors. To calculate emissions using these correction factors, only the length of queued vehicles is needed. The queue length can be calculated using the simplified relationships in Equation 3.15-18 or from any design handbooks such as Highway Capacity Manual (TRB, 2010).

NOx correction factors for Mobile6.2 emissions near signalized intersections were obtained by comparing emissions by the analytical method with the cruise 60km/h using a simple micro-emission model (Panis et al., 2006). The model was developed by emission testing of 17 passenger cars and two trucks under urban traffic conditions. It is difficult to justify that this limited number of cars and trucks can sufficiently represent the vehicle composition of on-road vehicles. Thus, it is suggested to repeat the methodology about correction factors with a more sophisticated micro-emission model such as the new EPA mobile source emission model, MOVES (EPA, 2010). Also, it is recommended to estimate correction factors for other hours of day, as the correction factors were developed only for the morning peak (9:00-10:00).

CHAPTER VI

6. CONCLUSIONS AND RECOMMENDATIONS

6.1 Conclusions

This study presented a multi-model approach for estimation of traffic-related air pollutant concentrations. This method has been used in the case study of Huron Church Road, Windsor, Ontario to estimate vehicular emissions and ambient concentrations of NO_2 and benzene. Mobile6.2 and AERMOD were used for estimation of vehicular emission and ambient air concentrations, respectively. Spatial and temporal variations of NO_2 and benzene concentrations were examined and major factors explaining the temporal variations were identified. Effects of input parameters on the estimated vehicular emission and air pollutant concentrations were evaluated.

Monthly and annual adjustment factors were derived using long-term vehicle counts (2004-2008) to adjust vehicle counts collected during different times to the base year of 2008 at Huron Church Road. The proposed traffic count adjustment method can be applied to the other urban arterial streets where long-term vehicle counts are available at a limited number of locations. Instead of extensive data collection at various locations in long terms, vehicle counts can be estimated by collecting the short-term counts at many locations and adjusting the counts for temporal variations using the long term data. Thus, this adjustment method could be a cost-effective alternative of vehicle count estimation.

Dispersion modeling results showed that annual mean NO_2 concentrations from traffic on the Huron Church Road were in the range of 27 $\mu g/m^3$ – 1.4 $\mu g/m^3$, at the receptors 40 – 1000 m from the centerline of the road. These traffic-related concentrations were additive to the background concentration of 21 $\mu g/m^3$. The

maximum of 48 μg/m^3 was observed at 40 m where some houses and commercial facilities were located. These results suggest that traffic on Huron Church Road significantly contributes to near-road human exposure. Concentrations decreased sharply with distance from the road. At distances of 200, 400, and 600 m from the road, the annual concentrations were 24%, 13%, and 9% of the concentrations at a distance of 40 m from the road, respectively. Concentrations were significantly higher (20%) in the east of the road than the west due to prevailing westerly wind. Similar patterns were observed for NO_2 and benzene.

Among the four seasons, simulated concentrations were the highest in fall due to high traffic counts and low wind speed. Concentrations were higher during the weekdays than Saturdays and Sundays because of heavier traffic. Nighttime concentrations were higher than the daytime due to low wind speed and poor mixings at night in spite of higher emissions in the daytime. Similar patterns were observed for NO_2 and benzene. The effects of meteorological parameters were further investigated by dispersion simulation using one-vehicle emission. During the nighttime, NO_2 concentrations were five times higher than during daytime due to poor mixing. This finding suggests the need to develop separate models for daytime and nighttime concentrations. AERMOD equations for calculation of lateral and vertical turbulence coefficients were examined, and it was found that high mixing during the daytime leads to high values of turbulence coefficients during the daytime.

From the comparison between the Unit Emission Case (constant emission rate) and the actual case (hourly variable emission rate), it was found that variations in simulated NO_2 concentrations were mainly due to meteorological parameters and less due to traffic

as they did not vary with hour-of-day as much as atmospheric dispersion. The two major factors, traffic counts and wind speed, explained 40% of variations in both the observed and simulated NO_2 concentrations. Temporal factors (hour of day, day of week, and season) combined with wind speed also explained 40% of variations in both the observed and simulated NO_2 concentrations. This was not unexpected because traffic counts were correlated with hour of day and day of week. This finding suggests that temporal factors can be used for prediction of concentrations where traffic counts are not available. These findings may help researchers develop simpler models using only major factors to predict air pollutant concentrations from traffic.

It was found that simple logarithmic regression models with predictors of car and truck counts, and wind speed can reasonably predict modeled hourly concentrations at fixed locations. Also, simple linear regression models using car and truck counts can reasonably predict modeled annual concentrations at different distances away from the road. The regression models were developed using the predictor "car-emission-equivalent". This makes the models applicable to other urban areas with a different truck percentage.

The relationship between the truck/car counts ratio and NO_2/benzene concentration ratio was found to be linear. The slope of the regression line, which reflects the increase in NO_2/benzene concentration ratio per one unit increase in truck/car ratio, was 212 and 238 for observed and simulated concentrations, respectively. Based on this relationship, the benzene concentrations can be estimated using the NO_2 concentrations and truck/car ratio. It should be noted that this relationship is valid only for traffic-related NO_2 and

benzene concentrations. If observed concentrations are used, the background contribution of both pollutants should be considered.

The comparison between simulated and observed concentrations indicates that the multi-model approach using the Mobile6.2 and AERMOD reasonably reproduced: 1) the observed hour-of-day pattern of NO_2 concentrations in 2008 at the Windsor West Station 1km west of the road, 2) the observed spatial fall-off pattern of NO_2 concentrations at 11 sites located at a transit line perpendicular to the road during a two-week period in May 2010, 3) the two major factor explaining majority of variations in observed concentrations, and 4) the observed incremental change in NO_2/benzene concentration ratio by change in truck/car ratio. However, the model-measurement comparison also revealed some differences. First, traffic counts explained more variations in observed (22%) than simulated concentrations (15%). Wind speed explained more variations in simulated (28%) than observed concentrations (21%). Season explained more variations in observed (9%) than simulated concentrations (4%). Second, seasonal patterns were quite different: observed NO_2 concentrations were high in winter and low in summer, but simulated NO_2 concentrations were high in fall and low and in winter. This discrepancy could be due to overestimation or underestimation of mixing by the AERMOD in some seasons. Third, the fall-off pattern was steeper for the simulated than the observed concentrations. This could be because simulated concentrations were from Huron Church Road only whereas observed concentrations were from both Huron Church road and local streets. Fourth, simulation results indicated that AERMOD underestimates concentrations during the daytime, especially around noon due to over mixing. In conclusion, despite the

small discrepancies, the multi-model approach accomplished well in replicating the key features observed in the field.

Results from the sensitivity study of Mobile6.2 showed that NOx and benzene emission factors of vehicles significantly varied with some input parameters. Overall, the emission factors were most sensitive to the choice of Ontario VMT (Vehicle Mile Traveled) compositions over the default values of US (NOx: 23% and benzene: -15%). For HDVs, the NOx emission factors increased by 39% while the benzene emission factor decreased by 27%. The choice of Ontario vehicle age distribution over the default values of US decreased both NOx (-7%) and benzene (-10%) emission factors. Emission factors were sensitive to the average speed, especially for Heavy Duty Vehicles (HDVs). Thus, when there is a significant percentage of HDVs on the road as on Huron Church Road, a small change in average speed can lead to a large change in emissions.

The changes due to the use of seasonal fuel properties and seasonal temperatures over annual values were less than 5%. It is concluded that VMT and vehicle age distribution specific to the study region should be used in Mobile6.2 applications. Appropriate choice of road type and average speed should be considered to reflect the actual driving cycle.

NO_2 concentrations were simulated using two methods of volume and area sources. It was observed that concentrations were generally higher by the area source than the volume source – especially during 10:00-17:00 by up to 22%.

It was found that the concentrations predicted by AERMOD were sensitive to the temporal resolution of emissions. When an annual emission rate was used, the annual mean concentrations were overestimated (NO_2: 19% and benzene: 24%) and the maximum hourly concentrations were underestimated (NO_2: 14% and benzene: 42%)

compared to using hour-of-day emissions. Thus, it is suggested to consider hour-of-day variation of vehicular emissions for dispersion modeling.

An analytical method was developed based on a queue estimation function with some typical acceleration and deceleration profiles of vehicles. The analytical model yields similar stop-and-go movement profiles as a microscopic traffic simulation model, but with fewer types of input data.

Using a Micro-emission model, it was found that stop-and-go movement on Huron Church Road increased the total NOx emission by 24% compared to the case of cruise speed of 50km/h during the morning peak hour (9:00-10:00). The increase was more pronounced, up to a factor of 4, at or near the 17 signalized intersections. However, emissions by Mobile 6.2 were only 7% higher when average speeds based on the traffic simulation for each 10m link were used rather than "Arterial 50km/h". This indicates that Mobile6.2 could not sufficiently capture the effects of stop-and-go movements on vehicular NOx emissions regardless of using link-specific average speed or "Arterial 50km/h". Thus, the correction (multiplication) factors were derived to adjust vehicular emissions by Mobile6.2 near the signalized intersections. The upstream correction factor was 3.2, which is applied to 75% of the length of queued vehicles behind the stop line to account for idling and acceleration emissions. The downstream correction factor was 1.6, which is applied to 85m after the stop line to account for emissions due to acceleration. It is concluded that stop-and-go movements significantly increase emission at the signalized intersections. Therefore, it is recommended to take into consideration stop-and-go movement of vehicles for estimation of emissions.

Results from this study are beneficial to the City of Windsor, future model developers, epidemiologists, policy makers, and users of AERMOD and Mobile6.2. Spatial and temporal distribution of traffic related air pollutant concentrations near Huron Church Road will help the City of Windsor identifying the time and location of high exposure and developing mitigation strategies. Epidemiologists could use the temporal and spatial distribution of air pollutants for estimating human exposure and its health effects. The regression models developed in this study could simplify the procedure of estimating the temporal and spatial distribution of air pollutants. This study helps the future model developers by identifying major factors explaining variations in concentrations. This study could help policy makers to divert the heavy-duty vehicles, which are high NOx and PM emitters, from local roads or highly populated areas to freeways or less populated area. This will reduce human exposure to air pollutants. Also, the spatial fall-off pattern of concentrations could help in determination of a minimum buffer distance to the road for building schools, and nursing homes. Users of AERMOD and Mobile6.2 could benefit by knowing that emissions are sensitive to VMT composition and local vehicle age distribution (local versus default values of US) in Mobile6.2, and AERMOD estimated concentrations are sensitive to hour of day variability in emissions input.

6.2 Recommendations

Limitations of this study are as below. First, background concentrations, pollutions from other sources such as other roads, point sources, and transboundary emissions were not considered. Second, hourly NO_2 concentrations used in model-measurement comparison were observed at a station approximately 1 km from the road, where the effects of Huron

Church Road traffic emissions are low. Third, the analytical method and traffic simulation presented in this study were not validated. Thus, field data should be collected for calibration and validations of these techniques. Fourth, the traffic simulations were limited to the middle lane, and one simulation run without consideration of actual lane assignment of cars and trucks.

Based on spatial fall-off of concentrations, a buffer distance of 600m from any busy arterial roads or freeways is suggested for residential settings, parks, schools, hospitals and nursing homes. At this distance, traffic related concentrations are 10% of those at 40m from the road. This will protect sensitive population from exposure to high traffic emission. For the City of Windsor, it is recommended to reduce the number of signalized intersections on Huron Church Road to improve traffic flow and to reduce emissions. Because trucks are high NOx and PM emitters, it is also suggested to divert trucks from Huron Church Road to freeways to reduce both emission and human exposure to traffic related air pollutants.

Future exposure and health studies should include background air pollutant concentrations. The new emerging technologies could also be used in air quality investigation. For example, the A-MAPS model (Spitzer et al., 2010) is a user friendly tool which provides a fast assessment of the impact of various traffic alternatives on air pollutant concentrations and health costs.

The multi-model approach for simulating NO_2 and benzene concentrations should be expand to all major roads in Windsor. Traffic counts of cars and trucks reported as Annual Average Daily Traffic (AADT) are available by City of Windsor. Hour-of day traffic counts by day of week can be estimated using either traffic profiles observed in

Windsor or those from the literature. The total length of major Windsor roads is approximately 500 km. Consequently, 60,000 links for simulation by AERMOD are needed. Thus, it demands immense computation cost.

It is also suggested to analyze spatial and temporal patterns of other traffic-related air pollutants such as CO, ultrafine PM, PM2.5, and PM10. It is worthwhile to investigate the relationships between the PM/CO concentration ratio and the truck/car counts ratio because trucks are high PM emitters and cars are high CO emitters (Transport Canada, 2006).

To mitigate border crossing traffic delays, Government of Canada plans to build a new bridge at the Windsor-Detroit border crossing and a freeway connecting the bridge is under construction. It is suggested to extend this study to analyze the impacts of traffic distribution between the existing Huron Church Road corridor and the new corridor on air quality. Results of this proposed study can help develop policy to divert most trucks to the new bridge to reduce the human exposure and health effects near Huron Church Road.

It is suggested to apply the multi-model approach used in this study in the other cities to see whether the findings are still valid. Most urban areas do not have a high truck percentage as Huron Church Road. However, both heavy and light duty vehicles should be considered in emission and dispersion modeling. This is because trucks are high NOx and PM emitters.

The spatial concentration pattern in this study should be compared with the Land-Use Regression model results, e.g. by Wheeler et al. (2008). Such comparison could provide

useful information about strengths and weaknesses of each model, which in turn could lead to improvement of modeling tools.

The simulated stop-and-go movement profiles of vehicles should be verified by collecting second-by-second speed and acceleration of vehicles using a probe sample, i.e. with GPS equipped vehicles. In addition, it is suggested to reflect the actual lane assignment patterns on the road in future traffic simulations.

Also, it is recommended to estimate correction factors for other hours of day and other pollutants on Huron Church Road. It is also suggested to develop correction factors for Mobile6.2 near signalized intersections using the new EPA mobile source emission model, MOVES (EPA, 2009), and to compare the correction factors with those developed in this study.

Hour-of-day variation in emission should be considered for estimation of concentrations. Without considering hour-of-day variation in emission, annual mean concentrations are overestimated and maximum hourly concentrations are underestimated. However, in many urban areas, only Average Annual Daily Traffic (AADT) is available. Thus, hourly traffic counts should be collected. Alternatively, users may use some typical traffic counts profiles, e.g. by hour-of-day, day of week, or season. Such profiles could be obtained from municipal or provincial transportation reports or literature. For Mobile6.2 model users, it is suggested to use 1) the local VMT composition and vehicle age distribution over the default values of US, and 2) the NOx correction factors developed in this study to adjust emission near signalized intersections. For AERMOD users, it is suggested to consider hour-of-day variation in emission input.

REFERENCES

Ahn K., Rakha H., 2008. The effects of route choice decisions on vehicle energy consumption and emissions, Transportation Research Part D: Transport and Environment, 13(3), 151-167

Akçelik R., Besley M., 2001. Acceleration and deceleration models. 23rd Conference of Australian Institutes of Transport Research (CAITR 2001), Monash University, Melbourne, Australia, 10-12 December 2001

Artaman A. Epidemiologist, Windsor Essex County Health Unit. Personal communication, June 2009.

Batterman, S.A., Zhang, K., & Kononowech, R., 2010. Prediction and analysis of near-road concentrations using a reduced-form emission/dispersion model. Environmental Health, 9, 29-29.

Beckerman, B., Jerrett, M., Brook, J.R., Verma, D.K., Arain, M.A., & Finkelstein, M.M., 2008. Correlation of nitrogen dioxide with other traffic pollutants near a major expressway, Atmos Environ, 42(2): 275–290.

Bell, M., Morgenstern, R., & Harrington, W., 2011. Quantifying the human health benefits of air pollution policies: Review of recent studies and new directions in accountability research. Environmental Science & Policy, 14(4): 357-368.

Benson, P.E., 1979. CALINE-3, A versatile dispersion model for predicting air pollutant concentrations near roadway. Final Report FHWA/CA/TL-79/23, California Department of Transportation, Sacramento, C A

Berkowicz, R., 2000. OPSM - A Parameterised Street Pollution Model Environmental Monitoring and Assessment 65: 323–331.

Boriboonsomsin, K., & Barth, M., 2008. Impacts of freeway high-occupancy vehicle lane configuration on vehicle emissions, Transportation Research Part D 13: 112–125.

Boulter P., McCrae I., & Green J., 2007. Primary NO_2 Emissions from Road Vehicles in the Hatfield and Bell Common Tunnels. Transport Research Foundation. http://trid.trb.org/view.aspx?id=841000 (Accessed November 2012).

Bureau of Transportation Statistics (BTS), 2009. US border crossing/entry data. http://www.bts.gov/programs/international/transborder/TBDR_BC/TBDR_BC_Index.html (Accessed January 2012).

Caltrans (California Department of Transportation), 1998. User's Guide for Cl4: A User-Friendly Interface for the CALINE4 Model for Transportation Project Impact

Assessments. http://www.dot.ca.gov/hq/env/air/documents/CL4Guide.pdf (Accessed July 2011).

Capparuccini, D., Faghri, A., Suarez, R., & Polus, A. 2008. Fluctuation and seasonality of hourly traffic and accuracy of design hourly volume estimates. Transportation Research Record: Journal of the Transportation Research Board, 2049: 63-70.

Carslaw, D.C., & Beevers, S.D., 2002. The efficacy of low emission zones in central London as a means of reducing nitrogen dioxide concentrations. Transportation Research Part D: Transport and Environment 7(1), 49-64.

CERC (Cambridge Environmental Research Consultants), 2010. ADMS-Roads Pollution Model. http://www.cerc.co.uk/environmental-software/ADMS-Roads-model.html (Accessed July 2011).

Chaix,B., Gustafsson, S., Jerrett, M., Kristersson, H., Lithman, T., Boalt, A. & Merlo, J., 2006. Children's exposure to nitrogen dioxide in Sweden: investigating environmental injustice in an egalitarian country, J Epidemiol Community Health, 60: 234–241.

Chen, C. H., Huang, C., Jing, Q. G., Wang, H. K., Pan, H. S., Li, L., Zhao, J., & Dai, Y. et al., 2007. On-road emission characteristics of heavy-duty diesel vehicles in Shanghai, Atmospheric Environment, 41(26), 5334–5344.

Claggett M., & Houk J., 2008. Comparing MOBILE6.2 and Emfac2007 Emission Factors. Journal of the Transportation Research Board, 2058 (1), 51-57.

Claggett M., 2012. Improvements to CAL3QHCR model. . Proceedings of the 105th Air & Waste Management Associations Conference, June 19-22 2012, San Antonio, TX, Paper 2012-A-497-AWMA.

Cook, R., & Glover, E., 2002. Technical Description of the Toxics Module for MOBILE6.2 and Guidance on Its Use for Emission Inventory Preparation. US EPA, Office of Transportation and Air Quality, Ann Arbor, MI.

Cook, R., Isakov, V., Touma, J., Benjey, W., Thurman, J., Kinnee, E., & Ensley, D., 2008. Resolving local scale emissions for near road modeling assessments, Journal of the Air & Waste Management Association 58: 451–461.

Cooper, C.D., & Arbrandt, M., 2004. Mobile Source Emission Inventories – Monthly or Annual Average Inputs to MOBILE6?, J. Air & Waste Manage. Assoc. 54:1006–1010.

Dennstaedt, S.C., 2006. Model Output Statistics Provide Essential Data for Small Airports. The front 2(2), 1-4. Published by NOAA's National Weather Service.

http://aviationweather.gov/general/pubs/front/docs/jun-06.pdf (Accessed November 2012) - Cited in Appendix A.

DMTI Spatial. 2002. DMTI CanMap RouteLogistics of Ontario (2001): Topographic Features - Land Use Layer. Markham, Ontario: DMTI Spatial Inc.

DRIC (Detroit River International Crossing) Study, 2008a. Environmental Assessment Study, Level 2 Traffic Operations Analysis of Practical Alternatives. http://www.partnershipborderstudy.com/reports_canada.asp (Accessed November, 2010)

DRIC, 2008b. Detroit River International Crossing Final Air Quality Monitoring Report October 1st, 2006 – October 31st, 2007. http://www.partnershipborderstudy.com/pdf/33900-7%2010APR08%20Quarterly%20Report%204%20-%20FINAL%20inc%20App.pdf (Accessed November, 2010).

DRIC, 2008c. Practical Alternatives Evaluation Working Paper - Air Quality Impact Assessment. http://www.partnershipborderstudy.com/pdf/AirQuality/WEB_PracticalAltsWP_AirQuality_May2008-report&apps.pdf (Accessed July 2011)

Eckhoff, P. A. & T. N. Braverman, 1995. Addendum to the user's guide to CAL3QHC version 2.0 (CAL3QHCR user's guide). US Environmental Protection Agency, Research Triangle Park, NC 27711.

Environment Canada, 2003. Gasoline and Diesel Fuel Survey: Driveability Index (DI) and Oxygenates in Gasoline; Cetane Index, Cetane Number, Aromatics and Polyaromatic Hydrocarbons (PAH) in Diesel. http://www.ec.gc.ca/Publications/default.asp?lang=En&xml=97F295AD-3476-4454-AF4B-D120DFF7C9FD (Accessed November, 2010).

Environment Canada, 2008. Benzene in Canadian Gasoline: Report on the Effect of the Benzene in Gasoline Regulations 2006. http://www.ec.gc.ca/Publications/default.asp?lang=En&xml=38479F21-23FA-48F9-AAEE-522C30E12098&printfullpage=true&nodash=1 (Accessed November, 2010).

Environment Canada. 2012a. Climate data online. http://www.climate.weatheroffice.ec.gc.ca/climateData/canada_e.html (Accessed November 2012)

Environment Canada, 2012b. Data Sources and Methods for the Sulphur Dioxide, Nitrogen Dioxide and Volatile Organic Compounds Air Quality Indicators.

http://www.ec.gc.ca/indicateurs-indicators/default.asp?lang=En&n=BA9D8D27-1&offset=4&toc=show (Accessed December 2012)

EPA (US Environment Protection Agency), 1995. User's guide for the Industrial Source Complex (ISC3) Dispersion models: volume I - user instructions. http://www.epa.gov/scram001/userg/regmod/isc3v1.pdf (Accessed November 2009).

EPA, 1997. Development of Speed Correction Cycles. Document Number M6.SPD.001. http://www.epa.gov/oms/models/mobile6/m6spd001.pdf (Accessed January 2012).

EPA, 1999a. Analysis of the impacts of control programs on motor vehicle toxics emissions and exposure in urban areas and nationwide. Report No. EPA-420/R-99-029-030. http://www.epa.gov/otaq/regs/toxics/r99029.pdf (Accessed November, 2010).

EPA, 1999b. Exhaust Emission Temperature Correction Factors for MOBILE6. Report No. EPA420-P-99-001 http://www.epa.gov/oms/models/mobile6/m6ste004.pdf (Accessed July 2011).

EPA, 1999c. Meteorological Processors and Accessory Programs: PCRAMMET. http://www.epa.gov/scram001/metobsdata_procaccprogs.htm (Accessed November 2009).

EPA, 2001. Final Facility Specific Speed Correction Factors. EPA420-R-01-060 www.epa.gov/oms/models/mobile6/r01060.pdf (Accessed September, 2011).

EPA, 2002a. Sensitivity Analysis of MOBILE6.0. EPA420-R-02-035 www.epa.gov/oms/models/mobile6/r02035.pdf

EPA, 2002b. Development of Heavy-Duty NOx Off-Cycle Emission Effects for MOBILE6, EPA420-R-02-004. http://nepis.epa.gov/Exe/ZyPURL.cgi?Dockey=P10022KB.txt

EPA, 2003. Mobile Source Emission Factor Model, Version 2, MOBILE6. http://www.epa.gov/otaq/m6.htm (Accessed November 2010).

EPA, 2004a. AERMOD: Description of model formulation. EPA-454/R-03-004 http://www.epa.gov/ttn/scram/models/aermod/aermod_userguide.zip (Accessed December 2010).

EPA, 2004b. User Guide for the AERMOD Meteorological Preprocessor (AERMET). EPA-454/B-03-002. www.epa.gov/scram001/7thconf/aermod/aermetugb.pdf (Accessed February 2011).

EPA, 2004c. User's Guide for the AERMOD Terrain Preprocessor (AERMAP). http://www.epa.gov/ttn/scram/models/aermod/aermap/aermap_userguide.zip (Accessed July 2011).

EPA, 2004d. AERMOD: Description of Model Formulation. Report No. EPA-454/R-03-004. http://www.epa.gov/scram001/7thconf/aermod/aermod_mfd.pdf (Accessed February 2013)

EPA, 2008. Fuel Trends Report: Gasoline 1995 – 2005. Report No. EPA420-R-08-002. http://www.epa.gov/otaq/regs/fuels/rfg/properf/420r08002.pdf (Accessed July 2011)

EPA, 2009. Motor Vehicle Emission Simulator, MOVES2010 User Guide. Report No. EPA-420-B-09-041. http://www.epa.gov/otaq/models/moves/420b09041.pdf (Accessed November 2012).

EPA, 2010. Transportation Conformity Guidance for Quantitative Hot-spot Analyses in PM2.5 and PM10 Nonattainment and Maintenance Areas. Report No. EPA-420-B-10-040. http://www.epa.gov/otaq/stateresources/transconf/policy/420b10040.pdf (Accessed November 2012).

EPA, 2012a. Mobile Source Emissions - Past, Present, and Future. http://www.epa.gov/otaq/invntory/overview/pollutants/index.htm (Accessed April 2012).

EPA, 2012b. Dispersion modeling home page. http://www.epa.gov/scram001/dispersionindex.htm (Accessed April 2012).

EPA, 2012c. Nitrogen Dioxide (NO_2) web page. http://www.epa.gov/iaq/no2.html (Accessed December 2012).

EPA, 2012d. Benzene web page. http://www.epa.gov/ttnatw01/hlthef/benzene.html (Accessed December 2012).

EPA, 2013a. AERMOD Model Change Bulletin, MCB#8, Date: 12/10/2012. http://www.epa.gov/ttn/scram/models/aermod/aermod_mcb8.txt (Accessed February 2013).

EPA, 2013b. AERSURFACE User's Guide. Report No. EPA-454/B-08-001. http://www.epa.gov/scram001/7thconf/aermod/aersurface_userguide.pdf (Accessed February 2013).

ESRI, 2010. ArcGIS: A Complete Integrated System. http://www.esri.com/software/arcgis/index.html (Accessed November 2010).

Faulkner, W.B., Shaw B.W., & Grosch R.. 2008. Sensitivity of Two Dispersion Models AERMOD and ISCST3 to Input Parameters for a Rural Ground-Level Area Source. J. Air and Waste Management 58: 1288-1296.

Federal Highway Administration (FHWA). 2004. Traffic Analysis Toolbox Volume III: Guidelines for Applying Traffic Microsimulation Modeling Software, No. FHWA-HRT-04-040.

Fu, J. & Yun J., 2010. An overview of models to estimate On-Road Vehicle Emissions and Their Dispersion. EM Magazine AWMA: 4-8.

Gan W.Q., Koehoorn M., Davies H.W., Demers P.A., & Tamburic L. et al., 2011. Long-Term Exposure to Traffic-Related Air Pollution and the Risk of Coronary Heart Disease Hospitalization and Mortality. Environ Health Perspect 119(4): 501-507.

GeoBase Canada, 2000. Land Cover. http://geobase.ca/geobase/en/data/landcover/index.html (Accessed July 2011).

Google Earth. 2010. Windsor, Ontario, Canada - Huron Church Road. Imagery year of 2007. Downloadable from http://earth.google.ca (Accessed November 2010).

Grosch T.G. & Lee R.F., 1999. Sensitivity of the AERMOD air quality model to the selection of land use parameters, Transactions on Ecology and the Environment., vol.37, 1999.

Hatzopoulou, M., & Hao J.Y. et al., 2011. Simulating the impacts of household travel on greenhouse gas emissions, urban air quality, and population exposure. Transportation 38(6): 871-887.

Hanrahan, P.L., 1999. The Plume Volume Molar Ratio Method for Determining NO2/NOx Ratios in Modeling—Part I: Methodology, Air & Waste Manage. Assoc. 49:1324-1331.

Health Canada, 2010a. Study Analyzes Impact of Air Pollution on Windsor Children. http://www.hc-sc.gc.ca/sr-sr/activ/environ/windsor-eng.php (Accessed July 2011).

Health Canada, 2010b, Canada - United States Border Air Quality Strategy. http://www.ec.gc.ca/air/default.asp?lang=En&n=D6F2B21E-1 (Accessed October 2010)

Health Canada, 2011. Health Effects of Air Pollution. http://www.hc-sc.gc.ca/ewh-semt/air/out-ext/effe/health_effects-effets_sante-eng.php (Accessed July 2011)

HEI (Health Effect Institute), 2010. Traffic-Related Air Pollution: A Critical Review of the Literature on Emissions, Exposure, and Health Effects. http://pubs.healtheffects.org/view.php?id=334 (Accessed April 2012)

Held, T., Chang, D.P.Y., Niemeier, D.A., 2003. UCD 2001: an improved model to simulate pollutant dispersion from roadways. Atmospheric Environment 37(1): 5325-5336.

Hellinga, B., & Abdy, Z. 2008. Signalized intersection analysis and design: Implications of day-to-day variability in peak-hour volumes on delay. Journal of Transportation Engineering, 134(7): 307-318.

Hendrick, E., Hanna, C.D.S., Egan, C.D.B., & Tino, C.V., 2012. Review and Evaluation of the Plume Volume Molar Ratio Method (PVMRM) and Ozone Limiting Method (OLM) for short-term (1-hour average) NO_2 Impacts. Epsilon Associates, Inc. http://mycommittees.api.org/rasa/amp/Modeling%20Documents/Review%20and%20Evaluation%20of%20PVMRM%20and%20OLM%20-%20Final%20Report.pdf (Accessed February 2012)

Infoplease.com, 2012. Climate of 100 Selected U.S. Cities. Infoplease. © 2000–2007 Pearson Education. http://www.infoplease.com/ipa/A0762183.html (Accessed February 2012)

ITE, 2008. Canadian Capacity Guide for Signalized Intersection, Institute of Transportation Engineers, Canada

Kim, D. 2003. Evaluation on simulation models for urban corridor signal optimizations. Proceedings of the Eastern Asia Society for Transportation Studies, 4: 512-525.

Kourtidis, K., Ziomas, I., Zerefos, C., Kosmidis, E., Symeonidis, P., & Christophilopoulos, E. et al. (2002). Benzene, toluene, ozone, NO_2 and SO_2 measurements in an urban street canyon in Thessaloniki, Greece. Atmospheric Environment, 36, 5355–5364.

Kumar, A., Varadarajan, C., Vijayan, A., & Pathan, S., 2011. Air Quality Modeling Case Studies, Advances in Environmental Research, Vol. 15, Chapter 6, pp. 135-163, Nova Science Publishers, Inc.

Kumar, A. Professor & Chairman. Department of Civil Engineering, The University of Toledo. Personal communication, February 2013.

Kun, C., & Lei, Y., 2007. Microscopic Traffic-Emission Simulation and Case Study for Evaluation of Traffic Control Strategies. J Transpn Sys Eng & IT, 7(1), 93−100.

Lakes Environmental, 2011. AERMOD View Gaussian Plume Air Dispersion Model. http://www.weblakes.com/products/aermod/index.html (Accessed July 2011).

Lindgren, A., Stroh E., Nihlén, U., Montnémery, P., Axmon, A. & Jakobsson, K., 2009. Traffic exposure associated with allergic asthma and allergic rhinitis in adults. A cross-sectional study in southern Sweden, International Journal of Health Geographics, 8:25.

Lindgren, A., Björk, J., Stroh E., & Jakobsson, K., 2010. Adult asthma and traffic exposure at residential address, workplace address, and self-reported daily time outdoor in traffic: A two-stage case-control study, BMC Public Health, 10:716.

Long, G.E., Cordova, J.F., & Tanrikulu, S. 2004. An Analysis of AERMOD Sensitivity to Input Parameters in the San Francisco Bay Area. 13th Conference on the Applications of Air Pollution Meteorology with the Air and Waste Management Association. Vancouver, B.C. Canada.

McCarthy, M.C., Hafner, H.R., & Montzka, S.A., 2006. Background concentrations of 18 air toxics for North America. Journal of the Air & Waste Management Association, 56(1), 3-11.

Minitab, 2011. Statistical and Process Management Software for Six Sigma and Quality Improvement. http://www.minitab.com (Accessed July 2011).

Minoura, H., & Ito, A., 2010. Observation of the primary NO_2 and NO oxidation near the trunk road in Tokyo. Atmospheric Environment, 44(1), 23-29.

Modig., L., Sunesson, A.L., Levin, J.O., et al. 2004. Can NO_2 be used to indicate ambient and personal levels of benzene and 1,3-butadiene in air?. J Environ Monit, 6:957–962.

MOE, 2009a. Historical Air Pollutant Data. Air Dispersion Modelling Guideline for Ontario. http://www.airqualityontario.com/history/index.php (Accessed July 2011).

MOE, 2009b. Air Dispersion Modelling Guideline for Ontario. http://www.ene.gov.on.ca/environment/en/resources/STD01_076487.html (Accessed Feb 2011).

MOE, 2010. Ontario Regional Meteorological Data. http://www.ene.gov.on.ca/environment/en/industry/standards/industrial_air_emissions/air_pollution/STDPROD_084097.html (Accessed July 2011).

MOE, 2011. Information: About Air Quality. http://www.airqualityontario.com (Accessed July 2011)

MOE, 2012. Air Quality in Ontario 2009 Report and Appendix. http://www.ene.gov.on.ca/environment/en/resources/STDPROD_081227.html (Accessed April 2012).

Mohan, M., Bhati, S., Sreenivas, A., & Marrapu, P., 2011. Performance evaluation of AERMOD and ADMS-Urban for total suspended particulate matter concentrations in megacity Delhi. Aerosol and Air Quality Research, 11(7), 883-894.

Mölter A., Lindley S., de Vocht F., Simpson A., & Agius R., 2010. Modelling air pollution for epidemiologic research — Part I: A novel approach combining land use regression and air dispersion, Science of The Total Environment, 408(23), 5862-5869

NOAA (National Oceanic and Atmospheric Administration), 2006. Fire Weather Annual Operating Plan, published by National Weather Service Weather Forecast Office in Upton, NY. http://www.erh.noaa.gov/okx/WFO-FireWXOperatingPlan.pdf (Accessed July 2011) - Cited in Appendix A.

NOAA, 2012, National Oceanic and Atmospheric Administration: NOAA/ESRL Radiosonde Database Access. http://www.esrl.noaa.gov/raobs/ (Accessed November 2012).

Panis L.I., Broekx S., & Liu R., 2006. Modelling instantaneous traffic emission and the influence of traffic speed limits. Science of The Total Environment, 371, 270-285.

Parra, M.A., Elustondo, D., Bermejo, R., & SantamarÃ-a, J.M., 2009. Ambient air levels of volatile organic compounds (VOC) and nitrogen dioxide (NO2) in a medium size city in Northern Spain, Science of the Total Environment, 407:999-1009.

Pénard-Morand, C., Schillinger, C., Armengaud, A., Debotte, G., Chrétien, E., Pellier, S., Annesi-Maesano, I., & ISSAC-France, 2006. Assessment of schoolchildren's exposure to traffic related air pollution in the French Six Cities Study using a dispersion model. Atmospheric Environment 40(1), 2274-2287.

Pierce T., Isakov V., Haneke B., & Paumier J., 2008. Emission and air quality modeling tools for near-roadway applications. EPA/600/R-09/001. http://www.epa.gov/nscep/index.html (Accessed April 2012).

PTV AG. 2008. VISSIM User Manual Version 5.10. Karlsruhe, Germany.

Schnitzhofer, R., Beauchamp, J., Dunkl, J., Wisthaler, A., Weber, A., & Hansel, A. 2008. Long term measurements of CO, NO, NO2, benzene, toluene and PM10 at a motorway location in an Austrian valley, Atmos. Environ., 42, 1012–1024.

Scire, J., Strimaitis, D.G., & Yamartino, R.J., 2000a. A User's Guide for the CALPUFF Dispersion Model (Version 5). Earth Tech Inc., Concord, Massachusetts. http://www.src.com/calpuff/download/CALPUFF_UsersGuide.pdf (Accessed July 2011).

Scire, J., Robe, F.R., Fernau, M.E., & Yamartino, R.J., 2000b. A User's Guide for the CALMET Meteorological Model (Version 5). Earth Tech Inc., Concord, Massachusetts. http://www.src.com/calpuff/download/CALMET_UsersGuide.pdf (Accessed July 2011).

Sillman S., 2003. 9.11 - Tropospheric Ozone and Photochemical Smog, Treatise on Geochemistry, Pergamon, Oxford, Pages 407-431, ISBN 9780080437514, 10.1016/B0-08-043751-6/09053-8.

Sosa T.M., Cheu R.L., & Li W.W., 2012. Air pollution reduction at the Bridge of the Americas. Proceedings of the 105th Air & Waste Management Associations Conference, June 19-22 2012, San Antonio, TX, Paper 2012-A-560-AWMA

Spitzer, D., O'Byrne, G., Urquizo, N., & Bojkov, B., 2010. Using satellite data to monitor the quality of urban air. Environmental Science & Engineering Magazine September 2010.

Statistics Canada, 2008. Canadian Vehicle Survey: Annual 2008. http://www.statcan.gc.ca/pub/53-223-x/53-223-x2008000-eng.htm (Accessed November, 2010).

Statistics Canada, 2012. Statistics Canada 2011 Census of Canada. http://www12.statcan.gc.ca/census-recensement/index-eng.cfm (Accessed February, 2013).

Tang T., Claggett M., Byun J., Roberts M., Granell J., & Aspy D.E., 2005. MOBILE6.2 Modeling of Exhaust Air Toxic Emission Factors: Trend and Sensitivity Analysis. Journal of the Transportation Research Board, 1941 (99-106).

Touma, J.S., Isakov, V., Cimorelli, A.J., Brode, R.W., & Anderson, B., 2007. Using Prognostic Model-Generated Meteorological Output in the AERMOD Dispersion Model: An Illustrative Application in Philadelphia, PA J. Air & Waste Manage. Assoc. 57:586–595.

Transport Canada, 2006. Urban Transportation Emission Calculator. http://wwwapps.tc.gc.ca/Prog/2/UTEC-CETU/ (Accessed November, 2010).

Transport Canada, 2010. Transportation in Canada 2009 – Addendum. http://www.tc.gc.ca/media/documents/policy/addendum2009.pdf (Accessed July 2011).

Transportation Research Borad (TRB), 2010. Highway Capacity Manual. Washington, D.C.

University of California, 2003. Comprehensive Modal Emission Model (CMEM). http://www.cert.ucr.edu/cmem/ (Accessed July 2011).

Venkatram, A., Isakov, V., Seila, R., & Baldauf, R., 2009. Modeling the impacts of traffic emissions on air toxics concentrations near roadways, Atmospheric Environment, 43: 3191–3199.

Vitale R., Boulton W., Lepage M., Gauthier M., Qiu X., & Lamy S., 2004. Modelling the Effects of E10 Fuels in Canada. 13th International Emission Inventory Conference "Working for Clean Air in Clearwater" Clearwater, FL, June 8 - 10, 2004. www.epa.gov/ttn/chief/conference/ei13/modeling/boulton.pdf (Accessed November, 2010).

Wallace, J., & Kanaroglou, P., 2008. Modeling NOx and NO_2 emissions from mobile sources: A case study for Hamilton, Ontario, Canada. Transportation Research Part D: Transport and Environment 13 (1), 323–333.

Wang S., Tang X., Fan Z., Wu X., Lioy P.J., & Georgopoulos P.G. 2009. Modeling of Personal Exposures to Ambient Air Toxics in Camden, New Jersey: An Evaluation Study. Journal of Air & Waste Management Association 59:733–746.

Wang, X., 2008. Spatial Analysis of Long-term Exposure to Air Pollution and Cardio-respiratory Mortalities in Brisbane, Australia. Master of Applied Science Thesis, School of Public Health, of Queensland University of Technology.

Wayson, J., 2012. Using AERMOD for highway projects. Proceedings of the 105th Air & Waste Management Associations Conference, June 19-22 2012, San Antonio, TX, Paper 2012-A-347-AWMA.

Westerlund, k.k. & Cooper C.D., 2012. Developing a Mobile Source Air Toxics (MSATs) Dispersion Model. Proceedings of the 105th Air & Waste Management Associations Conference, June 19-22 2012, San Antonio, TX, Paper 2012-A-478-AWMA.

Wheeler, A.J., Smith-Doiron, M., Xu, X., Gilbert, N.L., & Brook, J.R. 2008. Intra-urban variability of air pollution in Windsor, Ontario - Measurement and modeling for human exposure assessment. Environmental Research 106: 7-16.

Wulder, M., & Nelson, T., 2003. EOSD Land Cover Classification Legend Report 2003. Canadian Forest Service, Natural Resources Canada Victoria, British Columbia. http://www.pfc.forestry.ca/eosd/cover/EOSD_legend_report-v2.pdf (Accessed July 2011).

Zhang, K., & Batterman, S.,, 2010. Near-road air pollutant concentrations of CO and PM2.5: A comparison of MOBILE6.2/CALINE4 and generalized additive models. Atmospheric Environment 44(14): 1740-1748.

Zhou, Y., & Levy, J.I. (2008). The impact of urban street canyons on population exposure to traffic-related primary pollutants. Atmospheric environment, 42(13), 3087-3098.

Zou, B., & Zeng Y. et al. 2010. Sensitivity Analysis of AERMOD in Modeling Local Air Quality under Different Model Options, 4th International Conference on Bioinformatics and Biomedical Engineering (iCBBE), 18-20 June 2010, Chengdu, China.

APPENDICES

Appendix A: Meteorological data source and processing

Hourly surface air data, collected at the Windsor Airport (42.28 N, 82.96 W, WMO Identifier: 71538) was obtained from Environment Canada website (2012a). Radiosonde upper air data were collected twice daily at Pontiac, MI, U.S.A. (42.70N, 83.47W, WMO Station: 72632). This is the nearest upper air station to Windsor, approximately 60 km northwest of Windsor located in a forest area (Figure A1). Those data were obtained from the National Oceanic and Atmospheric Administration website (NOAA, 2012). Hourly surface data (converted to HUSWO format) and upper air data were used by AERMET (EPA, 2004b) to produce hourly input, surface and vertical profiles, for AERMOD (EPA, 2004a).

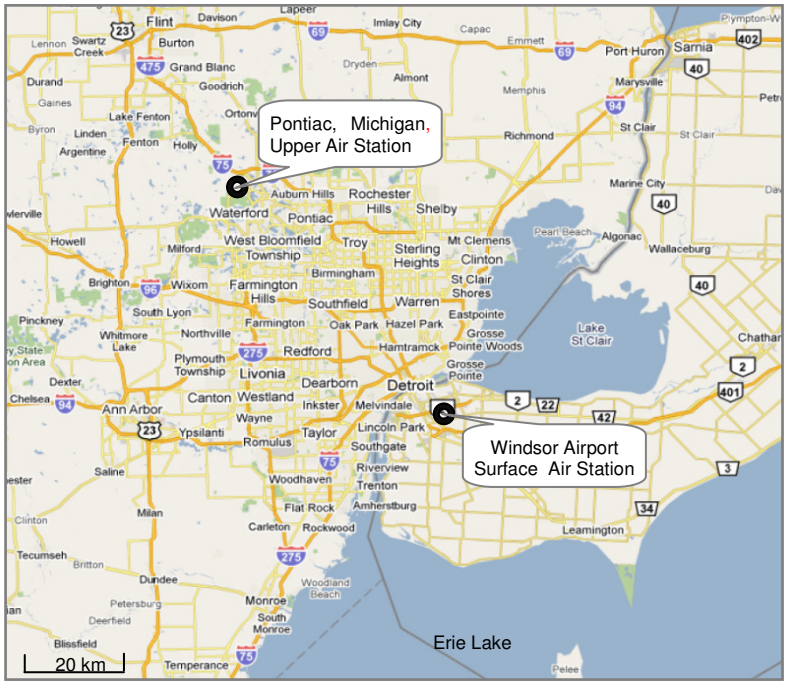

Figure A1: Map showing meteorological stations in Windsor and Michigan (base map from maps.google.com, 2009).

Table A1 lists surface data in HUSWO format. Table A2 shows a sample of surface data at the Windsor Airport.

Table A1: Surface data in HUSWO format.

	Parameters	Unit (Original data)	Unit (HUSWO format)	Flags for missing
1	Station#			
2	Year Month Day Time			
3	Global horizontal radiation			9999
4	Direct normal radiation			9999
5	Total cloud cover	Descriptive	Tenths	99
6	Opaque cloud cover		Tenths	99
7	Dry bulb temperature	Degree Celsius	Degree Fahrenheit	999.9
8	Dew point temperature	Degree Celsius	Degree Fahrenheit	999.9
9	Relative humidity	%	%	999
10	Station pressure	kPa	Hundredth of inches Hg 1 hundred inches of Hg = 3386.39 mb	9999
11	Wind direction	10's degree	degree	999
12	Wind speed	Km/h	mile/h	99.9
13	Visibility	Km	mile	9999.9
14	Ceiling height		feet	99999
15	Present weather			99999999
16	ASOS cloud layer 1			99999
17	ASOS cloud layer 2			99999
18	ASOS cloud layer 3			99999
19	Hourly precipitation			999
20	Snow depth			999

Note: Shaded rows are data available at the Windsor Airport (Environment Canada, 2012a).

Table A2: Sample data in Windsor Airport in Environment Canada website (2012a)

Year	Month	Day	Time (EST)	Temp (°C)	Dew Point Temp (°C)	Rel Hum (%)	Wind Dir (10's deg)	Wind Spd (km/h)	Visibility (km)	Stn Press (kPa)	Weather Condition
2008	2	1	13:00	-4.9	-6.1	91	9	7	4	100.88	Clear
2008	2	1	14:00	-4.7	-5.8	92	10	7	9.7	100.84	Clear

Since cloud cover (weather condition) was descriptive in the surface data (i.e. cloudy, clear), it was decoded according to a conversion table (Table A3) following Environment Canada guideline (2012a). Opaque cloud cover was not available in the surface data, and it was decoded from descriptive cloud cover according to a scheme by NOAA (2006) (Table A3). Ceiling height, called vertical visibility, was decoded from hourly visibility data using a conversion table (Table A4) by Dennstaedt (2006).

Table A3: Decoding scheme for sky cloud cover and opaque cloud cover from descriptive weather

Sky Cloud Cover (EC, 2009)		Opaque Cloud Cover (NOAA, 2006)	
Descriptive	Amount in tenths	Descriptive	Amount in tenths
Clear	0	Clear	0
Mainly Clear	1-4	Mostly Clear	1-3
		Partly Cloudy	4-7
Mostly Cloudy	5-9	Mostly Cloudy	8-9
Cloudy	10	Cloudy	10

Table A4: Decoding scheme for visibility and ceiling height (Dennstaedt, 2006)

Category	Visibility (mile)	Ceiling Height (ft)
1	Less than 0.5	Less than 200
2	0.5 – 1	200 – 400
3	1 – 2	500 – 900
4	2 – 3	1000 – 1900
5	3 – 5	2000 – 3000
6	5 – 6	3100 – 6500
7	Greater than 6	6600 – 12000

There were two hours missing surface air data at the Windsor Airport on September 29, 2008 during 22:00-23:00 and November 10, 2008 at 16:00-17:00. For these hours, surface air data were interpolated using data of the hours before and after the missing hours. All calm hours were replaced by a wind speed of 1.1 m/s following MOE Guideline (MOE, 2009b). There were 698 calm hours, about 8% of time in 2008.

Appendix B: Results of ANOVA and regression models

B1: Sample ANOVA Results

General Linear Model: NO2_Obs(ppb) versus CarNoxEqu(ve, WindSpeed(m/

```
Factor            Type   Levels  Values
CarNoxEqu(veh/h)  fixed     282  561, 567, 573, …
WindSpeed(m/s)    fixed      23  1.1, 1.7, 2.0, …


Analysis of Variance for NO2_Obs(ppb), using Adjusted SS for Tests

Source              DF     Seq SS    Adj SS   Adj MS      F      P
CarNoxEqu(veh/h)   281   51316.24  46979.21   167.19   4.31  0.000
WindSpeed(m/s)      22   39261.16  39261.16  1784.60  46.03  0.000
Error             2549   98817.52  98817.52    38.77
Total             2852  189394.93


S = 6.22633   R-Sq = 47.82%   R-Sq(adj) = 41.62%
```

General Linear Model: NO2_Sim(ug/m versus CarNoxEqu(ve, WindSpeed(m/

```
Factor            Type   Levels  Values
CarNoxEqu(veh/h)  fixed     282  561, 567, …
WindSpeed(m/s)    fixed      23  1.1, 1.7,…


Analysis of Variance for NO2_Sim(ug/m3), using Adjusted SS for Tests

Source              DF    Seq SS    Adj SS   Adj MS      F      P
CarNoxEqu(veh/h)   281  19854.52  13106.44    46.64   2.37  0.000
WindSpeed(m/s)      22  24302.98  24302.98  1104.68  56.10  0.000
Error             2566  50531.75  50531.75    19.69
Total             2869  94689.25


S = 4.43766   R-Sq = 46.63%   R-Sq(adj) = 40.33%
```

B2: Sample Regression Results

Regression Analysis: ln_NO2_0 versus ln_ws_0, Ln_car_nox_e_0

```
The regression equation is
ln_NO2_0 = - 2.43 - 1.50 ln_ws_0 + 0.915 Ln_car_nox_e_0


3186 cases used, 7 cases contain missing values


Predictor           Coef  SE Coef        T      P  VIF
Constant        -2.42856  0.09634   -25.21  0.000
ln_ws_0         -1.50320  0.01038  -144.76  0.000  1.0
Ln_car_nox_e_0   0.91475  0.01179    77.60  0.000  1.0


S = 0.362232   R-Sq = 88.8%   R-Sq(adj) = 88.8%


Analysis of Variance

Source            DF      SS      MS         F      P
Regression         2  3327.9  1664.0  12681.46  0.000
Residual Error  3183   417.6     0.1
Total           3185  3745.6
```

Regression Analysis: ln_NO2_1 versus Ln_car_nox_e_0_1, ln_ws_1

```
The regression equation is
ln_NO2_1 = - 4.09 + 0.923 Ln_car_nox_e_0_1 - 0.737 ln_ws_1


2339 cases used, 32 cases contain missing values


Predictor             Coef  SE Coef       T      P
Constant           -4.0949   0.1487  -27.54  0.000
Ln_car_nox_e_0_1   0.92342  0.01686   54.76  0.000
ln_ws_1           -0.73664  0.01039  -70.89  0.000


S = 0.269403   R-Sq = 77.4%   R-Sq(adj) = 77.3%


Analysis of Variance

Source            DF      SS      MS        F      P
Regression         2  579.04  289.52  3989.07  0.000
Residual Error  2336  169.54    0.07
Total           2338  748.58
```

Appendix C: Mobile6.2 – Road type and average speed

Table C1: Driving cycles considered for derivations of SCFs for Light Duty Vehicles (EPA, 2001).

Cycle	Average Speed (mph)	Maximum Speed (mph)	Maximum Acceleration (mph/s)	Length (seconds)	Length (miles)
Freeway, High Speed	63.2	74.7	2.7	610	10.72
Freeway, LOS A-C	59.7	73.1	3.4	516	8.55
Freeway, LOS D	52.9	70.6	2.3	406	5.96
Freeway, LOS E	30.5	63	5.3	456	3.86
Freeway, LOS F	18.6	49.9	6.9	442	2.29
Freeway, LOS "G"	13.1	35.7	3.8	390	1.42
Freeway Ramps	34.6	60.2	5.7	266	2.56
Arterial/Collectors LOS A-B	24.8	58.9	5	737	5.07
Arterial/Collectors LOS C-D	19.2	49.5	5.7	629	3.36
Arterial/Collectors LOS E-F	11.6	39.9	5.8	504	1.62
Local Roadways	12.9	38.3	3.7	525	1.87
Non-Freeway Area-Wide Urban Travel	19.4	52.3	6.4	1,348	7.25

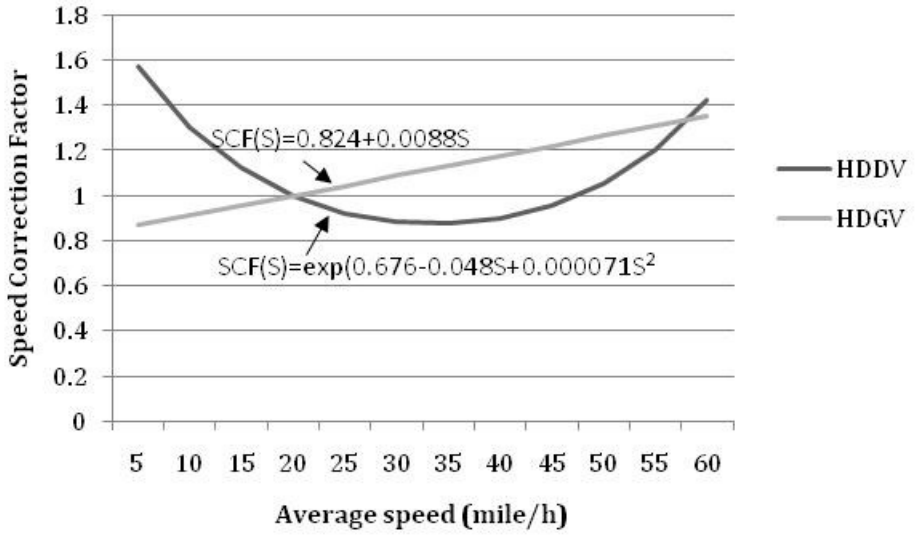

Figure C1: NOx speed correction factors for Heavy Duty Vehicles (source of data: EPA, 2001)

A more comprehensive study of effect of road type and average speed on estimated NOx and benzene vehicular emissions by Mobile6.2 was conducted. Figures C2 and C3 show NOx and benzene emission factors of LDVs and HDVs. NOx and benzene emission factors of LDVs were similar between the Arterial Road and the Freeway for average speeds from 30 to 80km. NOx and benzene emission factor of LDVs for the Arterial road decreased as average speed increased from 10 to 40 km/h and became almost constant in the average speeds above 40km/h. On the other hand, NOx emission factor of HDVs is slightly lower for the Arterial Road than Freeways. NOx emission factor of HDVs has a U-shape where emissions were low in the middle range of average speed.

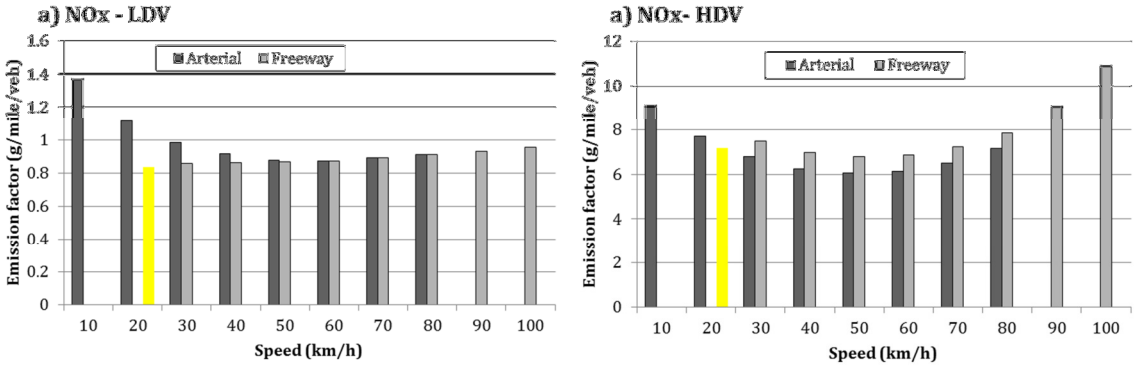

Figure C2: NOx emission factors of LDVs and HDVs with average speeds and road types (yellow bar shows the Local road)

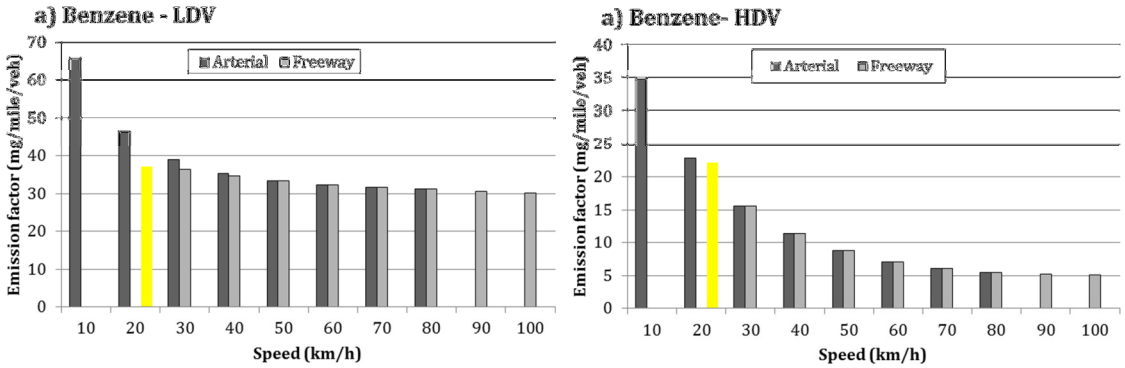

Figure C3: Benzene emission factors of LDVs and HDVs with average speeds and road types (yellow bar shows the Local road)

NOx emission factors of HDVs were slightly higher by the Freeway option than the Arterial option. In average speed of 20-30km/h which is close to the average speed of the Local Road, emission factors of LDVs by the Local Road option were lower than the Arterial option (NOx: -20% and Benzene: -25%).

For LDVs, there was a small difference among the three road types at low speed (≤ 40km/h); Arterial was slightly higher than Freeway and Local road emissions. There was no difference at high speed between Arterial and Freeway.

Appendix D: AERMOD formulation for estimation of turbulence coefficients

Equations D1-D6 show the model formulation for estimation of turbulence coefficients in AERMOD. These equations are from "AERMOD: DESCRIPTION OF MODEL FORMULATION" (EPA, 2004d).

Lateral turbulence coefficient (σ_{vT})

Equation D1 shows the lateral turbulence coefficient (σ_{vT}) as a function of mechanical and convective mixings.

$$\sigma_{vT}{}^2 = \sigma_{vm}{}^2 + \sigma_{vc}{}^2 \qquad \text{(D1)}$$

where:

σ_{vT}: Lateral turbulence coefficient

σ_{vm}: Mechanical mixing component for lateral turbulence coefficient (as defined in Equation D2 below)

σ_{vc}: Convective mixing component for lateral turbulence coefficient (as defined in Equation D3 below)

Mechanical mixing component for lateral turbulence is calculated as shown in Equation D2.

$$\sigma_{vm}{}^2 = \left[\frac{\sigma_{vm}{}^2(z_{im}) - \sigma_{v0}{}^2}{z_{im}}\right] z + \sigma_{v0}{}^2 \qquad for\ z \le z_{im} \qquad \text{(D2)}$$

$$\sigma_{vm}{}^2 = \sigma_{vm}{}^2(z_{im}) \qquad for\ z > z_{im}$$

where:

$\sigma_{v0}{}^2$: Initial mechanical mixing ($= 3.6\, u^*{}^2$)

z_{im}: Mechanical mixing height (m)

z: Elevation (m)

$$\sigma_{vm}{}^2(z_{im}) = \text{MIN}[\sigma_{v0}{}^2, 0.25]$$

Convective mixing component for lateral turbulence coefficient is calculated as shown in Equation D3.

$$\sigma_{vc}{}^2 = 0.35\, w^{*\ 2} \qquad \text{(D3)}$$

Vertical turbulence coefficient (σ_{wT})

Equation D4 shows the vertical turbulence coefficient (σ_{wT}) as a function of mechanical and convective mixings.

$$\sigma_{wT}{}^2 = \sigma_{wm}{}^2 + \sigma_{wc}{}^2 \qquad \text{(D4)}$$

where:

σ_{wT}: Vertical turbulence coefficient

σ_{wm}: Mechanical mixing component for vertical turbulence coefficient (as defined in Equation D5 below)

σ_{wc}: Convective mixing component for vertical turbulence coefficient (as defined in Equation D6 below)

Mechanical mixing (σ_{wm}) for vertical turbulence coefficient has two components: 1) contribution from boundary layer (σ_{wml}) and 2) contribution from the residual layer above the boundary layer (σ_{wmr}). Equation D5 shows how σ_{wml} was calculated.

$$\sigma_{wml} = 1.3u^* \sqrt{1 - \frac{z}{z_i}} \qquad for\ z < z_i \qquad \text{(D5)}$$

$$\sigma_{wml} = 0.0 \qquad for\ z \geq z_i$$

where:

σ_{wml}: Mechanical mixing in boundary layer

z_i: Maximum mixing height (=Max $[z_{im}, z_{ic}]$)

The convective mixing (σ_{wc}) for vertical turbulence coefficient is calculated as shown in Equation D6.

$$\sigma_{wc}{}^2 = 1.6 \left(\frac{z}{z_{ic}}\right)^{\frac{2}{3}} . w^{*\ 2} \qquad for\ z \leq 0.1 z_{ic} \qquad \text{(D6)}$$

$$\sigma_{wc}{}^2 = 0.35\ w^{*\ 2} \qquad for \quad 0.1 z_{ic} < z \leq z_{ic}$$

$$\sigma_{wc}{}^2 = 0.35\ w^{*\ 2}\ \ exp\left[-\frac{6(z - z_{ic})}{z_{ic}}\right] \qquad for \quad z > z_{ic}$$

Appendix E: Copyright permissions

E1: Permission for Akçelik & Besley, 2001

UWinGmail **Hassan Mohseni Nameghi <mohsenih@uwindsor.ca>**

Request for permission

Rahmi Akcelik <rahmi.akcelik@sidrasolutions.com> Fri, Dec 21, 2012 at 8:58 PM
To: Hassan Mohseni <mohsenih@uwindsor.ca>

Dear Hassan

You have our permission to use the specified figures provided due reference is given to the source.

Best wishes for Christmas and the New Year

Rahmi Akçelik
Director

SIDRA SOLUTIONS

From: Hassan Mohseni [mailto:mohsenih@uwindsor.ca]
Sent: Saturday, 22 December 2012 8:54 AM
To: Rahmi Akcelik
Subject: Request for permission

December 21, 2012

Dr. Rahmi Akçelik
Director, Akcelik & Associates Pty Ltd
P O Box 1075 G, Greythorn Victoria, Australia 3104

Dear Dr. Akçelik:

I am completing a doctoral dissertation at the University of Windsor entitled "A case study of integrated modelling of traffic, vehicular emissions, and air pollutant concentrations for Huron Church Road, Windsor." I would like your

permission to include in my thesis/dissertation the following material:

The following three figures from: Akçelik R., Besley M., 2001. Acceleration and deceleration models. 23rd Conference of Australian Institutes of Transport Research (CAITR 2001), Monash University, Melbourne, Australia, 10-12 December 2001

Figure 1 - Time-distance and speed-time diagrams showing the acceleration and deceleration manoeuvres of a vehicle stopping and starting at traffic signals

Figure 5 - Polynomial model: Acceleration, speed and distance profiles for a vehicle ACCELERATING from zero initial speed to a final speed of 60 km/h (The top figure)

Figure 6- Figure 6 - Polynomial model: Acceleration, speed and distance profiles for a vehicle DECELERATING from an initial speed of 60 km/h to zero final speed (The top figure)

My thesis will be deposited to the University of Windsor Leddy library.

[or]

My thesis will be deposited to the University of Windsor's online theses and dissertations repository (http://winspace.uwindsor.ca) and will be available in full-text on the internet for reference, study and / or copy.

I will also be granting Library and Archives Canada and ProQuest/UMI a non-exclusive license to reproduce, loan, distribute, or sell single copies of my thesis by any means and in any form or format. These rights will in no way restrict republication of the material in any other form by you or by others authorized by you.

Please confirm in writing or by email that these arrangements meet with your approval.

Thank you very much for your attention to this matter.

Sincerely,

Hassan Mohseni Nameghi
PhD Candidate in Environmental Engineering
University of Windsor

E2: Permission for Hanrahan (1999)

UWinGmail **Hassan Mohseni Nameghi <mohsenih@uwindsor.ca>**

Request for permission

Nancy Bernheisel <nbernheisel@awma.org> Wed, Mar 6, 2013 at 3:24 PM
To: Hassan Mohseni <mohsenih@uwindsor.ca>

Cc: Lisa Bucher <lbucher@awma.org>

Hi Hassan,

The material may be used in your dissertation, but not in any other sorts of materials/publications.

Nancy

Nancy E. Bernheisel
Publications Coordinator
Air & Waste Management Association
One Gateway Center, Third Floor
420 Fort Duquesne Blvd.
Pittsburgh, PA 15222 USA
P: +1-412-232-3444, ext. 6027
F: +1-412-232-3450
email: nbernheisel@awma.org

From: Hassan Mohseni [mailto:mohsenih@uwindsor.ca]
Sent: Wednesday, March 06, 2013 3:22 PM
To: Nancy Bernheisel
Cc: Lisa Bucher
Subject: Re: FW: Request for permission

Hi Nancy,

Thank you very much for giving me the permission to use the materials in my dissertation. However, I do not fully understand the statement "As long as the dissertation is not being formally published". After I deposit my dissertation, the hard copy will be available in the library and the e-copy will be available online. I am not sure whether this is called formal publication. Alternatively, you may mean that as long as the material is used in my dissertation, it it fine,

but I am not allowed to use the materials in other sorts of formal publications such as journal papers. I appreciate your help if you could clarify this statement.

Thank you for your time and patience.

Sincerely,

Hassan Mohseni Nameghi

On Wed, Jan 2, 2013 at 9:02 AM, Nancy Bernheisel <nbernheisel@awma.org> wrote:

Dear Hassan,

Thank you for your query.

As long as the dissertation is not being formally published, you have our permission to use in your thesis the material you state in your message below.

Best wishes in obtaining your Ph.D.

Nancy

Nancy E. Bernheisel
Publications Coordinator
Air & Waste Management Association
One Gateway Center, Third Floor
420 Fort Duquesne Blvd.
Pittsburgh, PA 15222 USA
P: +1-412-232-3444, ext. 6027
F: +1-412-232-3450
email: nbernheisel@awma.org

From: Hassan Mohseni [mailto:mohsenih@uwindsor.ca]
Sent: Sunday, December 30, 2012 11:39 AM
To: lbucher@awma.org
Subject: Request for permission

December 31, 2012

Lisa Bucher
Managing Editor
Journal of Air&Waste Management Association
One Gateway Center, 3rd Floor

420 Fort Duquesne Blvd.
Pittsburgh, PA 15222-1435

Dear Madam Bucher:

I am completing a doctoral dissertation at the University of Windsor entitled "A case study of integrated modelling of traffic, vehicular emissions, and air pollutant concentrations for Huron Church Road, Windsor." I would like your permission to include in my thesis/dissertation the following material:

Equations 1, 2, 3, and 9 from the following article:

Hanrahan, P.L., 1999. The Plume Volume Molar Ratio Method for Determining NO2/NOx Ratios in Modeling—Part I: Methodology, Air & Waste Manage. Assoc. 49:1324-1331.

My thesis will be deposited to the University of Windsor Leddy library.

[or]

My thesis will be deposited to the University of Windsor's online theses and dissertations repository (http://winspace.uwindsor.ca) and will be available in full-text on the internet for reference, study and / or copy.

I will also be granting Library and Archives Canada and ProQuest/UMI a non-exclusive license to reproduce, loan, distribute, or sell single copies of my thesis by any means and in any form or format. These rights will in no way restrict republication of the material in any other form by you or by others authorized by you.

Please confirm in writing or by email that these arrangements meet with your approval.

Thank you very much for your attention to this matter.

Sincerely,

Hassan Mohseni Nameghi
PhD Candidate in Environmental Engineering
University of Windsor

E3: Permission for Panis et al. (2006)

ELSEVIER LICENSE
TERMS AND CONDITIONS

Jan 10, 2013

This is a License Agreement between Hassan Mohseni Nameghi ("You") and Elsevier ("Elsevier") provided by Copyright Clearance Center ("CCC"). The license consists of your order details, the terms and conditions provided by Elsevier, and the payment terms and conditions.

All payments must be made in full to CCC. For payment instructions, please see information listed at the bottom of this form.

Supplier	Elsevier Limited The Boulevard,Langford Lane Kidlington,Oxford,OX5 1GB,UK
Registered Company Number	1982084
Customer name	Hassan Mohseni Nameghi
Customer address	401 Sunset Ave Windsor, ON N9B3P4
License number	3065330745758
License date	Jan 10, 2013
Licensed content publisher	Elsevier
Licensed content publication	Science of The Total Environment
Licensed content title	Modelling instantaneous traffic emission and the influence of traffic speed limits
Licensed content author	Luc Int Panis,Steven Broekx,Ronghui Liu
Licensed content date	1 December 2006
Licensed content volume number	371
Licensed content issue number	1–3
Number of pages	16
Start Page	270
End Page	285
Type of Use	reuse in a thesis/dissertation
Portion	figures/tables/illustrations
Number of figures/tables/illustrations	1
Format	both print and electronic
Are you the author of this Elsevier article?	No
Will you be translating?	No

Order reference number	
Title of your thesis/dissertation	A case study of integrated modelling of traffic, vehicular emissions, and air pollutant concentrations for Huron Church Road, Windsor
Expected completion date	Feb 2013
Estimated size (number of pages)	288
Elsevier VAT number	GB 494 6272 12
Permissions price	0.00 USD
VAT/Local Sales Tax	0.0 USD / 0.0 GBP
Total	0.00 USD
Terms and Conditions	

E4: Permission for Zhou and Levy (2006)

ELSEVIER LICENSE
TERMS AND CONDITIONS

Jan 10, 2013

This is a License Agreement between Hassan Mohseni Nameghi ("You") and Elsevier ("Elsevier") provided by Copyright Clearance Center ("CCC"). The license consists of your order details, the terms and conditions provided by Elsevier, and the payment terms and conditions.

All payments must be made in full to CCC. For payment instructions, please see information listed at the bottom of this form.

Supplier	Elsevier Limited The Boulevard,Langford Lane Kidlington,Oxford,OX5 1GB,UK
Registered Company Number	1982084
Customer name	Hassan Mohseni Nameghi
Customer address	401 Sunset Ave Windsor, ON N9B3P4
License number	3065331145482
License date	Jan 10, 2013
Licensed content publisher	Elsevier
Licensed content publication	Atmospheric Environment
Licensed content title	The impact of urban street canyons on population exposure to traffic-related primary pollutants
Licensed content author	Ying Zhou,Jonathan I. Levy
Licensed content date	April 2008

Licensed content volume number	42
Licensed content issue number	13
Number of pages	12
Start Page	3087
End Page	3098
Type of Use	reuse in a thesis/dissertation
Portion	figures/tables/illustrations
Number of figures/tables/illustrations	1
Format	both print and electronic
Are you the author of this Elsevier article?	No
Will you be translating?	No
Order reference number	
Title of your thesis/dissertation	A case study of integrated modelling of traffic, vehicular emissions, and air pollutant concentrations for Huron Church Road, Windsor
Expected completion date	Feb 2013
Estimated size (number of pages)	288
Elsevier VAT number	GB 494 6272 12
Permissions price	0.00 USD
VAT/Local Sales Tax	0.0 USD / 0.0 GBP
Total	0.00 USD
Terms and Conditions	

VITA AUCTORIS

NAME: Hassan Mohseni Nameghi

PLACE OF BIRTH: Iran

YEAR OF BIRTH: 1979

EDUCATION:

Khaje Nasir Toosi University of Technology, Tehran, Iran
1998 – 2003 BSc in Mechanical Engineering

Sharif University of Technology, Tehran, Iran
2003 – 2005 MSc in Energy Systems Engineering

University of Windsor, Windsor, ON
2009 – 2012 PhD in Environmental Engineering